Identifying genes underlying FHB QTLs in bread wheat

Lola González Penadés

A thesis submitted to the University of East Anglia

for the degree of Doctor of Philosophy

Department of Crop Genetics

John Innes Centre

March 2022

El verdadero acto del descubrimiento no consiste en salir

a buscar nuevas tierras, sino en aprender

a ver la vieja tierra con nuevos ojos.

MARCEL PROUST

Abstract

Fusarium Head Blight (FHB) is a destructive fungal disease which reduces wheat yield. *Fusarium* species produce deoxynivalenol (DON) mycotoxin, which is harmful to animals and humans that feed on contaminated grain. DON acts as a virulence factor enabling fungal spread in the wheat rachis and causing bleaching above the point of infection. Host resistance is broadly used to control FHB and is classified as type I, resistance to the initial penetration, or type II, resistance to fungal spread. Many Quantitative Trait Loci (QTLs) associated with FHB resistance have been identified.

FHB resistance QTLs located on the 5A and 2D chromosomes in bread wheat (*Triticum aestivum*), respectively, were studied in the present project. A recombinant inbred line (RIL) population (Hobbit *sib* x WEKH85A) and a near isogenic line (NIL) population (Crusoe x Wuhan) were tested for FHB type II resistance to fine-map the 5A and 2D QTLs, respectively. For the fine-mapping of both loci, a single marker analysis based on the physical position of SNPs in the Chinese Spring genome was performed. Results revealed that both 5A (*QFhb.WEK-5A*) and 2D (*QFhb.Wuhan-2DL*) loci were stable across years and were refined to 6.24 Mbp on the long arm of chromosome 5A and to 55.6 Mbp on the long arm of the 2D chromosome, respectively. Further fine-mapping is needed to refine *QFhb.Wuhan-2DL*.

Additionally, DON tolerance was assessed using wheat root assays. It was demonstrated that the *QFhb.WEK-5A* locus in line WEK8H5A may be associated with two traits: DON tolerance and FHB resistance. RNA-Seq identified a DON-responsive candidate gene *TraesCS5A02G191700* in the FHB *QFhb.WEK-5A* locus. Sequencing revealed that a 3 bp (CTT) deletion in the promoter region of gene *TraesCS5A02G191700* may be responsible for the enhanced expression of this gene upon challenge with DON or *F. graminearum* in line WEKH85A. Functionally validation is still needed.

Acknowledgements

The funding for this PhD project was provided by the Biotechnology and Biological Sciences Research Council (BBSRC) and Limagrain S.A. Thank you to both organisations for making this research possible.

Firstly, I would like to thank my supervisor Prof. Paul Nicholson for the opportunity, guidance, encouragement, support, his tremendously patience over the past years and his sense of humour. I am also grateful to my second supervisor, Prof. James Brown, for his guidance for the statistics analysis and his feedback throughout the project. I would also like to thank my industrial supervisor, Dr Simon Berry, and the collaborators at Limagrain S.A., specially to Mickael Throude and Jordi Comadran, for all their knowledge and work.

I am also grateful for the past and present members of the Nicholson and Brown groups for welcoming and helping me over these past years. My special thanks to Andrew Steed, Marianna Pasquariello, Emily Beardon, Laetitia Chartrain, Rachel Burns, Rachel Goddard, Martha Clarke, Martha Nicholson, Ben Hales and Catherine Chinoy for their invaluable help during poly tunnel or lab work. I would also like to thank the following people who have helped me with the project: the Horticultural services team at the JIC, Dr Pirita Paajanen and Dr Miguel Angelo Costa e Silva dos Santos for their bioinformatic assistance, Tom Lawrenson for his help and guidance during the ddPCR analysis, and the Transformation team at the JIC (specially Mark Smedley and Dr Sadiye Hayta).

Finally, I would like to thank my fellow students Beth, Miguel, John, Cyrielle and Jessica for their help, friendship and making the work and my time at the JIC so enjoyable. I am very grateful to my family and friends for their love and support, specially over the last year. I will always be extremely grateful for the sense of humour, encouragement, and the personal drive that Abraham has provided me during all these years of mutual support.

Abbreviations

ABC	ATP-binding cassette
AFLP	Amplified fragment length polymorphism
bp	Base pairs
CDS	Coding DNA sequence
CER	Controlled environment room
CIMMYT	Centro Internacional de Mejoramiento de Maíz y Trigo
Cq	Quantification cycle
CRISPR	Clustered regularly interspaced short palindromic repeats
CS	Chinese Spring
cv.	Cultivar
DAMPs	Damage-associated molecular patterns
ddPCR	Droplet digital PCR
DEG(s)	Differentially expressed gene(s)
DH	Doubled haploid
DNA	Deoxyribonucleic acid
DON	Deoxynivalenol
dpi	Day(s) post infection
DTI	DAMPs-triggered immunity
D3G	DON-3-O-glucoside
ERE	Ethylene-Responsive Element
ET	Ethylene
EU	European Union
FC	Fold change
FDK	Fusarium damaged kernels
FHB	Fusarium head blight
FRR	Fusarium root rot
GA_3	Gibberellic acid
Gbp	Giga base pares
GE	Genome editing
GSTs	Glutathione S-transferases
h	Hours
hai	Hours after infection

HCAAs	Hydroxycinnamic acid amides
HRC	Histidine-rich calcium
IWGSC	International Wheat Genome Sequence Consortium
JA	Jasmonic acid
JIC	John Innes Centre
KASP(s)	Kompetitive allele specific PCR
Kbp	Kilo base pares
Kg	Kilogram
L	Litre
LC	Low confidence
LMM	Linear mixed model
LOB	Lateral organ boundary
LTPs	Lipid transfer proteins
MAMPs	Microbe-associated molecular patterns
MAS	Marker-assisted selection
Mbp	Mega base pares
m^3	Cubic metre
min	Minutes
ml	Millilitre(s)
mM	Millimolar
MM	Master Mix
MTI	MAMPs-triggered immunity
ng	Nanogram(s)
NIL(s)	Near isogenic line(s)
NIV	Nivalenol
ONT	Oxford Nanopore Technology
Opt.	Optimal
PA(s)	Phosphatidic acid(s)
PAMPs	Pathogen-associated molecular patterns
PCR	Polymerase chain reaction
PFT	Pore-forming toxin-like domain
PI	Point of infection/inoculation
PP	Primer pairs
ppm	Parts per million
PR	Pathogenesis-related

PRRs	Pattern recognition receptors
PTI	PAMPs-triggered immunity
QTL(s)	Quantitative trait locus (loci)
RefSeq	Reference sequence
RFLP	Restriction fragment length polymorphism
RGA(s)	Resistance gene analogues
RIL(s)	Recombinant inbred line(s)
RNA	Ribonucleic acid
RNA-Seq	RNA sequencing
ROS	Reactive oxygen species
rpm	Revolutions per minute
RT-qPCR	Quantitative reverse transcription PCR
s	Seconds
SA	Salicylic acid
SFI	Single floret inoculation
SNP(s)	Single nucleotide polymorphism(s)
SPRAY	Spray inoculation
SSR	Simple sequence repeat
Tª	Temperature
TALEN	Transcription activator-like effector nuclease
TF(s)	Transcription factor(s)
TFBS	Transcription factor biding site
Tm	Melting temperature
TPM	Transcripts per million
UGT(s)	UDP-glucosyltransferases
UK	United Kingdom
WSB	Wangshuibai
ZEA	Zearalenone
µl	Microlitre(s)
µM	Micromole(s)
3-ADON	3-acetyl-DON
15-ADON	15-acetyl-DON
°C	Degrees Celsius
%	Percentage

Contents

List of Tables

List of Figures

Chapter 1

General Introduction

1.1. Wheat

1.1.1. Wheat genetics and evolution

Bread wheat (*Triticum aestivum*) allohexaploid genome is very large and complex, and it is the result of two hybridisation events (Petersen et al. 2006). The wheat genome is of 16 Gbp (Guan et al. 2020) and consists of 21 chromosome pairs. Indeed, an annotated reference sequence is available, giving access to 107.891 high-confidence genes (IWGSC 2018).

Wheat genome was originated by three diploid donor species (*Triticum urartu,* progenitor of *Aegilops speltoides* and *Aegilops tauschii*), each possessing 7 chromosome pairs. The first hybridisation and polyploidization event occurred approximately between 300-500 thousand years ago between *T. urartu* (AA) and a species believed to be an extinct ancestor of *Aegilops speltoides* (BB) to form the tetraploid *T. dicoccoides* (AABB). This tetraploid hybrid was later domesticated to form the tetraploid emmer wheat (*T. turgidum* ssp. *Dicoccum*) around 10 thousand years ago. The second hybridisation event is estimated to have taken place around 9 thousand years ago, between emmer wheat (AABB) and a wild grass, *A. tauschii* (DD), resulting in hexaploid *T. spelta* (AABBDD). Natural mutations led to the development of *T. aestivum* (AABBDD), known as bread wheat, and the modern durum wheat (*T. turgidum* ssp. *durum*) (AABB), which is used for making pasta (Figure 1.1.) (Rahman et al. 2020).

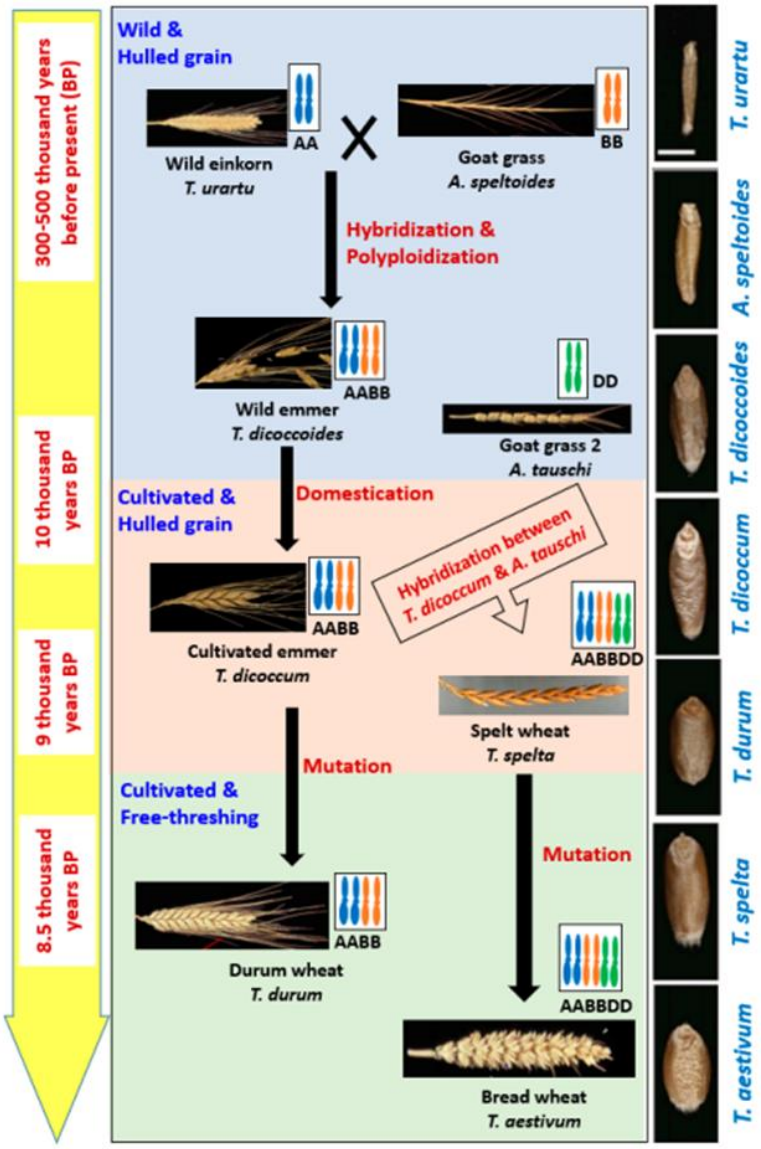

Figure 1.1. *Evolution of wheat through hybridization, allopolyploidization, domestication and mutation. The approximate time of those events is indicated on the left side in yellow. Pictures of spike for each wheat species are shown. The gradual changes in grain size and shape during evolution is represented on the right (Rahman et al. 2020).*

1.1.2. Importance of wheat

In the 21st century, food security has become an important challenge since global population is expected to increase to nine billion by 2050. In less than 20 years' time, cereal production will need to increase by 50 % to meet demand (Foresight 2011). A growing global population is, therefore, driving the world grain market.

Wheat (*Triticum* spp.) is one of the most important crops worldwide used for human and livestock feed. Wheat is the staple crop for an estimated 35 % of the world population (IDRC 2010). Indeed, more than two-thirds of global wheat is used for food and one fifth is used for livestock feed (OECD/FAO 2019).

1.1.3. Wheat production

Wheat production has increased almost 16 % between 2010 and 2020 (FAOSTAT 2021) and will need to continue this trend. Wheat is the dominant cereal crop grown in temperate countries (Shewry 2009) with a world global production in 2021 of around 770 million metric tonnes (FAOSTAT 2021). Indeed, wheat has become the world's second largest food source after maize (*Zea mays*) with an estimated worldwide 2021/22 production of 778.6 million metric tonnes (https://www.statista.com/).

The UK wheat yield has been increasing in the past years, with the wheat production in 2019 of 16.3 million tonnes, an increase of 20.1 % on 2018. However, wheat production in the UK in 2020 drastically declined to 9.6 million tonnes, a figure that has not been seen for at least 40 years (FAOSTAT 2021).

To maintain the increase in wheat supply, it is critical to protect wheat production. However, there are various threats to wheat production and among these, plant diseases are considered one of the most dangerous (Khan et al. 2020). Diseases of cereal crops cause yield reduction and, in some instances, grain contamination with toxins. Thus, to increase yield

and cereal production it is very important to obtain a better understanding of the interaction between pathogens and cereals.

1.2. Fusarium Head Blight – a threat to wheat production

One of the significant threats to wheat production is Fusarium Head Blight (FHB). This destructive fungal disease is also known as scab or ear blight. FHB affects wheat (*Triticum* spp.), barley (*Hordeum vulgare*), rye (*Secale cereale*), oats (*Avena sativa*), and other small grain cereal crops around the world. FHB causes yield losses and is a potential health risk to humans and animals that consume grain contaminated with mycotoxins (Parry, Jenkinson, and McLeod 1995). In fact, according to the International Maize and Wheat Improvement Centre (CIMMYT), FHB has been considered as one of the most destructive diseases impacting the production of wheat globally (Yi et al. 2018).

1.2.1. *Fusarium* spp. causing FHB

FHB can be caused by many different *Fusarium* species (Schroeder and Christensen 1963). The FHB species complex includes more than 16 species (Khan et al. 2020; O'Donnell et al. 2004), that infect a range of hosts (van der Lee et al. 2015). Some of these species are *Fusarium avenaceum*, *F. culmorum*, *F. graminearum*, *F. poae*, and *F. langsethiae*.

In a specific location, the predominant causal *Fusarium* species is determined by the environmental conditions, mainly temperature and rainfall (Goddard 2015; Nicholson 2009). In the UK and Northern Europe, the main causal agents are *F. graminearum* (teleomorph *Gibberella zeae*) and *F. culmorum* (Xu and Nicholson 2009). Irrespective of geographic origin, the optimum temperature growth of both *F. graminearum* and *F. culmorum* is 25°C (Brennan et al. 2003), temperate climate conditions.

Fusarium species are able to infect the plant host throughout most of its developmental stages (Goddard 2015). Many *Fusarium* species which cause FHB are also known to cause seedling blight and foot rot (Saharan 2020). Head blight is one of the most important *Fusarium* diseases because most cereal products are being generated from grains, which are produced in the head of the plant. Thus, if grain is infected during development, yield will be reduced due to kernel morphological changes and compromised grain quality.

1.2.2. Prevalence of FHB

FHB was first described as a major threat to wheat and barley in England in 1884 (Goswami and Kistler 2004; Smith 1884) and since then, numerous epidemics have been reported worldwide.

FHB epidemics have been reported to cause 10-70 % of production loss during the epidemic years (Zhang 2011). Given the current global warming associated with increased temperatures, major epidemics of FHB are likely to occur soon, particularly under high humidity conditions (Shah et al. 2014). The spread of FHB infection is affected by the variation in the temperature and humidity. However, the spread of infection may be also affected by the *Fusarium* isolate, since they can behave differently, regarding their aggressiveness, in lower or higher temperatures. Differential reaction with various *F. graminearum* isolates due to the variation in weather was observed by Saharan et al. (2007). Additionally, several studies have reported higher mycotoxin production at higher temperatures at the moment of initial infection (Xu, Nicholson, and Ritieni 2007).

During the last decades, the rapid global re-emerge of FHB along with contamination of grains with mycotoxins attributable to the disease led *F. graminearum* becoming one of the most intensively studied fungal plant pathogens (Goswami and Kistler 2004). FHB has become more prevalent in Asia, Europe, and South America. This pathogen is considered to

be one of the most important fungal plant pathogens in the world (Dean et al. 2012) causing serious economic, social, environmental and health issues (Kazan and Gardiner 2018). FHB causes major economic losses in both agriculture and grain producing industries every year (Kazan and Gardiner 2018), which leads to the impetus to decipher the key mechanisms to reduce FHB.

1.2.3. Life cycle of *Fusarium* sp. in wheat

The primary inoculum of FHB is the contaminated crop residue from previous harvests (Thompson 2010), since it has been demonstrated the *F. graminearum* can survive saprophytically over winter on plant debris from wheat, barley and maize (Goswami and Kistler 2004). Thus, this fungus can survive on living or dead tissues of many hosts.

Fusarium culmorum reproduces via asexual means only, while *F. graminearum* can use both types of reproduction (Doohan, Brennan, and Cooke 2003). *Fusarium graminearum* undergoes its sexual cycle on infested crop debris and its asexual cycle on living wheat tissues (Gunupuru, Perochon, and Doohan 2017). However, in both sexual stages, haploid mycelial structures are formed (Ma et al. 2013).

Fusarium sexual reproduction basically involves the production of ascospores, which are released from the ascus during periods of high humidity and wind. Asexual reproduction involves the production of three types of spores: microconidia, macroconidia and chlamydospores, which are most often distributed by splash dispersal (Figure 1.2.). Warm moist weather conditions in the spring are favourable for the development and maturation of conidia and ascospores, which occurs at the same time as flowering of cereal crops (Goswami and Kistler 2004). Indeed, ascospores of *F. graminearum* are the primary source of infection of cereal flowers (Trail 2009).

Fusarium graminearum is homothallic and so does not require a partner to develop sexual structures and produce ascospores. Sexual reproduction between isolates of *F. graminearum* increases genetic diversity of the pathogen and an adaptative response to its surroundings. In fact, there is a possibility of an increased adaptability of the fungus toward diverse environmental conditions via genetic exchange during the sexual reproduction (Cuomo et al. 2007).

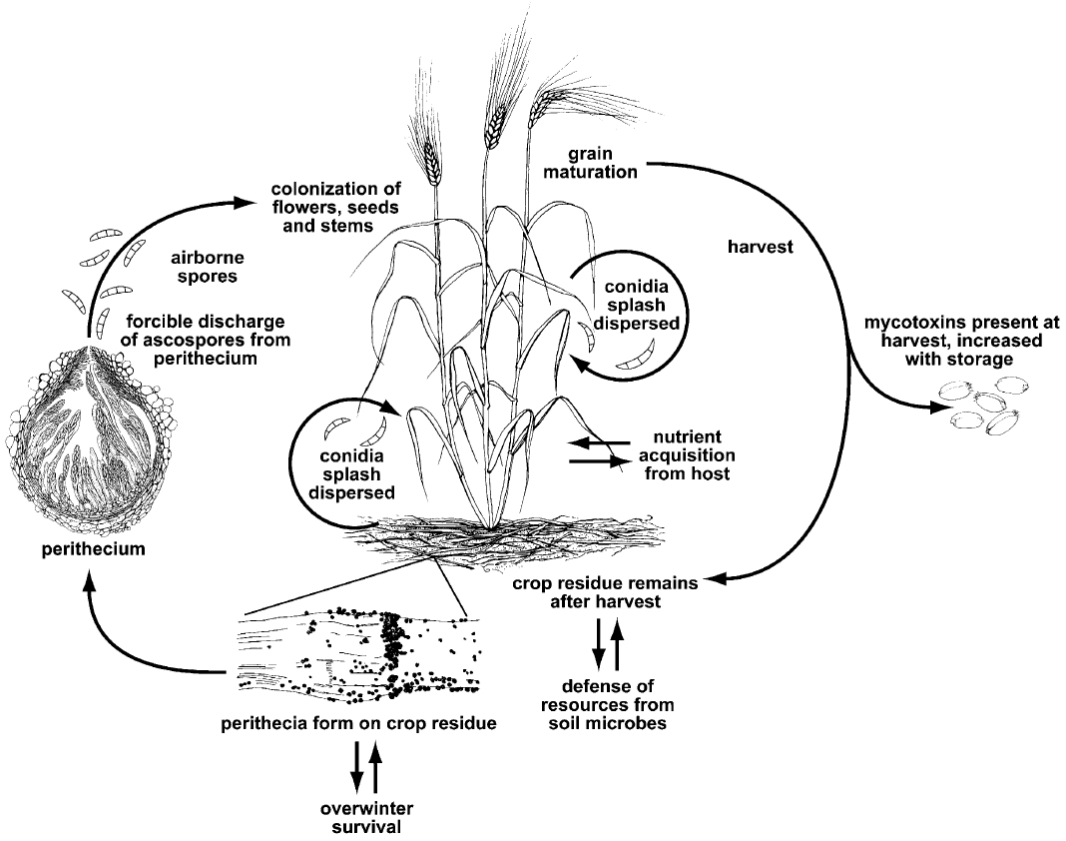

Figure 1.2. *The life cycle of F. graminearum, causal agent of FHB on wheat (Trail 2009).*

1.2.4. Host colonisation by *Fusarium* sp.

Fusarium colonization starts when fungal spores reach the external structures of wheat ears, such as lemma, palea or anther tissue (Bushnell, Hazen, and Pritsch 2003; Trail 2009). Anthers are very rapidly infected (Skinnes et al. 2010). This means that plants are more

sensitive to FHB at flowering stage (Walter, Nicholson, and Doohan 2010), during the period of anthesis.

The fungus germinates and does not penetrate directly through the epidermis. Hyphae develop on the surface of the epidermal cells of florets and glumes (Boenisch and Schaefer 2011) before penetrating the host via stomata or other susceptible sites on the cell wall, epidermis, or cuticle (Bushnell, Hazen, and Pritsch 2003). First, the fungus grows intercellularly and asymptomatically (Guenther and Trail 2005), and spreads from floret to floret inside a spikelet and from spikelet to spikelet through the xylem vessels in the rachis and rachilla (Ribichich, Lopez, and Vegetti 2000).

The lack of intracellular growth during the early stages of infection suggests that *F. graminearum* is a brief biotroph, therefore, it is considered a hemibiotroph (Jansen et al. 2005). When fungal structures develop intracellularly during both stem and head infections, *F. graminearum* starts acting as a necrotroph causing host cell death. Symptoms at this stage include water soaking in chlorenchyma tissues (Trail 2009), leading to the production of shrived kernels and premature bleaching of the spikes which affects photosynthesis (Bai and Shaner 1994).

1.2.5. Wheat symptoms caused by FHB infection

The most common symptom of FHB in wheat is the bleaching of infected spikelets (Figure 1.3.). The bleaching spreads from the initial point of infection as the fungus moves into the rachis of the wheat ear and into adjacent spikelets (Guenther and Trail 2005). Another disease symptom in wheat can be appreciated on the exterior surface of the florets and glume as brown, dark, purple to black necrotic lesions. The inflorescence will be then become bleached and tan coloured, with atrophied grain (Goswami and Kistler 2004).

Fusarium damaged grains have a lower weight which leads to them being dispersed more easily during harvesting and, therefore, increases fungal propagation and causes a potential reduction of yield in subsequent crops (Goddard 2015).

The extent and severity of symptoms and losses due to FHB depends on many aspects, including level of host susceptibility, environmental conditions, and inoculum density (Parry, Jenkinson, and McLeod 1995).

Figure 1.3. *Characteristic bleaching symptoms of FHB infection in wheat spikes.*

1.3. Mycotoxin production by *Fusarium* sp.

FHB not only causes yield losses but also contaminates grain with mycotoxins. Mycotoxins result in a direct yield loss and are of a great concern because of the associated health risks of wheat grain consumers (Thompson 2010). These toxins accumulate in the grains of infected crops, being stable during grain processing methods and reaching animals and human consumers.

Zearalenone (ZEA) and trichothecenes are among the mycotoxins of greatest agroeconomic importance (Zain, Bahkali, and Al-Othman 2012). Indeed, the most notable mycotoxins produced by several *Fusarium* species when infecting cereals, particularly wheat and maize, are ZEA and deoxynivalenol (DON). The predominant species responsible for ZEA production is *F. graminearum*. High concentrations of this compound appear to be produced during delayed wet harvests, which are more common in northern Europe (Edwards 2011).

The most widely studied and understood class of mycotoxins are the trichothecenes since their prevalence is higher in Northern Europe and America where cereal crops are commonly grown (Goddard 2015).

1.3.1. Trichothecenes – DON mycotoxin

Trichothecenes are the most interesting group of mycotoxins because they are produced by the most prevalent and pathogenic *Fusarium* species, including *F. graminearum* and *F. culmorum*. These secondary metabolites are a large class of structurally similar, water soluble sesquiterpenes (McCormick et al. 2011).

The most relevant trichothecenes of FHB are DON and nivalenol (NIV) (Desjardins and Proctor 2007). However, the most frequently encountered mycotoxin in Europe produced by *F. graminearum* and *F. culmorum* is DON, which has become a major concern due to the reduction of grain quality and risk to consumer health (Wegulo 2012). Apart from producing DON, *F. graminearum* also produces derivatives such as 3-acetyl-DON (3-ADON) and 15-acetyl-DON (15-ADON) (Bottalico and Perrone 2002). 3-ADON-producing *F. graminearum* isolates are often more aggressive and produce higher levels of DON than 15-ADON-producing strains (Puri and Zhong 2010).

1.3.2. DON is a virulence factor associated with FHB

DON is a key virulence factor associated with FHB infection. Following infection of wheat florets, the fungus starts producing DON and this facilitates the spreading of the fungus from spikelet to spikelet and from spikelet to rachis. Therefore, if the biosynthesis of DON is supressed, then colonisation can be reduced (Dweba et al. 2017; Maier et al. 2006).

The transcription factors *TRI6* and *TRI10* regulate the expression of trichothecene biosynthesis genes in *F. graminearum* (Seong et al. 2009). The Tri-cluster encodes key proteins involved in the biosynthesis of trichothecenes such as DON. *FgTRI5* gene encodes the enzyme trichodiene synthase which catalyses the first step of the trichothecene biosynthesis (Maier et al. 2006). Interestingly, when the *FgTRI5* gene was disrupted, *F. graminearum* mutants lacked the ability to spread in wheat spikes (Bai, Desjardins, and Plattner 2002).

However, by using a *ΔFgtri5* (deletion) strain, infection structures of *F. graminearum* were still observed, which suggested that DON production occurs distinctively during infection and may be unnecessary for the formation of such structures or necrotic lesions surrounding them. This would mean that trichothecenes are not crucial during the initial stages of infection since infection structures and necrotic lesions developed independent of DON production (Boenisch and Schaefer 2011). It appears that at this stage, trichothecenes might be crucial for suppressing host plant defence systems. This may suggest that trichothecene synthesis is not required during the biotrophic life of *F. graminearum* at the early infection phase and that it controls the necrotrophic life at later infection phases (Dweba et al. 2017).

Interestingly, the production of DON in dead host tissue remains low, despite significant fungal growth (Boedi et al. 2016). This may suggest that the host is also involved in triggering DON biosynthesis in the pathogen (Gardiner et al. 2010). Various polyamine

compounds, such as putrescine, arginine and cadaverine, produced by the host plant during infection, are known to induce DON biosynthesis in *F. graminearum* (Gardiner, Kazan, and Manners 2009).

1.3.3. Regulations for mycotoxin content

An association exists between DON biosynthesis and the colonization of developing tissues leading to shrunken grains (Jansen et al. 2005). Infestation of cereal grains in the field and in storage by DON may cause adverse effects on health. Some of these negative effects are the inhibition of DNA synthesis, cell growth and causing cell cycle suspension (Pestka 2010a).

DON is associated with human gastroenteritis, which is why it is colloquially known as “vomitoxin” (Pestka 2010b). This disease involves both the immune and gastrointestinal systems, and causes diarrhoea, vomiting, leukopenia, haemorrhage and toxic shock (Joffe 1978).

Due to the health concerns in humans and animals, strict regulations govern the permitted mycotoxin content of all cereal grains and the products derived from cereals. In Europe, maximum acceptable limits of mycotoxins in food and feed were set in the Commission regulation (EC) No 1881/2006, in which it established a maximum level of 1250 µg/Kg (1.25 ppm) in unprocessed cereals (Union 2006).

1.4. FHB control strategies

To perform an effective management of FHB, a single control strategy cannot be used because each of them has limitations. Employment of different strategies including cultural,

biological, chemical and host plant resistance are known to be more effective for FHB management (Dweba et al. 2017).

Nevertheless, the most reviewed and known approaches to control and management of FHB are chemical, agricultural and host resistance strategies. These strategies are aimed at decreasing primary inoculum, preventing the spread of the pathogen and decreasing the chance of infection if the inoculum is present (Parry, Jenkinson, and McLeod 1995). The use of bio-controls agents including bacteria and fungi have been also reported to reduce *F. graminearum* and associated toxin production. However, complete eradication of FHB has not yet been achieved and further studies are required (Dweba et al. 2017).

1.4.1. Chemical treatment

Fungicides have been used as a method to reduce FHB severity. The efficacy of different fungicides for FHB management was evaluated and it was reported that azoxystrobin and triazole fungicides best controlled the disease as compared to unsprayed control in wheat varieties (Bagga 2012). However, outcomes of using fungicides have not been successful in many instances because they are dependent on the environmental conditions, the fungicide selected and the *Fusarium* species present.

Additionally, it has been shown that the use of fungicides to control FHB had inconsistent yield results and may not reduce the mycotoxin content of grain to the tolerable level (Parry, Jenkinson, and McLeod 1995). These findings are also supported by other studies in which inoculated field trials in the UK indicate that few fungicides have significant activity against FHB and they may not be able to reduce the level of DON below the EU limit (Simpson et al. 2001).

Fungicide application is expensive, and application of these treatments repeatedly has the risk of generating fungicide insensitive *Fusarium* isolates. Therefore, this method is not an effective long term solution to prevent FHB infection (Goddard 2015).

1.4.2. Agricultural practice

Agricultural practices influence the incidence of FHB in the field. It has been shown that crop rotation affects the occurrence of FHB in the field, with crops following maize more prone to FHB infection (Osborne and Stein 2007). Maize is a good host for *Fusarium spp*., especially *F. graminearum*, in its senescence stage, which leads to a large reservoir of fungal biomass. Maize residues that remain on the soil surface provide a large increase in the niche available for the fungus and the production of ascospores and conidia (Pereyra, Dill-Macky, and Sims 2004).

The abundance of colonized cereal debris contributes to airborne inoculum throughout the area increasing the incidence of the fungal infection in the next crop. Therefore, previous crop and the amount of crop residue on the soil surface are considered to be major factors in local inoculum levels (Dill-Macky and Jones 2000). However, long-distance spore dispersal has also been reported (Maldonado-Ramirez et al. 2005) affecting crops nearby.

1.4.3. Genetic resistance

The use of sources of genetic resistance to FHB is more favourable to minimise the incidence and severity of the disease. It has become a primary control strategy to reduce yield losses and mycotoxin contamination. Indeed, host resistance has been considered a

particularly cost-efficient and environmentally friendly strategy to control FHB (Ittu et al. 2006).

Improvement of cereal cultivars with relatively high levels of FHB resistance is an essential breeding objective. The development of resistance against FHB in wheat can be performed by combining of molecular techniques with classical breeding methods (Khan et al. 2020). However, progress in developing FHB-resistant cultivars has been hindered by the complexity of this resistance. This is due to resistance to FHB being a quantitative trait. FHB resistance is polygenic, which means that many genes in the host, each with relatively small effects, are generally involved in disease resistance although a few genes have been shown to have a major effect on FHB resistance (Bai 2004).

The regions within genomes that contain genes associated with a particular quantitative trait are known as quantitative trait loci (QTLs) (Collard et al. 2005). Identification of QTLs related with FHB and DON resistance and the genes underlying these QTLs are urgently required to reveal new knowledge to develop resistant cereals and avoid yield losses and mycotoxin contamination.

1.5. Types of host resistance against FHB

Several categories of host resistance to FHB in cereal crops have been described. The most important and relevant ones for this project are type I and type II resistance. Type I is the resistance to the initial penetration of the host tissue by *Fusarium*, while type II is the resistance to fungal spread from infected to non-infected spikelets via the rachis (Schroeder and Christensen 1963). Type II resistance is primarily important in DON-producing *Fusarium* isolates, such as *F. graminearum* and *F. culmorum*, since these species can spread within the

wheat spike (Boenisch and Schaefer 2011) with DON acting as a virulence factor required to facilitate the spread.

Type III resistance has been reported for toxin decomposition (Miller, Young, and Sampson 1985), less grain infection and yield tolerance (Mesterházy 1995). Type IV resistance is measured as Fusarium damaged kernels (FDK) (Wegulo and Dowell 2008). Type V resistance (tolerance) is commonly defined as the ability of certain genotypes to yield higher than others when both have the same level of visual disease relative to uninoculated controls (Shaner 2002). In a much simplistic way, type III, IV and V have been described as resistance to mycotoxin accumulation, grain infection and tolerance, respectively (Mesterházy et al. 1999). These resistances tend to be more difficult to measure, especially in the field, and they are not very often used.

1.6. Breeding for FHB resistance

Breeding for disease control is a reliable and environmentally friendly approach that increases yield production as well as increasing selection intensity for desirable genotypes. The best way to manage FHB of wheat is the use of resistant cultivars. Development of disease resistant cultivars is an important factor to improve cultivation around the world (Shah et al. 2017). It is widely known that different wheat cultivars differ in their FHB resistance level but, so far, there is no genotype which is immune to the disease (Saharan 2020).

FHB resistance is controlled by many genes and it is influenced by the environment (Bai 2004). Plant breeding aims to combine multiple favourable traits into a single cultivar, thus, plant breeding for FHB resistance aims to combine multiple QTLs associated with different types of resistance into a single cultivar. However, QTLs for FHB resistance overlap

with QTLs linked to other traits, which means that FHB resistance is regulated by many underlying genetic factors and involves pleiotropy (Khan et al. 2020).

1.6.1. Trade-offs of breeding for FHB

Introducing a single desirable trait into breeding programmes may result in potential trade-offs, which are less favourable. For instance, reduced height allele (*Rht*) is involved in phytohormone signalling, producing a semi-dwarf phenotype. The European wheat cultivars that possess the *Rht-B1b* allele have been demonstrated to show a reduction of type I resistance but the opposite effect on type II resistance to FHB (Srinivasachary et al. 2009). The outcome, therefore, is a trade-off between reduced plant height and FHB resistance.

Another example is the introduction of the rye (*Secale cereale*) resistance genes to leaf rust, stem rust and powdery mildew into commercial wheat. This introduction of genes involved a translocation between the 1BL chromosome segment in bread wheat and 1RS in rye (Dhaliwal, Mares, and Marshall 1987). Increased resistance to FHB is associated with the presence of the *GliR1* allele, which resides within the 1BL/1RS translocation region (Ittu et al. 2000).

QTL mapping of the Romanian wheat variety Fundulea 201R, which also carries the 1RS segment, was detected to possess a major QTL associated with type II resistance on chromosome 1B within the 1BL/1RS region (Shen, Ittu, and Ohm 2003). However, the presence of the translocation has been proved to produce a poor performance during the commercial bread making process (Zhao et al. 2012). Thus, selection for FHB resistance within the 1BL/1RS region may give a potential quality trade-off.

It is important to highlight that avoiding trade-offs between disease resistance and agronomically important traits could be managed by the more accurate identification of

genomic regions associated with the trait of interest by fine-mapping interesting QTLs that have been already identified. The identification of QTLs of interest can be done by marker assisted selection.

1.6.2. Marker Assisted Selection – an approach to enhance breeding programmes

Marker-assisted selection (MAS) is a tool used by plant breeders to elucidate the genes or QTLs underlying control for FHB resistance and integrate them into elite material. MAS relies on DNA markers, which provide the means to rapidly screen segregating populations for resistance alleles (Landjeva, Korzun, and Börner 2007). Thus, markers tightly linked with QTL are used to improve the transfer of resistance genes from donor parent to recurrent parent, which is known as the backcross method of gene introduction (Shah et al. 2017).

MAS also allows gene pyramiding, which involves the introduction of genes for multiple types of resistance into an elite cultivar. In conjunction with traditional phenotypic selection, MAS may be the most efficient approach for increasing FHB resistance (Miedaner et al. 2009) by the production of durable disease resistant varieties of wheat.

For instance, in the study of Jia et al. 2018, QTL pyramiding was performed by crossing different near isogenic lines (NILs). Lines with different combinations of the four major-effect QTLs (*Fhb1*, *Fhb2*, *Fhb4* and *Fhb5*) were developed and additive effects were particularly significant for both type I and II resistances when all four QTLs were introduced.

Effective MAS for FHB resistance depends on knowledge of the genetic relationship of the germplasm to be improved with identified FHB resistance QTLs (Ittu et al. 2006). As more QTLs are being identified, novel and closely linked markers are being developed, which

may contribute to increasing the efficiency of MAS and the development of resistant cultivars against FHB.

1.7. Wheat germplasm and loci contributing to FHB resistance

Identification of resistance genes for stable and reliable resistance to FHB is challenging. In field studies, the environment causes a large influence on the disease incidence resulting in significant variation between trials and even between the replicates within a trial. In addition to resistance to FHB being polygenic, it has a moderate heritability, which makes gene identification more difficult (Goddard 2015). Nevertheless, molecular genetics has greatly speeded up FHB resistance research in wheat in the past years.

1.7.1. Major-effect FHB QTLs in wheat

Large numbers of QTLs providing quantitative resistance have been identified in diverse cereal germplasm. QTLs for FHB resistance have been found on all wheat chromosomes except in chromosome 7D (Buerstmayr, Ban, and Anderson 2009). Currently, more than 250 QTLs have been reported (Jia et al. 2018). Most of these QTLs have small effects and have not been verified yet. Additionally, the genes underlying most of these QTLs have not been identified and, thus, research is ongoing to clone FHB resistance genes.

The four major-effect QTLs identified in common wheat are *Fhb1* on chromosome 3B (Cuthbert, Somers, Thomas, Cloutier, and Brule-Babel 2006; Liu et al. 2006); *Fhb2* on chromosome 6B (Cuthbert, Somers, and Brule-Babel 2007); *Fhb4* on chromosome 4B (Xue et al. 2010); and *Fhb5* on chromosome 5A (Xue et al. 2011). Very recent findings have shown the successful cloning of *Fhb7* from the Triticeae E genome and the characterization of its molecular mechanisms (Wang et al. 2020).

Other important loci such as *Fhb3*, *Fhb6* and *Fb7AC* have revealed new insights into FHB resistance. *Fhb3* was discovered in an alien species, *Leymus racemosus*, and wheat-*Leymus* introgression lines. *Fhb3* was mapped to the distal region of the short arm of chromosome 7Lr#1 (Qi et al. 2008). *Fhb6* is a novel FHB resistance gene that was initially identified and mapped on the sub-terminal region of the short arm of chromosome $1E^{IS}$#1S of a perennial grass *Elymus tsukushiensis* (Cainong et al. 2015). When *Fhb6* was transferred to wheat an increase of FHB resistance was observed. Moreover, chromosome 7A was shown to harbour another novel QTL for FHB, designated as *Fhb7AC*, providing both type II and type III resistance (Jayatilake, Bai, and Dong 2011).

1.7.1.1. *Fhb1* locus

One of the major QTL is *Fhb1* and it is derived from the Chinese wheat cultivar Sumai 3, which is widely used as a source of resistance. *Fhb1* (*Qfhs.ndsu-3BS*) is associated with type II resistance (Cuthbert, Somers, Thomas, Cloutier, and Brule-Babel 2006), resistance to pathogen spread. Cuthbert et al. (2006) mapped this QTL to the distal segment of chromosome 3BS of spring wheat using Sumai 3 as a resistant parent. *Fhb1* was validated to be a major QTL in FHB resistance using the Chinese wheat line W14 (Chen et al. 2007) and it was further fine mapped to 261 Kbp region housing seven candidate genes (Liu et al. 2008).

Different mechanisms of this locus have been suggested to contribute to FHB resistance. Transcriptomic analysis in Sumai 3 showed that the phenylalanine ammonia-lyase pathway allows the production of defence-related metabolites (Golkari et al. 2007). Additionally, *Fhb1* locus in wheat landrace Wangshuibai (WSB) seems to contribute to FHB resistance by positively influencing the expression of jasmonic acid (JA) signalling (Xiao et al. 2013). *Fhb1* has been also implicated in harbouring a locus which controlled the conversion

of DON into non-toxic DON-3-O-glucoside (D3G) or a regulatory gene affecting detoxification capability (Lemmens et al. 2005).

A recent study confirms that *Fhb1* in WSB and Sumai 3 are placed within the same interval, delimited by *Xwgrb597-Xmag9404* markers (Jia et al. 2018). Only three SNPs differ between these two Chinese cultivars. These findings may imply that both Chinese cultivars possess the same source of resistance on chromosome 3B.

Very recent and independent studies have reported the cloning of *Fhb1*. Both studies used a map-based cloning approach to delimit *Fhb1* to a small interval on chromosome 3BS. Functional validation showed that *HRC*, a gene that encodes a putative histidine-rich calcium-binding protein, is the key determinant of *Fhb1*-mediated resistance to FHB. The protein localizes to the nucleus, but its exact function in conferring FHB resistance remains unknown (Li, Zhou, et al. 2019; Su et al. 2019). Although both studies agreed on the *HRC* gene responsible for *Fhb1* resistance, they reached very contrasting conclusions regarding the causative allele (Lagudah and Krattinger 2019). On the one hand, Su et al (2019) claimed that the *Fhb1*-mediated resistance is the result of a loss-of-function mutation. On the other hand, Li et al. (2019) claimed that the same deletion results in a gain of function.

In addition, a previous study also reported the cloning of *Fhb1* from Sumai 3 (Rawat et al. 2016). The gene identified was a chimeric lectin with agglutinin domains and a pore-forming toxin-like domain (*PFT*). The biochemical mechanism of *PFT*-mediated FHB resistance is still unknown, but it was suggested that *PFT* may participate in the recognition of fungus-specific carbohydrates and cause toxicity to the fungus. The *PFT* gene is found adjacent to the *HRC* gene. Plants have been shown to have operon-like gene clusters, in which closely linked but structurally unrelated genes are involved in the same biochemical processes (Boycheva et al. 2014). That is why Lagudah and Krattinger (2019) suggested that both *PFT* and *HRC* genes may quantitatively contribute toward FHB resistance. However,

further research is needed to clarify the contradictory results provided by the three papers claiming the cloning of *Fhb1*.

Moreover, work performed by Jia et al. (2018) contradicts findings of Rawat et al (2018) regarding the *PFT* cloning. Among other reasons, they demonstrated that the *PFT* gene does not show a role in DON detoxification since the truncation mutants of the gene did not exhibit any bleaching of wheat spikes. These findings are controversial since it is known that *Fhb1* loci is involved in type II resistance potentially by detoxifying DON. This may indicate then that the *PFT* is not playing a role in DON detoxification.

1.7.1.2. *Fhb2* locus

The QTL located on the short arm on chromosome 6B, also known as *Fhb2*, confers an increase in type II resistance to FHB. *Fhb2* is flanked by *GWM133* and *GWM644* (Cuthbert, Somers, and Brule-Babel 2007). Several genes involved in the detoxification of DON and cell wall reinforcement have been identified in this QTL region. Thus, these genes are postulated to be involved in decreasing the spread of the pathogen within the spike (Dhokane et al. 2016).

1.7.1.3. *Fhb4* locus

Qfhi.nau-4B is also a major QTL identified within WSB. To fine map this chromosomal region, a series of RILs were developed from Nanda2419 x WSB. *Qfhi.nau-4B* was confined between *Xhbg226* and *Xgwm149*, and named *Fhb4* (Xue et al. 2010). In this case, *Fhb4* provides type I resistance (Jia et al. 2018) by making the heads less susceptible to initial infection.

1.7.1.4. *Fhb5* locus

This QTL located on chromosome 5A is known to provide type I resistance to FHB. This QTL, *Qfhs.ifa-5A*, was identified in CM-82036, a line derived from Sumai 3 (Buerstmayr et al. 2003). *Fhb5* is also known to be a major QTL in WSB since genetic analysis of NILs derived from this resistant cultivar showed that it is inherited like a single dominant gene. However, in this cultivar it is referred to as *Qfhi.nau-5A* (Xue et al. 2011).

Recently, *Qfhs.ifa-5A* from Sumai 3 has been fine mapped into two separated QTLs: *Qfhs.ifa-5Ac*, located in the proximity of the centromere, and *Qfhs.ifa-5AS,* located on the distal half of the 5AS (Steiner et al 2019). The interval of *Fhb5* from WSB (*Qfhi.nau-5A*) has been refined very close to the centromere and, therefore, partially overlapping with *Qfhs.ifa-5Ac* (Jia et al. 2018). This means that *Fhb5* partially overlaps with *Qfhs.ifa-5Ac,* and that Sumai 3 and Wangshuibai may share a common type I resistance gene. However, due the pericentromeric position of this locus and the low recombination rate, fine-mapping of *Qfhs.ifa-5Ac* is still a challenge (Steiner et al. 2019).

A transcriptomic characterization study revealed that one of the mechanisms of resistance provided by *Fhb5* may be conferred by non-specific lipid transfer proteins (LTPs) (Schweiger, Steiner, et al. 2013). It is known that LTPs from wheat can affect the growth of fungal pathogens, including *F. graminearum* (Sun et al. 2008).

1.7.1.5. *Fhb7* locus

The FHB resistance gene *Fhb7* was cloned from *Thinopyrum elongatum*, a species used in wheat distant hybridization breeding. *Fhb7* encodes a glutathione S-transferase and confers broad resistance to *Fusarium* species by detoxifying trichothecenes via de-epoxidation (Wang et al. 2020). Indeed, *Fhb7* has been claimed by Wang et al (2020) to show a similar effect on FHB resistance as *Fhb1*. Introgression of the *Fhb7* locus in wheat conferred

resistance to both FHB and crown rot in diverse wheat backgrounds without yield penalty. This means that this novel source of resistance could be used in combating FHB and reducing DON contamination in wheat and other cereals crops through breeding.

Interestingly, *Fhb7* coding sequence has no obvious homology to any known sequence in the entire plant kingdom but shares 97 % sequence identity with a species of endophytic fungus (*Epichloë aotearoae*) known to infect temperate grasses. These findings provided Wang et al (2020) the evidence that *Fhb7* in the *Th. elongatum* genome might be derived from that fungus via horizontal gene transfer.

1.7.2. Resistant germplasm

Resistance to FHB in wheat has been identified mainly from three gene pools: winter wheats from Eastern Europe; spring wheats from China and Japan; and spring wheats from Brazil (Shen, Ittu, and Ohm 2003).

In the wheat germplasm, the Chinese Spring cultivar Sumai 3 has been one of the most widely used sources of genetic resistance to FHB (Buerstmayr et al. 2003). The Sumai 3 source of resistance has proven to be stable, heritable and consistent across environments (Rudd et al. 2001). This cultivar exhibits high-level FHB resistance and other important agronomic traits. For this reason, Sumai 3 has been used, along with its derivatives, in breeding programs globally (Niwa et al. 2014).

Jia et al (2018) summarized major findings on chromosome locations of wheat FHB resistance QTLs and showed that in Sumai 3 the QTLs responsible for FHB resistance are located on chromosome 3BS (*Fhb1*) and 6BS (*Fhb2*). However, it has been proven that Sumai 3 also provides FHB on chromosome 5AS (*Qfhs.ifa-5A*) (Anderson et al. 2001; Buerstmayr et al. 2002; Buerstmayr et al. 2003; Cuthbert, Somers, and Brule-Babel 2007).

WSB is also a Chinese cultivar and it is known to carry the highest number of validated FHB resistance QTLs, followed by the Brazilian cultivar Frontana (Jia et al. 2018). WSB cultivar harbours 11 QTLs within the 21 chromosomes, which shows the great importance of this Chinese wheat landrace for FHB resistance studies. Wuhan-1 cultivar is also a Chinese cultivar which has been reported to contain two QTLs: one is a major-effect QTL in chromosome 4B proximal to the centromere (*Fhb4*) and the other resides on 2DL (Somers, Fedak, and Savard 2003).

1.8. Wheat defensive mechanisms against FHB

FHB resistance mechanisms can also be categorized in two groups, morphological and physiological (Rudd et al. 2001). Regarding morphological mechanisms, they seem to help the plant during the initial infection by the pathogen. It has been shown that short genotypes tend to have higher disease severity relative to taller genotypes. This may be due to shorter distance between the wheat heads and inoculum sources in the soil. Additionally, awned genotypes can also show higher levels of infection compared to awnless genotypes possibly due to the increased surface resulting in more chances for deposition of fungal spores (Mesterházy 1995). Physiological mechanisms of resistance involve biochemical pathways which can produce fungal inhibiting compounds (Gilsinger et al. 2005).

When the interaction with a pathogen occurs, plants can induce defence genes that provide a variety of biochemical responses. These reactions can help to prevent the initial infection as well as slowing down the growth and spread of the pathogen. Transcriptomic analysis has been very useful in advancing our understanding of cereal- *F. graminearum* interactions by the identification of the general classes of genes expressed in the host in response to FHB infection (Kazan and Gardiner 2018).

1.8.1. Host response to pathogen infection

During infection, it has been shown in many transcriptomics studies that *F. graminearum* activates host defences similar to those induced in many other plant-microbe interactions. General classes of host genes altered in wheat spikes during infection are genes encoding: pathogenesis-related (PR) proteins; transporters; primary metabolism; lipid transfer proteins; metabolite transformation; ubiquitin-proteasome pathway; hormone biosynthesis and signalling phenylpropanoid biosynthesis; primary carbohydrate metabolism and transport; citric acid cycle; primary nitrogen metabolism; ABC transporters; lipases; UDP-glycosyltransferases (UGTs); lectins; regulators of oxidative burst (Kazan and Gardiner 2018).

A comparative transcriptomic analysis of genes expressed in infected spikes and in spikes without *F. graminearum* infection revealed 163 up-regulated genes which were classified into different functional categories. Almost 50 % of these genes encoded proteins for synthesis of antimicrobial compounds, modulation of the oxidative state, and resistance gene analogues (RGAs) or kinase proteins. Interestingly, some RGAs were found only in spikes under pathogen attack, which may imply unique roles in defence against *F. graminearum*. Additionally, RGAs and kinases are important regulators of communication between signalling pathways mediated by phytohormones in response to infection (Jia et al. 2018).

Pathogen infection activates phytohormone signalling pathways, which control many aspects of plant immunity (Schenk et al. 2000). Through proteomic and transcriptomic analysis, different pathways were identified to be activated after *F. graminearum* infection (Ding et al. 2011). The first phase, within 6 hours after infection (hai), was associated with the biotrophic stage of the pathogen in which salicylic acid (SA) signalling, phosphatidic acid (PA) signalling, and reactive oxygen species (ROS) production and scavenging were activated. These activities are associated with hyper-sensitive responses and plant cell death which may help reducing the growth of the pathogen. The second phase is observed to occur between

6 and 24 hai and is likely associated with the necrotrophic stage of *F. graminearum*. At this stage, activation of the JA and ethylene (ET) signalling pathways occur, in which the ET pathways help to facilitate the transition from SA to JA defence signalling.

1.8.2. Host responses to DON

The role of host responses to trichothecene accumulation is an important aspect of plant defence and resistance to fungal infection. DON is the most prevalent trichothecene mycotoxin found in *Fusarium*-infected grains. DON is a fungal virulence factor for *Fusarium*, facilitating disease spread within wheat heads (Gunupuru, Perochon, and Doohan 2017) and contributing to the symptoms of FHB disease.

DON can be detoxified by several studied enzymatic reactions which include deepoxidation, oxidation, epimerization and glycosylation (Tian et al. 2016). The active epoxide group in DON determines its toxicity for interrupting protein synthesis, but DON can be deepoxidated to deepoxy DON (DOM-1) which is less toxic. Different bacterial species have been identified using this mechanism (Gratz, Duncan, and Richardson 2013; Guan et al. 2009; Islam et al. 2012; Li, Zhu, et al. 2011; Young et al. 2007). Other detoxification processes found in bacteria that convert DON into low-toxic products, such as oxidation of DON to 3-keto DON and epimerization of DON to 3-epi DON, have been reported (McCormick 2013; He et al. 2015; Ikunaga et al. 2011; Sato et al. 2012).

1.8.2.1. DON detoxification by UGT genes

Plants have the capacity to detoxify mycotoxins by conjugation with sugars, which is known as glycosylation (Berthiller et al. 2007) and is catalysed by UDP-glucosyltransferase (UGT) enzymes. The first UGT was identified in *Arabidopsis thaliana* (*DOGT1*) and can detoxify

DON by converting 15-ADON to less toxic D3G, via the transfer of glucose to the 3-OH position (Poppenberger et al. 2003).

Several UGTs have been identified in cereal crops which increase DON resistance. The first monocot UGT gene identified was *HvUGT13248*, which was up regulated by *F. graminearum* infection and DON application in barley (Schweiger et al. 2010). Transgenic *Arabidopsis* expressing *HvUGT13248* exhibited increased resistance to DON and converted DON to D3G (Shin et al. 2012). Transgenic wheat expressing *HvUGT13248* exhibited significantly higher resistance to disease spread (type II) compared with non-transformed controls (Li et al. 2015). *Brachypodium distachyon* possesses two UGT homologs to *HvUGT13248*, which also conferred an increased resistance to DON by converting DON to D3G when expressed in yeast (Schweiger, Pasquet, et al. 2013).

Moreover, the *Brachypodium distachyon Bradi5g03300* UGT was shown to confer tolerance to DON through glycosylation of DON into D3G *in planta* and to be involved in quantitative resistance to FHB (Pasquet et al. 2016). Recently, it has been reported that transgenic wheat lines expressing *Bradi5g03300* UGT gene exhibited a higher level of type II resistance and a strong reduction of mycotoxin content (Gatti et al. 2019).

It has been also demonstrated that *HvUGT13248* is also capable of converting NIV into the non-toxic nivalenol-3-O-β-D-glucoside. Thus, this important UGT gene from barley provides resistance to both DON- and NIV-producing *Fusarium* (Li et al. 2017). Another UGT gene from barley variety 10W1 (*HvUGT-10W1*) located on chromosome 7H was also identified to confer disease resistance to FHB to some extent. Seeds of cultivar 10W1 also showed lower DON accumulation. However, its role in DON detoxification needs to be further studied (Xing et al. 2017).

1.8.2.2. UGT genes for FHB resistance in wheat

Only a few candidate UGT genes have been identified in wheat. These genes are *TaUGTB2*, *TaUGT1*, *TaUGT2*, *TaUGT3*, *TaUGT4*, *TaUGT5*, *TaUGT6*, and *TaUGT12887*, with the last five genes closely related to FHB resistance (He et al. 2020; Lin et al. 2008; Lulin et al. 2010; Ma et al. 2015; Schweiger, Pasquet, et al. 2013; Zhou et al. 2016).

The first DON-resistance related gene was cloned and characterized from the FHB resistant wheat variety Wangshuibai. The UGT gene *TaUGT3* showed high similarity in amino acid level with *DOGT1* gene in *Arabidopsis*, which can detoxify DON. However, whether *TaUGT3* has the same function in wheat it is unknown. Functional analysis by transformation of *A. thaliana* showed that *TaUGT3* could also improve DON tolerance levels at its seedling stage. Nevertheless, this needs to be further verified by transformation of *TaUGT3* into FHB susceptible wheat varieties (Lulin et al. 2010).

Additionally, *TaUGT4* was cloned from the FHB resistant cultivar Sumai 3 (Ma et al. 2015). *TaUGT5* may enhance DON tolerance, protecting the plant cell from pathogen infection and resulting in better maintenance of the cell structure, which slows down *Fusarium* proliferation in plant tissue (Zhao, Ma, et al. 2018). Moreover, transformation of *TaUGT6* into *Arabidopsis* increased root tolerance when grown on agar plates containing DON, and resistance to *F. graminearum* spread when *TaUGT6* was overexpressed in wheat (He et al. 2020).

Additionally, a wheat UGT gene *TaUGT12887* was identified in a transcriptomic study to be associated with two majors FHB resistance QTLs, *Fhb1* and *Qfhs.ifa-5A*. When expressed in a yeast strain, *TaUGT12887* was shown to provide DON tolerance, although much weaker than that previously observed with the characterized barley *HvUGT13248* (Schweiger, Steiner, et al. 2013).

Chapter 2

A QTL (*QFhb.WEK-5A*) on chromosome 5AL of WEK0609 increases Fusarium head blight type II resistance in wheat

2.1. Abstract

Quantitative trait locus (QTL) associated with both FHB type I and type II resistance have been previously reported on the 5A chromosome of bread wheat. The location of those QTLs on the 5A depends on the pedigree of the wheat cultivar. WEK0609 is an American winter wheat line that carries a QTL on the 5A and significantly showed reduced fungal colonization and DON content of the grain. The type of resistance as well as the location on the 5A chromosome was unknown.

A single chromosome substitution line named WEKH85A had been created by the introgression of the 5A chromosome of WEK0609 into a susceptible winter wheat (Hobbit *sib*) background. The purpose of this project was to assess the type of resistance provided by WEK0609 and to identify the physical location of the 5A QTL. A single marker analysis in a set of recombinant lines derived from the cross between the resistant line WEKH85A and the susceptible line Hobbit *sib* was performed.

This study confirmed that the source of FHB resistance provided by WEK0609 is type II. Data collected from three summer poly tunnel trials in Norwich (UK) confirmed the location of the 5A locus, named *QFhb.WEK-5A*, on the long arm of the 5A chromosome. *QFhb.WEK-5A* was fine-mapped to a region of 6.24 Mbp, containing 44 annotated genes in the Chinese Spring reference genome.

2.2. Introduction

WEK0609 is an American winter wheat line that has been previously used in QTL studies of FHB resistance. Previous field and controlled environment trials indicated that WEK0609 possesses both type I and type II resistance (Gosman et al. 2005). In that study, WEK0609 significantly reduced symptom development, yield loss, fungal colonization, and DON content of grain relative to the susceptible parent used in the study, Hobbit *sib*.

A QTL for FHB resistance was mapped by using a double haploid (DH) population from the cross WEK0609 x Hobbit *sib* (Gosman 2001). This QTL located on the 5A chromosome, reduced DON content, increased yield tolerance and reduced levels of fungal biomass. In addition, this QTL was also associated with reduced sensitivity to DON so appeared that WEK0609 may possess mechanisms underlying FHB resistance and DON tolerance on the 5A chromosome, but the location of the locus and its origins are unknown. Alongside the DH population, a single chromosome substitution line was created by the introgression of the 5A chromosome of WEK0609, which carries the FHB resistance, into a susceptible winter wheat (Hobbit *sib*) background.

Examination of the pedigree of WEK0609 revealed two potential donors of the 5A resistance: Sumai 3 and Fundulea F201R. Sumai 3 harbours *Qfhs.ifa-5A* in the short arm of 5A, near the centromere, and confers type I resistance (Somers, Fedak, and Savard 2003). Fundulea F201R also harbours the 5A locus in the short arm but confers type II resistance (Shen, Ittu, and Ohm 2003). The source of resistance of WEK0609 on the 5A chromosome may, thus, be provided by the Chinese line Sumai 3, by the Romanian line Fundulea F201R, or it may be a new source of FHB resistance.

2.2.1. Chapter aims

The single chromosome substitution line WEKH85A carries the 5A chromosome of WEK0609, carrying FHB resistance in a Hobbit *sib* background. The line WEKH85A was crossed to Hobbit *sib* and a bi-parental population was generated using a single seed descendant.

The objectives for this work were:

1) Characterisation of the 5A QTL over three summer trials (2018-2020) using recombinant inbred lines (RILs).
2) Fine-mapping of the 5A locus using a single marker analysis based on the physical position of single nucleotide polymorphisms (SNPs) in the Chinese Spring reference genome (IWGSC RefSeq v1.1).
3) Establishing the possible origin of the 5A QTL: whether the 5A source of resistance is type I from Sumai 3 or type II from Fundulea F201R or is a novel source.

2.3. Material and Methods

2.3.1. Plant material

The seed used in this project originated from previous work performed on the 5A chromosome, after which seed were bulked for use in experiments.

2.3.1.1. Parental lines

Hobbit *sib* is a semi-dwarf winter wheat cultivar, which was selected for these studies because it has been reported to have no appreciable resistance to FHB. Hobbit *sib* is closely related to the winter wheat cultivar Hobbit, which was commercially grown in the UK during the 1970s (Buerstmayr et al. 1999).

The original source of FHB resistance was present in the line WEK0609. Chromosome substitution lines were generated in a susceptible background through use of a monosomic series in the variety Hobbit *sib* (A.J. Worland and E. Sayers, unpublished). The line WEKH85A is a single chromosome substitution line genetically similar to Hobbit *sib* except for chromosome 5A, which comes from the resistant cultivar WEK0609.

2.3.1.2. Recombinant-inbred lines

One hundred and seventy-one RILs derived from the cross between Hobbit *sib* and WEKH85A (F_6) were generated by Andrew Steed (unpublished). These RILs were used for the 5A QTL FHB characterisation and mapping in the Summer of 2018. For subsequent summer trials, only specific RILs containing the 5A locus were selected to be tested for FHB resistance.

2.3.1.3. Plant location and growth conditions

Seed of the selected RILs were sown in 96-cell-trays of John Innes F2 Starter. Plants were placed in a controlled environment room (CER) for a pre-vernalisation period of two

weeks (day Tª of 20 ºC and night Tª of 16 ºC; with 70 % humidity); in a cereals-CER for a vernalisation period of eight weeks (day and night Tª of 6 ºC; with 70 % of humidity); in a polytunnel for one/two weeks of cold and, finally, plants were transplanted into John Innes Cereals Mix in 1L-pots (Supplementary data Table S1), with one plant per pot. Plants were located at the John Innes Centre, Norwich (UK) and were staked and tied as appropriate.

2.3.1.4. Polytunnel experiment design

In Summer 2018, plants were arranged in a randomised incomplete block design. The trial consisted of three blocks with each block containing 8 plots of thirty-two 1L-pots in each. As the number of RILs to be tested was high, only four replicates per line were selected and were equally distributed throughout the polytunnel. In following years, plants were arranged in a polytunnel at the JIC in an Alpha Lattice design within different blocks and plots per block. Depending on the trial and number of plants selected, different numbers of blocks were used.

In the 2019 trial, plants were arranged in eight blocks (N1-4, S1-4) containing three plots each (Supplementary data Figure S1). A small number of RILs were selected with a total of 24 replicates per line.

In the 2020 trial, experimental design was much smaller since it was performed to confirm the 5A locus. Plants were arranged in twelve blocks (N1-6, S1-6) containing two plots each (Supplementary data Figure S2). A higher number of RILs were selected with total of six replicates per line. Randomization was generated using the Design Computing Gendex DOE Toolkit 8.0. (Module IBD, http://designcomputing.net/).

2.3.2. Evaluation of type II FHB resistance

2.3.2.1. Fungal point-inoculation of wheat spikes

Parents (WEKH85A and Hobbit *sib*) and RILs were evaluated for type II FHB resistance (resistance to fungal spread in the spikes) by using the point-inoculation method. Production

of inoculum was carried out as described previously in Gosman et al. (2005) by using highly virulent DON-producing strains of *F. culmorum*.

Conidia of *F. culmorum* isolates Fc2037 and Fc2076 combined were produced on sterile barley kernels and harvested by Andrew Steed. To enhance the uniformity of inoculum, aliquots were prepared and stored at -20°C and were defrosted on the inoculation day. Prior to inoculation, heads that had reached mid-anthesis were tagged and numbered for identification and tracking. Plants were inoculated with fungal conidial suspension (0.5 x 10^7 spores ml^{-1}) injected in the middle of the spike at mid-anthesis. A minimum of two heads per plant were inoculated.

2.3.2.2. Scoring FHB type II symptoms in wheat spikes

FHB disease symptoms were scored after different days post-infection (dpi), depending upon the rate of movement of the pathogen in the spike or spread of bleaching symptoms. Scoring of symptoms in Summer 2018 was done at 10, 14 and 18 dpi. Scoring in subsequent trials was done across two consecutive days due to the large number of plants, depending on the flowering time for each set of plants, and data was analysed together as 'Score 1', 'Score 2', and so on. Data for Summer 2019 was collected at 11-12 dpi (Score 1), at 14-15 dpi (Score 2), at 17-18 dpi (Score 3), at 21 dpi (Score 4) and at 23-24 dpi (Score 5); and for Summer 2020 at 12-13 dpi (Score 1), at 14-15 dpi (Score 2), at 16-17 dpi (Score 3), at 18-19 dpi (Score 4) and at 21-22 dpi (Score 5).

FHB disease symptoms were recorded by counting the number of infected or bleached spikelets below and above the point of infection (PI), respectively. Complete bleached spikes above the PI were given a '10' score, the approximate number of total spikelets above the PI. Pre-bleached spikes were given a '5' score. Resistant spikes showed a reduced spread of FHB infection and un-inoculated spikelets remained green (Figure 2.1.). While spikes in Figure 2.1.A-C were inoculated with *F. culmorum* and disease spread was

observed, since there was bleaching, spike in Figure 2.1.D was inoculated in the middle, but it was not infected because disease was not established. That is the reason why this spike remained green.

Figure 2.1. *Scoring FHB disease symptoms in wheat spikes. FHB symptoms were recorded by counting the number of infected or bleached spikelets above and under the PI in the middle of the spike (red arrow): A) complete bleached spike = 10 score; B) pre-bleached spike = 5 score; C) three bleached spikelets = 3 score; D) zero bleached spikelets = 0 score.*

2.3.3. Genotyping

2.3.3.1. Leaf sampling and DNA extraction

Leaf material from 1-week-old seedling was sampled for each plant and placed into 1.2 ml deep 96-well plates. Plates containing leaf samples were freeze-dried overnight. Then, a single tungsten bead was added to each well and samples were grounded into a fine powder using a Spex GenoGrinder 2010 at 1500 rpm for 2 min, checking samples every

minute. Plates were then centrifuge at 4000 rpm for 10 min to settle the ground leaf samples and prevent sample loss.

Genomic DNA was extracted from freeze-dried leaf tissue using the extraction protocol for 96-well plates, adapted from (Pallotta et al. 2003), with minor modifications. DNA was quantified using the spectrophotometer NanoDrop 2000 (Thermo Scientific) and diluted to 50 ng μl^{-1}.

2.3.3.2. Developing and using KASP markers

SNP genotyping information for the 5A chromosome was obtained from different sources: Cereals DB web site (www.cerealsdb.uk.net), RNA-Seq data (performed in Chapter 3), in-house 18K SNP array and exome capture data provided by the iCase partner, Limagrain S.A.

Based on the sequence of identified SNPs, two allele-specific forward primers and one common reverse primer were designed for each kompetitive allele-specific PCR (KASP) assay. KASP primers, designed using Chinese Spring RefSeq 1.0., were developed and downloaded from PolyMarker (www.polymarker.tgac.ac.uk) (Ramirez-Gonzalez, Uauy, and Caccamo 2015).

KASP markers were generated by adding the corresponding tail sequences of FAM (GAAGGTGACCAAGTTCATGCT) and VIC (GAAGGTCGGAGTCAACGGATT) dyes at the 5' end of the specific primers. Sequence information of KASP markers used to genotype the 5A QTL population over the trials is found in Table 2.1. KASPs markers were produced by Sigma-Aldrich (www.sigmaaldrich.com).

KASP assays were performed in 384-well PCR plates in a 4.07 µl volume with 2 µl KASP 2x reaction mix, 0.07 µl assay mix (12 µl each allele-specific forward primer (100 µM), 30 µl reverse primer (100 µM), and 46 µl dH_2O) and 2 µl genomic DNA (50 ng μl^{-1}). The PCR

conditions were as follows: 94°C for 15 min; 35 cycles of 94°C for 20 s, and 57°C for 60 s. Fluorescence detection of the PCR products was performed with PHERAstar (BMG LABTECH) and were amplified for an additional 5 cycles of 94°C 20 s, 57°C 60 s, when necessary. KLUSTERCALLER software (LGC Genomics) was used for analysing results.

Table 2.1. *KASP markers used for the genotyping of the 5A chromosome. Associated RefSeqv1.1 gene models (where available) and physical position on RefSeqv1.0 assembly are shown. Fam, Vic and common primers (seq from 5' to 3') are shown for each KASP. Source of markers used for the analysis is described.*

Marker	SNP position (RefSeqv1.0)	Reference allele	Alternative allele	Associated gene (RefSeqv1.1)	Fam (seq 5' to 3')	Vic (seq 5' to 3')	Common (seq 5' to 3')	Source
BS00021708	30,411,062	G	A	intergenic	GCAACACCACAACTGCGCTCA	GCAACACCACAACTGCGCTCG	CCGTGGTGTTGCAGAGGACGAT	CerealsDB
BA00374543	32,883,071	C	G	intergenic	CAGCATACGGCTTCTTGTCACG	CAGCATACGGCTTCTTGTCACC	CCCATGACCTCGGCAAAATGGATTT	CerealsDB
S1	118,661,064	C	T	*TraesCS5A02G088100*	-	-	-	18K SNP array
S2	213,403,509	G	A	intergenic	-	-	-	18K SNP array
S3	300,205,197	A	C	intergenic	-	-	-	18K SNP array
BA00219976	317,234,298	C	T	*TraesCS5A02G143000*	GCCTTTGCAAACTACTACATGC	GCCTTTGCAAACTACTACATGT	TGAATTCCAGGCTATTCACAGG	CerealsDB
S4	321,894,801	G	A	*TraesCS5A02G145600*	AGAGTGGAGAGGAAGACCGG	AGAGTGGAGAGGAAGACCGA	TCACCGCGGCAATGGCTA	RNA-Seq
S5	381,755,729	G	A	*TraesCS5A02G182000*	GCCTCCCATCCTTTGACGAG	GCCTCCCATCCTTTGACGAA	GTGCTATCTTGGACATCTTGTCT	RNA-Seq
S6	382,105,017	C	A	*TraesCS5A02G182400*	TGTAATTTGTTTGCTGCAGAGAC	TGTAATTTGTTTGCTGCAGAGAA	CTTAGCAGATGGTTCTTTAGTATGC	RNA-Seq
S7	382,286,059	G	A	intergenic	CACTTGGAGAACCATGAGTCTTG	CACTTGGAGAACCATGAGTCTTA	TCTCGAGACGATGGAGGTCT	RNA-Seq
S8	383,192,473	C	T	*TraesCS5A02G183500*	GCGTTATGCACCGATCAATAC	GCGTTATGCACCGATCAATAT	TGCAGTGTACTTTACCAGAGTGT	RNA-Seq
S9	383,465,301	A	G	*TraesCS5A02G183800*	CTGTCCAATCTTCCGTGGGA	CTGTCCAATCTTCCGTGGGG	ACCTGAGCAACAATTCCCTCTC	exome capture
S10	384,014,520	G	A	intergenic	GCCAGCCATCTCACTTCTCTG	GCCAGCCATCTCACTTCTCTA	GTCCTATTTATGGTAACTTGTTGCT	exome capture
S11	389,637,157	G	C	*TraesCS5A02G187800*	CGACGGGTTCTTGAATCTCTG	CGACGGGTTCTTGAATCTCTC	CCTCACATTGTCGCTCTACG	exome capture
S12	390,237,437	G	A	*intergenic*	CAGTTGATAAGTTGACCACATTCA	CAGTTGATAAGTTGACCACATTCG	CAAACATACTGGGTCTCGGAAG	exome capture
S13	394,752,864	G	A	intergenic	TCGCAGTATGATTTAGTTTCGAGG	TCGCAGTATGATTTAGTTTCGAGA	TCGCGTGCAAGTTCTATGACT	exome capture
S14	394,753,217	C	T	*TraesCS5A02G190200*	CCAAACACAAAACAGCCTTGC	CCAAACACAAAACAGCCTTGT	CGTCGGCAAAGAGTCTGAAAC	exome capture
BA00228977	395,057,684	C	T	*TraesCS5A02G190600*	CGGTGTCCATGACAGACCG	CGGTGTCCATGACAGACCA	GGTGATGCAGCTGAGTTAGT	CerealsDB
S15	395,832,889	C	T	*TraesCS5A02G191500*	ACTGCCTCTCCTTTCAGCCC	ACTGCCTCTCCTTTCAGCCT	CCATTTCAGGTCTTGGCTGGTAT	RNA-Seq
S16	395,833,610	C	T	*TraesCS5A02G191500*	TACTGCCTCTCCTTTCAGCCC	TACTGCCTCTCCTTTCAGCCT	CCATTTCAGGTCTTGGCTGGTAT	exome capture
S17	395,834,363	G	A	*TraesCS5A02G191500*	GCGACCAAGGGTATGAGGAG	GCGACCAAGGGTATGAGGAA	TTAGGTGATATGTGGACAGATTTTG	exome capture
S18	395,886,197	A	G	intergenic	AACCTAAATCATCGCCACCA	AACCTAAATCATCGCCACCG	CCTCGCTGAGTTCGCTACC	exome capture
S19	398,269,789	T	C	*TraesCS5A02G194700*	CAGGACATACGTAGAACAGGT	CAGGACATACGTAGAACAGGC	GTTCGTGAACCCACCCAC	exome capture

Table 2.1. Continued. *KASP markers used for the genotyping of the 5A chromosome. Associated RefSeqv1.1 gene models (where available) and physical position on RefSeqv1.0 assembly are shown. Fam, Vic and common primers (seq from 5' to 3') are shown for each KASP. Source of markers used for the analysis is described.*

Marker	SNP position (RefSeqv1.0)	Reference allele	Alternative allele	Associated gene (RefSeqv1.1)	Fam (seq 5' to 3')	Vic (seq 5' to 3')	Common (seq 5' to 3')	Source
S20	400,786,018	C	T	*TraesCS5A02G197000*	CTTGTGCATTTAACTGGCAAAATC	CTTGTGCATTTAACTGGCAAAATT	AAGCTGCCCAAGGTGTACTT	exome capture
S21	401,139,323	A	T	*TraesCS5A02G197200*	GGATGTCGGAGAAGTGTAGAAAAT	GGATGTCGGAGAAGTGTAGAAAAA	ACGTACAAAAGTTCATTCGAGTT	exome capture
S22	404,438,674	G	A	intergenic	-	-	-	18K SNP array
S23	405,034,925	C	T	intergenic	-	-	-	18K SNP array
S24	407,955,815	C	T	intergenic	-	-	-	18K SNP array
BA00061052	408,930,186	T	C	*TraesCS5A02G202200*	GACATCATCCCGCGAATACC	GACATCATCCCGCGAATACT	GAATTTGTTCTCTAGAGGATGCG	CerealsDB
S25	409,319,878	T	C	*TraesCS5A02G202300*	CCTACAGTGCCCCCATCTTT	CCTACAGTGCCCCCATCTTC	CCAAGAGCAACAATCGCTTT	RNA-Seq
S26	410,499,218	A	G	*TraesCS5A02G202700*	GCAAGGAGACTCCGCCGA	GCAAGGAGACTCCGCCGG	GGGACTATATTTCCTGGAGCTC	RNA-Seq
S27	410,803,424	C	T	*TraesCS5A02G203000*	-	-	-	18K SNP array
BA00919063	412,226,288	C	T	intergenic	CTGCTCTACTCATCCTCGCTG	AATTCTGCTCTACTCATCCTCGCTA	ACAGAGGTGATTCTGATCTAAACGAACTA	CerealsDB
S28	413,043,503	C	A	*TraesCS5A02G203500*	CATTTTGCTGTAGGCTGGAAC	CATTTTGCTGTAGGCTGGAAA	CTTCCAGCTGAAGTCTGTTGA	RNA-Seq
S29	417,051,540	T	G	*TraesCS5A02G206600*	GTTAAAGCCCCTCGCCGT	GTTAAAGCCCCTCGCCGG	CAGGAGACGATCTTGCCC	RNA-Seq
S30	417,897,180	T	C	*TraesCS5A02G207100*	-	-	-	18K SNP array
S31	419,204,071	C	T	intergenic	-	-	-	18K SNP array
BA00710203	419,363,482	A	G	*TraesCS5A02G207400*	CGCAGGAACTTCGTTTGTGTT	CGCAGGAACTTCGTTTGTGTC	GAACAGATGGTATCTCTAGGCC	CerealsDB
S32	421,825,888	A	C	*TraesCS5A02G208200*	-	-	-	18K SNP array
S33	427,896,043	C	T	intergenic	-	-	-	18K SNP array
S34	429,751,662	C	T	intergenic	-	-	-	18K SNP array
S35	430,050,339	A	G	intergenic	-	-	-	18K SNP array
BA00160245	430,246,218	C	T	*TraesCS5A02G215000*	AGTATCGGGGCAGCTTCTA	AGTATCGGGGCAGCTTCTG	TCGGCTAATATCAGGGGCTG	CerealsDB
S36	430,604,205	G	A	intergenic	-	-	-	18K SNP array
S37	433,030,768	T	C	intergenic	-	-	-	18K SNP array
BA00617086	438,266,961	G	A	*TraesCS5A02G222100*	CATTCCTCTGTAGAGCTGCTATG	CCCTATGCACAATGTCCAGAGC	CGGCATCAACTGCTGATCGCATTAA	CerealsDB

Table 2.1. Continued. *KASP markers used for the genotyping of the 5A chromosome. Associated RefSeqv1.1 gene models (where available) and physical position on RefSeqv1.0 assembly are shown. Fam, Vic and common primers (seq from 5' to 3') are shown for each KASP. Source of markers used for the analysis is described.*

Marker	SNP position (RefSeqv1.0)	Reference allele	Alternative allele	Associated gene (RefSeqv1.1)	Fam (seq 5' to 3')	Vic (seq 5' to 3')	Common (seq 5' to 3')	Source
S38	438,267,579	G	A	*TraesCS5A02G222100*	-	-	-	18K SNP array
BA00156148	438,471,823	T	C	*TraesCS5A02G222500*	CCCTATGCACAATGTCCAGAGT	CATTCCTCTGTAGAGCTGCTATA	AGGTATCAATGCTGACCGAGTA	CerealsDB
BA00569895	439,186,565	A	G	*TraesCS5A02G223300*	GATATTGCGATAGTGAACAGTCTCCA	ATATTGCGATAGTGAACAGTCTCCG	TACTGCCTTTGCATGATGCTCCCAT	CerealsDB
BA00639663	552,162,031	G	A	*TraesCS5A02G348600*	CGCAACGCTGGCGTGCCTTT	GCAACGCTGGCGTGCCTTC	GCTGCCAATCTGCCCGTCGAT	CerealsDB

2.3.4. Statistical analysis

Disease data was analysed using a linear mixed model (LMM) in the statistical software R 3.5.3 (https://cran.r-project.org/bin/windows/base/). Genstat software (v18.1) was also used to confirm results (https://www.vsni.co.uk/software/genstat/). The LMM analysis was used to assess the variation attributable to block (random), line (random), inoculation date (fixed) and marker (fixed). For the trial performed in 2018, inoculation date was not added into the analysis. The analysis was performed for each marker located on the 5A chromosome. Visual analysis of residues was undertaken for all analyses to assess normality of data. All data was log10 transformed to achieve normality of residuals and to ensure residuals were independent of fitted values. Predicted mean and standard error values were calculated for those lines included in the analysis.

2.4. Results

2.4.1. Characterisation of the 5A QTL under polytunnel conditions

FHB disease trials to assess type II resistance were performed over three Summers (2018-2020) under polytunnel conditions at the JIC (Norwich, UK). FHB type II disease symptoms were scored when disease symptoms (bleaching) were observed/spread within wheat spikes as in Figure 2.1.A-D. Scoring of symptoms above and below the PI of wheat spikes was done every 2-4 dpi.

The genomic information was obtained by screening each line with polymorphic markers identified between the parental lines. This allows the determination of which parental allele is present in each line for each marker on the 5A locus. SNPs were used to developed KASP markers. Different numbers of markers were used for each year's analysis depending on the availability and discovery of new SNPs along the 5A locus (Table 2.1.). To begin with, markers from Cereals BD were used, followed by markers developed by the iCase collaborators using the 18K SNP array and, finally, by KASPs obtained from the RNA-Seq data (see Chapter 3) and Exome capture data (Limagrain S.A., personal communication).

A LMM analysis was then performed for each individual marker located on the 5A chromosome using the phenotypic data obtained from above and below the PI in each summer season and the genotypic data of the parental lines and RILs.

2.4.1.1. Summer 2018

Graphical genotype of parental lines and RILs used in Summer 2018 is provided in Supplementary data (Figure S5). Line names are specified on each raw and markers used are specified on each column. Yellow is the allele provided by WEKH85A and blue the one by Hobbit *sib*. Green is the heterozygous allele. White is missing value.

Variation of FHB was characterized using 171 RILs from the cross between Hobbit *sib* and WEKH85A (F_6) in the summer 2018 trial. Figure 2.2. represents how the distribution of symptoms changed over time using the phenotypic data collected at 10, 14 and 18 dpi. The parent Hobbit *sib* was more susceptible than parent WEKH85A when focusing on the spread of the pathogen above the PI. The resistance of WEKH85A to FHB disease spread above the PI was maintained over time. However, both parental lines had similar number of infected spikelets below the PI.

The 171 RILs showed significant variation for disease spread, being 0 as non-infected/bleached spikelets and 10 as totally infected/bleached spikelets (Figure 2.2.). At 10 dpi, number of infected spikelets below and above the PI ranged from 0 to 5, indicating that this was an early time point to observe differences in FHB disease severity. Data collected at 18 dpi showed the opposite, with the number of infected spikelets below and above the PI ranging from 5 to 10. Thus, indicating that in this case, it was a late time point to observe differences.

The distribution of FHB disease above the PI at 14 dpi showed that many RILs were severely infected by the pathogen (ranging from 5-10), but several lines were still as resistant as parental line WEKH85A, which had a mean of 5.3 infected spikelets (Supplementary data Figure S5). The distribution below the PI showed that just a few RILs were severely infected by the pathogen.

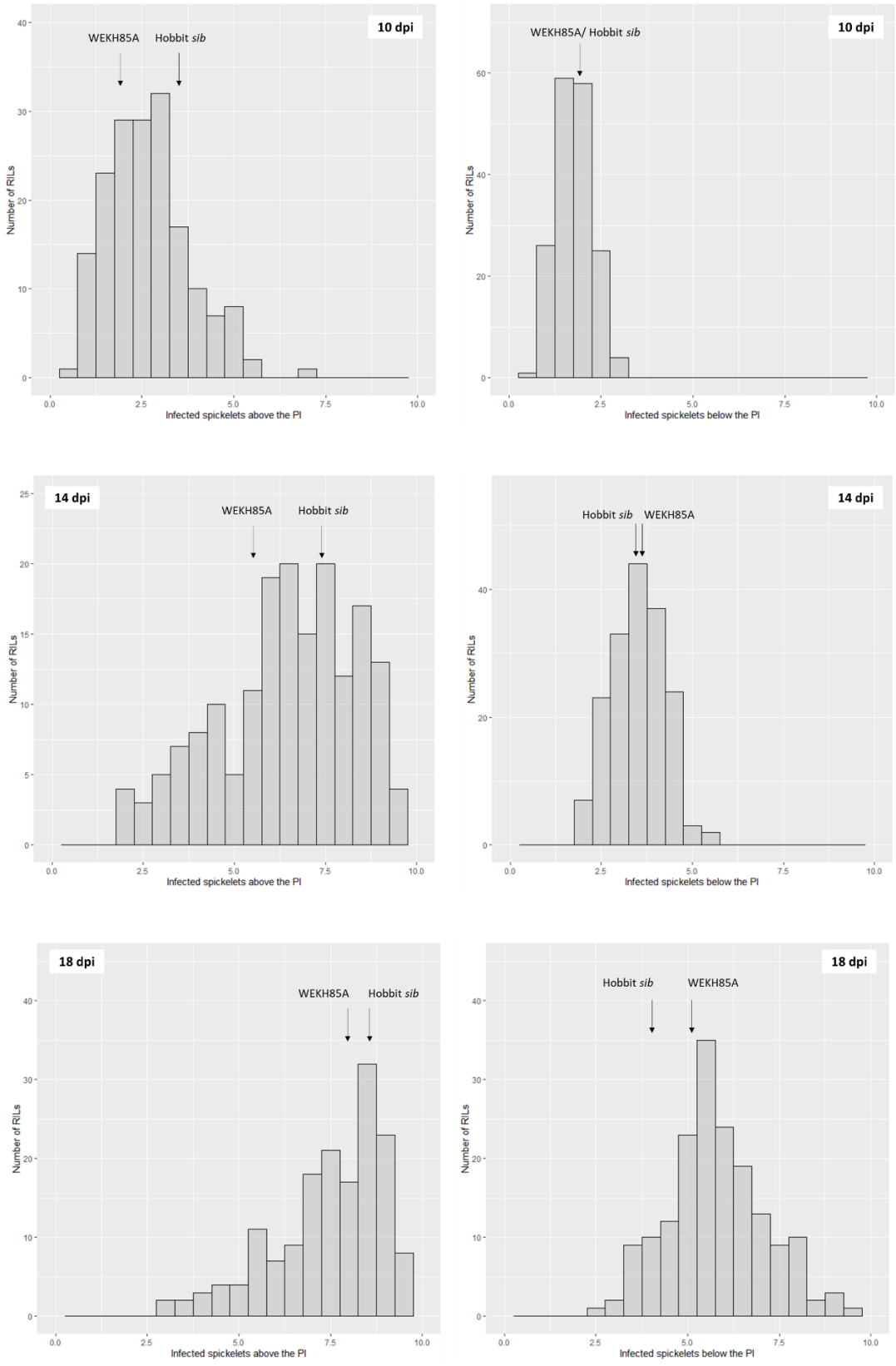

Figure 2.2. *Frequency distribution of FHB disease above (left) and below (right) the PI of 171 RILs from the cross between Hobbit sib (susceptible parent) and WEKH85A (resistant parent) at three dates post-infection: 10 dpi (top), 14 dpi (middle) and 18 dpi (bottom). Position of parental lines are represented in each histogram with black arrows.*

P-value data obtained from the LMM analysis performed for each individual marker located on the 5A chromosome is shown in Table 2.2. and Table 2.3., for scoring data above and below the PI, respectively. Source of markers used for the analysis are described, mainly obtained from Cereals DB (www.cerealsdb.uk.net). Associated RefSeqv1.1 gene models (where available) and physical position on RefSeqv1.0 assembly are shown.

LMM analysis of Summer 2018 data revealed that three markers were associated with FHB type II resistance ($P < 0.05$) at 14 dpi on the long arm of chromosome 5A (Table 2.2. and Table 2.3.). These markers are *BA00061052*, *BA00919063* and *BA00710203*, which are located at 408.93, 412.23 and 419.36 Mbp, respectively. The analysis may not have provided a stronger association with the disease because the scoring performed on that Summer was severe. Indeed, the difference in the number of infected spikelets between 'Hs' and 'WEK' alleles is only half of a spikelet (and), with the parent WEKH85A conferring the resistant allele to *Fusarium* spread on the long arm of the 5A chromosome (Table S2 and Table S3).

Table 2.2. *P-value data obtained from a LMM analysis performed for each individual marker located on the 5A chromosome. Source of markers used for the analysis are described. Associated RefSeqv1.1 gene models (where available) and physical position on RefSeqv1.0 assembly are shown. Symptoms above the point of infection were assessed at 10 dpi, at 14 dpi, and at 18 dpi in Summer 2018. Data was transformed using a log10 transformation. P-value data of markers associated with FHB type II resistance are highlighted in light green (P < 0.05).*

Source	CerealsDB	CerealsDB	CerealsDB	CerealsDB	CerealsDB	CerealsDB	CerealsDB	CerealsDB
RefSeqv1.1 Gene model	intergenic	intergenic	*TraesCS5A02G143000*	*TraesCS5A02G190600*	*TraesCS5A02G202200*	intergenic	*TraesCS5A02G207400*	*TraesCS5A02G215000*
RefSeqv1.0 (bp)	30,411,062	32,883,071	317,234,298	395,057,684	408,930,186	412,226,288	419,363,482	430,246,218
Marker	***BS00021708***	***BA00374543***	***BA00219976***	***BA00228977***	***BA00061052***	***BA00919063***	***BA00710203***	***BA00160245***
10 dpi	0.857	0.937	0.685	0.560	0.414	0.275	0.322	0.602
14 dpi	0.428	0.747	0.860	0.252	0.049	0.024	0.049	0.221
18 dpi	0.490	0.571	0.274	0.550	0.109	0.069	0.050	0.301

Source	CerealsDB	CerealsDB	CerealsDB	CerealsDB
RefSeqv1.1 Gene model	*TraesCS5A02G222100*	*TraesCS5A02G222500*	*TraesCS5A02G223300*	*TraesCS5A02G348600*
RefSeqv1.0 (bp)	438,266,961	438,471,823	439,186,565	552,162,031
Marker	***BA00617086***	***BA00156148***	***BA00569895***	***BA00639663***
10 dpi	0.660	0.562	0.646	0.568
14 dpi	0.350	0.361	0.519	0.833
18 dpi	0.628	0.622	0.724	0.690

Table 2.3. *P-value data obtained from a LMM analysis performed for each individual marker located on the 5A chromosome. Source of markers used for the analysis are described. Associated RefSeqv1.1 gene models (where available) and physical position on RefSeqv1.0 assembly are shown. Symptoms below the point of infection were assessed at 10 dpi, at 14 dpi, and at 18 dpi in Summer 2018. Data was transformed using a log10 transformation. P-value data of markers associated with FHB type II resistance are highlighted in light green (P < 0.05).*

Source	CerealsDB	CerealsDB	CerealsDB	CerealsDB	CerealsDB	CerealsDB	CerealsDB	CerealsDB
RefSeqv1.1 Gene model	intergenic	intergenic	*TraesCS5A02G143000*	*TraesCS5A02G190600*	*TraesCS5A02G202200*	intergenic	*TraesCS5A02G207400*	*TraesCS5A02G215000*
RefSeqv1.0 (bp)	30,411,062	32,883,071	317,234,298	395,057,684	408,930,186	412,226,288	419,363,482	430,246,218
Marker	***BS00021708***	***BA00374543***	***BA00219976***	***BA00228977***	***BA00061052***	***BA00919063***	***BA00710203***	***BA00160245***
10 dpi	0.915	0.967	0.641	0.271	0.114	0.060	0.051	0.263
14 dpi	0.693	0.796	0.389	0.199	0.042	0.033	0.026	0.192
18 dpi	0.457	0.515	0.756	0.561	0.186	0.206	0.195	0.611

Source	CerealsDB	CerealsDB	CerealsDB	CerealsDB
RefSeqv1.1 Gene model	*TraesCS5A02G222100*	*TraesCS5A02G222500*	*TraesCS5A02G223300*	*TraesCS5A02G348600*
RefSeqv1.0 (bp)	438,266,961	438,471,823	439,186,565	552,162,031
Marker	***BA00617086***	***BA00156148***	***BA00569895***	***BA00639663***
10 dpi	0.420	0.403	0.458	0.884
14 dpi	0.319	0.403	0.284	0.544
18 dpi	0.515	0.535	0.431	0.847

The genomic region on the 5AL locus most associated with FHB resistance in Summer 2018 was of 35.19 Mbp, between markers *BA00228977* (at 395.06 Mbp) and *BA00160245* (at 430.25 Mbp).

Heterozygous lines not being tested during this trial were bulked and genotyped to identify new recombinant lines containing the 5AL locus. From this bulking material, four lines (RIL 20, 107, 152 and 230), which were fixed and had interesting recombination points along the 5A locus, were selected for the following year's trial. Moreover, lines RIL 97, 103 and 323 tested in Summer 2018 were again selected because they were also promising recombinants. A total amount of seven recombinants and the parental lines were selected to be tested in Summer 2019 (Table 2.4.).

Table 2.4. *Graphical genotype of parental lines and recombinant inbred lines selected to be tested in Summer 2019. The 5A QTL is located between markers BA00228977 (at 395.06 Mbp) and BA00160245 (at 430.25 Mbp). Source of markers is described. Associated RefSeqv1.1 gene models (where available) and physical position on RefSeqv1.0 assembly are shown. Predicted means and standard errors (S.E.) of FHB scoring data above the point of infection (PI) of lines tested in Summer 2018 is also showed at 14 dpi. 'Hs' is the allele provided by parental line Hobbit sib; 'WEK' is the allele provided by parental line WEKH85A.*

	Source	CerealsDB	CerealsDB	CerealsDB	CerealsDB	CerealsDB	**14 dpi**	
	RefSeqv1.1 Gene model	*TraesCS5A02G190600*	*TraesCS5A02G202200*	intergenic	*TraesCS5A02G207400*	*TraesCS5A02G215000*		
	RefSeqv1.0 (bp)	395,057,684	408,930,186	412,226,288	419,363,482	430,246,218		
Line ID	**Type of line**	***BA00228977***	***BA00061052***	***BA00919063***	***BA00710203***	***BA00160245***	**Mean**	**S.E.**
Hobbit *sib*	Parental (Hs)	Hs	Hs	Hs	Hs	Hs	7.44	1.29
WEKH85A	Parental (WEK)	WEK	WEK	WEK	WEK	WEK	5.30	1.92
RIL 20	Recombinant	WEK	WEK	WEK	WEK	WEK	-	-
RIL 97	Recombinant	WEK	WEK	WEK	Hs	Hs	2.38	1.14
RIL 103	Recombinant	Hs	WEK	WEK	WEK	WEK	3.17	1.53
RIL 107	Recombinant	Hs	Hs	Hs	WEK	WEK	-	-
RIL 152	Recombinant	Hs	WEK	WEK	WEK	WEK	-	-
RIL 230	Recombinant	Hs	WEK	WEK	WEK	WEK	-	-
RIL 323	Recombinant	WEK	Hs	Hs	Hs	Hs	8.50	1.03

2.4.1.2. Summer 2019

Graphical genotype of parental lines and RILs used in Summer 2019 is provided in Figure 2.3. For this trial, a smaller set of seven RILs (RIL 20, 97, 103, 107, 152, 230 and 323) were selected to fine-map the 5A QTL. Parental lines were also tested.

Line RIL 20 had the WEK allele from 382.10 Mbp on the 5AL; RIL 97 between 321.90 Mbp to 417.05 Mbp; RIL 103 and RIL 323 from 395.83 Mbp. However, RIL 152 was like parental line WEKH85A across the 5A chromosome, except the beginning of the short arm which it was still heterozygous, and at maker *BA00228977* (at 395.06 Mb) which has 'Hs' allele. On the other hand, RIL 107 was like parental line Hobbit *sib*, it was still segregating at marker S29 (417.05 Mbp), but it had 'WEK' allele on the long arm of the 5A from marker *S30* (at 417.90 Mbp).

Figure 2.4. represents how the distribution of disease spread above the PI changes for these lines over time using phenotypic data collected at 11-12 dpi (Score 1), at 14-15 dpi (Score 2), at 17-18 dpi (Score 3) and at 21 dpi (Score 4). As expected, parent Hobbit *sib* was more susceptible than parent WEKH85A when observing disease spread above and below the PI. The resistance of WEKH85A to FHB disease spread above the PI was maintained over time (Figure 2.3.). This figure shows the total number of infected spikelets (scoring data above + below) for each line.

Phenotypic data in 2019 showed different levels of FHB disease spread depending on the line. Recombinant lines showing a high level of FHB resistance over time were RILs 103, 152 and 230. On the contrary, RILs 107 and 323 were very susceptible (Figure 2.3.).

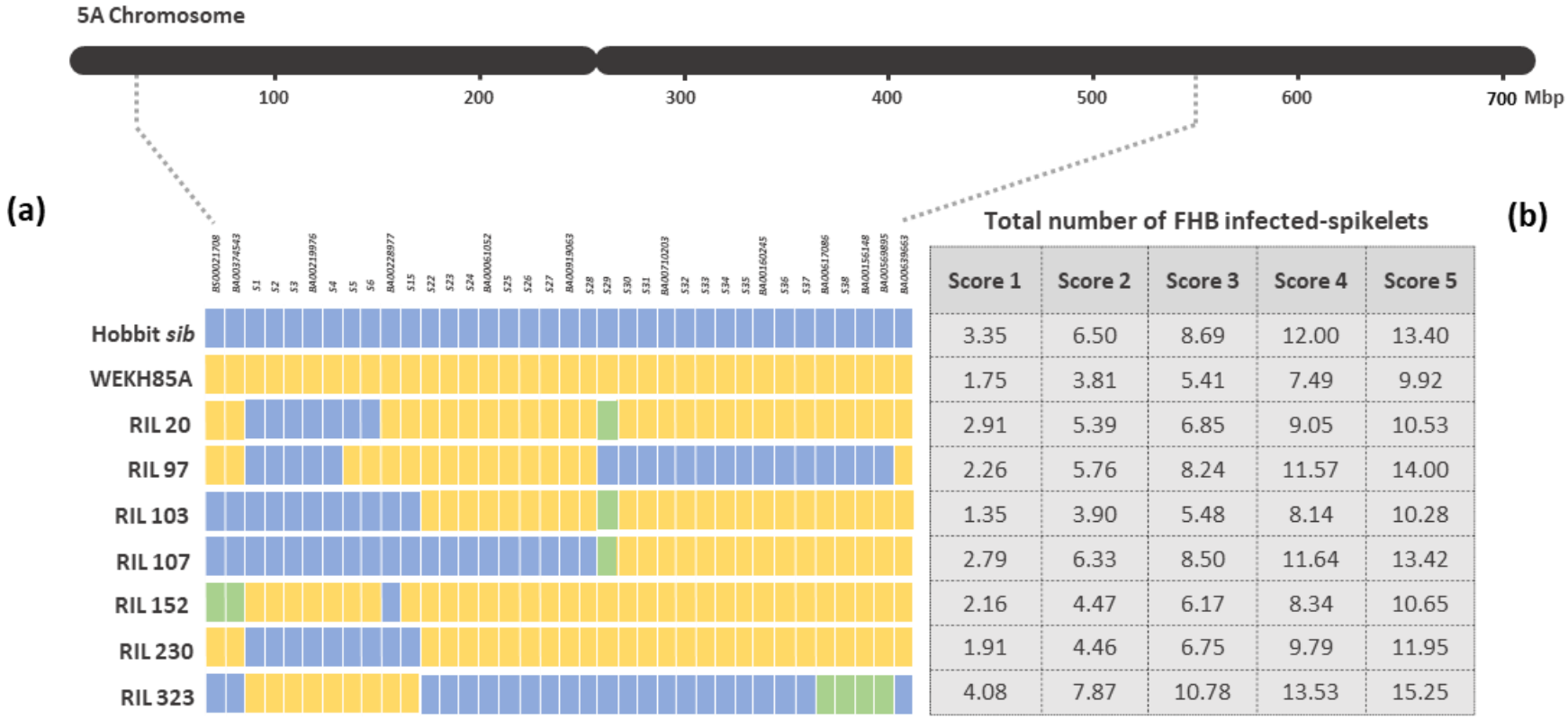

Total number of FHB infected-spikelets

Score 1	Score 2	Score 3	Score 4	Score 5
3.35	6.50	8.69	12.00	13.40
1.75	3.81	5.41	7.49	9.92
2.91	5.39	6.85	9.05	10.53
2.26	5.76	8.24	11.57	14.00
1.35	3.90	5.48	8.14	10.28
2.79	6.33	8.50	11.64	13.42
2.16	4.47	6.17	8.34	10.65
1.91	4.46	6.75	9.79	11.95
4.08	7.87	10.78	13.53	15.25

Figure 2.3*. a) Graphical genotype on the 5A chromosome of parental lines and recombinant inbred lines used on Summer 2019. Lines names are specified on each raw and markers used are specified on each column. Yellow is the allele provided by WEKH85A and blue the one by Hobbit sib.* ***b)*** *Total number of FHB infected-spikelets (scoring data above and below the point of infection) obtained for each line at different scoring dates: Score 1 (11-12 dpi), Score 2 (14-15 dpi), Score 3 (17-18 dpi), Score 4 (21 dpi) and Score 5 (23-24 dpi).*

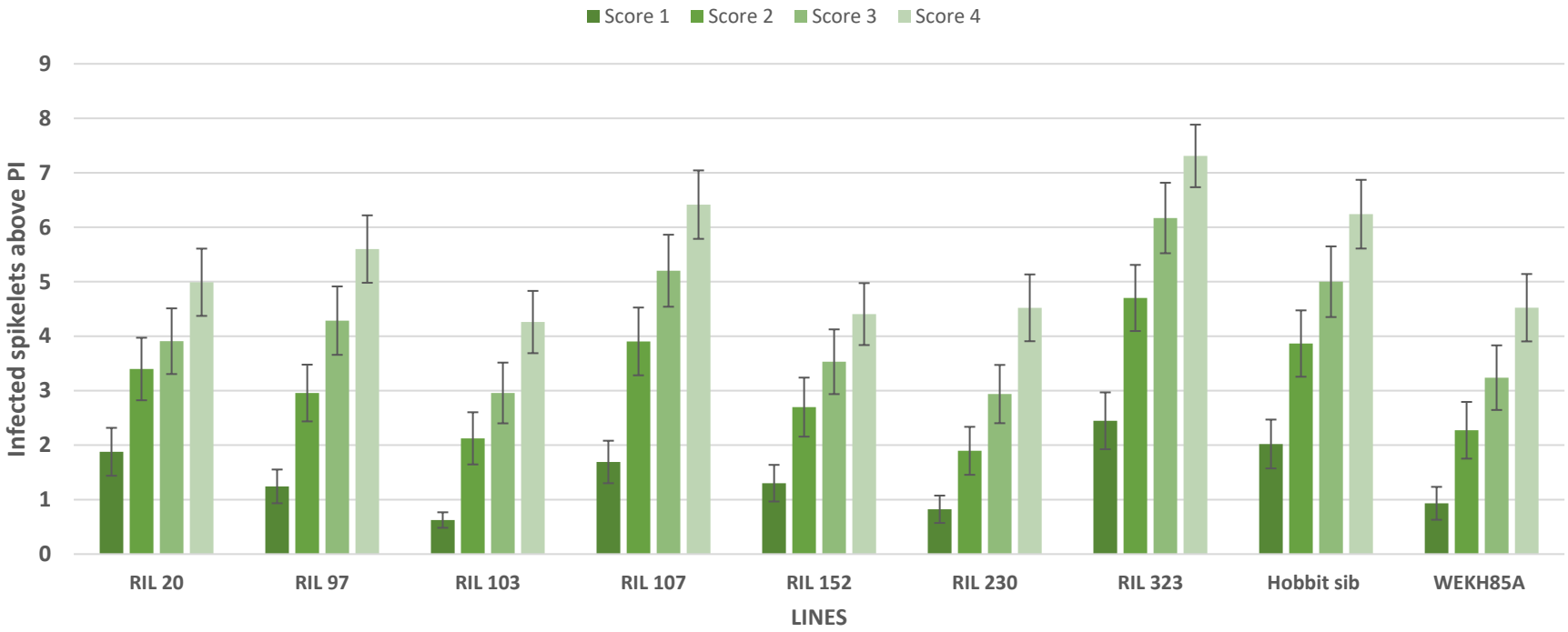

Figure 2.4. *FHB disease above the PI or number of bleached spikelets above the PI of RILs and parental lines (Hobbit sib and WEK8H5A) tested for type II on Summer 2019. Scoring symptoms were collected at 11-12 dpi (Score 1), at 14-15 dpi (Score 2), at 17-18 dpi (Score 3) and at 21 dpi (Score 4). Predicted means were generated using a LMM analysis. Error bars are ± standard error.*

P-value data obtained from the LMM analysis performed for each individual marker located on the 5A chromosome is shown in Table 2.5. and Table 2.6., for scoring data above and below the PI, respectively. Source of markers used for the analysis are described. Associated RefSeqv1.1 gene models (where available) and physical position on RefSeqv1.0 assembly are shown.

LMM analysis of Summer 2019 data revealed that nine markers were associated with FHB type II resistance ($P = 0.006$) at 17-18 dpi on the long arm of chromosome 5A. These markers are *S22*, *S23*, *S24*, *BA00061052*, *S25*, *S26*, *S27*, *BA00919063* and *S28* (source: 18K SNP array, Cereals DB and RNA-Seq), which are located at 404.44, 405.03, 407.96, 408.93, 409.32, 410.50, 410.80, 412.23 and 413.04 Mbp, respectively (Table 2.5.). There is a stronger association with the resistance over time ($P < 0.0001$) at 21 and 23-24 dpi when using scoring data above the PI. The same nine markers were associated with the disease when using the scoring data below the PI, being stronger ($P = 0.001$) at 11-12 dpi, and thus confirming the genomic region of the 5AL. The difference in the number of infected spikelets between 'Hs' and 'WEK' alleles is two and one spikelets of resistance for scoring data above and below the PI, respectively (Table S4 and Table S5).

Table 2.5. *P-value data obtained from a LMM analysis performed for each individual marker located on the 5A chromosome. Source of markers used for the analysis is described. Associated RefSeqv1.1 gene models (where available) and physical position on RefSeqv1.0 assembly are shown. Symptoms above the point of infection were assessed in five sets at different dpi: at 11-12 dpi (Score 1), at 14-15 dpi (Score 2), at 17-18 dpi (Score 3), at 21 dpi (Score 4) and at 23-24 dpi (Score 5) in Summer 2019. Data was transformed using a log10 transformation. P-value data of markers associated with FHB type II resistance are highlighted in light green (P < 0.05) and markers strongly associated with the resistance in dark green (P < 0.01).*

Source	CerealsDB	CerealsDB	18K SNP array	18K SNP array	18K SNP array	CerealsDB	RNA-Seq	RNA-Seq
RefSeqv1.1 Gene model	intergenic	intergenic	*TraesCS5A02G088100*	intergenic	intergenic	*TraesCS5A02G143000*	*TraesCS5A02G145600*	*TraesCS5A02G182000*
RefSeqv1.0 (bp)	30,411,062	32,883,071	118,661,064	213,403,509	300,205,197	317,234,298	321,894,801	381,755,729
Marker	***BS00021708***	***BA00374543***	***S1***	***S2***	***S3***	***BA00219976***	***S4***	***S5***
Score 1	0.473	0.473	0.813	0.813	0.813	0.813	0.813	0.829
Score 2	0.413	0.413	0.911	0.911	0.911	0.911	0.911	0.967
Score 3	0.381	0.381	0.929	0.929	0.929	0.929	0.929	0.834
Score 4	0.241	0.241	0.857	0.857	0.857	0.857	0.857	0.911
Score 5	0.136	0.136	0.936	0.936	0.936	0.936	0.936	0.903

Source	RNA-Seq	CerealsDB	RNA-Seq	18K SNP array	18K SNP array	18K SNP array	CerealsDB
RefSeqv1.1 Gene model	*TraesCS5A02G182400*	*TraesCS5A02G190600*	*TraesCS5A02G191500*	intergenic	intergenic	intergenic	*TraesCS5A02G202200*
RefSeqv1.0 (bp)	382,105,017	395,057,684	395,833,610	404,438,674	405,034,925	407,955,815	408,930,186
Marker	***S6***	***BA00228977***	***S15***	***S22***	***S23***	***S24***	***BA00061052***
Score 1	0.829	0.630	0.803	0.019	0.019	0.019	0.019
Score 2	0.967	0.491	0.739	0.012	0.012	0.012	0.012
Score 3	0.834	0.533	0.829	0.006	0.006	0.006	0.006
Score 4	0.911	0.662	0.962	<0.0001	<0.0001	<0.0001	<0.0001
Score 5	0.903	0.754	0.834	<0.0001	<0.0001	<0.0001	<0.0001

Table 2.5. Continued. *P-value data obtained from a LMM analysis performed for each individual marker located on the 5A chromosome. Source of markers used for the analysis is described. Associated RefSeqv1.1 gene models (where available) and physical position on RefSeqv1.0 assembly are shown. Symptoms above the point of infection were assessed in five sets at different dpi: at 11-12 dpi (Score 1), at 14-15 dpi (Score 2), at 17-18 dpi (Score 3), at 21 dpi (Score 4) and at 23-24 dpi (Score 5) in Summer 2019. Data was transformed using a log10 transformation. P-value data of markers associated with FHB type II resistance are highlighted in light green (P < 0.05) and markers strongly associated with the resistance in dark green (P < 0.01).*

Source	RNA-Seq	RNA-Seq	18K SNP array	CerealsDB	RNA-Seq	RNA-Seq	18K SNP array
RefSeqv1.1 Gene model	*TraesCS5A02G202300*	*TraesCS5A02G202700*	*TraesCS5A02G203000*	intergenic	*TraesCS5A02G203500*	*TraesCS5A02G206600*	*TraesCS5A02G207100*
RefSeqv1.0 (bp)	409,319,878	410,499,218	410,803,424	412,226,288	413,043,503	417,051,540	417,897,180
Marker	***S25***	***S26***	***S27***	***BA00919063***	***S28***	***S29***	***S30***
Score 1	0.019	0.019	0.019	0.019	0.019	0.080	0.096
Score 2	0.012	0.012	0.012	0.012	0.012	0.041	0.059
Score 3	0.006	0.006	0.006	0.006	0.006	0.040	0.040
Score 4	<0.0001	<0.0001	<0.0001	<0.0001	<0.0001	0.026	0.029
Score 5	<0.0001	<0.0001	<0.0001	<0.0001	<0.0001	0.030	0.028

Source	18K SNP array	CerealsDB	18K SNP array	18K SNP array	18K SNP array	18K SNP array	CerealsDB	18K SNP array
RefSeqv1.1 Gene model	intergenic	*TraesCS5A02G207400*	*TraesCS5A02G208200*	intergenic	intergenic	intergenic	*TraesCS5A02G215000*	intergenic
RefSeqv1.0 (bp)	419,204,071	419,363,482	421,825,888	427,896,043	429,751,662	430,050,339	430,246,218	430,604,205
Marker	***S31***	***BA00710203***	***S32***	***S33***	***S34***	***S35***	***BA00160245***	***S36***
Score 1	0.096	0.096	0.096	0.096	0.096	0.096	0.096	0.096
Score 2	0.059	0.059	0.059	0.059	0.059	0.059	0.059	0.059
Score 3	0.040	0.040	0.040	0.040	0.040	0.040	0.040	0.040
Score 4	0.029	0.029	0.029	0.029	0.029	0.029	0.029	0.029
Score 5	0.028	0.028	0.028	0.028	0.028	0.028	0.028	0.028

Table 2.5. Continued. *P-value data obtained from a LMM analysis performed for each individual marker located on the 5A chromosome. Source of markers used for the analysis is described. Associated RefSeqv1.1 gene models (where available) and physical position on RefSeqv1.0 assembly are shown. Symptoms above the point of infection were assessed in five sets at different dpi: at 11-12 dpi (Score 1), at 14-15 dpi (Score 2), at 17-18 dpi (Score 3), at 21 dpi (Score 4) and at 23-24 dpi (Score 5) in Summer 2019. Data was transformed using a log10 transformation. P-value data of markers associated with FHB type II resistance are highlighted in light green (P < 0.05) and markers strongly associated with the resistance in dark green (P < 0.01).*

Source	18K SNP array	CerealsDB	18K SNP array	CerealsDB	CerealsDB	CerealsDB
RefSeqv1.1 Gene model	intergenic	*TraesCS5A02G222100*	*TraesCS5A02G222100*	*TraesCS5A02G222500*	*TraesCS5A02G223300*	*TraesCS5A02G348600*
RefSeqv1.0 (bp)	433,030,768	438,266,961	438,267,579	438,471,823	439,186,565	552,162,031
Marker	***S37***	***BA00617086***	***S38***	***BA00156148***	***BA00569895***	***BA00639663***
Score 1	0.096	0.483	0.483	0.483	0.483	0.062
Score 2	0.059	0.389	0.389	0.389	0.389	0.057
Score 3	0.040	0.297	0.297	0.297	0.297	0.065
Score 4	0.029	0.238	0.238	0.238	0.238	0.048
Score 5	0.028	0.238	0.238	0.238	0.238	0.031

Table 2.6. *P-value data obtained from a LMM analysis performed for each individual marker located on the 5A chromosome. Source of markers used for the analysis is described. Associated RefSeqv1.1 gene models (where available) and physical position on RefSeqv1.0 assembly are shown. Symptoms below the point of infection were assessed in five sets at different dpi: at 11-12 dpi (Score 1), at 14-15 dpi (Score 2), at 17-18 dpi (Score 3), at 21 dpi (Score 4) and at 23-24 dpi (Score 5) in Summer 2019. Data was transformed using a log10 transformation. P-value data of markers associated with FHB type II resistance are highlighted in light green (P < 0.05) and markers strongly associated with the resistance in dark green (P < 0.01).*

Source	CerealsDB	CerealsDB	18K SNP array	18K SNP array	18K SNP array	CerealsDB	RNA-Seq	RNA-Seq
RefSeqv1.1 Gene model	intergenic	intergenic	*TraesCS5A02G088100*	intergenic	intergenic	*TraesCS5A02G143000*	*TraesCS5A02G145600*	*TraesCS5A02G182000*
RefSeqv1.0 (bp)	30,411,062	32,883,071	118,661,064	213,403,509	300,205,197	317,234,298	321,894,801	381,755,729
Marker	***BS00021708***	***BA00374543***	***S1***	***S2***	***S3***	***BA00219976***	***S4***	***S5***
Score 1	0.278	0.278	0.638	0.638	0.638	0.638	0.638	0.411
Score 2	0.321	0.321	0.432	0.432	0.432	0.432	0.432	0.480
Score 3	0.365	0.365	0.500	0.500	0.500	0.500	0.500	0.594
Score 4	0.357	0.357	0.338	0.338	0.338	0.338	0.338	0.566
Score 5	0.440	0.440	0.332	0.332	0.332	0.332	0.332	0.606

Source	RNA-Seq	CerealsDB	RNA-Seq	18K SNP array	18K SNP array	18K SNP array	CerealsDB
RefSeqv1.1 Gene model	*TraesCS5A02G182400*	*TraesCS5A02G190600*	*TraesCS5A02G191500*	intergenic	intergenic	intergenic	*TraesCS5A02G202200*
RefSeqv1.0 (bp)	382,105,017	395,057,684	395,833,610	404,438,674	405,034,925	407,955,815	408,930,186
Marker	***S6***	***BA00228977***	***S15***	***S22***	***S23***	***S24***	***BA00061052***
Score 1	0.411	0.902	0.633	0.001	0.001	0.001	0.001
Score 2	0.480	0.901	0.466	0.012	0.012	0.012	0.012
Score 3	0.594	0.920	0.530	0.022	0.022	0.022	0.022
Score 4	0.566	0.662	0.363	0.027	0.027	0.027	0.027
Score 5	0.606	0.645	0.430	0.030	0.030	0.030	0.030

Table 2.6. Continued. *P-value data obtained from a LMM analysis performed for each individual marker located on the 5A chromosome. Source of markers used for the analysis is described. Associated RefSeqv1.1 gene models (where available) and physical position on RefSeqv1.0 assembly are shown. Symptoms below the point of infection were assessed in five sets at different dpi: at 11-12 dpi (Score 1), at 14-15 dpi (Score 2), at 17-18 dpi (Score 3), at 21 dpi (Score 4) and at 23-24 dpi (Score 5) in Summer 2019. Data was transformed using a log10 transformation. P-value data of markers associated with FHB type II resistance are highlighted in light green (P < 0.05) and markers strongly associated with the resistance in dark green (P < 0.01).*

Source	RNA-Seq	RNA-Seq	18K SNP array	CerealsDB	RNA-Seq	RNA-Seq	18K SNP array
RefSeqv1.1 Gene model	*TraesCS5A02G202300*	*TraesCS5A02G202700*	*TraesCS5A02G203000*	intergenic	*TraesCS5A02G203500*	*TraesCS5A02G206600*	*TraesCS5A02G207100*
RefSeqv1.0 (bp)	409,319,878	410,499,218	410,803,424	412,226,288	413,043,503	417,051,540	417,897,180
Marker	***S25***	***S26***	***S27***	***BA00919063***	***S28***	***S29***	***S30***
Score 1	0.001	0.001	0.001	0.001	0.001	0.240	0.213
Score 2	0.012	0.012	0.012	0.012	0.012	0.174	0.091
Score 3	0.022	0.022	0.022	0.022	0.022	0.147	0.063
Score 4	0.027	0.027	0.027	0.027	0.027	0.124	0.052
Score 5	0.030	0.030	0.030	0.030	0.030	0.150	0.073

Source	18K SNP array	CerealsDB	18K SNP array	18K SNP array	18K SNP array	18K SNP array	CerealsDB	18K SNP array
RefSeqv1.1 Gene model	intergenic	*TraesCS5A02G207400*	*TraesCS5A02G208200*	intergenic	intergenic	intergenic	*TraesCS5A02G215000*	intergenic
RefSeqv1.0 (bp)	419,204,071	419,363,482	421,825,888	427,896,043	429,751,662	430,050,339	430,246,218	430,604,205
Marker	***S31***	***BA00710203***	***S32***	***S33***	***S34***	***S35***	***BA00160245***	***S36***
Score 1	0.213	0.213	0.213	0.213	0.213	0.213	0.213	0.213
Score 2	0.091	0.091	0.091	0.091	0.091	0.091	0.091	0.091
Score 3	0.063	0.063	0.063	0.063	0.063	0.063	0.063	0.063
Score 4	0.052	0.052	0.052	0.052	0.052	0.052	0.052	0.052
Score 5	0.073	0.073	0.073	0.073	0.073	0.073	0.073	0.073

Table 2.6. Continued. *P-value data obtained from a LMM analysis performed for each individual marker located on the 5A chromosome. Source of markers used for the analysis is described. Associated RefSeqv1.1 gene models (where available) and physical position on RefSeqv1.0 assembly are shown. Symptoms below the point of infection were assessed in five sets at different dpi: at 11-12 dpi (Score 1), at 14-15 dpi (Score 2), at 17-18 dpi (Score 3), at 21 dpi (Score 4) and at 23-24 dpi (Score 5) in Summer 2019. Data was transformed using a log10 transformation. P-value data of markers associated with FHB type II resistance are highlighted in light green (P < 0.05) and markers strongly associated with the resistance in dark green (P < 0.01).*

Source	18K SNP array	CerealsDB	18K SNP array	CerealsDB	CerealsDB	CerealsDB
RefSeqv1.1 Gene model	intergenic	*TraesCS5A02G222100*	*TraesCS5A02G222100*	*TraesCS5A02G222500*	*TraesCS5A02G223300*	*TraesCS5A02G348600*
RefSeqv1.0 (bp)	433,030,768	438,266,961	438,267,579	438,471,823	439,186,565	552,162,031
Marker	***S37***	***BA00617086***	***S38***	***BA00156148***	***BA00569895***	***BA00639663***
Score 1	0.213	0.233	0.233	0.233	0.233	0.054
Score 2	0.091	0.204	0.204	0.204	0.204	0.064
Score 3	0.063	0.132	0.132	0.132	0.132	0.053
Score 4	0.052	0.169	0.169	0.169	0.169	0.093
Score 5	0.073	0.226	0.226	0.226	0.226	0.151

The phenotypic data is related to the parental alleles (WEKH85A or *Hobbit sib*) in each RIL at each marker position, while the genomic data reveals the location of the QTL in these lines. Once the single marker analysis is performed, it is when any maker associated with the resistance (provided by WEK8H5A allele) can be identified.

The genomic region on the 5AL locus most associated with FHB resistance in Summer 2019 was of 21.22 Mbp, between markers *S15* (at 395.83 Mbp) and *S29* (at 417.05 Mbp). All recombinant lines tested in Summer 2019 contained the resistant allele (WEKH85A) on that genomic region on the 5AL except RIL 107, which was like Hobbit sib (Figure 2.3.). Generally, FHB disease severity was very high in 2019 trial, but lines showing the best resistant effect were RIL 103, RIL 152 and RIL 230 (Figure 2.3.). In contrast, RIL 107 showed high levels of FHB susceptibility over time. Despite RIL 97 containing the 5A QTL region and exhibiting high levels of FHB resistance in Summer 2018, severity of the disease was extremely high in Summer 2019.

The lack of homozygous recombinant lines on that region lead to a search among heterozygous lines that could segregate on the region. Heterozygous lines - some not previously tested (RILs 125, 132, 170 and 188) and RILs 266 and 271 tested during the first trial - were bulked and genotyped to identify new recombinant lines containing the 5AL locus. Several lines were selected and bulked again to obtain different recombination points on the 5AL. Fixed and homozygous lines containing recombination events on the 5AL locus were then selected. These lines were recoded and used in the type II disease assessment in the 2020 summer trial to confirm the mapping of the QTL. Some of these lines were sister lines, like for example RILs 4A and 4B, which were obtained from RIL 4 (Table 2.7.).

Table 2.7. *Graphical genotype of parental lines and recombinant inbred lines used on Summer 2020. Source of markers is described. Associated RefSeqv1.1 gene models (where available) and physical position on RefSeqv1.0 assembly are shown. Predicted means and standard errors (S.E.) of FHB scoring data above the point of infection (PI) of lines tested in Summer 2018 is also showed at 14 dpi. 'Hs' is the allele provided by parental line Hobbit sib; 'WEK' is the allele provided by parental line WEKH85A; 'Het' is the heterozygous allele.*

		Source	CerealsDB	CerealsDB	CerealsDB	CerealsDB	CerealsDB	**14 dpi**	
		RefSeqv1.1 Gene model	*TraesCS5A02G143000*	*TraesCS5A02G190600*	*TraesCS5A02G202200*	intergenic	*TraesCS5A02G207400*		
		RefSeqv1.0 (bp)	317,234,298	395,057,684	408,930,186	412,226,288	419,363,482		
old-Line ID	**Line ID**	**Type of line**	***BA00219976***	***BA00228977***	***BA00061052***	***BA00919063***	***BA00710203***	**Mean**	**S.E.**
Hobbit *sib*	**Hobbit *sib***	Parental (Hs)	Hs	Hs	Hs	Hs	Hs	7.44	1.29
WEKH85A	**WEKH85A**	Parental (WEK)	WEK	WEK	WEK	WEK	WEK	5.30	1.92
RIL 125	**RIL 4**	Recombinant	WEK	Het	Het	Het	Het	-	-
RIL 132	**RIL 5**	Recombinant	Het	Het	Het	Het	Het	-	-
RIL 170	**RIL 7**	Recombinant	Het	Het	Het	Het	Het	-	-
RIL 188	**RIL 9**	Recombinant	Hs	Het	Het	Het	Het	-	-
RIL 188	**RIL 10**	Recombinant	Hs	Het	Het	Het	Het	-	-
RIL 188	**RIL 11**	Recombinant	Hs	Het	Het	Het	Het	-	-
RIL 266	**RIL 14**	Recombinant	WEK	Het	Het	Het	Het	9.38	0.63
RIL 266	**RIL 15**	Recombinant	WEK	Het	Het	Het	Het	9.38	0.63
RIL 266	**RIL 16**	Recombinant	WEK	Het	Het	Het	Het	9.38	0.63
RIL 266	**RIL 17**	Recombinant	WEK	Het	Het	Het	Het	9.38	0.63
RIL 271	**RIL 19**	Recombinant	Het	Het	Het	Het	Het	7.88	1.39

2.4.1.3. Summer 2020

Graphical genotype of parental lines and RILs used in Summer 2020 is provided in Figure 2.5. For this trial, a set of fifteen RILs (RIL 4A, 4B, 5A, 7A, 7B, 9A, 9B, 10B, 11A, 14A, 15A, 16A, 17A, 17B and 19A) were selected to fine-map the 5A QTL. Parental lines were also tested.

Figure 2.6. represents how the distribution of disease spread above the PI changes for these lines over time using phenotypic data collected at 12-13 dpi (Score 1), at 14-15 dpi (Score 2), at 16-17 dpi (Score 3) and at 18-19 dpi (Score 4). During this trial, both parental lines, Hobbit *sib* and WEKH85A, had similar number of infected spikelets above and below the PI over time (Figure 2.5.). No differences between parental lines were observed in the 2020 trial suggesting that these plants were incorrectly identified, since there were clear phenotypical differences in previous years.

However, phenotypic data in 2020 showed different levels of FHB disease spread depending on the recombinant line. Recombinant lines showing a very good level of FHB resistance over time were RILs 4A, 4B, 7B, 9A and 10B. In contrast, RILs 16A, 17B and 19A were very susceptible (Figure 2.5.).

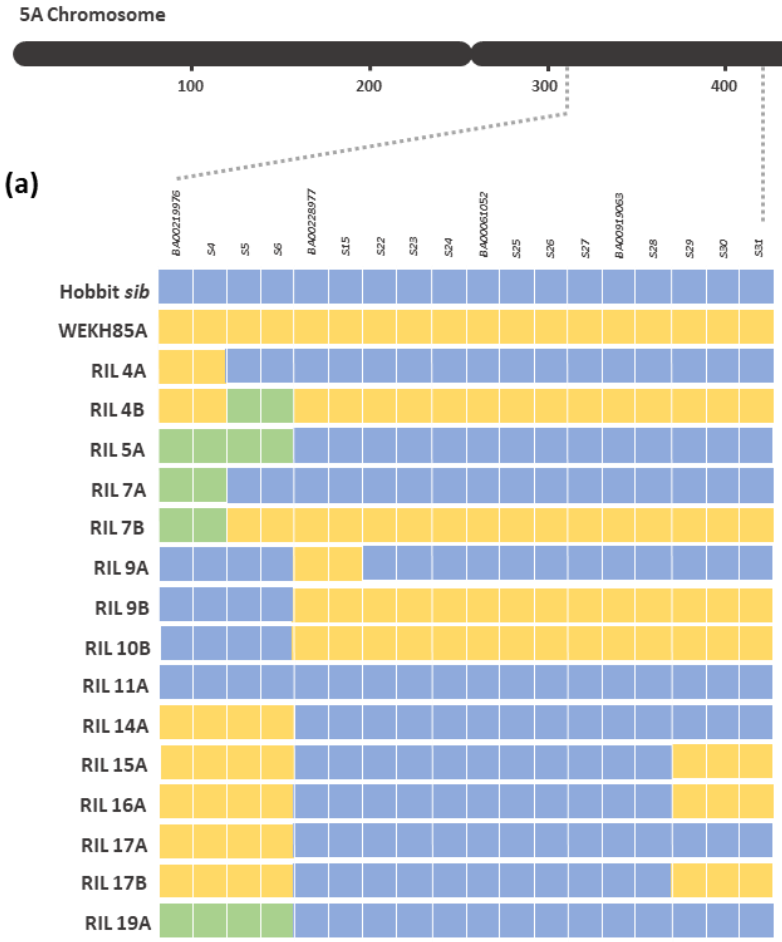

(b)

Total number of FHB infected-spikelets

Score 1	Score 2	Score 3	Score 4	Score 5
1.83	3.28	5.07	6.07	8.16
2.11	3.78	4.85	6.72	8.78
0.45	1.10	1.90	3.15	6.05
0.44	1.19	2.00	2.83	5.00
2.00	3.50	5.00	7.14	8.86
3.71	5.54	6.46	8.04	12.36
0.44	1.11	1.76	3.07	5.70
0.74	1.29	2.22	3.79	6.84
2.54	2.42	3.75	4.83	6.58
0.49	1.31	2.21	3.04	5.04
1.47	2.78	4.32	5.22	6.97
1.38	3.31	4.57	6.93	10.22
2.92	4.58	6.34	8.45	11.42
2.64	5.21	7.96	9.72	12.64
2.00	3.50	4.69	7.35	9.27
3.43	5.86	7.82	8.93	11.54
3.45	5.05	6.86	8.77	11.36

Figure 2.5. *a) Graphical genotype on the 5A chromosome of parental lines and recombinant inbred lines used on Summer 2020. Line names are specified on each raw and markers used are specified on each column. Yellow is the allele provided by WEKH85A and blue the one provided by Hobbit sib. b) Total number of FHB infected-spikelets (scoring data above and below the point of infection) obtained for each line at different scoring dates: Score 1 (12-13 dpi), Score 2 (14-15 dpi), Score 3 (16-17 dpi), Score 4 (18-19 dpi) and Score 5 (21-22 dpi).*

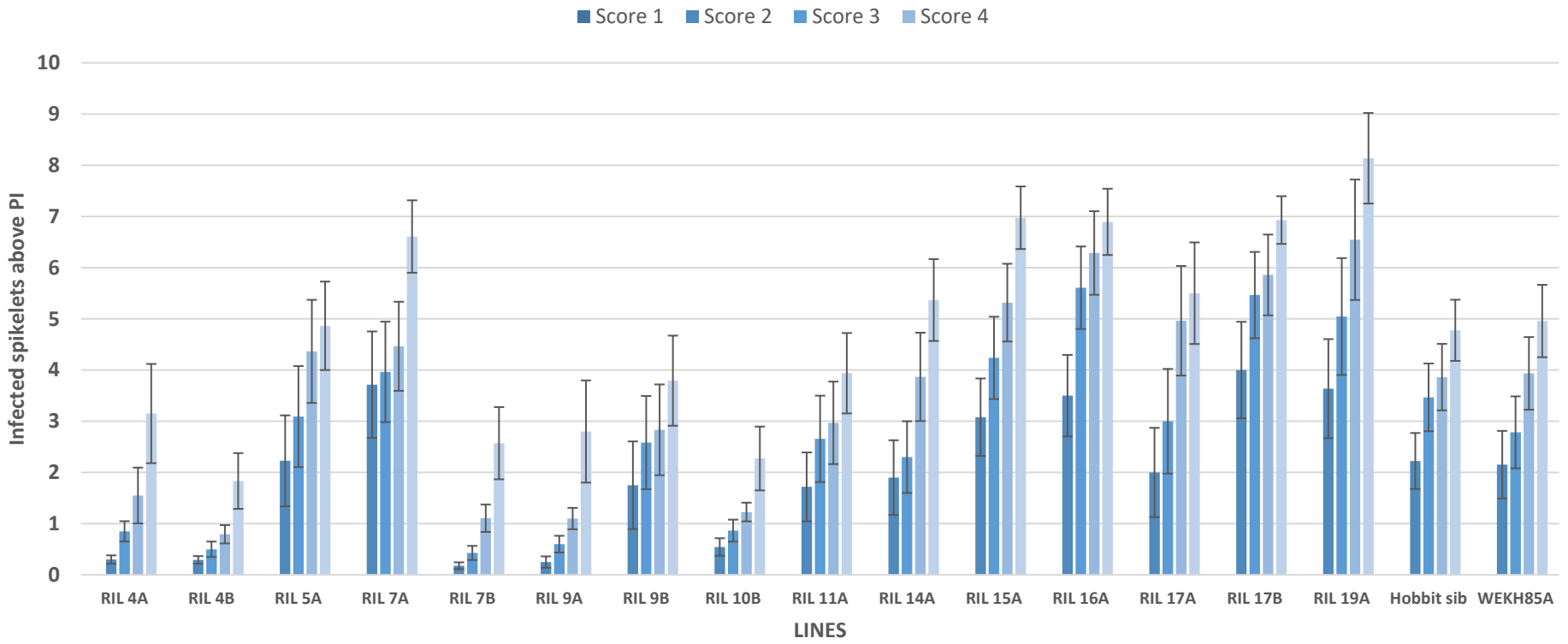

Figure 2.6. *FHB disease above the PI or number of bleached spikelets above the PI of RILs and parental lines (Hobbit sib and WEK8H5A) tested for type II on Summer 2020. Scoring symptoms were collected at 12-13 dpi (Score 1), at 14-15 dpi (Score 2), at 16-17 dpi (Score 3) and at 18-19 dpi (Score 4). Predicted means were generated using a LMM analysis. Error bars are ± standard error.*

LMM analysis of Summer 2020 data revealed that two markers were strongly associated with FHB type II resistance ($P < 0.01$) at all scoring dates within the trial. These markers are *BA00228977* and *S15* (source: Cereals DB and RNA-Seq), which are located at 395.06 and 395.83 Mbp (Table 2.8.). The same markers were associated with the disease when using the scoring data below the PI, being stronger ($P < 0.01$) at 12-13 and 14-15 dpi, and thus confirming the genomic region. The difference in the number of infected spikelets between 'Hs' and 'WEK' alleles is two and half of a spikelet of resistance for scoring data above and below the PI, respectively (Table S6 and Table S7).

The genomic region most associated with FHB resistance on the 5AL in Summer 2020 was of 22.33 Mbp, between markers *S6* (at 382.11 Mbp) and *S22* (at 404.44 Mbp). Recombinants containing the WEK allele on this interval were RIL 4B, RIL 7B, RIL 9A, RIL 9B and RIL 10B (Figure 2.5.). All these lines had a high level of FHB type II resistance over time (Figure 2.6.). The other recombinants had the 'Hs' allele and showed higher levels of susceptibility to FHB. However, RIL 4A possessed 'Hs' allele across the 5A QTL but showed higher levels of resistance. The opposite was observed for parental line WEKH85A (Figure 2.5. and Figure 2.6.).

Table 2.8. *P-value data obtained from a LMM analysis performed for each individual marker located on the 5A chromosome. Source of markers used for the analysis is described. Associated RefSeqv1.1 gene models (where available) and physical position on RefSeqv1.0 assembly are shown. Symptoms above the point of infection were assessed in five sets at different dpi: at 12-13 dpi (Score 1), at 14-15 dpi (Score 2), at 16-17 dpi (Score 3), at 18-19 dpi (Score 4) and at 21-22 dpi (Score 5) in Summer 2020. Data was transformed using a log10 transformation. P-value data of markers associated with FHB type II resistance are highlighted in light green (P < 0.05) and markers strongly associated with the resistance in dark green (P < 0.01).*

Source	CerealsDB	RNA-Seq	RNA-Seq	RNA-Seq	CerealsDB	RNA-Seq	18K SNP array
RefSeqv1.1 Gene model	*TraesCS5A02G143000*	*TraesCS5A02G145600*	*TraesCS5A02G182000*	*TraesCS5A02G182400*	*TraesCS5A02G190600*	*TraesCS5A02G191500*	intergenic
RefSeqv1.0 (bp)	317,234,298	321,894,801	381,755,729	382,105,017	395,057,684	395,833,610	404,438,674
Marker	***BA00219976***	***S4***	***S5***	***S6***	***BA00228977***	***S15***	***S22***
Score 1	0.799	0.799	0.932	0.932	0.008	0.008	0.031
Score 2	0.481	0.481	0.449	0.449	0.004	0.004	0.033
Score 3	0.780	0.780	0.409	0.409	0.005	0.005	0.028
Score 4	0.267	0.267	0.371	0.371	0.006	0.006	0.026
Score 5	0.387	0.387	0.203	0.203	0.005	0.005	0.015

Source	18K SNP array	18K SNP array	CerealsDB	RNA-Seq	RNA-Seq	18K SNP array	CerealsDB
RefSeqv1.1 Gene model	intergenic	intergenic	*TraesCS5A02G202200*	*TraesCS5A02G202300*	*TraesCS5A02G202700*	*TraesCS5A02G203000*	intergenic
RefSeqv1.0 (bp)	405,034,925	407,955,815	408,930,186	409,319,878	410,499,218	410,803,424	412,226,288
Marker	***S23***	***S24***	***BA00061052***	***S25***	***S26***	***S27***	***BA00919063***
Score 1	0.031	0.031	0.031	0.031	0.031	0.031	0.031
Score 2	0.033	0.033	0.033	0.033	0.033	0.033	0.033
Score 3	0.028	0.028	0.028	0.028	0.028	0.028	0.028
Score 4	0.026	0.026	0.026	0.026	0.026	0.026	0.026
Score 5	0.015	0.015	0.015	0.015	0.015	0.015	0.015

Table 2.8. Continued. *P-value data obtained from a LMM analysis performed for each individual marker located on the 5A chromosome. Source of markers used for the analysis is described. Associated RefSeqv1.1 gene models (where available) and physical position on RefSeqv1.0 assembly are shown. Symptoms above the point of infection were assessed in five sets at different dpi: at 12-13 dpi (Score 1), at 14-15 dpi (Score 2), at 16-17 dpi (Score 3), at 18-19 dpi (Score 4) and at 21-22 dpi (Score 5) in Summer 2020. Data was transformed using a log10 transformation. P-value data of markers associated with FHB type II resistance are highlighted in light green (P < 0.05) and markers strongly associated with the resistance in dark green (P < 0.01).*

Source	RNA-Seq	RNA-Seq	18K SNP array	18K SNP array
RefSeqv1.1 Gene model	*TraesCS5A02G203500*	*TraesCS5A02G206600*	*TraesCS5A02G207100*	intergenic
RefSeqv1.0 (bp)	413,043,503	417,051,540	417,897,180	419,204,071
Marker	***S28***	***S29***	***S30***	***S31***
Score 1	0.031	0.946	0.946	0.946
Score 2	0.033	0.861	0.861	0.861
Score 3	0.028	0.809	0.809	0.809
Score 4	0.026	0.890	0.890	0.890
Score 5	0.015	0.949	0.949	0.949

Table 2.9. *P-value data obtained from a LMM analysis performed for each individual marker located on the 5A chromosome. Source of markers used for the analysis is described. Associated RefSeqv1.1 gene models (where available) and physical position on RefSeqv1.0 assembly are shown. Symptoms below the point of infection were assessed in five sets at different dpi: at 12-13 dpi (Score 1), at 14-15 dpi (Score 2), at 16-17 dpi (Score 3), at 18-19 dpi (Score 4) and at 21-22 dpi (Score 5) in Summer 2020. Data was transformed using a log10 transformation. P-value data of markers associated with FHB type II resistance are highlighted in light green (P < 0.05) and markers strongly associated with the resistance in dark green (P < 0.01).*

Source	CerealsDB	RNA-Seq	RNA-Seq	RNA-Seq	CerealsDB	RNA-Seq	18K SNP array
RefSeqv1.1 Gene model	*TraesCS5A02G143000*	*TraesCS5A02G145600*	*TraesCS5A02G182000*	*TraesCS5A02G182400*	*TraesCS5A02G190600*	*TraesCS5A02G191500*	intergenic
RefSeqv1.0 (bp)	317,234,298	321,894,801	381,755,729	382,105,017	395,057,684	395,833,610	404,438,674
Marker	***BA00219976***	***S4***	***S5***	***S6***	***BA00228977***	***S15***	***S22***
Score 1	0.264	0.264	0.254	0.254	0.004	0.004	0.009
Score 2	0.111	0.111	0.081	0.081	0.009	0.009	0.017
Score 3	0.293	0.293	0.188	0.188	0.011	0.011	0.018
Score 4	0.392	0.392	0.266	0.266	0.015	0.015	0.024
Score 5	0.429	0.429	0.148	0.148	0.008	0.008	0.015

Source	18K SNP array	18K SNP array	CerealsDB	RNA-Seq	RNA-Seq	18K SNP array	CerealsDB
RefSeqv1.1 Gene model	intergenic	intergenic	*TraesCS5A02G202200*	*TraesCS5A02G202300*	*TraesCS5A02G202700*	*TraesCS5A02G203000*	intergenic
RefSeqv1.0 (bp)	405,034,925	407,955,815	408,930,186	409,319,878	410,499,218	410,803,424	412,226,288
Marker	***S23***	***S24***	***BA00061052***	***S25***	***S26***	***S27***	***BA00919063***
Score 1	0.009	0.009	0.009	0.009	0.009	0.009	0.009
Score 2	0.017	0.017	0.017	0.017	0.017	0.017	0.017
Score 3	0.018	0.018	0.018	0.018	0.018	0.018	0.018
Score 4	0.024	0.024	0.024	0.024	0.024	0.024	0.024
Score 5	0.015	0.015	0.015	0.015	0.015	0.015	0.015

Table 2.9. Continued. *P-value data obtained from a LMM analysis performed for each individual marker located on the 5A chromosome. Source of markers used for the analysis is described. Associated RefSeqv1.1 gene models (where available) and physical position on RefSeqv1.0 assembly are shown. Symptoms below the point of infection were assessed in five sets at different dpi: at 12-13 dpi (Score 1), at 14-15 dpi (Score 2), at 16-17 dpi (Score 3), at 18-19 dpi (Score 4) and at 21-22 dpi (Score 5) in Summer 2020. Data was transformed using a log10 transformation. P-value data of markers associated with FHB type II resistance are highlighted in light green (P < 0.05) and markers strongly associated with the resistance in dark green (P < 0.01).*

Source	RNA-Seq	RNA-Seq	18K SNP array	18K SNP array
RefSeqv1.1 Gene model	*TraesCS5A02G203500*	*TraesCS5A02G206600*	*TraesCS5A02G207100*	intergenic
RefSeqv1.0 (bp)	413,043,503	417,051,540	417,897,180	419,204,071
Marker	***S28***	***S29***	***S30***	***S31***
Score 1	0.009	0.589	0.589	0.589
Score 2	0.017	0.739	0.739	0.739
Score 3	0.018	0.731	0.731	0.731
Score 4	0.024	0.875	0.875	0.875
Score 5	0.015	0.659	0.659	0.659

2.4.2. Location of the 5AL locus over Summers 2018-2020

The fine-mapping of the 5A locus over the period of three Summers (2018-2020) on the long arm of the 5A chromosome is graphically represented in Figure 2.7. Graphical genotypes of the 5A QTL location for each of the three summer trials are represented in yellow (WEKH85A-like allele).

The genomic region on the 5AL locus most associated with FHB resistance in Summer 2018 was of 35.19 Mbp, between markers BA00228977 (at 395.06 Mbp) and BA00160245 (at 430.25 Mbp); on Summer 2019 was of 21.22 Mbp, between markers S15 (at 395.83 Mbp) and S29 (at 417.05 Mbp); and on Summer 2020 was of 22.33 Mbp, between markers S6 (at 382.11 Mbp) and S22 (at 404.44 Mbp).

The 5AL locus was stable over a period of three years and was fine-mapped to a relatively small genetic interval. The peak of the QTL moved slightly closer to the centromere in that data from the last summer trial, as can be observed in Figure 2.7. Over three years of trials, thus, the genomic region on the 5AL consistently associated with FHB type II resistance is located between markers *S15* (at 395.83 Mbp) and *S22* (at 404.44 Mbp).

To conclude, this genomic region between *S15* and *S22* allowed a robust and stable effect of FHB type II resistance over three summer trials.

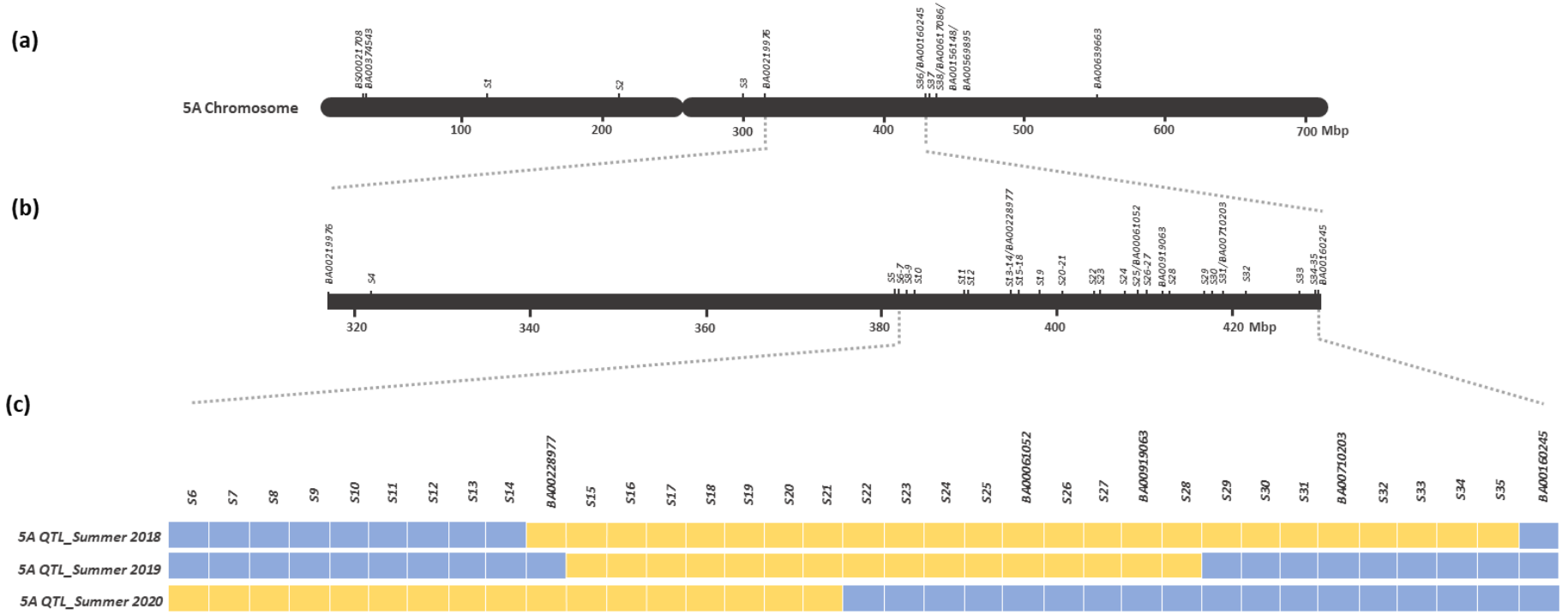

Figure 2.7. *(a) Physical map of the wheat chromosome 5A using KASP markers. (b) Region comprising between markers BA00219976 (317.23 Mbp) and BA00160245 (430.25 Mbp) is amplified to show the location of markers used to refine the QTL located on the long arm of chromosome 5A. (c) Graphical genotypes of the 5A QTL over three summer trials (2018-2020). Yellow region represents the size and location of the QTL for that specific year.*

2.4.3. Refining the 5AL locus

In collaboration with the iCase partner, Limagrain S.A., new SNPs were identified using exome capture and RNA-Seq data (see Chapter 3). New KASP markers were developed and several RILs used in summer trial 2020 (RIL 9A, RIL 10B, RIL 16A and RIL 17B) were genotyped to fine-map the QTL on the long arm of the 5A chromosome. These new markers were not included for the single marker analysis performed on that year since only those specific RILs above mentioned were screened by our collaborators.

However, the combination of FHB phenotypic data collected in 2020 and the new genotypic data obtained with those novel markers helped to refine the 5AL locus to 6.24 Mbp, between markers *S11* (389.64 Mbp) and *S18* (395.89 Mbp). Potential lines carrying the 5AL locus are RILs 9A and 10B (Figure 2.8.). While both lines showed the best performance against FHB, RILs 17B and 16A (not carrying the 5AL locus) were very susceptible to the disease with high number of infected spikelets above the PI.

Since the 5AL locus consistently associated with FHB over three trials was located from markers *S15* to *S22*, the potential genomic region on the 5AL locus associated with the resistance, thus, resides on its right flank, between markers *S15* (at 395.83 Mbp) and *S18* (at 395.89 Mbp) (Figure 2.8.).

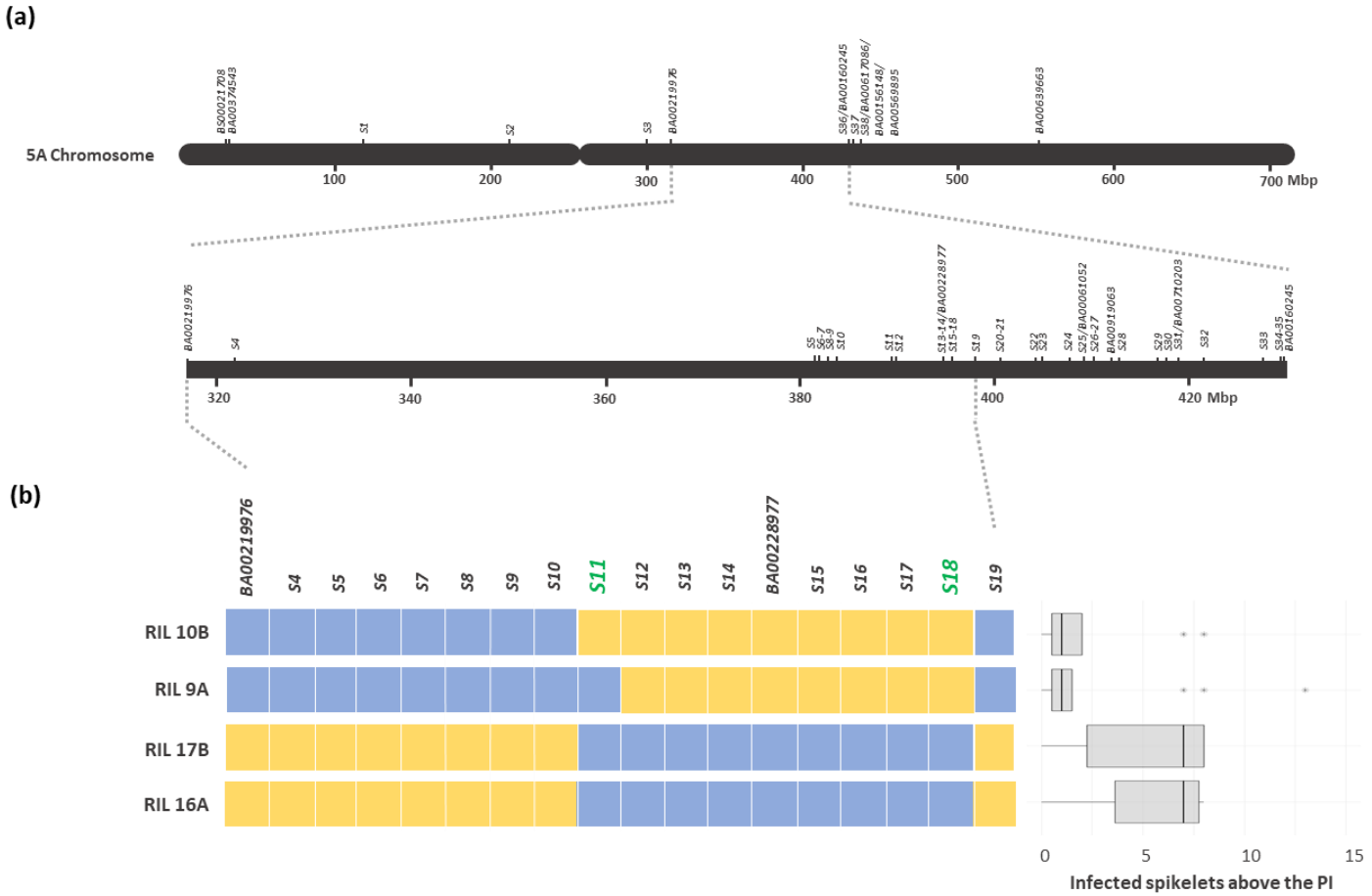

Figure 2.8. *a) Physical map of the wheat chromosome 5A using KASP markers. Region comprising between markers BA00219976 (317.23 Mbp) and BA00160245 (430.25 Mbp) is amplified to show the location of markers used to refine the 5AL locus, QFhb.WEK-5A. (b) Graphical genotypes of recombinant inbred line (RILs). The genotypes are defined by having either the Hobbit sib-like (blue) or the WEKH85A-like (yellow) allele at each marker shown across the interval. QFhb.WEK-5A is of 6.24 Mbp, between markers S11 and S18 (bold green). Box plot of infected spikelets above the PI using Summer 2020 data is represented for each genotype.*

2.5. Discussion

2.5.1. *QFhb.WEK-5A* is located on the long arm of the 5A chromosome

In this study, a set of RILs derived from the cross between the resistant line WEKH85A and the susceptible line Hobbit *sib* were genotyped using a diverse set of KASP markers on the 5A chromosome and were phenotyped for type II FHB resistance over three summer trials (2018-2020). A single marker analysis for each KASP along on the 5A chromosome was performed to map the resistance. Indeed, based on the Chinese Spring reference genome (IWGSC RefSeq v1.0) a physical map of the wheat 5A chromosome was developed using KASP markers (Figure 2.7. and Figure 2.8.).

This study confirms that the source of resistance provided by WEK0609 is type II. Data collected from three summer poly tunnel trials in Norwich (UK) confirmed the location of the 5A locus, named *QFhb.WEK-5A*, on the long arm of the 5A chromosome. *QFhb.WEK-5A* was fine-mapped to a region from 389.64 and 395.89 Mbp (6.24 Mbp) between markers *S11* and *S18* and contains 44 annotated genes, which were extracted from Ensembl Plants (EMBL-EBI 2022).

Moreover, the type II resistance associated with *Qfhb.WEK-5A* may function against DON, since a reduction of bleaching above the point of infection was observed in 2018-2020 trials. This suggests that *Qfhb.WEK-5A* may restrict fungal colonisation and confer resistance or tolerance to DON or that a QTL conditioning low DON accumulation may be located close to the region of the gene or genes controlling disease spread, as has been previously reported (Bai, Shaner, and Ohm 2000).

2.5.2. FHB QTLs on the 5A chromosome

To investigate FHB resistance in wheat, many studies initially used specific markers such as RFLP (restriction fragment length polymorphism), SSR (simple sequence repeat), and AFLP (amplified fragment length polymorphism) to create genetic maps and identify QTLs. Recently, a revolution of genotyping technology has taken place and different technologies for SNP detection have been developed. These high-throughput SNP detection technologies are cost-effective and accelerate plant breeding programmes.

Wheat research has highly improved due to the completion of the genome sequence (International Wheat Genome Sequencing Consortium 2014) and the genome annotation (IWGSC 2018). These recent advances allow the genetic architecture of FHB resistance in wheat to be studied in more detail (Venske et al. 2019).

Previous studies have identified numerous different QTLs located on the 5A chromosome related with different sources of FHB resistance. A detailed list including information on the source of the QTL resistance, the mapping population and the phenotyping methods for a great number of studies is given in Table 2.10., which has been adapted (Buerstmayr, Ban, and Anderson 2009).

Table 2.10. *Detected 5A QTLs for Fusarium head blight resistance in wheat (adapted from Buerstmayr et al 2009). SFI = Single floret inoculation. SPRAY = spray inoculation. PI = Point inoculation.*

Source of resistance allele	Chromosome location	FHB resistance	Marker/s linked to the QTL	Plant material	Phenotyping	References
CM-820306	5AS (Qfhs.ifa-5A)	Type II *	Xgwm293 – Xgwm304	CM-82036 x Remus; 239 DH	F. graminearum, F. culmorum, SFI: 4 field exp.	(Buerstmayr et al. 2002)
CM-820306	5AS (Qfhs.ifa-5A)	Type I (FHB severity) *	Xgwm293 – Xgwm156	CM-82036 x Remus; 239 DH	F. graminearum, F. culmorum, SPRAY: 4 field exp.	(Buerstmayr et al. 2003)
Renan	5AL (QHt.inra-5a2)	Type I (FHB severity)	Xgwm639b and B1	Renan x Récital; 194 RIL	F. culmorum, SPRAY: 3 field exp.	(Gervais et al. 2003)
Fundulea F201R	5A	Type II	Xgwm304	Patterson x F201R; 318 (118) RIL	F. graminearum, SFI: 3 field exp.	(Shen, Ittu, and Ohm 2003)
Nyu Bai [a]	5AS (Qfhs.ifa-5A)	Type I and DON content/accumulation	Xgwm96	Wuhan 1 x Nyu Bai; 110 DH2	F. graminearum, SFI: 2 greenhouse exp., SPRAY: 2 field exp.	(Somers, Fedak, and Savard 2003)
93FHB21	5A	Type II	Xgwm291	AC Foremost x 93FHB21; 76 DH	F. graminearum, SFI: 1 greenhouse exp.	(Yang et al. 2003)
Arina	5A	Type I (FHB severity)	Xgwm291 – Xglk348c	Arina x Forno; 240 RIL	F. culmorum, SPRAY: 6 field exp.	(Paillard et al. 2004)
Frontana	5A	Type I (FHB severity)	Xgwm129 – Xbarc197	Remus x Frontana; 180 DH	F. graminearum, F. culmorum, SPRAY: 3 field exp.	(Steiner et al. 2004)
Wangshuibai	5A	Type I (FHB severity)	Xgwm129 – Xgwm156	Wangshuibai x Alondra	F. graminearum, Natural FHB infection evaluated for 3 years	(Jia et al. 2005)
DH181	5AS	Type I (FHB incidence)	Xgwm293 – xgwm305	DH181 x AC Foremost; 174 DH	F. graminearum, SFI: 3 greenhouse exp., SPRAY: 2 field exp.	(Yang et al. 2005)
W14 [b]	5AS	Type I, type II and DON accumulation *	Xbarc117 – Xbarc56	W14 x Pioneer Brand-2684 (Pion2684); 96 DH	F. graminearum, SFI: 2 greenhouse exp., SPRAY: 1 field exp.	(Chen et al. 2006)
Wangshuibai	5A (Qfhi.nau-5A)	Type I (FHB incidence)	Xwmc96 – Xgwm304 (from Xbarc56 – Xbarc100)	Nanda2419 x Wangshuibai; 154 RIL	F. graminearum, SPRAY: 3 field exp., grain spawn: 1 field exp.	(Lin et al. 2006)
Wangshuibai	5A	Type II and DON content	XmCCAeAAG.2 – Xgwm156 and Xgwm186 – XmCCA.eAAG.2	Wangshuibai x Annong8455; 118 RIL	F. graminearum, SFI: 2 field exp.	(Ma et al. 2006)
CJ 9306	5AS (QFhs.nau-5AS)	Type II and DON content	Xgwm425 – Xbarc186	Veery x CJ 9306; 152 RIL	F. graminearum, SFI: 3 greenhouse exp.	(Jiang et al. 2007)
Ernie	5A	Type II	Xbarc165	Ernie x MO94-317; 243 RIL	F. graminearum, SFI: 2 greenhouse exp.	(Liu et al. 2007)
Nyu Bai or Sumai 3	5AS	Type I (FHB severity) and DON content	Xwmc705, Xgwm304, Xgwm154	3 backcross populations involving: Nyu Bai, Wuhan 1 and Sumai 3	F. graminearum, SPRAY: 2 field exp.	(McCartney et al. 2007)
CM-82036	5A	Type I (FHB severity) and DON content	Xgwm156 – Xgwm304a	DH [CM-82036/Remus]/ Nandu/2/DH [Frontana/ Remus]/Munk	F. culmorum, SPRAY: 4 field exp.	(Miedaner et al. 2006; Wilde et al. 2007)

Table 2.10. Continued. *Detected 5A QTLs for Fusarium head blight resistance in wheat (adapted from Buerstmayr et al 2009). SFI = Single floret inoculation. SPRAY = spray inoculation. PI = Point inoculation.*

Source of resistance allele	Chromosome location	FHB resistance	Marker/s linked to the QTL	Plant material	Phenotyping	References
Sumai 3	5AS	Type II	Xgwm293 and Xgwm129	WSY developed from Sumai 3, Wangshuibai and Nobeokabouzo	F. graminearum, SFI: 1 greenhouse, SPRAY: 1 field exp. (nursery)	(Shi et al. 2008)
Wangshuibai	5AS (Qfhi.nau-5A or Fhb5)	Type I	barc180, barc117, gwm415, gwm304, mag3794	Wansghuibai x Mianyang 99-323; RILs NW66 and NW87	F. graminearum, SPRAY: 2 field exp.	(Xue et al. 2010)
T. macha	5AL	Type I and II	Xs20m18_11 – Xbarc319; peak at Q locus	Furore x T. macha (accession 1240001); 321 BC_2F_3	F. graminearum and F. culmorum, SPRAY: 6 field exp., grain spawn: 1 field exp	(Buerstmayr et al. 2011)
PI 277012	5AS (Qfhb.rwg-5A.1) and 5AL (Qfhb.rwg-5A.2)	Type I, II and DON accumulation	5AS (peak at Xbarc40; Xcfa2104 – Xgwm617) and 5AL (peak at Xcfd39; Xwmc470 – Xbarc48)	Grandin (PI 531005) x PI 277012; 130 DH	F. graminearum, SFI: 3 greenhouse and 2 field exp.	(Chu et al. 2011)
Haiyanzhong	5AS (QFhb.hyz-5A)	Type II (minor effect)	Xbarc56 – Xgwm129 or Xbarc141 – Xgwm129	Wheaton x HFZ	F. graminearum, SFI: 3 greenhouse and 1 field exp. (nursery)	(Li, Bai, et al. 2011)
Wangshuibai	5AS (Qfhi.nau-5A or Fhb5)	Type I	Xgwm304 – Xgwm415	Mianyang 99-323 recombinants; PH691 recombinants; Nanda2419 x Wansghuibai, 530 RIL	F. graminearum, grain spawn: 2 field exp.	(Xue et al. 2011)
Huangfangzhu	5AS	Type II (minor effect)	Xbarc117 and Xbarc186	Wheaton x HFZ	F. graminearum, SFI: 3 greenhouse and 1 field exp. (nursery)	(Li et al. 2012)
CM-82036	5A (Qfhs.ifa-5A)	Type I	5AS: barc186, gwm1057, barc56, gwm293, barc117 and gwm129; 5AL: barc1, barc180, barc40 and gmw156	CM-82036 x Remus; selection of NILs containing the 5A locus	F. graminearum, SFI: 1 greenhouse and 1 field exp.	(Schweiger, Steiner, et al. 2013)
PI 41025 (durum wheat)	5AL (Qfhb.rwg-5A.3)	Type II	Xwmc110 – IWA7009, peak at Xfcp650	PI 41025 x Ben (PI 596557)	F. graminearum, SFI: 3 greenhouse and 1 field exp. (nursery)	(Zhang et al. 2014)
Soru	5AL	Type I, II and DON accumulation	Type I: Vrn-A1 – Ex_c31769_793; Type II: Vrn-A1 – Ex_c7729_144	Soru#1 x Naxos; 131 RIL	F. graminearum, SFI: 1 field exp., SPRAY: 1 field exp., grain spawn: 1 field exp.	(He et al. 2016)
CM-82037 [b]	5AS (Qfhs.ifa-5A)	Type I (FHB severity)	C-5AS3-0.75 bin	CM-82036 x Remus; 364 DH	Map comparison	(Buerstmayr et al. 2018)
Yangmai 13	5AL (QFhbp-jaas.5AL-1)	Type II	BS00069175_51	C615 x Yangmai 13; 198 RIL	F. graminearum, SFI: 1 greenhouse exp., SPRAY: 2 field exp.	(Yi et al. 2018)
FL62R1	5AL	Type II	BS00036839_51 and BobWhite_c2236_111	FL62R1 x Stettler; 185 DH	F. graminearum, PI in greenhouses	(Zhang et al. 2018)
10Ae564 (durum wheat)	5AL (Qfhb.ndwp-5A)	Type II and DON content	IWB71377 – IWB8656, peak at IWB26525	Joppa (PI 673106) x 10Ae564 (PI 277012); 205 RIL	F. graminearum, SFI: 2 greenhouse and 2 field exp. (nursery)	(Zhao, Leng, et al. 2018)

Table 2.10. Continued. *Detected 5A QTLs for Fusarium head blight resistance in wheat (adapted from Buerstmayr et al 2009). SFI = Single floret inoculation. SPRAY = spray inoculation. PI = Point inoculation.*

Source of resistance allele	Chromosome location	FHB resistance	Marker/s linked to the QTL	Plant material	Phenotyping	References
CM-82036	5AS (Qfhs.ifa-5A)	Type I	Qfhs.ifa-5Ac (cfa2250 – wmc705) and Qfhs.ifa-5AS (barc56 – ldk49)	CM-82036 x Remus; selection of NILs containing the 5A locus	F. graminearum, SPRAY: 1 field and 1 greenhouse exp. In multiple years	(Steiner et al. 2019)
Yangmai 158	5AL (QFhb-5A)	Type II	IAAV5294 – BS00060445_51	Ningmai 9 x Yangmai 158; 282 RIL	F. graminearum, SFI: field exp.	(Jiang et al. 2020)

[a] Published as Wuhan 1 x Maringa (Somers, Fedak, and Savard 2003) but corrected to Wuhan 1 x Nyu Bai (McCartney et al. 2007).

[b] Composite interval mapping study.

*The effect of the 5A QTL was stronger after spray inoculation than after single floret inoculation.

Wheat 5A chromosome has been previously reported to carry FHB type I (Xu et al. 2001) and type II resistance genes (Buerstmayr et al. 1999; Buerstmayr et al. 2002) in different chromosomal regions based on corresponding marker positions. A compilation of the FHB QTLs type I and II resistances on the 5A chromosome are represented in their physical location (megabases) in Figure 2.9., which has been adapted from Jiang et al. 2020.

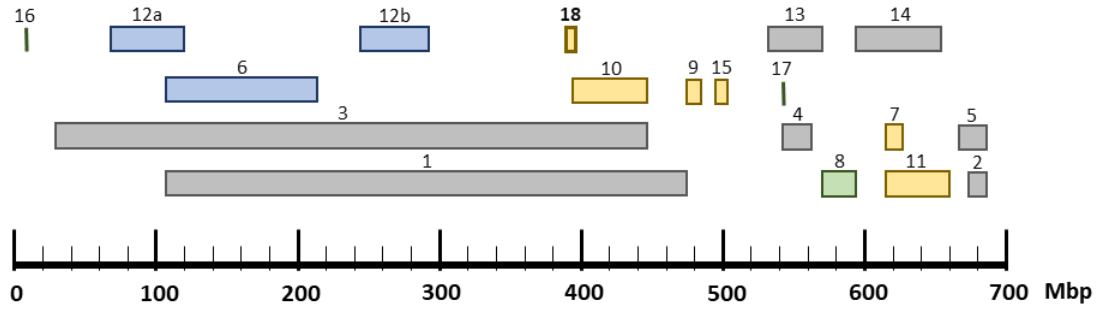

Figure 2.9. *Putative physical distribution of the quantitative trait loci for resistance to Fusarium head blight (FHB) on chromosome 5A (adapted from Jiang et al. 2020). '1' and '2' were proposed from the QTL meta-analysis by Löffler et al. (2009); '3','4' and '5' were proposed from the QTL meta-analysis by Liu et al. (2009); '6' was Fhb5 (Xue et al., 2011); '7', '8' and '9' were proposed by Zhang et al (2014), He et al. (2016) and Yi et al. (2018), respectively; '10' was proposed by Zhang et al. (2018); '11' was identified by Zhao et al. (2018); '12' was fine-mapped by Steiner et al. (2019) being '12a' the locus Qfhs.ifa-5AS and '12b' the locus Qfhs.ifa-5Ac; '13' and '14' were proposed from the QTL meta-analysis by Venske et al. (2019), who identified five QTL intervals but not all where represented; '15' was identified by Jiang et al. (2020); '16' and '17' were identified by Zhu et al. (2020); '18' was identified in this study. Grey rectangles indicate QTL meta-analysis studies. Blue rectangles indicate FHB type I resistances. Yellow rectangles indicate FHB type II resistances. Green rectangle indicates both type I and II resistances.*

QTLs for FHB type I resistance, measured as FHB severity and FHB incidence, have been identified on the 5A chromosome from cultivars: Nyu Bai, CM-820306, Renan, Frontana, Arina, DH181 and Wangshuibai (Table 2.10.) (Buerstmayr et al. 2003; Buerstmayr et al. 2018; Gervais et al. 2003; Jia et al. 2005; Li, Bai, et al. 2011; Lin et al. 2006; McCartney et al. 2007; Miedaner et al. 2006; Paillard et al. 2004; Schweiger, Steiner, et al. 2013; Somers, Fedak, and Savard 2003; Steiner et al. 2019; Steiner et al. 2004; Wilde et al. 2007; Xue et al. 2011; Yang et al. 2005).

One of the most mentioned 5A QTLs providing type I resistance is *Fhb5* (see Figure 2.9. '6'). The source of resistance of *Fhb5* is Wangshuibai and this QTL was mapped to the short arm of chromosome 5A using *Xwmc96–Xgwm304* (Lin et al. 2006; Xue et al. 2011; Xue et al. 2010). This locus was also identified by QTL meta-analysis (Liu et al. 2009; Löffler, Schön, and Miedaner 2009), and most probably by Venske et al 2019.

The 5A QTL found in cv. CM-820306 (*Qfhs.ifa-5A*) has been located on the short arm of chromosome 5A near the centromere and has been confirmed to be associated with type I resistance in numerous studies (Buerstmayr et al. 2003; Miedaner et al. 2006; Schweiger, Steiner, et al. 2013; Steiner et al. 2019; Wilde et al. 2007). The SSR markers *Xgwm293, Xgwm156 and Xgwm304* have been widely used to identify *Qfhs.ifa-5A* (Buerstmayr et al. 2003). Recently, Steiner et al (2019) fine mapped the FHB resistance QTL *Qfhs.ifa-5A* from Sumai 3 into two separated QTLs: *Qfhs.ifa-5Ac*, located in the proximity of the centromere, and *Qfhs.ifa-5AS,* located on the distal half of the 5AS (see Figure 2.9.'12a' and '12b').

Recently, it has been refined the interval of *Fhb5* very close to the centromere and therefore, partially overlapping with *Qfhs.ifa-5Ac* (Jia et al. 2018). This means that *Fhb5* partially overlaps with *Qfhs.ifa-5Ac,* and it is proposed that Sumai 3 and Wangshuibai share a common type I resistance gene. Due the pericentromeric position of this locus and the low recombination rate, fine-mapping of *Qfhs.ifa-5Ac* is still a challenge (Steiner et al. 2019).

QTLs on the 5A chromosome for FHB type II resistance, measured as FHB spread, have been also detected from cultivars Fundulea F201R, 93FHB21, CJ 9306, Ernie and Yangmai 158 (Table 2.10.) (Jiang et al. 2007; Jiang et al. 2020; Liu et al. 2007; Shen, Ittu, and Ohm 2003; Yang et al. 2003). To identify the Romanian cv. Fundulea F201R, *Xgwm304* was used to monitor the type II resistance (Shen, Ittu, and Ohm 2003).

In cv. CM-820306, Huangfangzhu and Haiyanzhong, the effect of the 5A QTL was stronger after spray inoculation than after single floret inoculation, but a minor effect on type

II resistance was observed (Buerstmayr et al. 2002; Li, Bai, et al. 2011; Li et al. 2012). For several cultivars, such as W14 and PI277012, the 5A QTL was associated with both type I and type II resistances, and with DON accumulation (Chen et al. 2006; Chu et al. 2011).

A QTL providing FHB type I and II resistances from a CIMMYT bread wheat line Soru#1 was identified on 5AL in a distal location (He et al. 2016). Novel QTLs on the 5AL were also identified in wheat accession PI 277012 (Chu et al. 2011), emmer wheat (Zhang et al. 2014), Yangmai 13 (Yi et al. 2018), and Yangmai 158 (Jiang et al. 2020). Recently, two QTLs associated with FHB resistance were identified on the 5A chromosome by using a genome-wide association analysis in Chinese elite wheat lines (Zhu et al. 2020). The 5AS QTL was associated with marker *IWB21456* at 9.6 Mbp and the 5AL QTL was associated with marker I*WB42293* at 540.6 Mbp.

QTL-meta-analysis is an efficient approach to verify whether QTLs observed in isolated studies correspond to different loci or whether they represent a common position on the genetic map. The aim of this type of analysis is to establish the occurrence of QTL "hotspots" in a consensus map. QTL meta-analysis studies have been performed for FHB resistance in wheat (Liu et al. 2009; Löffler, Schön, and Miedaner 2009; Mao et al. 2010; Venske et al. 2019). Based on the meta-analysis study of Liu et al (2009), a major cluster of type II resistance is located around the centromere in cultivars Sumai 3, Wangshuibai, CM82036, Ernie, Frontana and W14, and is separated from another cluster on the 5AL provided by Renan. For FHB type I resistance, two QTLs on the 5A were identified from Wangshuibai and Sumai 3 sources.

A type II resistance QTL from an eastern Canadian line, FL62R1, flanked by *BS00036839_51* and *BobWhite_c2236_111*, was also identified (Zhang et al. 2018). Physical location of the marker *BS00036839* is at 394 Mbp on the 5AL. Interestingly, *QFhb.WEK-5A* from the present study resides in a close genomic interval to that for FL62R1 (see Figure 2.9.

'10' and '18'). However, the genetic linkage map of the 5A chromosome suggested that the QTL region covered the entire centromeric region, leading Zhang et al. (2018) to assume that this QTL on the 5A is neighbouring *Fhb5*. The *Fhb5* QTL from Wangshuibai is reported to play a major role in type I resistance (Xue et al. 2011), but Zhang et al (2018) also indicate that *Fhb5* is also having a minor effect on type II resistance. Regardless, additional work is needed to confirm whether the 5AL QTL from FL62R1 is in fact *Fhb5* or is just very proximal to *Fhb5*.

Literature for the 5A FHB QTLs is complex and controversial since some loci associated with different types of FHB resistance and from various sources have been sometimes clustered in the same regions on the 5A chromosome (Table 2.10.). Since genetic maps created for many of these studies do not use the physical location, the chromosome location of target markers is unavailable. This means that the exact location of the 5A locus on the 5A chromosome was not determined for many of the previous studies. Nevertheless, it seems clear that the wheat chromosome 5A carries type I as well as type II resistance at different locations.

2.5.3. A new source of FHB resistance on the 5AL

From previous field and controlled environment trials, it is known that resistant cultivar WEK0609 may possess both type I and II FHB resistance (Gosman et al. 2007). The hypothesis at the start of the study was that the source of FHB resistance on chromosome 5A of WEK0609, and therefore from the population used for the current project, was derived from the Chinese wheat line Sumai 3 as a type I, or by the Romanian winter wheat cultivar Fundulea 201R (F201R) as a type II.

It is known that the cultivar Sumai 3 possesses resistance on the short arm of the 5A near the centromere (Buerstmayr et al. 2003; Somers, Fedak, and Savard 2003). Steiner et al. (2019) dissected the 5AS locus into *Qfhs.ifa-5Ac* and *Qfhs.ifa-5AS* (Figure 2.9. '13a-b'). Both QTLs peaks are more than 140 Mbp apart: *Qfhs.ifa-5AS* is located at 70.7-119.9 Mbp and

Qfhs.ifa-5Ac is located at 245.9-290 Mbp on the 5A chromosome of Chinese Spring reference genome (IWGSC RefSeq v1.0).

To characterize the 5A QTL for FHB resistance the allele sizes of SSR at this locus have been used in several studies (Gosman et al. 2007; McCartney et al. 2004). In these studies, SSR allele sizes of the cultivars under test were compared with those of known and characterised FHB resistance sources to establish whether haplotypes associated with FHB resistance were present and infer the origin of these in specific cultivars. For the study of McCartney et al. (2004), the haplotype of the *Qfhs.ifa-5A* locus for the cv. Sumai 3 and CM-82036 and Frontana was the same, differing from the haplotype for Wangshuibai, Ernie and Nyuubai. For the study of Gosman et al. (2007), two distinct haplotypes were identified at the *Qfhs.ifa-5A* locus. One was identical to cv. CM-82036, which is also shared by cv. Sumai-3, and the other is identical to the Russian cultivar Aurora shared by WEK0609 and Renan. Fundulea F201R, which carries a potent QTL for resistance in a similar position to *Qfhs.ifa-5A* (Shen, Ittu, and Ohm 2003), differed at the *Xgwm156* locus.

Cultivar F201R has been reported to have resistant genes against FHB derived from cultivars NS732, Amigo and possibly other parents involved in its complex genealogy (Ittu, Săulescu, and Ittu 2001). Gosman et al (2007) also carried out a study to infer the origin of resistance in different wheat cultivars based on allele sizes of SSR markers linked to QTLs. In this study, different haplotypes were identified at the 5A QTL locus. Interestingly, cultivar WEK0609 had a more similar haplotype to F201R than to Sumai 3. This may suggest that both WEK0609 and F201R cultivars are genetically more closely related, but they may not possess the same source of type II FHB resistance on the 5A. Indeed, a minor QTL for type II resistance in cultivar F201R was identified near the end of the short arm of the 5A (Shen, Ittu, and Ohm 2003). The exact location of this QTL on the 5AS is not known since a linkage map was developed using SSR markers for that study.

This suggests that neither Sumai 3 nor F201R provide the source of resistance in the population used for the present study, since *QFhb.WEK-5A* has been mapped on the 5AL (Figure 2.9. '18'). Hence, my findings suggest that the 5A type II resistance of WEK0609 may be derived from another cultivar, maybe from the Russian cultivar Aurora or similar pedigree. As the origin of the source of type II resistance provided by cv. WEK0609 is still not clear, it is possible that *QFhb.WEK-5A* may be a novel source of FHB resistance on chromosome 5A.

2.5.4. Conclusions and future work

In summary, data from the present study showed that a novel *QFhb.WEK-5A* for FHB type II resistance was identified. *QFhb.WEK-5A* has been mapped to 6.24 Mbp on the 5AL and there are 44 candidate genes that need to be further examined. It is also important to establish whether *QFhb.WEK-5A* is also associated with DON tolerance. If it is associated with both FHB type II resistance and DON tolerance, it will be important to determine whether there any genes associated with both traits. These questions will be addressed in the next chapter.

Due to the high genetic diversity for FHB resistance in wheat it is important to increase its effectiveness by pyramiding more than one gene into a cultivar, as has been demonstrated in the past with the Chinese cultivar Sumai 3. By using markers closely linked to QTLs, breeders can pyramid different resistance genes with MAS to achieve this purpose. *QFhb.WEK-5A* identified in this study could be implemented, together with other resistances, into UK breeding programmes to achieve more effective FHB resistance.

Chapter 3

Identification of differentially expressed DON responsive genes associated with the 5AL QTL (*QFhb.WEK-5A*) for Fusarium head blight resistance in bread wheat

3.1. Abstract

Fusarium Head Blight (FHB) is well-known to decrease yield but also contaminating the grain with mycotoxins. Some *Fusarium* sp. produce deoxynivalenol (DON). DON acts as a virulence factor in wheat since it promotes the spread of the pathogen infection. Resistance to DON may be underlying FHB type II resistance observed in the QTL on the 5A chromosome.

To confirm whether the 5A QTL associated with FHB type II resistance also confers DON tolerance, seedlings containing and not containing the locus were exposed to the mycotoxin and development of roots and shoots was monitored. To identify potential candidate genes involved in DON resistance on the 5A QTL, an RNA-Seq analysis was also performed.

In the present study, two orphan genes were identified on the 5A QTL to be potential associated with DON tolerance: *TraesCS5A02G191700* and *TraesCS5A02G191800*. Further expression studies also confirmed that both genes may be also associated with *Fusarium* resistance. Sequencing of both genes may reveal genomic differences with Chinese Spring reference genome.

3.2. Introduction

FHB not only decreases yield but also results in the contamination of grain with trichothecene mycotoxins, one of the most relevant being deoxynivalenol (DON) (McMullen, Jones, and Gallenberg 1997). The accumulation of DON in infected wheat grains is a risk for humans and livestock that consume the contaminated grain posing a risk to world food security (Pestka et al. 2004).

DON is a protein synthesis inhibitor and one of the most important mycotoxins that inhibits peptidyl transferase activity (Rocha, Ansari, and Doohan 2005). In wheat, DON is a virulence factor that enables the spread of FHB within the spike. *Fusarium graminearum* requires DON to spread from the initial point of infection to the adjacent spikelets and penetrate the rachis (Jansen et al. 2005). Thus, there is a close relationship between DON resistance and type II FHB resistance (Lemmens et al. 2005). Trichodiene synthase, encoded by *TRI5* in *F. graminearum*, is the first enzyme in the trichothecene biosynthetic pathway (Rynkiewicz, Cane, and Christianson 2001; Trapp et al. 1998). When the *TRI5* gene was disrupted, the DON-nonproducing mutants of *F. graminearum* lacked the ability to spread in wheat spikes (Bai, Desjardins, and Plattner 2002). Since DON promotes plant disease, the role of host responses to the accumulation is considered an important aspect of plant defence and resistance to *Fusarium* infection.

DON accumulation in FHB-susceptible wheat genotypes has been shown to be higher than in resistant ones (Goswami and Kistler 2005). Therefore, DON resistant wheat cultivars may be more likely to resist the spread of FHB in the spikes because DON accumulation is lower. This may be caused by the presence of genes involved in DON detoxification or similar mechanisms.

Wheat can detoxify DON by glycosylation, which is the main metabolic pathway of transforming the toxin to a less toxic compound. This has been demonstrated in *Arabidopsis*

thaliana, where a UDP glycosyltransferase (UGT) gene, known as *AtUGT73C5* or *DOGT1* (deoxynivalenol-glucosyltransferase 1), converts DON to the less toxic compound DON-3-*O*-glucoside (D3G) (Poppenberger et al. 2003). This conversion and the overexpression of the gene are correlated with DON resistance. The UGT *HvUGT1324* was identified in barley after infection with DON-producing *F. graminearum* (Boddu, Cho, and Muehlbauer 2007) and DON application (Gardiner et al. 2010). The ability of the product of this gene to convert DON to D3G was successfully demonstrated in both *A. thaliana* and yeast (Shin et al. 2012; Schweiger et al. 2010). *HvUGT1324* was then transformed into wheat and results showed high levels of FHB resistance (Li et al. 2015).

Despite this commonly well-known DON detoxifying mechanism, there are other means by which wheat plants can detoxify or reduce levels of DON inside plant cells. For instance, membrane transporters also play a role in protecting cells against the toxicity of DON. One of the most well-known are the multidrug resistance protein ABC (ATP-binding cassette) transporters, which have been identified through increased expression in response to DON and the fungal pathogen. In wheat *TaABCC3* was expressed very early after DON exposure, and virus induced gene-silencing targeting the homoeologous genes on 3A and 3B chromosomes led to an increase in bleaching of the spikelets upon DON inoculation (Walter et al. 2015).

Additional DON-related mechanisms may play an important role in FHB resistance in wheat. Through comparative genomics it has been possible to identify a portion of eukaryotic genes referred to as orphan genes, which are taxonomically restricted genes. These genes are phylogenetically restricted and do not encode any previously identified protein domain (Khalturin et al. 2009). Their functions remain unknown, but recent studies have revealed that these genes are key in favouring agronomic traits. This is the case with the *Triticum*

aestivum gene *Fusarium* Resistance Orphan Gene (*TaFROG*) which is highly DON-responsive and enhances wheat resistance to FHB (Perochon et al. 2015).

3.2.1. Chapter aims

I hypothesized that a mechanism of DON detoxification, or a similar mechanism, may be involved in the reduction of bleaching symptoms in wheat spikes by reducing the accumulation of DON and, consequently, decreasing the spread of FHB.

To confirm whether the genomic interval of 6.24 Mbp associated with FHB type II resistance also confers DON tolerance and, to identify potential candidate genes involved, the objectives were:

1) To determine whether +/- 5A QTL lines differ in DON tolerance by exposing seedlings to the mycotoxin and monitoring root and shoot development over time.
2) Perform an RNA-Seq analysis of +/- 5A QTL lines to identify DON responsive genes at the FHB 5A locus.
3) Establish whether the DON-responsive genes identified in the RNA-Seq are differentially expressed between +/- 5A QTL lines.

3.3. Material and Methods

3.3.1. DON assay on roots and shoots using +/- 5A QTL lines

3.3.1.1. Selection of lines

A recombinant inbred line population was created from a cross between Hobbit *sib* (susceptible parent) and WEKH85A (resistant parent), which is genetically similar to Hobbit *sib* except for chromosome 5A which comes from the resistant cultivar WEK0609 as described in Chapter 2.

Several RILs derived from the Hobbit *sib* x WEKH85A (F_7) were used in assays to determine relative DON tolerance. These RILs were chosen because of the specific recombination events on the long arm of chromosome 5A, between 317 - 418 Mbp: RIL 97, RIL 103, RIL 107 and Hobbit sib (Table 2.4.). Line RIL 97 contains the 5A QTL, while lines RIL 103, RIL 107 and Hobbit *sib* lack the 5A QTL.

3.3.1.2. DON assay

Around twenty seed of +/- 5A QTL lines were stratified for four days in Petri dishes containing 5 ml sterile distilled water on filter paper discs. To allow uniform germination, gibberellic acid (GA_3) (0.8 µl/ml) was added to the water. Seed was germinated at room temperature for 24 h and germinated seeds were transferred to individual, racked 15 ml tubes. Nine seeds were used per treatment: control tubes contained 8 ml of 0.4 % agar (Formedium) while DON tubes were supplemented with DON (5 µM). This concentration of DON was selected because previous work (by Dr Miguel Angelo Costa e Silva dos Santos) had demonstrated that the inhibition of root growth in susceptible varieties was not too severely affected.

Tubes were randomised in different racks and placed in a tray lined with wet paper and trays were covered with a clear lid to maintain high humidity. Trays were incubated in a

growth cabinet at 15°C under 16 h/8 h light/dark cycle. Root and shoot length of individual seedlings were measured every day after germination for a total of 7-10 days. Photos of tubes were taken every day, and final photos of seedlings removed from the tubes were taken on the last day of the experiment at 10 days post-infection (dpi).

3.3.1.3. Statistical analysis

Root and shoot length data of the +/- 5A QTL lines was analysed using Microsoft Excel (2016). The slope ('a' value from the 'y = ax' formula; where 'x' is dpi, and 'y' is the length of roots or shoots measured on each dpi) for both root and shoot data was calculated for each replicate on each treatment. Slope data was then analysed using an Unbalanced ANOVA in the Genstat software (v18.1), since the number of observations for all factors levels was unequal. Predicted means and S.E. of root and shoot data were calculated for each treatment and line. The percentage of the slope ratio between predicted means for treated (DON) and untreated (control) tissues was calculated for each line using Microsoft Excel (2016).

3.3.2. RNA-Seq analysis of roots of +/- 5A QTL lines exposed to DON

3.3.2.1. Selection of lines

Seed of RIL 97 (+ 5A QTL) and Hobbit *sib* (- 5A QTL) were selected for analysis. The selection of RIL 97 as the line containing the 5A QTL was done after the FHB summer trial in 2019. This line was selected because it was the only recombinant that harboured the entire 5A locus as identified at that time (see genotyping on Table 2.4. in Chapter 2). Despite not showing a very good performance against FHB in 2019 (Figure 2.3.), RIL 97 showed very good level of FHB type II resistance in 2018 (Figure S5) with low infected spikelets above (2.38 ± 1.14) and below (3.25 ± 1.65) the PI which were similar to those of the resistant parental line WEK5AH8 (5.30 ± 1.92 and 3.50 ± 0.22, above and below, respectively) at 14 dpi.

3.3.2.2. Seed preparation, inoculation, and experimental design

Four replicate Petri dishes were prepared for each treatment (Mock control and 5 µM DON) and line and were arranged in a propagator tray with clear lid to maintain humidity. Around twenty-five seeds of each corresponding line were stratified for three days in Petri dishes containing 5 ml sterile distilled water on filter paper discs. Seed was germinated at room temperature for 24 h. Roots were developed on the plate and after three days post-germination at room temperature, 20 ml of DON (5 µM) or water were applied accordingly to each plate, for DON and control treatments, respectively (Figure 3.1.). Roots were incubated for 6 h and then root tissue was harvested and immediately frozen in liquid nitrogen.

Figure 3.1. *Roots of lines RIL 97 (+ 5A QTL) and Hobbit sib (- 5A QTL) were developed on Petri dishes for three days. After this time, roots were incubated for 6 h with 20 ml of DON (5 µM) or water and root tissue was harvested and immediately frozen in liquid nitrogen.*

3.3.2.3. RNA extraction and sequencing

Samples were ground using a pestle and mortar under liquid nitrogen. Total RNA from roots were extracted using the RNeasy® Plant Mini Kit (Qiagen) following manufacturer's instructions (eluting in 30 µl water). An on-column DNase digestion was

performed with the RNase-free DNase Set (Qiagen), according to manufacturer's instructions, to purify the RNA. RNA integrity and quality were initially tested by separation on denaturing 1.5 % agarose gel electrophoresis and quantification using the spectrophotometer NanoDrop 2000 (Thermo Scientific). All samples had an RNA-integrity number > 6. At least 500 ng of RNA for sixteen samples (four replicates per treatment) was submitted to Genewiz (UK) for quality control, library preparation and RNA sequencing by Illumina HiSeq to create 15-20 million 150 bp paired-end reads per sample.

3.3.2.3. RNA-Seq data analysis

To analyse the RNA-Seq data, I sought help from Dr Pirita Paajanen (Computational and Systems Biology, JIC), who wrote very useful scripts which I could use for the analysis. A lot of support during the analysis was also provided by Dr Miguel Angelo Costa e Silva dos Santos, from our group.

Raw data was obtained as fasta files. To begin with, a quality control assessment (FastQC version 0.11.3) was performed on all raw files of each sample (each sample has a file for its forward and reverse strand). Trimmomatic (version 0.33) was used to trim the ends of each read of any remaining Illumina adapter sequences, followed by another FastQC assessment. Resultant reads were then mapped using HISAT2 (version 2.1.0) (Kim, Langmead, and Salzberg 2015) to wheat Chinese Spring reference genome (IWGSC RefSeq v1.0), sequence available from EnsemblPlants (EMBL-EBI 2022). Reads were sorted using Samtools (version 1.9). Kallisto (version 0.44.0) was used to map each read to a gene coding sequence and DESeq2 was used to quantify the abundance of each transcript when comparing treatments.

A gene count matrix was obtained containing a table with gene counts and transcripts per million (TPM). Additional tables were obtained for gene $\log_2$ fold change (FC) and statistical significance when comparing the following treatments and lines: RIL 97 upon

DON vs. control; RIL 97 upon DON vs. Hobbit *sib* upon DON; Hobbit *sib* upon DON vs. control; RIL 97 control vs. Hobbit *sib* control.

Venn diagrams were produced using the webtool Venny v2.1 and used to obtain lists of shared up- and down-regulated genes with a false-discovery-rate cut off 0.01 and a $\log_2$ FC > 2/-2 (Oliveros 2007-2015).

3.4. Results

3.4.1. Assessment of +/- 5A QTL lines for DON tolerance in roots and shoots

Root and shoot length were measured every day for a total of 9 dpi, and final photos of seedling development were taken at 10 dpi (Figure 3.2.), when seedlings were removed from agar tubes. Photos represent a random selection of three seedlings per line and treatment. Clear differences can be observed between control and DON treatments on the development of roots with a lesser effect observed for shoots. Another visual observation was that root length of RIL 97 (+5A QTL) was less inhibited than the other lines tested following exposure to DON.

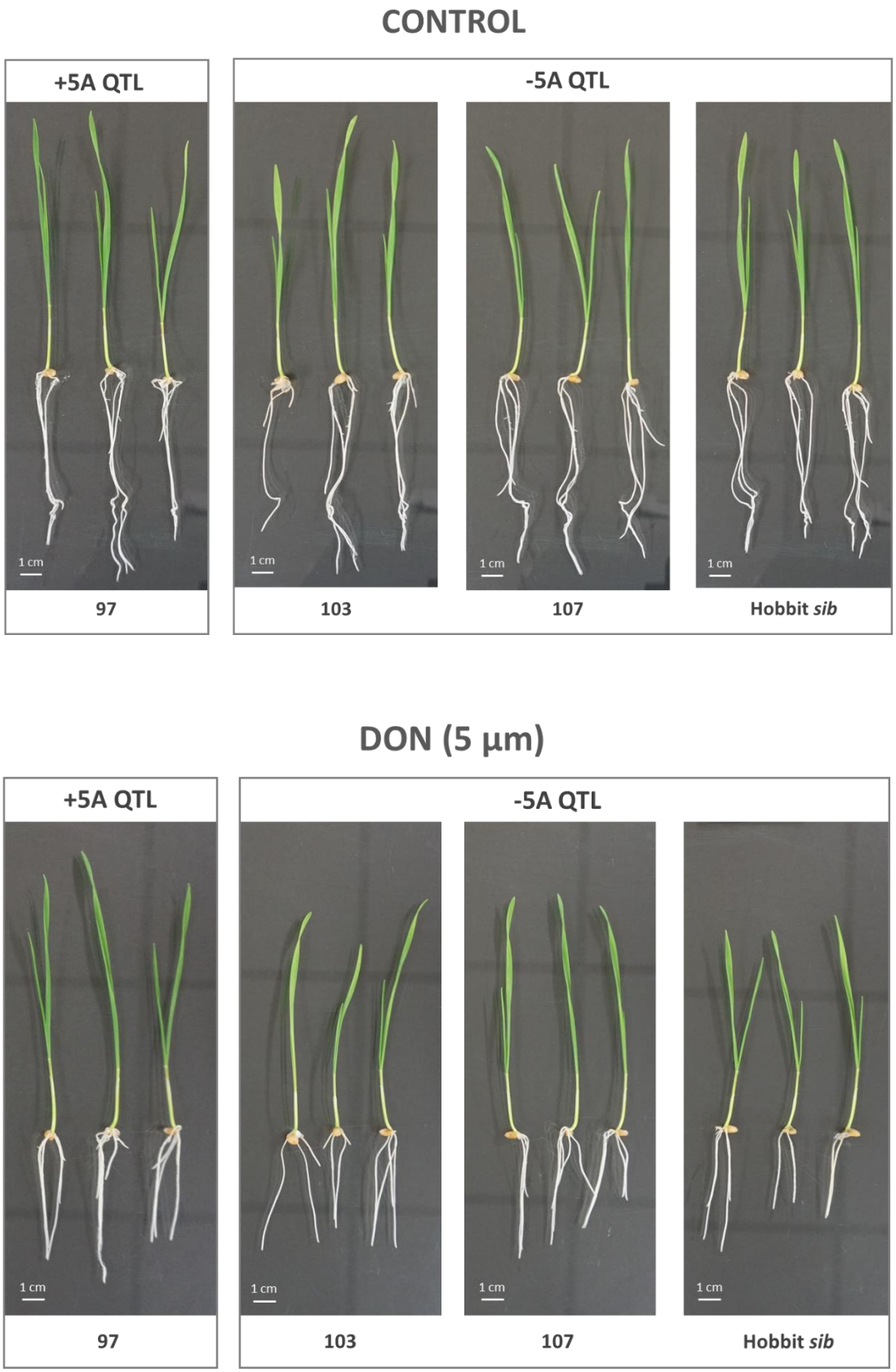

Figure 3.2. *Roots and shoots at 10 dpi of the + 5A QTL line (RILs 97) and - 5A QTL lines (RIL 103, RIL 107 and Hobbit sib) of seedlings grown in agar (control) and agar + DON (5 µM). Three random samples were selected of each line and treatment.*

To identify differences in DON tolerance, control and DON treatments for each line were compared. First, the slope data (see section 3.2.1.3.) was calculated for each replicate of a line given at each day post-infection (dpi; starting at 3 dpi). This was calculated for both root and shoot data. The slope data represents the average rate of root or shoot growth change over time after the application of treatments.

Roots and shoots slope data showed that lines *(P*-value < 0.05 and < 0.001, respectively) and treatments *(P*-value < 0.001 and < 0.05, respectively) significantly differ while the interaction between line and treatment had no significant influence, indicating that the two factors are independent of each other (Table 3.1. and Table 3.2.).

Table 3.1. *P-value of roots slope data of +/- 5A QTL wheat lines tested under DON (5 µm) and control treatments at different days post infection (dpi).*

	3 dpi	4 dpi	5 dpi	6 dpi	7 dpi	8 dpi	9 dpi
Line	0.001	0.005	0.004	0.002	0.005	0.006	0.007
Treatment	<.001	<.001	<.001	<.001	<.001	<.001	<.001
Line x Treatment	0.143	0.391	0.344	0.184	0.135	0.151	0.194

Table 3.2. *P-value of shoots slope data of +/- 5A QTL wheat lines tested under DON (5 µm) and control treatments at different days post infection (dpi).*

	3 dpi	4 dpi	5 dpi	6 dpi	7 dpi	8 dpi	9 dpi
Line	0.003	0.004	<.001	<.001	<.001	<.001	<.001
Treatment	0.011	0.009	0.005	0.007	0.007	0.008	0.01
Line x Treatment	0.457	0.369	0.405	0.429	0.467	0.380	0.489

The slope ratio (DON treatment/ control treatment) for each line was calculated and represented as percentage of root or shoot development (Figure 3.3.). The ratio DON/Control shows the effect of the DON treatment compared with the control.

Results revealed that roots of the line containing the 5A QTL (RIL 97) were less inhibited compared with lines no containing the 5A QTL (RIL 103, RIL 107 and Hobbit *sib*). The difference of root length between RIL 97 and Hobbit *sib* at 4 dpi was 21 % (Figure 3.3.-A), which decreased over time being of 14 % at 9 dpi (see Supplementary Data Table S8).

Differences of root length between RIL 97 and RIL 103 started at 12 % at 4 dpi and decreased to 9 % at 9 dpi; and between RIL 97 and RIL 107 were 14 % at 4 dpi and 12 % at 9 dpi.

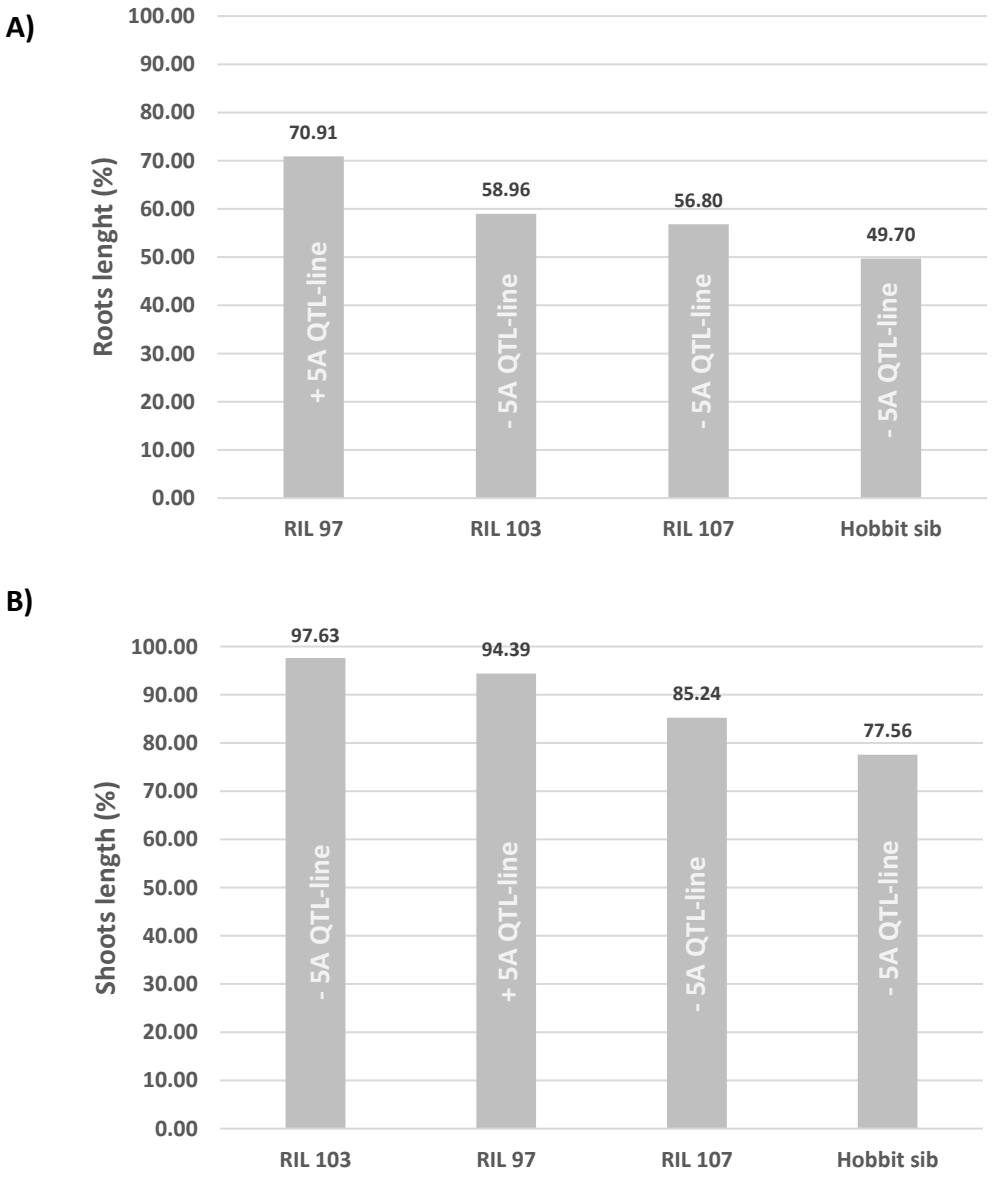

Figure 3.3. *Ratio DON/control (%) of roots (**A**) and shoots (**B**) at 4 dpi of a + 5A QTL line (RIL 97) and - 5A QTL lines (RIL 103, RIL 107 and Hobbit sib). Predicted means were generated using an Unbalanced ANOVA. The percentage of the ratio of root and shoots length between predicted mean treated (DON) and untreated (control) was calculated for each line. Percentage values for each line are shown on the top of each bar.*

Data collected for shoot development showed differences between treatments and lines (Table 3.2.). However, differences between lines did not necessarily correlate with the possession of the *QFhb.WEK5A* locus (Figure 3.3.-B). Clear differences in shoot development were observed between RIL 97 and Hobbit *sib* for DON treated seedlings. The inhibition of shoot length between RIL 97 and parental line Hobbit *sib* at 4 dpi was 17 % (see Supplementary Data Table S9), which also decreased over time being of 12 % at 9 dpi. Differences of shoot length between RIL 97 and RIL 107 started at 9 % at 4 dpi and decreased to 5 % at 9 dpi. However, RIL 103, which does not possess the *QFhb.WEK5A* locus, showed less inhibition upon DON exposure of shoot development than RIL 97.

In summary, the average percentage difference between DON and control treatments in roots was 41 % of inhibition, while in shoots was only 11 % of inhibition. The effect of DON exposure, thus, was greater on roots than on shoots. This may imply that shoot growth was not a good indicator of DON tolerance in wheat.

To conclude, these findings support the hypothesis that line RIL 97, which harbours the 5AL locus for FHB type II resistance, may also harbour genes associated with DON tolerance in the same genomic region. To identify which genes responding to the presence of DON, and so may be involved in DON tolerance, in the 5A QTL, RNA-Seq analysis was performed.

3.4.2. RNA-Seq analysis of +/- 5A QTL lines in response to DON

Previous work using *Brachypodium distachyon* to identify genes differentially expressed upon exposure to DON (Santos 2021) had revealed that response to DON (5 µM) after 6 h was much greater than at 24 h.

RNA sequencing data was analysed to create a list of differentially expressed genes (DEGs) for both +/- 5A QTL lines between DON and the control treatments. Firstly, I wanted

to recheck which genes were differentially expressed wherever in the entire genome for both RIL 97 (+ 5A QTL) and Hobbit *sib* (- 5A QTL) in response to DON.

DEGs (*P*-value ≤ 0.01) between DON and control treatments of RIL 97 and Hobbit *sib* lines were extracted from the entire genome. Then, those DEGs with a $\log_2$ FC ≥ 2.0/ ≤ -2.0 were identified for both lines. Up-regulated genes ($\log_2$ FC ≥ 2.0), whether the gene is more expressed upon DON, and down-regulated genes ($\log_2$ FC ≤ -2.0), whether the gene is more expressed in the control treatment, for both +/- 5A QTL lines were represented in a Venn diagram (Venny 2.1.0) (Figure 3.4.-A).

Detailed information about all the genes in the wheat genome which showed a response upon DON exposure can be seen in Supplementary Excel file (Tables EF1-4), in which specifications about gene annotations, gene start and end (bp) location, $\log_2$ FC and *P*-values are listed.

RIL 97 (+ 5A QTL) showed a greater response to DON in its entire genome than Hobbit *sib* with 581 genes being specifically more highly expressed and 55 genes being significantly less expressed (Supplementary Excel file Table EF1 and Table EF2). In contrast, only 27 genes were specifically more highly expressed in the susceptible line Hobbit *sib* (- 5A QTL) on exposure to DON (Supplementary Excel file Table EF3). Additionally, both lines shared 202 DEGs in response to DON (Supplementary Excel file Table EF4, and Figure 3.4.-A).

The most common type of genes which were up-regulated were protein detoxification-related genes and UGT genes. However, many of the DEGs identified have not been yet annotated in the Chinese Spring reference genome (IWGSC RefSeq v1.0.).

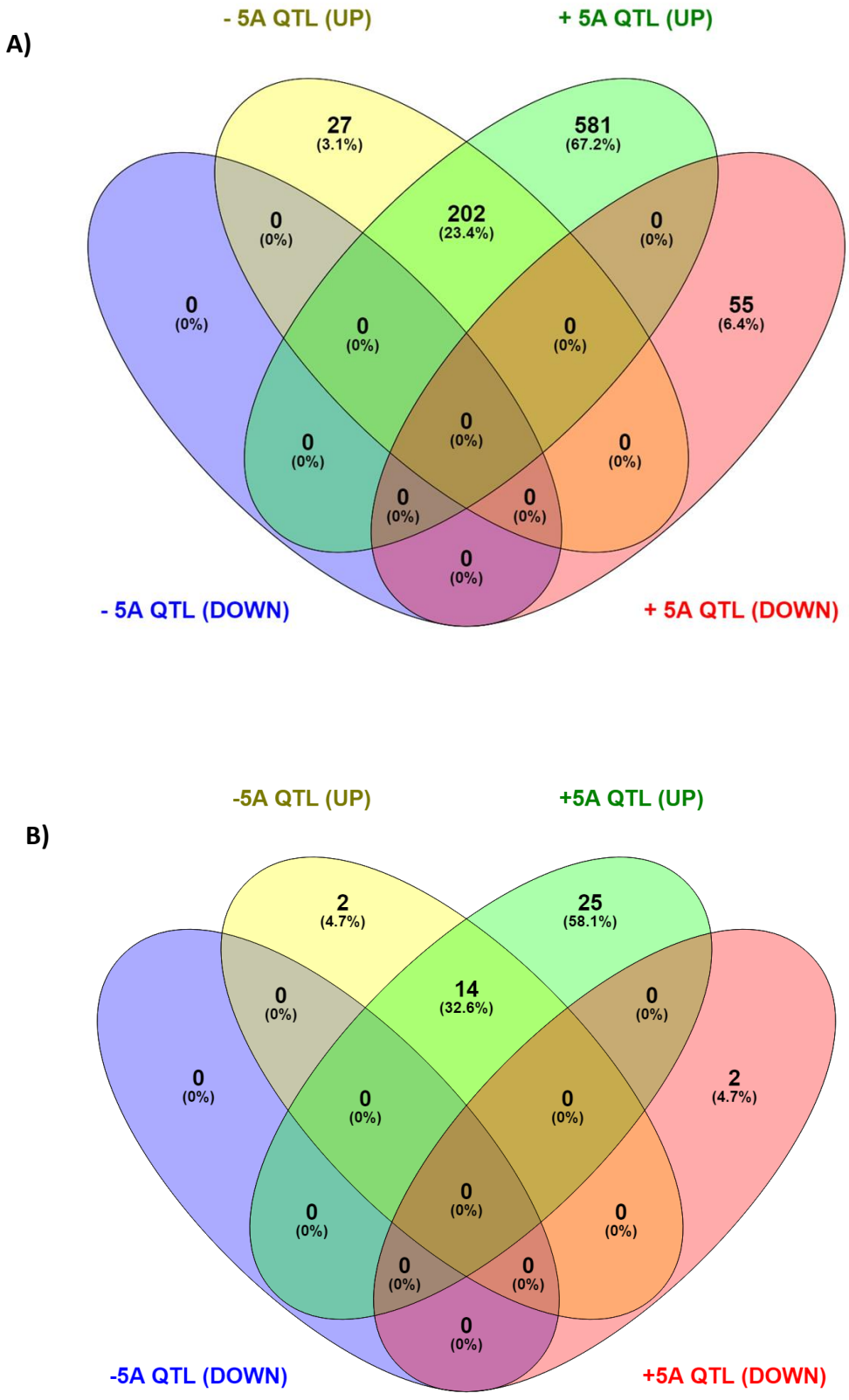

Figure 3.4. A) *Up-regulated (DON) and down-regulated (control) differentially expressed genes (DEGs) of RIL 97 and Hobbit sib lines (+ 5A QTL and - 5A QTL, respectively) on the full genome of wheat.* ***B)*** *Up-regulated (DON) and down-regulated (control) DEGs of RIL 97 and Hobbit sib lines on the 5A chromosome of wheat.*

Several protein detoxification genes with a very high expression value in RIL 97 were genes *TraesCS7D02G484500*, *TraesCS7A02G497300* and *TraesCS7B02G400500* with a $\log_2$ FC of 9.33, 8.81 and 8.23, respectively (Supplementary Excel file Table EF1). *TraesCS7A02G497300* and *TraesCS7D02G484500* were specific of RIL 97 but were not identified as being highly expressed upon DON exposure in Hobbit *sib*.

Common DEGs identified upon DON for both +/- 5A QTL lines (and that have been annotated) were *TraesCS7B02G400500* ($\log_2$ FC = 8.23 in RIL 97, $\log_2$ FC = 4.84 in Hobbit *sib*), and *TraesCS2A02G463300*, which encodes a UGT gene ($\log_2$ FC = 5.70 in RIL 97, $\log_2$ FC = 3.45 in Hobbit *sib*) (Supplementary Excel file Table EF4).

Then, to identify significant DEGs on the 5A chromosome the same parameters (*P*-value ≤ 0.01; $\log_2$ FC ≥ 2.0/ ≤ -2.0) were used but only those genes located on the 5A were selected for both lines. RIL 97 also showed a greater response to DON than Hobbit *sib* with 25 genes being more highly expressed and two genes being significantly less expressed. In contrast, Hobbit *sib* had only two genes highly expressed upon DON exposure (Figure 3.4.-B). Detailed information about these DEGs in the 5A chromosome can be seen in Supplementary data (Table S10, Table S11, Table S12 and Table S13).

TraesCS5A02G545100LC, which is a low confidence (LC) gene, was identified in RIL 97 as being highly expressed upon DON ($\log_2$ FC = 7.02), but not in Hobbit *sib.* *TraesCS5A02G368900* was also highly expressed upon DON in RIL 97 ($\log_2$ FC = 4.45) but not in Hobbit *sib*. Neither of these genes have annotations in the reference genome, so gene function is unknown. Nevertheless, *TraesCS5A02G368900* may encode for a protein involved in detoxification since this gene is in a very close proximity to genes *TraesCS5A02G368600, TraesCS5A02G368700* and *TraesCS5A02G368800*. These genes are highly differentially expressed in RIL 97 ($\log_2$ FC = 4.00, 3.40 and 4.36, respectively), and located on the long arm of chromosome 5A at 569 Mbp (Supplementary data Table S10). These three genes were also

identified to be highly expressed in Hobbit *sib* (log_2 FC = 2.71, 2.65 and 3.05, respectively) (Supplementary data Table S12).

Expression of only two 5A genes was significantly reduced upon control treatment in RIL 97. These genes, which have not been annotated, were *TraesCS5A02G535900* and *TraesCS5A02G023700* (log_2 FC = -2.02 and -2.36, respectively) (Supplementary data Table S11).

DEGs identified in the 5A chromosome of wheat and specific of Hobbit *sib* were *TraesCS5A02G545000LC* (log_2 FC = 3.44) and *TraesCS5A02G300000LC* (log_2 FC = 2.55) (Supplementary data Table S12), which are LC genes and have not been annotated in the Chinese Spring reference genome.

Additionally, both lines shared 14 DEGs in response to DON (Figure 3.4.-B). While *TraesCS5A02G065500* (log_2 FC = 5.24 in RIL 97, log_2 FC = 3.26 in Hobbit *sib*) was more highly differentially expressed in RIL 97, *TraesCS5A02G325100* (log_2 FC = 2.51 in RIL 97, log_2 FC = 4.22 in Hobbit *sib*) was more highly expressed in Hobbit *sib.* Both lines shared the three DEGs previously mentioned (*TraesCS5A02G368600, TraesCS5A02G367600* and *TraesCS5A02G368800),* which are involved in protein detoxification. There was also a gene encoding a UGT, gene *TraesCS5A02G149600* (log_2 FC = 3.86 in RIL 97, log_2 FC = 2.35 in Hobbit *sib*) (Supplementary data Table S13).

3.4.3. DEGs in response to DON on the 5A locus of RIL 97

Recombinant line RIL 97 (+5A QTL) harbours the FHB type II resistance provided by parental line WEKH85A on the 5A chromosome. The WEKH85A introgression in this line is of at least 101 Mbp, from 322 to 417 Mbp (see Figure 2.3 in Chapter 2) since recombination points are located between markers *S4-S5* and *S28-S29*. Thus, the question to be asked is,

which of those DEGs previously identified on the 5A chromosome are located within the 5A locus of RIL 97?

When focusing only on the DEGs located on the WEKH85A introgression of RIL 97, there are just eight genes that are up-regulated upon DON exposure. No gene in this interval was down-regulated following DON exposure, which explains the simplification of the Venn diagram (Figure 3.5.).

Five DEGs are specific to RIL 97 (+ 5A QTL) and, therefore, are specific of the parental line providing the resistance, WEKH85A (Figure 3.5 and Table 3.3). These genes, which have not been annotated on the reference genome, are *TraesCS5A02G149700, TraesCS5A02G180900, TraesCS5A02G298500LC, TraesCS5A02G304000LC* and *TraesCS5A02G191800*. Two of these genes have been annotated with LC by IWGSC.

Three genes are differentially expressed in common for both RIL 97 and Hobbit *sib*, so they are highly expressed upon DON treatment in both +/- 5A QTL lines (Figure 3.5 and Table 3.4.). These genes are *TraesCS5A02G149600, TraesCS5A02G183500* and *TraesCS5A02G196400,* and only the first of these has been annotated (glycosyltransferase).

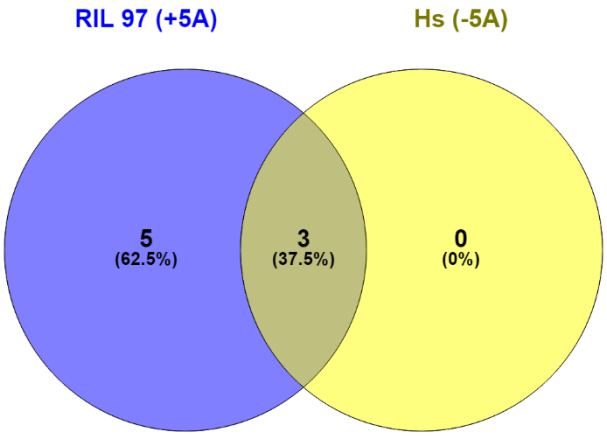

Figure 3.5. *DEGs upon DON for RIL 97, on the 5A locus (from 322 to 417 Mbp), and Hobbit sib (Hs).*

Table 3.3. *Specific DEGs of RIL 97 (+ 5A QTL), and from parental line WEKH85A, located on the introgression (from 322 to 417 Mbp). For each DEG, the log_2 FC and the P-value are shown. Gene ID, start and end (bp) location obtained from the IWGSC RefSeq v1.1. Annotation of genes (when available) are shown.*

IWGSC RefSeq v1.1			Annotation	log_2(FC)	*P*-value
Name	**Start (bp)**	**End (bp)**			
TraesCS5A02G149700	327575915	327577750	n/a	2.30	8.3E-06
TraesCS5A02G180900	379355434	379356264	n/a	2.24	1.2E-05
TraesCS5A02G298500LC	382284803	382285946	n/a	4.25	1.8E-17
TraesCS5A02G304000LC	391512387	391513778	n/a	2.52	1.1E-06
TraesCS5A02G191800	395847109	395848224	n/a	2.29	3.7E-06

Table 3.4. *Common DEGs for both RIL 97 (+ 5A QTL) and Hobbit sib (- 5A QTL) located on WEK5A (from 322 to 417 Mbp). For each DEG, the log2 FC and the P-value are shown. Gene ID, start and end (bp) location obtained from the IWGSC RefSeq v1.1. Annotation of genes (when available) are shown.*

IWGSC RefSeq v1.1			Annotation	RIL 97		Hobbit *sib*	
Name	**Start (bp)**	**End (bp)**		log_2(FC)	*P*-value	log_2(FC)	*P*-value
TraesCS5A02G149600	327573796	327581013	Glycosyltransferase	3.86	1.8E-37	2.35	4.9E-33
TraesCS5A02G183500	383191065	383192590	n/a	2.37	4.6E-06	2.57	1.9E-14
TraesCS5A02G196400	400410933	400413943	n/a	4.44	3.4E-21	2.99	1.1E-19

3.4.4. DON-candidate genes on the FHB type II *QFhb.WEK5A* locus

By the end of Summer 2020, and with the collaboration of the iCase partner Limagrain, the 5A QTL for FHB type II resistance was refined to 6.24 Mbp on the long arm of chromosome 5A (see Figure 2.8. on Chapter 2). This was achieved thanks to the combination of specific RILs tested for FHB type II resistance in Summer 2020, and the development of new KASP markers at the 5A locus.

The identification of novel SNPs between +/- 5A QTL lines was performed by the 'Marker development and genomic resources team' at Limagrain by using the RNA-Seq data as well as an Exome capture data set (unpublished data). Only SNPs identified on the 5A chromosome were provided. Then, I selected those SNPs located on the 5A chromosome, between 317 - 418 Mbp, and developed new KASPs - detailed protocol of KASP development can be found in the Materials and Methods section of Chapter 2. Specific RILs (RIL 9A, RIL 10B, RIL 16A and RIL 17B) and parental lines, WEKH85A and Hobbit *sib*, were then screened with those markers (see Figure 2.8. on Chapter 2).

Only two DON- responsive genes are located on the 6.24 Mbp-interval and are specifically expressed in RIL 97 (+ 5A QTL), so are provided by the resistant parent WEKH85A. These genes are a low confidence gene, *TraesCS5A02G304000LC*, located at 391.5 Mbp, and *TraesCS5A02G191800* at 395.8 Mbp (Figure 3.6).

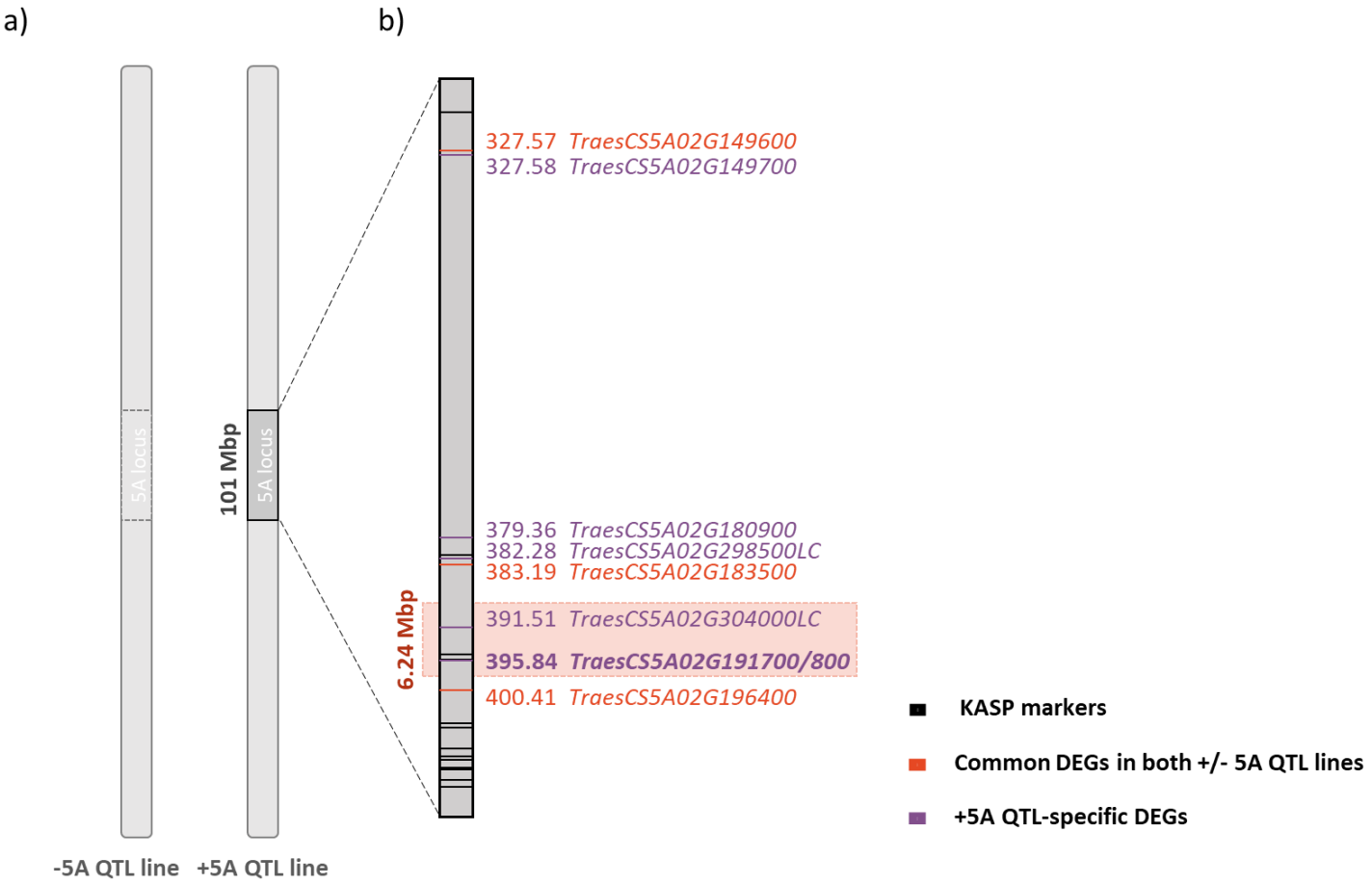

Figure 3.6. *a) Physical representation of the 5A chromosome for parental line Hobbit sib (- 5A QTL line) and RIL 97 (+ 5A QTL line), and the location of the 5A WEKH85A on RIL 97. b) Location on the 5A locus of the differentially expressed genes (DEGs) identified in the RNA-Seq analysis of roots exposed to DON. Specific DEGs of line RIL 97 (+5A QTL) are highlighted in purple. Common DEGS in both +/- 5A QTL lines are highlighted in red. Black lines on the 5A locus represent the KASPs markers used for the fine-mapping of the 5A QTL. Location of each DEGs is represented in Mbp next to the gene ID. Fine-mapping of the 5A QTL (6.24 Mbp) after Summer 2020 for FHB type II resistance is highlighted with a red rectangle.*

The paralogue of gene *TraesCS5A02G191800* is the adjacent gene *TraesCS5A02G191700* located very close by at 395 Mbp (Figure 3.6.). Gene *TraesCS5A02G191700* was also selected as a promising DON-candidate gene on the 5A locus based on its high level of protein sequence similarity with gene *TraesCS5A02G191800* which indicates that both genes may contribute to DON tolerance (Figure 3.7.).

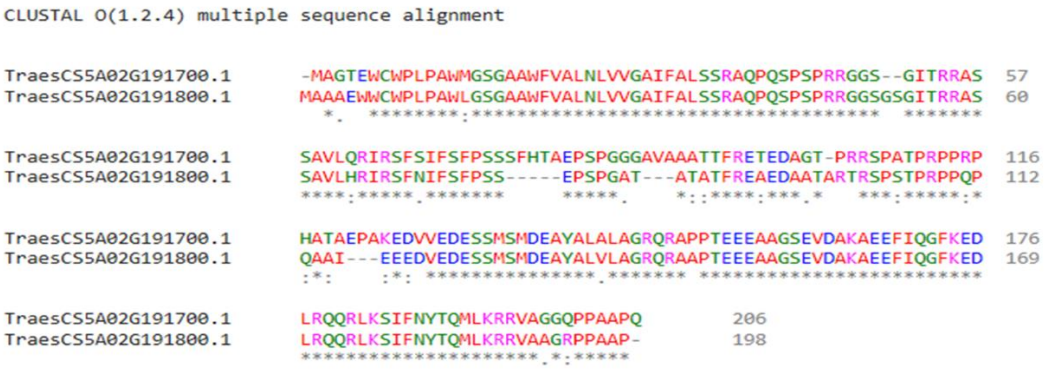

Figure 3.7. *Protein sequences similarly between TraesCS5A02G191700 and gene TraesCS5A02G191800 located on the 5AL at 395 Mbp. Alignment of sequences was performed using Clustal Omega (https://www.ebi.ac.uk/Tools/msa/clustalo/).*

Gene *TraesCS5A02G191700* was not identified during the RNA-Seq analysis because for the data analysis a $\log_2$ FC ≥ 2 was used to filter the DEGs expressed upon DON treatment. This gene had a $\log_2$ FC = 1.84 when comparing DON and control treatments of RIL 97 (+ 5A QTL), and $\log_2$ FC = 1.06 when comparing DON and control treatments of Hobbit *sib* (- 5A QTL) (Table 3.5.). Thus, it was excluded from the analysis. In contrast, gene *TraesCS5A02G191800* had a $\log_2$ FC = 2.24 when comparing DON and control treatments of RIL 97 (+ 5A QTL) and, therefore, it was identified during the analysis.

Expression of gene *TraesCS5A02G191700* was statistically significantly different when comparing both DON and control treatments of RIL 97 (+ 5A QTL) and Hobbit *sib* (- 5A QTL) (*P*-value = 5.50 x 10^{-8} and 0.001, respectively). This outcome meant that while expression of *TraesCS5A02G191800* is increased upon DON treatment and is specific of RIL

97, the + 5A QTL line, expression of *TraesCS5A02G191700* is increased in both +/- 5A QTL lines. However, when comparing the expression level of this gene upon DON treatment in both lines, there was a significant difference in gene expression (*P*-value = 0.02) between RIL 97 and Hobbit *sib* being more expressed in the + 5A QTL line (RIL 97) (Table 3.5.).

Table 3.5. *Log_2 FC and P-value data extracted from the RNA-Seq analysis performed in roots upon DON and control treatments for lines RIL 97 (+ 5A QTL) and Hobbit sib (- 5A QTL) for paralogues genes TraesCS5A02G191700 and TraesCS5A02G191800.*

		TraesCS5A02G191700	TraesCS5A02G191800
RIL 97 DON vs. Control	**log_2 FC**	1.84	2.29
	P-value	5.50×10^{-8}	3.68×10^{-6}
Hobbit sib DON vs. Control	**log_2 FC**	1.06	0.40
	P-value	0.001	0.200
DON RIL 97 vs. Hobbit sib	**log_2 FC**	0.71	0.40
	P-value	0.020	0.230
Control RIL 97 vs. Hobbit sib	**log_2 FC**	0.30	-0.24
	P-value	0.330	0.390

Information about gene counts and the TPM obtained from the RNA-Seq analysis for these nine genes in the 5A QTL interval (Figure 3.6.) can be found in Table S14 and Table S15, respectively, of the Supplementary data. Gene counts and TPM showed that gene *TraesCS5A02G191700* was more highly expressed than *TraesCS5A02G191800* in RIL 97 upon DON (TPM = 11.85, gene count = 177.61) (Table 3.6.).

Table 3.6. *TPM and gene counts data extracted from the RNA-Seq analysis performed in roots upon DON and control treatments for lines RIL 97 (+ 5A QTL) and Hobbit sib (- 5A QTL) for paralogues genes TraesCS5A02G191700 and TraesCS5A02G191800.*

			TraesCS5A02G191700	TraesCS5A02G191800
RIL 97	**DON**	**TPM**	11.85	3.13
		Gene counts	177.61	44.75
	Control	**TPM**	2.79	0.25
		Gene counts	38.5	4.00
Hobbit sib	**DON**	**TPM**	6.37	1.47
		Gene counts	53.75	11.25
	Control	**TPM**	2.01	0.52
		Gene counts	27.25	7.25

Expression levels of the homoeologous genes of *TraesCS5A02G191700* and *TraesCS5A02G191800* were also verified (see Table S16 and Table S17, respectively, in the Supplementary data).

The homoeologous gene of *TraesCS5A02G191700* on the 5B chromosome is *TraesCS5B02G191400*. This gene was differentially expressed between DON and control treatments for both lines, with the response for RIL 97 (+5A QTL) being greater (log_2 FC = 1.59, P-value = 1×10^{-7}) than for Hobbit *sib* (log_2 FC = 0.69, P-value = 0.04) (Table S16). The homoeologous gene of *TraesCS5A02G191800* on the 5B chromosome is *TraesCS5B02G191300*, which had the same pattern of expression again being more highly expressed in RIL 97 (log_2 FC = 1.84, P-value = 1×10^{-5}) than in Hobbit *sib* (log_2 FC = 0.96, P-value = 0.005). Expression of *TraesCS5B02G191300* was significantly enhanced following DON treatment in both lines (log_2 FC = 1.00, P-value < 0.001). The homoeologous gene of *TraesCS5A02G191800* on the 5D chromosome, *TraesCS5D02G199100*, was very highly differentially expressed between treatments for RIL 97 (log_2 FC = 2.43, P-value = 1×10^{-8}) but not significantly affected in Hobbit *sib* (log_2 FC = 0.56, P-value = 0.095) (Table S17).

In summary, there appear to be two potential DON-responsive candidate genes in the 5A QTL interval for FHB type II resistance that have been annotated with high confidence by IWGSC. These genes are *TraesCS5A02G191700* and *TraesCS5A02G191800*. The public availability of RNA-Seq expression data from wheat allowed two additional questions to be posed. Are these genes also expressed upon *Fusarium*? Is there any other gene in the QTL interval that is also expressed upon the pathogen?

3.4.5. DON-candidate genes also expressed upon *Fusarium* sp.

There are 44 annotated genes (IWGSC RefSeq v1.0) within the 6.24 Mbp interval, any of which could be potential candidates for FHB type II resistance on the 5A chromosome. The online browser expVIP (Ramírez-González et al. 2018; Borrill, Ramirez-Gonzalez, and Uauy 2016), was used to examine expression of the 44 genes following infection by *Fusarium*. The browser contains three *Fusarium* studies (Gou et al. 2016; Schweiger et al. 2016; Kugler et al. 2013) that were used to investigate the expression level of the 44 annotated genes.

Information on the 44 genes (location and annotation), and expression when exposed to *Fusarium* are shown in Table 3.7., which also summarises the expression of these genes when exposed to DON from the present work.

Expression of several genes (*TraesCS5A02G189500, TraesCS5A02G189700, TraesCS5A02G190400, TraesCS5A02G191200* and *TraesCS5A02G191900*) were slightly expressed upon infection by the pathogen, while DON-candidate genes *TraesCS5A02G191700* and *TraesCS5A02G191800* were highly expressed upon *Fusarium* infection (Table 3.7., highlighted in yellow and green, respectively).

When visualizing the expression levels of both DON-candidate genes *TraesCS5A02G191700* and *TraesCS5A02G191800* in expVIP for the three *Fusarium* studies previously mentioned (Figure 3.8., Figure 3.9. and Figure 3.10.), I observed that gene *TraesCS5A02G191700* is higher expressed than *TraesCS5A02G191800*. The expression levels of both genes increased over time being very high after 2 dpi (48-50 h) (Schweiger et al. 2016; Kugler et al. 2013) and at 4 dpi (Gou et al. 2016). These findings may suggest that both genes are promising genes involved in DON tolerance as well as FHB type II resistance and merit further study.

Table 3.7. *Annotated genes located on the 5AL locus of 6.24 Mbp. IWGSC RefSeqv1.1 gene name and physical location of gene start and end (bp) are shown. Gene description is also provided when available. Increased expression upon DON[1] treatment (Yes or No) was obtained from the RNA-Seq analysis, and increased expression upon Fusarium[2] treatment (Yes or No) from expVIP studies performed with the pathogen in wheat (http://www.wheat-expression.com/).*

IWGSC RefSeq v1.1			Gene description	Expression upon DON[1]	Expression upon *Fusarium*[2]
Name	**Start (bp)**	**End (bp)**			
TraesCS5A02G187900	389713723	389715786	n/a	No	No
TraesCS5A02G188000	389716642	389718098	n/a	No	No
TraesCS5A02G188100	389719370	389724310	Enolase 1 // chloroplastic	No	No
TraesCS5A02G188200	389724313	389726710	n/a	No	No
TraesCS5A02G188300	389763146	389764957	n/a	No	No
TraesCS5A02G188400	390229534	390231245	n/a	No	No
TraesCS5A02G188500	390234284	390237986	n/a	No	No
TraesCS5A02G188600	390242133	390244439	n/a	No	No
TraesCS5A02G188700	390365810	390370864	n/a	No	No
TraesCS5A02G188800	390552710	390563403	n/a	No	No
TraesCS5A02G188900	390730454	390734791	n/a	No	No
TraesCS5A02G189000	391516937	391521446	n/a	No	No
TraesCS5A02G189100	391542907	391548314	Tetratricopeptide repeat protein 1	No	No
TraesCS5A02G189200	391548711	391554182	n/a	No	No
TraesCS5A02G189300	391977248	391978991	n/a	No	No
TraesCS5A02G189400	391998137	392000722	n/a	No	No
TraesCS5A02G189500	392035064	392038145	MFS domain-containing protein	No	**Yes**
TraesCS5A02G189600	392574715	392585765	MPN domain-containing protein // spliceosomal tri-snRNP complex assembly	No	No
TraesCS5A02G189700	393252482	393254499	VQ domain-containing protein	No	**Yes**
TraesCS5A02G189800	393363595	393365096	Succinate dehydrogenase [ubiquinone] iron-sulfur subunit 3 // mitochondrial	No	No
TraesCS5A02G189900	393469551	393478023	n/a	No	No
TraesCS5A02G190000	394181080	394183400	Trehalose 6-phosphate phosphatase	No	No
TraesCS5A02G190100	394556419	394558559	n/a	No	No
TraesCS5A02G190200	394753167	394754858	n/a	No	No
TraesCS5A02G190300	394753672	394754694	n/a	No	No
TraesCS5A02G190400	394755631	394759459	HCC2 // copper ion homeostasis // mitochondrial cytochrome c oxidase assembly	No	**Yes**
TraesCS5A02G190500	395000985	395001446	chaperone?	No	No
TraesCS5A02G190600	395053634	395058676	FAD synthase?	No	No
TraesCS5A02G190700	395062528	395063210	chaperone?	No	No
TraesCS5A02G190800	395074525	395076886	n/a	No	No
TraesCS5A02G190900	395284820	395286256	glutathione transferase	No	No

Table 3.7. Continued. *Candidate genes located on the 5AL locus of 6.24 Mbp. IWGSC RefSeqv1.1 gene name and physical location of gene start and end (bp) are shown. Gene description is also provided when available. Expression upon DON[1] (Yes or No) was obtained from the RNA-Seq analysis, and expression upon Fusarium[2] (Yes or No) from expVIP studies performed with the pathogen in wheat (http://www.wheat-expression.com/).*

TraesCS5A02G191000	395303048	395304338	FLZ-type domain-containing protein // zinc finger	No	No
TraesCS5A02G191100	395680588	395692509	DUF3883 domain-containing protein // embryo development // root development // Histidine kinase putative	No	No
TraesCS5A02G191200	395697117	395704282	Laccase? // L-ascorbate oxidase activity // oxidoreductase activity	No	Yes
TraesCS5A02G191300	395759513	395760415	Molybdopterin synthase catalytic subunit	No	No
TraesCS5A02G191400	395804995	395807284	n/a	No	No
TraesCS5A02G191500	395832889	395835769	G domain-containing protein?	No	No
TraesCS5A02G191600	395835819	395838322	n/a	No	No
TraesCS5A02G191700	395838634	395839780	n/a	Yes	Yes
TraesCS5A02G191800	395847109	395848224	n/a	Yes	Yes
TraesCS5A02G191900	395851340	395852914	LOB domain-containing protein? // multicellular organism development	Yes	Yes
TraesCS5A02G192000	395868700	395873140	Zinc finger CCCH domain-containing protein 59?	No	No
TraesCS5A02G192100	395874247	395879691	Disease resistance protein RPM1 (NLR)?	No	No
TraesCS5A02G192200	395885773	395886123	n/a	No	No

[1] DON assay data performed in the present study. Expression of DEGs upon DON when log_2 >1 (P-value < 0.02). Yellow, log_2 fold change is ≥1 but <2; green, log_2 fold change is ≥2.

[2]ExpVIP data of Fusarium studies performed by Gou et al 2016, Kugler et al 2013, Schweiger et al 2016. Yellow means that the gene is slightly expressed, while green means that it is highly expressed upon Fusarium when comparing with a mock treatment.

Figure 3.8. *Differential expression levels of genes TraesCS5A02G191700 and TraesCS5A02G191800 after 4 days of mock and Fusarium-infection in rachis of Chinese Spring (http://www.wheat-expression.com/) (Gou et al. 2016).*

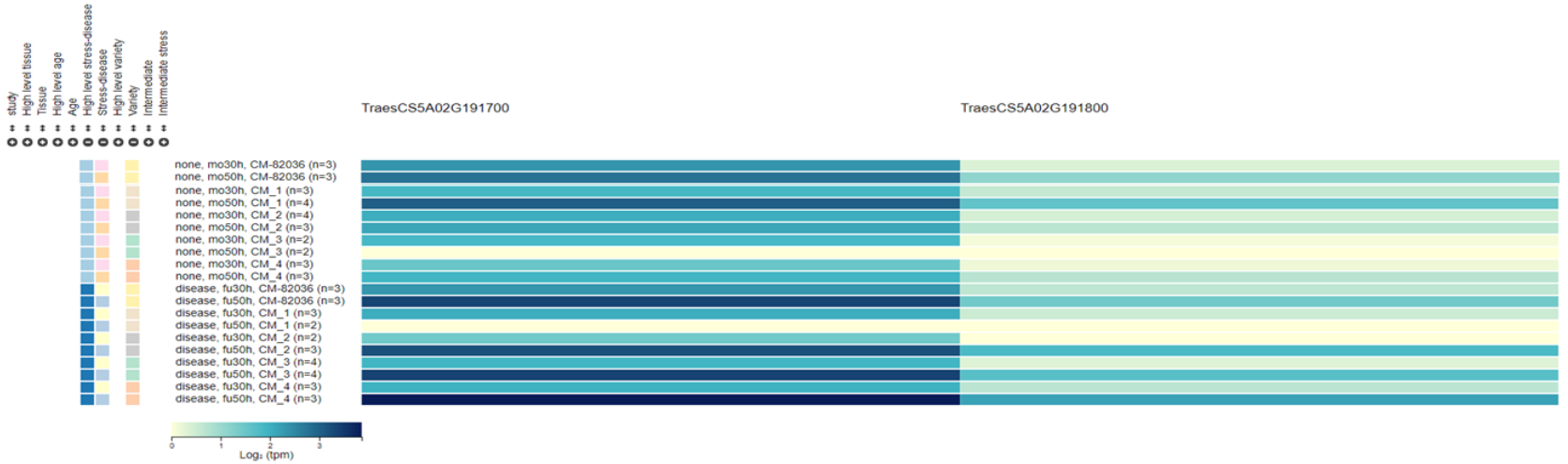

Figure 3.9. *Differential expression levels of genes TraesCS5A02G191700 and TraesCS5A02G191800 after 30 and 50 hours of mock and Fusarium-infection in spikes of NILs derived from the cross of the highly resistant cultivar CM-82036 and the highly susceptible cultivar Remus (http://www.wheat-expression.com/) (Kugler et al. 2013).*

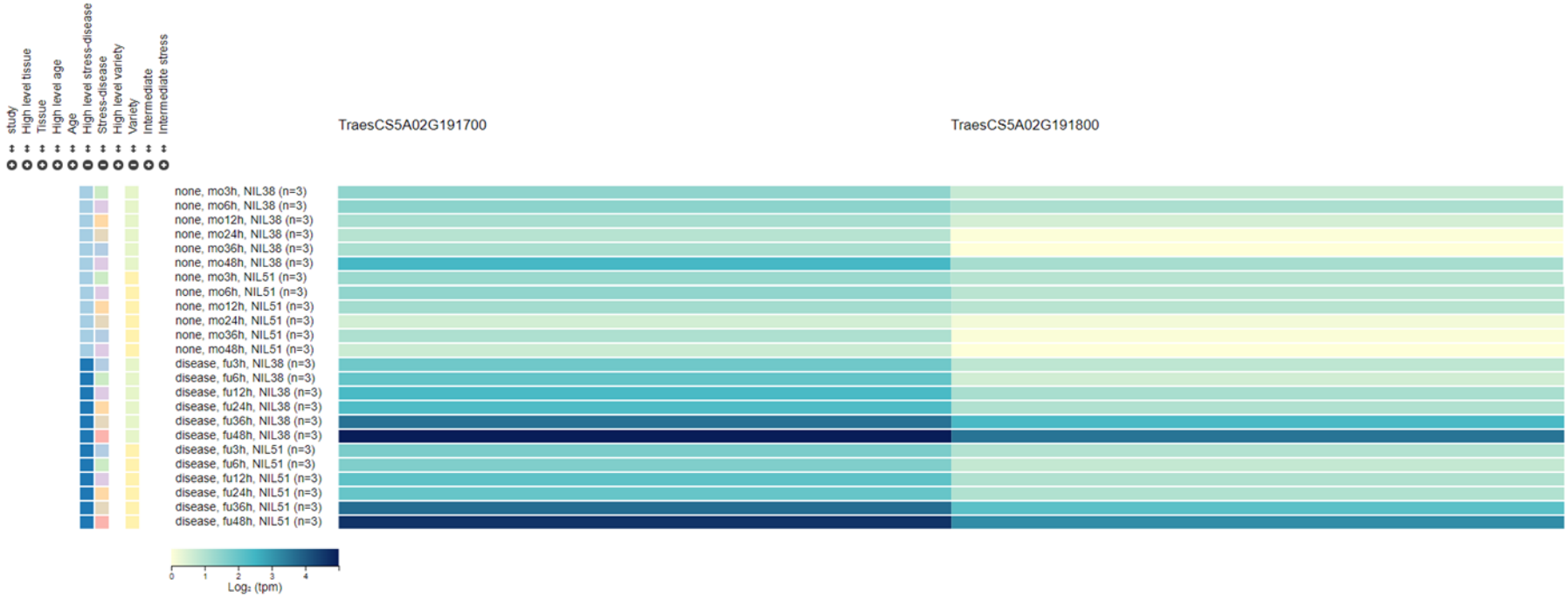

Figure 3.10. *Differential expression levels of genes TraesCS5A02G191700 and TraesCS5A02G191800 after a time-course of 48 hours of mock and Fusarium-infection in spikes of NILs derived from the cross of the highly resistant cultivar CM-82036 and the highly susceptible cultivar Remus (http://www.wheat-expression.com/) (Schweiger et al. 2016).*

3.5. Discussion

3.5.1. The 5A locus in RIL 97 confers DON tolerance

It was demonstrated in Chapter 2 that the 5A QTL reproducibly confers FHB type II resistance when infecting wheat spikes with *F. culmorum* conidia. Spread of the pathogen infection was measured by counting the number of bleached spikelets. Bleaching above the point of infection was reduced in resistant lines compared with susceptible lines. The outcome of the single marker analysis performed on specific RILs from the cross of WEK8H5A (resistant parent) and Hobbit *sib* (susceptible parent) helped to reduce the QTL interval to an interval of 6.24 Mbp on the long arm of chromosome 5A.

It is known that DON acts as virulence factor in wheat since it promotes the spread of the pathogen infection (Bai et al. 2008; Langevin, Eudes, and Comeau 2004). In this manner, DON contributes towards FHB type II susceptibility by promoting the spread of the pathogen within the spike. It is possible that the resistance provided by the 5A QTL may reflect reduced sensitivity to DON and not to the fungus itself. Therefore, resistance to DON may be underlying the type II resistance observed on the 5AL QTL. For these reasons I examined whether the 5A QTL was also conferring DON tolerance by using +/- 5A QTL lines exposed to the mycotoxin.

By exposing +/- 5A QTL lines to a fixed amount of DON, the complexity of gene expression upon pathogen infection is reduced since the focus of the experiment would be on the effects of the mycotoxin without the influences of the fungus itself. Moreover, the use of seedlings for the experiment implies the use of an economically and fast assay to test DON tolerance in those selected lines instead of growing and infecting wheat plants with the pathogen, which is time consuming.

Thus, the simplicity of the experiment relied on using seedlings of selected lines, growing them in agar (control and DON) and observing differences in root and shoot development (length) between treatments over time. If the 5A locus is involved in DON tolerance the + 5A QTL-line, when exposed to the mycotoxin, will develop roots and shoots closed in development as the control treatment, while the - 5A QTL-line will show an inhibition of development.

A potential drawback would be if DON tolerance was provided by different pathways on the seedling and adult stage of the wheat plant, and therefore, despite observing the resistance in early stages of development, the genes which are triggering that resistance could have changed or switch expression patterns in a late stage of plant development. That is why it would be also relevant to check what genes are highly expressed upon DON in wheat spikes.

In previous studies, it has been shown that DON is phytotoxic in plants (Wegulo 2012). The potential phytotoxicity of DON has recently been assessed on bread wheat seedlings' growth by analysing root and shoot development at four days after the mycotoxin application (Ederli et al. 2021). The results of this study showed that bread wheat was very sensitive to DON, causing a significant decrease in both shoot (-16.25 %) and root (-11.5 %) growth in comparison to the untreated control.

Older studies also showed these toxic effects. DON strongly inhibited root growth in seedlings of seven wheat cultivars (Shimada and Otani 1990). An *in vitro* assay using germinating maize (*Zea mays*) embryos was performed to assess the phytotoxic effects of DON and other mycotoxins (McLean 1995). In this study, DON showed to have an inhibitory effect in roots and shoots.

Additionally, it has been demonstrated that DON strongly inhibited growth of wheat coleoptile tissue at a concentration of 10^{-6} M, with the inhibition being greater at a higher

concentration (Wang and Miller 1988). *Arabidopsis* and wheat roots were also inhibited when grown on the surface of media containing DON (Masuda et al. 2007). In this study they also demonstrated that shoot growth was inhibited by all trichothecenes in a concentration-dependent manner.

In the present study I demonstrated that DON exposure on wheat roots led to an inhibition of roots and shoots. Since DON is water soluble (Snijders 2004), it can be translocated to other parts of the plant where it can cause physiological effects. However, in the RILs tested in this study, the inhibition of DON was better observed in the roots (41 %) than in the shoots (11 %).

RIL 103, which does not possess the *QFhb.WEK5A* locus, showed less inhibition of shoot development upon DON exposure than RIL 97. This may imply that this line may have other genes favouring DON tolerance in other locations on the 5AL chromosome, or it may imply that shoot growth rate was not a good indicator of the effect of DON tolerance. However, line RIL 97 (+ 5A QTL) showed higher levels of DON resistance compared to the *Fusarium*-susceptible parental line Hobbit *sib* (- 5A QTL).

Overall, these findings suggest that the 5A locus from WEKH85A may also function against DON since a reduction of bleaching was observed in infected wheat spikes, and it may be associated with FHB type II resistance.

3.5.2. Protein detoxification genes and UDP-glycosyltransferases (UGTs) identified upon DON exposure

RNA was extracted from roots exposed to control (H_2O) or DON (5 µM) treatments on +/- 5A QTL lines. This approach was taken in an effort to refine the RNA-Seq analysis of the lines differing for the *QFhb*.WEK5A QTL to identify those genes exhibiting a differential response to DON.

Firstly, DEGs between DON and control treatments for both RIL 97 (+ 5A QTL) and Hobbit *sib* (- 5A QTL) were extracted in the whole wheat genome. Three homoeologues genes *TraesCS7A02G497300*, *TraesCS7B02G400500* and *TraesCS7D02G484500,* which are annotated as being protein detoxification genes, were very highly expressed upon exposure to DON. Increased expression of the homoeologues located on the 7A and 7D chromosomes were specific of RIL 97. Indeed, these genes were very highly expressed upon *Fusarium* after 50 h post-inoculation but not after 30 h (Kugler et al. 2013). Data obtained from the study of Schweiger et al (2016) revealed that these genes increased in expression 36 h post-inoculation. In fact, the expression of these homoeologues genes (*TraesCS7A02G497300*, *TraesCS7B02G400500* and *TraesCS7D02G484500*) were also highly expressed (log_2 FC = 5.95, 6.95 and 7.00, respectively) upon *Fusarium* infection after 4 dpi (Gou et al. 2016).

Genes *TraesCS7A02G497300*, *TraesCS7B02G400500* and *TraesCS7D02G484500* encode proteins from the MATE (Multi antimicrobial extrusion protein) family (http://www.ebi.ac.uk/interpro/entry/InterPro/IPR002528/). These general types of proteins are involved in exporting metabolites across the cell membranes and are often responsible for multidrug resistance to a wide range of molecules. It seems that these genes start being expressed and increased very rapidly the level of expression during the third day post-pathogen infection. It has been showed that in controlled experiments, DON was detected at 36 h after inoculation of wheat spikelets with *F. culmorum* (Kang and Buchenauer 1999). These genes, thus, may start being highly expressed upon DON detection to reduce the levels of the mycotoxin inside the plant cells.

Other genes which were identified to be highly expressed upon DON were those annotated as being UDP-glycosyltransferases (UGTs), such as gene *TraesCS2A02G463300* (http://www.ebi.ac.uk/interpro/entry/InterPro/IPR002213/), which was highly expressed upon DON for both RIL 97 and Hobbit *sib*, being more highly expressed in line RIL 97.

One of the most common methods for DON detoxification in plants is the use of UGTs. The function of this type of genes was first described in *A. thaliana*. *DOGT1* of *A. thaliana* can transfer the glucose group from the UDP-glucose to modify the hydroxyl group of carbon 3 of DON. This process leads to the production of a less toxic compound called D3G (Poppenberger et al. 2003). Other UGTs with similar function have been discovered in other plants such as *Bradi5g03300* in *B. distachyon* (Gatti et al. 2019; Pasquet et al. 2016; Schweiger, Pasquet, et al. 2013), *HvUGT13248* in barley (Li et al. 2015; Shin et al. 2012; Schweiger et al. 2010), and *TaUGT3* (Lulin et al. 2010) and *TaUGT12887* (Schweiger, Steiner, et al. 2013) in wheat.

Genes which were more highly differentially expressed between DON and control treatments for both +/- 5A QTL lines were then extracted for the 5A chromosome. Genes *TraesCS5A02G368600, TraesCS5A02G368700* and *TraesCS5A02G368800* were highly differentially expressed for both RIL 97 and Hobbit *sib*, while increased expression of *TraesCS5A02G368900* was specific for RIL 97. These adjacent genes are located at 569 Mbp on the long arm of the 5A chromosome and encode proteins from the MATE family.

When checking the expression of genes *TraesCS5A02G368600, TraesCS5A02G368700* and *TraesCS5A02G368800* upon pathogen infection in wheat spikelets, these three genes were highly expressed after 4 dpi (Gou et al. 2016). *TraesCS5A02G368600* and *TraesCS5A02G368700* expression levels rapidly increased from 36 h post-infection (Schweiger et al. 2016) and were still highly expressed at 50 h post-infection (Kugler et al. 2013). As previously mentioned, this type of genes may start being highly expressed upon DON detection to reduce the levels of toxicity inside the plant cells.

Another gene which was identified to be highly expressed upon DON was *TraesCS5A02G149600,* being annotated as a UGT and located at 327 Mbp on the 5A

chromosome. This gene was highly expressed upon DON for both RIL 97 and Hobbit *sib*, being more expressed in the introgression line.

The two genes that were more expressed upon control treatment (H_2O) in RIL 97 were *TraesCS5A02G023700* and *TraesCS5A02G535900*, located at 18.8 Mbp in the short arm of the 5A chromosome and at 692.3 Mbp on the long arm of the 5A chromosome, respectively. These genes, therefore, are not located within the 5A QTL interval and so appear not to be involved in resistance to FHB.

3.5.3. DON-candidate genes identified on the *QFhb*.WEK5A locus

Finally, detailed attention was paid into those DEGs previously identified on the 5A chromosome that were located within the 5A locus of RIL 97. This recombinant line harbours the FHB type II resistance provided by parental line WEKH85A on the 5A chromosome, within a region from 322 to 417 Mbp (see Table 3.3.).

Eight genes located on the 5A chromosome were identified as being highly expressed upon exposure to the mycotoxin. Five genes increased in expression levels only in the line harbouring the QTL (RIL 97), while the other three genes were highly expressed in both +/- 5A QTL lines upon DON treatment. One of these genes, *TraesCS5A02G149600* (located at 327.60 Mbp), was annotated to encode a UGT. None of the other genes were annotated on the Chinese Spring reference genome.

Although *TraesCS5A02G149600* may be involved in DON resistance through a similar mechanism of DON detoxification in both RIL 97 and Hobbit *sib*, this gene is not located within the 6.24 Mbp-QTL (see Table 3.4.), making it highly unlikely to be involved in the functioning of the *QFhb*.WEK5A QTL. Nonetheless, it is possible that the DON insensitivity

and FHB resistance are due to two independent genes so the reduced DON sensitivity of RIL 97 may be due to this gene.

DEGs between +/- 5A QTL lines were then specifically extracted on the 6.24 Mbp-QTL associated with FHB type II resistance. Only one high confidence annotated gene, *TraesCS5A02G191800*, located at 395.84 Mbp, was identified as a potential DON-responsive gene specific to the + 5A QTL line. This gene was not annotated on the reference genome and, thus, no information about its putative function or description was available. However, its gene paralogue *TraesCS5A02G191700* (also not annotated), was identified as also of interest as a DON-responsive gene. Levels of expression of gene *TraesCS5A02G191700* upon exposure to the mycotoxin were not as high as for gene *TraesCS5A02G191800* (that is why it did not appear during the data filtration process), but it was differentially expressed between +/- 5A QTL lines upon DON exposure.

TraesCS5A02G191700 and *TraesCS5A02G191800* were described as containing motifs for DUF761 a family of proteins of unknown function (https://www.ebi.ac.uk/interpro/entry/InterPro/IPR008480/). Indeed, this type of family proteins includes pathogen-associated molecular pattern-induced protein A70, which was identified in *Arabidopsis*. This protein was induced in *Arabidopsis* during *Pseudomonas syringae* infection by jasmonic acid and wounding (Truman et al. 2007).

3.5.4. Is there any other DON-candidate gene on the *QFhb*.WEK5A locus?

The bread wheat genome is approximately 16 Gbp and has a repeat content of approximately of 80 %. One of the major obstacles to the analysis of the wheat transcriptome until recently was the lack of a suitable mapping reference. The spring wheat Chinese Spring (CS) IWGSC RefSeq v1.0. genome assembly was finalised in 2018 (IWGSC 2018), which has revolutionised wheat genomics.

RNA-sequencing enables the identification of differentially expressed genes under specific conditions and in a particular plant tissue. During the RNA-Seq analysis, reads of DEGs obtained from the +/- 5A QTL lines were aligned to the CS reference genome. Only the genes that are annotated as low or high confidence on CS could be identified to match the alignment of those reads. The main problem resides on the length of those reads, since the RNA-Seq method produces transcripts of around 150 bp. When these small transcripts are assembled to generate longer transcripts to be mapped into the reference genome, some transcript isoforms are 'lost'.

Additionally, it may not be possible to map novel genes into the reference genome since there will be no equivalent for those genes. Additionally, some genes may have transposed into the 5A QTL interval in WEKH85A. As I used the reference genome during the analysis, the location given to those specific DEGs identified were based in reference to CS. It is, thus, also important to consider DEGs identified the whole genome of wheat (see section 3.4.2.), no matter where they mapped in CS, as they may have moved into the *QFhb*.WEK5A locus in the parental line WEKH85A from elsewhere in the genome. As the full genome of the parental line WEKH85A have not been sequenced, it is unknown what are the differences at the genomic level with CS.

3.5.5. *TraesCS5A02G191700* and *TraesCS5A02G191800* may be orphan genes

Orphan genes are a set of genes specific to a taxonomic group which lack homology outside of a given species or lineage. These subsets of clade-specific genes generally confer lineage-specific adaptations in conjunction with the plant's ability to cope with abiotic and biotic stresses. Both DON-candidate genes *TraesCS5A02G191700* and *TraesCS5A02G191800*, for which gene function is unknown, appear to be specific genes found only in the Poaceae

family and, thus, they both may be orphan genes. Orphan genes may have emerged in this family of plants from the need adapt to certain environmental or biological stresses.

An orphan gene peculiar to the grass family Poaceae has recently been identified as a key gene in DON tolerance in wheat. Overexpression of *TaFROG* has been demonstrated to improve plant DON tolerance as well as FHB resistance. When *TaFROG* expression is downregulated, DON and FHB severity increase (Perochon et al. 2015). Little is known about the cellular function of this gene, but it is known that *TaFROG* interacts with *TaSnRK1α*. A Poaceae-divergent NAC-like transcription factor (TF) named *TaNACL-D1,* also interacts with *TaFROG*. *TaFROG* and *TaNACL-D1* are both co-expressed in an early response after *F. graminearum* infection and DON inoculation. Wheat lines overexpressing the TF were more resistant to FHB, and it has been suggested that *TaFROG* may form a protein complex with *TaSnRK1α* and *TaNACL-D1* to produce a disease response evolved within the *Triticeae* (Perochon et al. 2019).

The orthologous gene of *TaFROG*, *Bradi4g22656*, was identified as being highly expressed upon DON (5 µM) when roots of *B. distachyon* (FHB susceptible line Bd21) were exposed to the mycotoxin for 6 h (log_2 FC = 6.58) (Santos 2021). The homoeologous *TaFROG* genes in wheat (*TraesCS4A02G201900*, *TraesCS4D02G102800* and *TraesCS4B02G106100*), located on group 4 chromosomes, were also identified in the present study as being expressed upon the toxin in RIL 97 (log_2 FC = 4.39, 3.31 and 1.85, respectively) (see Supplementary Excel Files, Table EF1) and in Hobbit *sib* (log_2 FC = 1.48, 1.95 and 2.42, respectively) (see Table EF3).

3.5.6. Expression of *TraesCS5A02G191700* and *TraesCS5A02G191800* increase upon *Fusarium* infection

DON-responsive genes, *TraesCS5A02G191700* and *TraesCS5A02G191800*, have been identified in the present study by being differentially expressed between +/- 5A QTL lines after DON application.

Expression studies of FHB in wheat showed that they both were highly expressed after several hours and days post-infection. For instance, both genes were up-regulated at 4 dpi in the rachis in the variety CS (Gou et al. 2016) (Figure 3.8.). The level of expression of these genes also increased in the spikelets of *Fusarium*-infected NILs after a time-course experiment of 48 h (Schweiger et al. 2016). Gene *TraesCS5A02G191700* was more highly differentially expressed (log_2 FC > 4) at 48 h post-infection than gene *TraesCS5A02G191800* (log_2 FC > 3) (Figure 3.10.). For this study, NILs were developed from a cross of a highly FHB resistant donor CM-82036 (originated from the cross Sumai 3 and Thornbird-S) and the highly susceptible cultivar Remus. Additionally, both DON-responsive genes were highly expressed in NILs derived from the same cross when compared with the control treatment at 50 h after *Fusarium* infection (Kugler et al. 2013). In this case, gene *TraesCS5A02G191700* was also more highly differentially expressed (log_2 FC > 3) in the majority of the NILs at 50 h post-infection than gene *TraesCS5A02G191800* (log_2 FC > 1) (Figure 3.9.).

Homoeologues of gene *TraesCS5A02G191800* on the 5B and 5D chromosomes, genes *TraesCS5B02G191300* and *TraesCS5D02G199100*, respectively, were also differentially expressed in RIL 97 between DON and control treatments (*P*-value < 0.001) (Table S17). These genes were highly expressed in wheat spikes 36 h after infection with *Fusarium* (Schweiger et al. 2016), and expression of *TraesCS5D02G199100* was higher than *TraesCS5A02G191800* (log_2 FC > 2 at 36 h and log_2 FC > 3 at 48 h), and even at 4dpi (Gou et al. 2016).

Homoeologues of gene *TraesCS5A02G191700* on the 5B and 5D chromosomes, are genes *TraesCS5B02G191400* and *TraesCS5D02G199200*, respectively. Only

TraesCS5B02G191400 was differentially expressed between control and DON treatments in RIL 97 (*P*-value < 0.001) and to a lesser extent in Hobbit *sib* (*P*-value < 0.05) (Table S16). However, *TraesCS5A02G191700* and *TraesCS5D02G199200* were highly expressed in spikes 50 h after *Fusarium* infection (Kugler et al. 2013), with the expression of the DON-responsive gene *TraesCS5A02G191700* being much greater than that of *TraesCS5D02G199200*. However, the expression levels of the three homoeologous genes were similar at 4 dpi (log_2 FC of around 6.00) (Gou et al. 2016).

3.5.7. Expression of the orthologous genes of *TraesCS5A02G191700* and *TraesCS5A02G191800* in *Brachypodium distachyon*

The orthologous genes of *TraesCS5A02G191700* and *TraesCS5A02G191800* in *B. distachyon* are *Bradi4g28890* and *Bradi4g28900*, which have been shown to have an association with DON tolerance and FHB resistance by members of the group (Bankes-Jones 2021; Haidoulis 2021; Santos 2021).

The description for both genes is "Cotton fibre expressed protein 1 (CFE1)" (https://www.uniprot.org/uniprot/O81373). Very little it is said about this type of family proteins of unknown function. These proteins may be integral components of the cellular membrane. In addition, these types of proteins have the same transmembrane helices as the ones mentioned above (DUF761) identified in *Arabidopsis thaliana*. These types of proteins also have another domain of unknown function (DUF4408), which is found at the N-terminus of the CFE1 family.

Gene *Bradi4g28890* was up-regulated in *B. distachyon* ecotype Bd21 (log_2 FC > 2; *P*-value < 0.001) after exposure to DON (5 µM) for 6 h (Unpublished data provided by Dr Miguel Angelo Costa e Silva dos Santos). This gene was also up-regulated in *B. distachyon* ecotypes

Bd21 and Bd2-3 (log_2 FC > 3; *P*-value < 0.001) when applying a higher concentration of DON (20 µM) for 6 h (Unpublished data provided by Dr Elizabeth Anna Bankes-Jones).

A study was performed to identify genes expressed upon infection of either DON-producing or DON non-producing *Fusarium* isolates in *Brachypodium* ecotype Bd21 (Pasquet et al. 2014). Both *Bradi4g28890* and *Bradi4g28900* were highly differentially expressed (log_2 FC > 3; *P*-value < 0.001) between the producing and non-producing DON isolates. Expression of both genes was higher in spikelets infected with the DON-producing *Fusarium* isolate. *Bradi4g28890* was also identified to be highly expressed in spikes of ecotype Bd3-1 after 3 dpi with *F. graminearum* (log_2 FC = 2.45; *P*-value < 0.001). Expression of *Bradi4g28900* was slightly increased upon *Fusarium* infection (log_2 FC = 1.21; *P*-value < 0.001) after 1 dpi in a Fusarium root rot (FRR) assay (Unpublished data provided by Dr John Francis Haidoulis).

To conclude, the expression levels of orthologous genes to *TraesCS5A02G191700* and *TraesCS5A02G191800 in Brachypodium* also increased upon DON and *Fusarium* infection.

3.5.8. How may DON-candidate genes be triggering DON tolerance?

Expression levels of most of the 44 candidate genes located on the 5A locus remained low upon DON exposure (see Table 3.7.). Only one gene (*TraesCS5A02G191800)* had a very high expression level (log_2 FC ≥ 2), and two genes (*TraesCS5A02G191700* and *TraesCS5A02G191900)* had a slightly increased expression (log_2 FC ≥ 1) in RIL 97, the line containing the 5A QTL, upon mycotoxin exposure. Two of these DEGs are the DON-responsive genes already mentioned.

The remaining gene is *TraesCS5A02G191900* (located at 395.85 Mbp), is annotated as encoding a lateral organ boundary (LOB) domain-containing protein and it may be involved

in a multicellular organism development. These LOB domain genes are a gene family encoding plant-specific transcription factors that play key roles in plant growth and development (Zhang et al. 2020).

Gene *TraesCS5A02G191700* is expressed in both +/- 5A QTL lines, but the expression level is much greater in the line containing the 5A locus from WEKH85A. It seems, thus, that the primary response to DON by the plant host in the WEKH85A resistant line appears to be through increasing the expression of genes, *TraesCS5A02G191700* and *TraesCS5A02G191800*, that consequently may trigger a cascade of gene activation that increases DON tolerance and, consequently, FHB resistance.

3.5.9. Conclusions and future work

It seems that DON-candidate genes *TraesCS5A02G191700* and *TraesCS5A02G191800* identified on the 5AL locus may be promising candidate genes for FHB resistance by increasing their level of expression upon DON exposure. Examination of the expVIP database also reveals that these genes, particularly *TraesCS5A02G191700*, are both highly responsive to challenge by *Fusarium* species.

However, it is also important to identify whether DON tolerance and FHB type II resistance are two independent loci or whether one locus is conferring a pleiotropic effect on the 5AL QTL. The 5A QTL interval was refined to 6.24 Mbp using specific RILs tested in Summer 2020. This interval was smaller than that used for the RILs used for the RNA-Seq analysis to identify DEGs responding to DON. Therefore, RILs (RIL 9A, RIL 10B, RIL 16A and RIL 17B) will be tested on the next chapter to check if they also show differential sensitivity to DON.

The expression levels of both genes in response to DON treatment will be confirmed by Q-RT-PCR, and they will be sequenced to identify any possible difference between the resistant and susceptible lines at the DNA sequence level.

Additionally, expression analysis of genes expressed upon DON exposure in wheat spikes could help to verify if the expression of those candidates' genes, *TraesCS5A02G191700* and *TraesCS5A02G191800*, are tissue-specific or they are also identified in the spikes. Moreover, it would be also important to check whether the higher expression of both genes is also observed in wheat spikes infected upon *Fusarium*, as expVIP data is supporting.

Chapter 4

Fine mapping the Fusarium Head Blight 5AL QTL (*QFhb.WEK-5A*) and identification of candidate genes for FHB and DON resistance

4.1. Abstract

The use of cultivars showing and increase in FHB resistance and low DON content is the most economical and effective method to avoid wheat yield losses. *Fhb1* is the first major QTL associated with FHB type II resistance on the 3B chromosome in cultivar Sumai 3. Sumai 3 is being used as a source of resistance in wheat breeding programmes worldwide. *Fhb1* provides DON tolerance by a detoxification mechanism. Different studies have claimed the identification of genes associated with the resistance but there are still many controversies.

In the present study it was important to identify whether DON tolerance and FHB type II resistance are two independent loci or whether *QFhb.WEK-5A* locus is conferring a pleiotropic effect on the 5AL QTL. The association of DON tolerance and FHB type II resistance in specific-selected recombinants from the cross of WEKH85A (resistant) and Hobbit *sib* (susceptible) lines was further studied. Sequencing and examination of both DON and FHB candidate genes, *TraesCS5A02G191700* and *TraesCS5A02G191800*, was performed.

Results revealed that the *QFhb.WEK-5A* locus for FHB type II resistance of 6.24 Mbp also confers DON tolerance in the introgression line WEK8H5A. The most promising candidate gene located in the 5A locus is the DON-responsive gene *TraesCS5A02G191700*. This gene contains a deletion in the promoter region in the parental line WEKH85A which may be the key component of a transcriptional activation response that could lead to the increase in expression of this gene when expose to the mycotoxin.

4.2. Introduction

FHB resistance in wheat is a complex and quantitative trait. Indeed, FHB resistance may involve a complex and interacting network of signalling pathways. To reduce losses caused by *Fusarium* sp., the employment of cultivars with high FHB resistance and low DON content is the most economical and effective method (Bai 2004).

Immune germplasm to FHB has not been identified but it is well known that Chinese cultivar Sumai 3 possesses a good combination for both FHB resistance and DON accumulation traits. Sumai 3 has been successfully used as a resistant parent in wheat breeding programs worldwide (Bai, Su, and Cai 2018).

Many identified FHB resistance QTL have been associated with low DON accumulation (Somers, Fedak, and Savard 2003; Ma et al. 2006), but only few have been tested for their ability to either detoxify DON or enhance resistance to the toxin (Gunupuru, Perochon, and Doohan 2017). The first major QTL associated with type II resistance was *Fhb1*, identified on chromosome 3B in cultivar Sumai 3 (Bai et al. 1999; Anderson et al. 2001; Zhou et al. 2002; Cuthbert, Somers, Thomas, Cloutier, and Brulé-Babel 2006). Indeed, the first functional characterisation of *Fhb1* was related with DON detoxification, since plants carrying the *Fhb1* allele were more resistant to DON-induced bleaching and were able to convert DON into a less toxic derivate D3G (Lemmens et al. 2005).

Recent studies on the *Fhb1* have claimed to identify the gene underlying the locus. Using a map-based cloning approach, a pore-forming toxin-like (PFT) gene was identified as a potential candidate conferring the resistance to FHB at the *Fhb1* locus (Rawat et al. 2016). Moreover, two most recent studies revealed that a mutation of the histidine-rich calcium-binding gene “His” (*TaHRC*) confers FHB resistance at the *Fhb1* locus (Li, Zhou, et al. 2019; Su et al. 2019), but the role of mutated *TaHRC* in FHB resistance is still not very clear (Lagudah and Krattinger 2019; Li, Zhou, et al. 2019; Su et al. 2019).

It was demonstrated in Chapter 2 that a combination of three summer trials enabled the refining of the FHB QTL interval. The *QFhb.WEK-5A* locus of 6.24 Mbp for FHB type II resistance was fine mapped at the end of Summer 2020, once new markers were identified and were used to reduce the QTL. Additionally, I demonstrated in Chapter 3 that the 5A QTL from WEKH85A conferred DON tolerance since line RIL 97 (+ 5A QTL) showed higher levels of DON resistance when compared with Hobbit *sib* (- 5A QTL). Line RIL 97 harbours the 5A QTL associated with FHB type II resistance within a region from 322 to 417 Mbp on the 5A chromosome.

During summer 2020 trial, several RILs were tested for FHB type II resistance under polytunnel conditions. Specific resistant and susceptible RILs for FHB type II resistance were selected from this trial. These RILs were also selected for the presence/absence of the *QFhb.WEK-5A* locus of 6.24 Mbp. These specific recombinant lines selected from Summer 2020 were selected to be tested for DON tolerance. As the locus had been fine mapped and RILs were tested for FHB resistance, I wanted to identify whether RILs resistant to the pathogen also tolerate the mycotoxin. If this was the case, it would mean that the *QFhb.WEK-5A* locus of 6.24 Mbp harbours the genes associated with both traits: DON tolerance and FHB type II resistance. If FHB resistant RILs were susceptible to the mycotoxin, it would mean that the two traits are independent of one another on *QFhb.WEK-5A* locus but may reside close in the 5A QTL region of RIL 97, from 322 to 417 Mbp on the 5A chromosome.

Therefore, by performing this experiment the aim was to examine whether two genomic regions residing very close on the *QFhb.WEK-5A* locus (different genes) are associated with DON tolerance and FHB resistance, or whether it is just one genomic region associated with the two traits. As FHB resistance possess a polygenic and quantitative mode of inheritance, the resistance to FHB infection and DON accumulation may be controlled by independent loci and (or) genes as previously suggested by Somers et al 2003. Therefore,

both traits in the present study could be controlled by a single gene located within the 6.24 Mbp FHB QTL, but they could still be controlled by separate genes within this interval.

Additionally, the RNA-Seq analysis of roots exposed to DON in RIL 97 revealed the identification of two potential DON-candidate genes (*TraesCS5A02G191700* and *TraesCS5A02G191800*) within the *QFhb.WEK-5A* locus of 6.24 Mbp for FHB type II resistance. It would be relevant to sequence parental lines Hobbit *sib* and WEKH85A to identify potential polymorphisms that could not be identified during RNA sequencing. These genes were sequenced and further examined at the genomic level.

Moreover, it would be also crucial to confirm the expression of both *TraesCS5A02G191700* and *TraesCS5A02G191800* genes obtained from the RNA-Seq data, so the expression profile of these genes was examined. Indeed, high levels of expression of the two genes may occur due to different number of copies in the parental lines when compared with the Chinese Spring (CS) reference genome. The *QFhb.WEK-5A* locus could have been duplicated in the FHB resistant parental line WEKH85A. Gene duplication could have led to higher expression of candidate genes upon the exposure to the mycotoxin. Thus, confirming the number of copies of both *TraesCS5A02G191700* and *TraesCS5A02G191800* in both parental lines was also crucial to provide insight into the mechanism of resistance provided by WEKH85A.

A powerful and recent approach to confidently generate copy number measurements in a different array of crops, such as rice, citrus, potato, maize, tomato, and wheat, is the droplet digital PCR-based method (Collier et al. 2017). This method uses specific primers to amplify target transgenes, and endogenous reference genes in a single duplexed reaction containing thousands of droplets. The method relies on the detection of the endpoint amplicon production in the droplets and the quantification using sequence-specific fluorescently labelled probes.

4.2.1. Chapter aims

To further study the association of DON tolerance and FHB type II resistance in the *QFhb.WEK-5A* locus and to further examine the two DON-candidate genes *TraesCS5A02G191700* and *TraesCS5A02G191800*, the objectives were:

1) Perform a DON assay using critical FHB type II resistant and susceptible RILs to test whether DON tolerance and FHB type II resistance reside in the same 6.24 Mb region on the 5AL chromosome.
2) Sequence both candidate genes to identify any difference at the genomic level between the FHB susceptible parental line Hobbit *sib* and the FHB resistant line WEKH85A.
3) Confirm the expression level of both DON-candidate genes by quantitative reverse transcription PCR (RT-qPCR) analysis.
4) Confirm the gene copy number of both DON-candidate genes by ddPCR analysis.

4.3. Material and Methods

4.3.1. DON assay on roots using +/- 5A QTL RILs

4.3.1.1. Selection of lines

A recombinant inbred line population was created from a cross between Hobbit *sib* (susceptible parent) and WEKH85A (resistant parent), which is genetically similar to Hobbit *sib* except for chromosome 5A which comes from the resistant cultivar WEK0609 as described in Chapter 2.

Several RILs derived from the Hobbit *sib* x WEKH85A were used for the DON assay to test DON tolerance. These RILs were chosen because of the presence or absence of the 6.24 Mbp-QTL on the 5A chromosome, between markers *S11* (389.64 Mbp) and *S18* (395.89 Mbp). While lines RIL 9A and RIL 10B contained the *QFhb.WEK-5A* locus of 6.24 Mbp (+ 5A QTL), lines RIL 16A and RIL 17B lacked the 5A QTL (- 5A QTL) (see Figure 2.8. in Chapter 2). Lines RIL 97 (+ 5A QTL) and parental line Hobbit *sib* (- 5A QTL) were also included in the experiment.

4.3.1.2. DON assay

The same protocol as previously described in Chapter 3 (section 3.3.1.2.) was used. For this assay, around twenty-five seed of +/- 5A QTL lines were used to ensure that sufficient seed at the same germination stage were available for the experiment.

4.3.1.3. Statistical analysis

The same statistical method as previously described in Chapter 3 (section 3.3.1.3.) was used.

4.3.1.4. Genotyping analysis

Genotyping of selected RILs to confirm the presence/absence of the 5A locus was performed as previously described in Section 2.3.3. of Chapter 2. DNA extraction and screening was done by Richard Goram (Genotyping Services, JIC) using the following KASP markers: *S4, S11, S13, S18, S20* and *S25* (see Table 2.1. in Chapter 2).

4.3.2. Sequencing DON-candidate genes *TraesCS5A02G191700* and *TraesCS5A02G191800*

4.3.2.1. Designing primers

Sequence information for both DON-candidate genes *TraesCS5A02G191700* and *TraesCS5A02G191800* and their homoeologous genes located on chromosomes 5B and 5D were extracted from Ensembl Plants (EMBL-EBI 2022). Each DNA sequence was downloaded from the Chinese Spring reference genome (IWGSC RefSeq v1.0) with around +3000 bp and with +1000 bp of genomic sequencing upstream and downstream of each gene, respectively. This was done to ensure that the promoter region and the full coding sequence (CDS) for each gene was sequenced.

Alignment of each candidate gene with its respective homoeologous gene was performed using Geneious Prime software (version 2021.2.2). Primer pairs (PP) were manually developed to be specific for each DON-candidate gene and were modified according to specific settings by using OligoEvaluator™ (Sigma-Aldrich). These general parameters were a primer length between 18-25 bp, a melting temperature (Tm) between 55-62°C and a GC content between 40-60 %.

Different set of PPs were developed to amplify the CDS and the promotor of genes *TraesCS5A02G191700* (Table 4.1. and Table 4.2.) and *TraesCS5A02G191800* (Table 4.3. and Table 4.4.). For each left (5') (L) or right (3') (R) primers, the sequence (5' to 3'), the length (in bp), the Tm (°C) and GC content (%) is specified. For each PP the product size (in bp) is also specified.

Table 4.1. *Primer sequences used to sequence the coding region of gene TraesCS5A02G191700. Sequence (from 5' to 3'), length (bp), melting temperature (Tm), and GC content (%) for each left (5') (L) and right (3') (R) primers are specified. Product size (bp) for each primer pair is shown.*

Primer Pairs	Left Primer (5') (L)				Right Primer (3') (R)				Product size (bp)
	seq 5' to 3'	length (bp)	Tm (°C)	GC (%)	seq 5' to 3'	length (bp)	Tm (°C)	GC (%)	
L1/R1	TGATTTGGTCCCTGCCTACC	20	59.4	55.0	AATGTTCAGACCAGCTGCGA	20	59.9	50.0	985
L4/R4	TGGAGTGCATACAAGCCAAG	20	58.2	50.0	CGCTCCACAATGATACCG	18	55.7	55.6	350
L5/R5	AACGATCAGACCAACAACCA	20	57.4	45.0	GCTCCTTCAGCATCTTCTC	19	55.4	52.6	466
L7/R7	TGTTTCTCGTGCGCTGCT	18	60.3	55.6	AAATGGAAGGCATGCCTG	18	55.6	50.0	271
L8/R8	ACAGAGACGGTCAGACGGA	19	59.9	57.9	TGCTGATTTGCAAGGAAAGAGC	22	60.0	45.5	464
L10/R10	CGGTATCATTGTGGAGCG	18	55.7	55.6	AGCAGCGCACGAGAAACA	18	60.3	55.6	662

Table 4.2. *Primer sequences used to sequence the promoter of gene TraesCS5A02G191700. Sequence (from 5' to 3'), length (bp), melting temperature (Tm), and GC content (%) for each left (5') (L) and right (3') (R) primers are specified. Product size (bp) for each primer pair is shown.*

Primer Pairs	Left Primer (5') (L)				Right Primer (3') (R)				Product size (bp)
	seq 5' to 3'	length (bp)	Tm (°C)	GC (%)	seq 5' to 3'	length (bp)	Tm (°C)	GC (%)	
L2/R2	CATTTCGAATGCTCCTGCTTG	21	58.20	47.60	GATTGCGTGCACGTTTGGAA	20	60.30	50.00	446
L3/R3	TGCTGGTTTCTTATTCACCGGTT	23	60.70	43.50	TGAGTGTAGGAGGCAGCAA	19	58.20	52.60	447
L4/R4	CGCTTAGTGTGCACATAA	18	52.80	44.40	AGAACGGCTGGTTCACG	17	57.10	58.80	434
L5/R5	CATGGATCTCGCCACTACTG	20	57.90	55.00	ATCTTGGGTGAACAATTGCA	20	55.80	40.00	392
L7/R7	GCATGTGATTTCTCACATCTGG	22	57.70	45.50	CTAGAAGAACGCTCGTGC	18	55.70	55.60	440
L8/R8	GATGGATTATGGTCCCGTACT	21	56.70	47.60	ATCCCTACCGGACCATCT	18	56.20	55.60	531
L9/R9	CCTTCCCAATTACCATTCCC	20	55.70	50.00	CCAAGACTTGGCCCAGTA	18	56.10	55.60	543
L10/R10	ATTCATGCTTCGTTCCACTC	20	56.10	45.00	AGCCACAGCTCCAAGAAT	18	56.10	50.00	416

Table 4.3. *Primer sequences used to sequence the coding region of gene TraesCS5A02G191800. Sequence (from 5' to 3'), length (bp), melting temperature (Tm), and GC content (%) for each left (5') (L) and right (3') (R) primers are specified. Product size (bp) for each primer pair is shown.*

Primer Pairs	Left Primer (5') (L)				Right Primer (3') (R)				Product size (bp)
	seq 5' to 3'	length (bp)	Tm (°C)	GC (%)	seq 5' to 3'	length (bp)	Tm (°C)	GC (%)	
L1/R1	TTCTCGAGGAGAAGAGGCCA	20	59.96	55.00	GCTTGCCCTCGTGAACATAAC	21	59.87	52.38	857
L3/R3	TGTCGGTTGAGCAATCTTTCA	21	58.20	42.90	ACGTCGCCGCCTTTGATT	18	60.40	55.60	369
L5/R5	TCCATGCTCATCGAGCTCT	19	58.20	52.60	TCATCTGTGCGATCAGATATTC	22	55.90	40.90	525
L6/R6	GCGTTGCTCTGCTTTGTGAA	20	60.00	50.00	TTGATGTGGAGGAGAAAGAAG	21	55.20	42.90	641
L11/R11	GGCCAGCTCTCCCTTTAT	18	55.90	55.60	GCTATCTTCGCCCTGTCCT	19	58.90	57.90	671

Table 4.4. *Primer sequences used to sequence the promoter of gene TraesCS5A02G191800. Sequence (from 5' to 3'), length (bp), melting temperature (Tm), and GC content (%) for each left (5') (L) and right (3') (R) primers are specified. Product size (bp) for each primer pair is shown.*

Primer Pairs	Left Primer (5') (L)				Right Primer (3') (R)				Product size (bp)
	seq 5' to 3'	length (bp)	Tm (°C)	GC (%)	seq 5' to 3'	length (bp)	Tm (°C)	GC (%)	
L1/R1	TGAAAGGCTCGAGAGACA	18	55.10	50.00	CTTGGACCAAACACATCC	18	53.20	50.00	383
L2/R2	CCGCATTAATTCGTTGCTG	19	55.60	47.40	CCGACCCACTGTTAGTTG	18	55.00	55.60	561
L3/R3	TTGGGTCCAGTAGGTCGA	18	56.70	55.60	AGGTTCCCGTACGTTTGG	18	56.90	55.60	470
L4/R4	CTCTTCGGTCCAGATATTTGG	21	55.90	47.60	TCCTTTCAGAATCGTCCGATA	21	56.30	42.90	468
L5/R5	AGCTCGTTTCTCAATCAGGTA	21	56.80	42.90	ACGATGACTCAGCCTACTAGA	21	57.40	47.60	443
L7/R7	GGAATTACTTGTCGCAGAAG	20	54.40	45.00	GAGATGATACCGTGTCACTCTT	22	57.40	45.50	425
L8/R8	TAGGAGCACCATTCAGTGTG	20	57.20	50.00	GCAGAGGTAGACGGTTCA	18	56.00	55.60	399
L9/R9	AACCGTTTGATAGATGGCCTTC	22	58.70	45.50	GACGAGACGGAGCAACTA	18	56.10	55.60	377
L10/R10	TCAAGTTTCATACTCGCCTG	20	55.50	45.00	CAAAAGCACATACCAAGTTCACTC	24	58.80	41.70	338
L11/R11	TACCGTGTACGTCTAATGCTAC	22	57.50	45.50	CCGGTCAGAATTACTTGTCTC	21	56.10	47.60	386

4.3.2.2. Gene amplification and DNA clean-up

Primers (Table 4.1., Table 4.2., Table 4.3. and Table 4.4.) were ordered from Merck/Sigma Aldrich UK. To amplify the genes and test the PP efficacies, a PCR was carried out using a Gstorm or a Mastercycler X50s (Eppendorf) PCR machines. Concentrations and volumes for the PCR are shown in Table 4.5., and parameters used for the amplification in Table 4.6. Genomic DNA template used for the PCR reaction was obtained from parental lines WEKH85A and Hobbit *sib* (protocol can be seen in section 2.3.3.1. in Chapter 2). Quality of PCR amplicons was determined using gel electrophoresis and visualized in a Bio-Rad Gel Imaging System. DNA fragments were excised from the agarose gel and purified using the QIAquick® Gel Extraction Kit (QIAGEN), following manufacture's protocol.

Table 4.5. *PCR reagents for primer quality assays.*

	Reagent	Initial concentration	Volume per well (µl)
Master Mix (MM)[1]	Buffer	5x	4
	$MgCl_2$	25 µM	1.2
	dNTPs	10 mM	0.4
	TaqPol*	5 U/µl	0.1
	F primer	10 µM	1.3
	R primer	10 µM	1.3
	DNA template	-	4
	dH_2O	-	7.7
	Total		**20**

*Gotaq G2 Flexi DNA polymerase from Promega. [1]All the components are mixed in a MM for the appropriate number of samples except the DNA template and dH_2O.

Table 4.6. *PCR thermo-cycling parameters.*

Activity	Temperature (°C)	Cycles	Time
Denaturation I	95	x1	2 min
Denaturation II	95		30 s
Annealing	61	x35	1 min
Extension I	72		40 s
Extension II	72	x1	5 min
Storage	10	-	Indefinitely

4.3.2.3. Cloning of PCR products

PCR products were cloned using the protocol of pGEM®-T Easy Vector Systems (Promega), following manufacturer's instructions. Reactions used for the ligation, as well as for the positive and background controls are shown in Table 4.7.

Table 4.7. *Ligation reagents and reactions for cloning PCR products into a vector system.*

Reagent	Standard reaction (µl)	Positive reaction (µl)[1]	Background reaction (µl)[2]
2X Rapid Ligation Buffer, T4 DNA Ligase	5	5	5
pGEM®-T Easy Vector Systems (50 µl)	1	1	1
PCR product	2	-	-
Control Insert DNA	-	2	-
T4 DNA Ligase (3 Weiss units/ µl)	1	1	1
dH_2O	1	1	3
Total	**10**	**10**	**10**

[1] Ligation with a control DNA provided with the kit (positive control). [2]Ligation with just the vector (negative control).

Plasmids were inserted into competent *Escherichia coli* cells using the manual of One Shot™ TOP10 Chemically Competent Cells (Invitrogen™). Blue-white colony screening was done on plates of X-Gal agar with ampicillin to identify recombinant bacterial colonies. Colonies that contain the inserted-PCR product were white. Then, plasmid DNA purification from selected white colonies was performed with the QIAprep Spin Miniprep Kit (QIAGEN), following manufacturer's instructions.

4.3.2.4. Sanger sequencing

DNA obtained from both the clean-up as well as from the purification method was quantified using a NanoDrop 2000 (Thermo Scientific) spectrophotometer and diluted accordingly with the company's sequencing requisites. Diluted DNA samples (15 µl) were sent to Eurofins Genomics for Sanger sequencing. For each PP, two DNA samples were sent containing the 5' and the 3' primers. Thus, for each PCR product, a sequence file for its

forward and reverse strand was obtained. Sequences were analysed using Geneious Prime software (version 2021.2.2).

4.3.3. Characterisation of *TraesCS5A02G191700* expression profile

4.3.3.1. cDNA synthesis and quality check

RNA of +/- 5A QTL lines roots exposed to 6 h of DON (5 µM) or control (H_2O) treatments (see section 3.3.2. in Chapter 3) was transformed into cDNA to run a RT-qPCR. Samples of cDNA were prepared using the SuperScript® III First-Strand Synthesis System for RT-PCR (Invitrogen), following manufacturer's instructions. cDNA was quantified using a NanoDrop 2000 spectrophotometer.

To test cDNA quality, a normal PCR was carried out using a Gstorm or a Mastercycler X50s (Eppendorf) PCR machines. Concentrations and volumes for the PCR reaction are shown in the previous Table 4.5., and parameters used for the amplification are shown in Table 4.6.

To amplify gene *TraesCS5A02G191700*, a pair of primers were manually developed on the CDS (700_CDS) using Geneious Prime software (version 2021.2.2). The housekeeping gene of wheat hn-RNPQ (heterogeneous nuclear ribonucleoprotein Q, *TraesCS2A02G390200*) was obtained from other study (Hu et al. 2019b). Primers were ordered from Sigma-Aldrich (Table 4.8.) and tested in the cDNA. Quality of PCR amplicons was determined using gel electrophoresis and visualized in a Bio-Rad Gel Imaging System.

Table 4.8. *Primer pair sequences used to sequence the coding region of gene TraesCS5A02G191700 (700_CDS) and the housekeeping gene of wheat hn-RNPQ (heterogeneous nuclear ribonucleoprotein Q, TraesCS2A02G390200). Sequence (from 5' to 3'), length (bp), melting temperature (Tm), and GC content (%) for each left (L) and right (R) primers are specified. Product size (bp) for each primer pair is shown.*

Gene	Primer Pairs	seq 5' to 3'	length (bp)	Tm (°C)	GC (%)	Product size (bp)
700_CDS	**L**	ATCGAGCTCTCGTCTTCCA	19	57.80	52.60	200
	R	TCCGCTCCTTCAGCATCT	18	58.00	55.60	
hn-RNPQ	**L**	TCACCTTCGCCAAGCTCAGAACTA	24	69.90	50.00	127
	R	AGTTGAACTTGCCCGAAAC	19	61.70	47.40	

4.3.3.2. RT-qPCR assay

Following quality check, the cDNA obtained for each treatment was then used for RT-qPCR reactions (Table 4.9.). To test PP 700_CDS (Table 4.8.) two or three biological replicates, and two-three technical replicates were prepared. To test PP for housekeeping gene hn-RNPQ (Table 4.8.) three or four biological replicates, and two-three technical replicates were prepared. RT-PCR was carried out on a CFX96^{TM} Real-Time PCR detection system (BIO RAD) using the Scan mode SYBR/FAM only, using the parameters specified in Table 4.10.

Table 4.9. *Reagents for the RT-qPCR assay.*

	Reagent	Initial concentration	Volume per well (µl)
Master Mix (MM)[1]	SYBR green*	2x	5
	F primer	10 µM	0.6
	R primer	10 µM	0.6
	cDNA	**	2
	dH_2O	-	1.8
	Total		**10**

*SYBR Green JumpStart Taq ReadyMix from Sigma-Aldrich. ** A 1/10, 1/50, 1/100, 1/500 and 1/1000 cDNA dilution series from stock were developed. [1]All the components are mixed in a MM for the appropriate number of samples except the DNA template and dH_2O.

Table 4.10. *PCR thermo-cycling parameters for gene TraesCS5A02G191700 expression analysis.*

Activity	Temperature (°C)	Cycles	Time
Denaturation I	95	x1	4 min
Denaturation II	94		10 s
Annealing	60	x39	10 s
Extension I	72		30 s
Extension II	72	x1	10 min
Meltcurve capture	65-95	-	5 s

For both the target gene *TraesCS5A02G191700* and the housekeeping gene hn-RNPQ, the quantification cycles (Cq) were obtained from BioRad CFX Manager Software V3.1. Then, the log_2-fold change in expression was calculated using the Livak method for relative gene expression and following the Equation 4.1. The primer efficiency was experimentally

determined in a dilution series experiment using the same procedures stated in Table 4.9. and Table 4.10. Microsoft Excel (2016) was used to analyse and calculate the log_2-fold change, and to perform a standard student t-Test.

Equation 4.1. *Calculation for the log-fold change in expression of the target gene TraesCS5A02G191700 from Cq values between two treatments (DON vs. Control) using a housekeeping gene as a reference. Cq = Quantification cycle. GOI = Gene of Interest. HK = Housekeeping gene. Primer efficiency was calculated from standard curves developed for the GOI and HK. Equation from Dr John Francis Haidoulis (thesis).*

$$\Delta Ct = (GOI\ Cq - HK\ gene\ Cq)$$

$$\Delta\Delta Ct = (DON\ Treatment\ \Delta\ Cq - Control\ Treatment\ \Delta\ Cq)$$

$$Log_2 fold\ change = Log_2(Primer\ Efficiency^{\Delta\Delta\ Cq})$$

4.3.4. Gene copy number estimation of *TraesCS5A02G191700*

4.3.4.1. Designing primers and TaqMan® probe for gene *TraesCS5A02G191700*

To amplify gene *TraesCS5A02G191700*, a pair of primers and a TaqMan® probe were manually developed on the upstream region of the CDS using both Geneious Prime software (version 2021.2.2) and Primer3Plus (Untergasser et al. 2007). Primers were ordered from Sigma-Aldrich and the TaqMan® probe from Thermo Fisher Scientific. Sequences (5' to 3') for the left (L) and the right (R) primers, and the probe, are shown in Table 4.11., where the length (in bp), the Tm (°C), the GC content (%), primer dimer, secondary structure, and the product size of the PP (in bp) are also specified.

Table 4.11. *Primer pair and TaqMan® probe sequences used for the ddPCR of gene TraesCS5A02G191700. Sequence (from 5' to 3'), length (bp), melting temperature (Tm), GC content (%), primer dimer, and secondary structure for each left (L) and right (R) primers and probe are specified. Product size (bp) for the PP is shown. OligoEvaluatorTM (Sigma-Aldrich) was used to recheck primers parameters.*

Primer Pairs	seq 5' to 3'	length (bp)	Tm (°C)	GC (%)	Primer dimer	Secondary Structure	Product size (bp)
L	TTTCTCGTGCGCTGCT	16	62.3	56.2	No	None	263
R	AAATGGAAGGCATGCCTG	18	63.7	50.0	No	Weak	
Probe	ATCAGCGCCACTCACAAGTCAC	22	68.8	54.5	No	Very Weak	-

To develop the probe to be specific of gene *TraesCS5A02G191700*, an alignment with its respective homoeologous genes (*TraesCS5B02G191400* and *TraesCS5D02G199200*), its paralogue gene *TraesCS5A02G191800*, and its homoeologous genes (*TraesCS5B02G191300* and *TraesCS5D02G199100*) was performed (see Figure 4.1.).

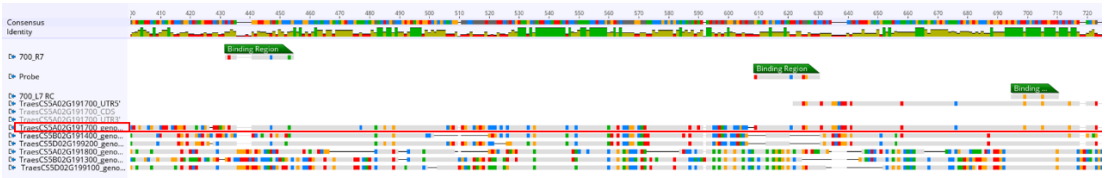

Figure 4.1. *Alignment of TraesCS5A02G191700 and TraesCS5A02G191800, and its homoeologues genes to develop a primer pair and a probe to be specific of gene TraesCS5A02G191700 (underlined in red). PP left (700_L7) and right (700_R7), and probe are shown on the left.*

Specific parameters were used to design the PP and probe. General settings for the PP were: product (amplicon) size ranging from 60-200 bp; primer size between 18-25 bp (Opt. 20 bp); primer Tm between 57-63°C (Opt. 60°C); primer GC content between 50-60 % (Opt. 55 %). General settings for the internal oligo (probe) were oligo size between 18-29 bp (Opt. 25 bp); oligo Tm between 64-70°C (Opt. 66°C); oligo GC content between 30-80 % (Opt. 50 %).

Due to sequence similarity between paralogues and homoeologues it was not possible to develop a specific probe to the CDS of gene *TraesCS5A02G191700*, so a probe was designed upstream of the CDS within the 5' untranslated region, as Figure 4.1. represents.

4.3.4.2. Reference genes in wheat

The sequence information of the two reference control genes (Ref. gene 1 and Ref. gene 2) for wheat were provided by Tom Lawrenson from the transformation team (Crop Genetics, JIC). Primers were ordered from Sigma-Aldrich, but probes aliquots were provided by Tom (Table 4.12. and Table 4.13.).

One reference gene (Ref. gene 1) is present as a single copy in each wheat genome; therefore, it has a total of three copies in the hexaploid bread wheat genome (*TraesCS6A02G289400*, *TraesCS6B02G319500* and *TraesCS6D02G269500*). This gene is *TaHd1-1*, and it is involved in zinc ion binding and regulation of flower development. It belongs to the zinc finger protein CONSTANS-LIKE (https://www.uniprot.org/uniprot/Q76K62). The other gene (Ref. gene 2) is present only on the B genome (*TraesCS6B02G307300*) with no homoeologues.

Table 4.12. *Primer pair and TaqMan® probe sequences used for the ddPCR of Ref. gene 1. Sequence (from 5' to 3'), length (bp), melting temperature (Tm), GC content (%), primer dimer, and secondary structure for each left (L) and right (R) primers and probe are specified. Product size (bp) for the PP is shown. OligoEvaluatorTM (Sigma-Aldrich) was used to recheck primers parameters.*

Primer Pairs	seq 5' to 3'	length (bp)	Tm (°C)	GC (%)	Primer dimer	Secondary Structure	Product size (bp)
L	TGCTAACCGTGTGGCATCAC	20	67.1	55.0	No	Weak	107
R	GGTACATAGTGCTGCTGCATCTG	23	65.7	52.2	No	Weak	
Probe	CATGAGCGTGTGCGTGTCTGCG	22	76.6	63.6	No	None	-

Table 4.13. *Primer pair and TaqMan® probe sequences used for the ddPCR of Ref. gene 2. Sequence (from 5' to 3'), length (bp), melting temperature (Tm), GC content (%), primer dimer, and secondary structure for each left (L) and right (R) primers and probe are specified. Product size (bp) for the PP is shown. OligoEvaluatorTM (Sigma-Aldrich) was used to recheck primers parameters.*

Primer Pairs	seq 5' to 3'	length (bp)	Tm (°C)	GC (%)	Primer dimer	Secondary Structure	Product size (bp)
L	TCAAAATGACTGGCCTAATCAGATAA	30	65.3	34.6	No	Weak	78
R	GATCAATTGTTCGACAGTGAAGGT	24	65.1	41.7	No	Very weak	
Probe	TCCGCTGGGCATAATTCCAATGAGC	25	75.4	52.0	No	Weak	-

4.3.4.3. Leaf sampling and DNA extraction

Genomic DNA from seedlings of parental lines WEKH85A, Hobbit *sib* and Chinese Spring was extracted using the QIAamp® 96 DNA QIAcube® HT Kit (QIAGEN), following manufacturer's instructions, to obtain high quality DNA.

4.3.4.4. PCR assay

To test the PP efficacies for gene *TraesCS5A02G191700* and Ref. gene 1 and 2, a PCR was carried out using a Gstorm or a Mastercycler X50s (Eppendorf) PCR machines. Concentrations and volumes for the PCR are shown in Table 4.14., and parameters used for the amplification in the previous Table 4.6. in section 4.2.2.2. A restriction enzyme (EcoRI) was used to cut the template DNA (5'…G/AATTC…3') and aid quantification. The EcoRI mix was prepared (Table 4.15.) and added as the last component of the Master Mix (MM). Genomic DNA template used for the PCR reaction was obtained from parental lines WEKH85A, Hobbit *sib* and Chinese Spring.

Table 4.14. *PCR reagents for primer quality assays when using EcoRI-HF restriction enzyme.*

	Reagent	Initial concentration	Volume per well (µl)
Master Mix (MM)[1]	Buffer	5x	4
	$MgCl_2$	25 µM	1.2
	dNTPs	10 mM	0.4
	TaqPol*	5 U/µl	0.1
	F primer	10 µM	1.3
	R primer	10 µM	1.3
	EcoRI mix[2]	10x	1
	DNA template	-	3
	dH_2O	-	7.7
	Total		**20**

*Gotaq G2 Flexi DNA polymerase from Promega. [1]All the components are mixed in a MM for the appropriate number of samples except the DNA template and dH_2O. [2]See Table 4.15. for protocol.

Table 4.15. *Reagents and volumes needed to prepare the EcoRI mix (10x).*

Reagent	Initial concentration	Volume per well (µl)
Smartcut Buffer	10x	8
EcoRI-HF®**	20 U/µl	10
dH_2O		62
Total		80

**High-Fidelity (HF®) restriction enzyme (10000 U) from NEW ENGLAND BioLabs.

4.3.4.5. ddPCR assay

To quantify the copy number for *TraesCS5A02G191700*, a ddPCR assay was performed following the QIAcuity™ Probe PCR Kit (QIAGEN), following manufacturer's instructions, and using TaqMan® probes in a multiplex reaction. The ddPCR assay was carried out using a QIAGEN's QIAcuity instrument for digital PCR (dPCR).

Concentrations and volumes for the ddPCR are shown in Table 4.16. The primer-probe mix (10x) was prepared as it is shown in Table 4.17. for both Ref. gene 1 with *TraesCS5A02G191700*, and Ref. gene 2 with *TraesCS5A02G191700*. The EcoRI mix (Table 4.15.) was added as the last component of the MM. A QIAcuity Nanoplate 8.5k 24-well (QIAGEN) and specific QIAcuity Nanoplate seal were used as protocol described.

Table 4.16. *ddPCR reagents using EcoRI-HF restriction enzyme.*

	Reagent	Initial concentration	Volume per well (µl)
Master Mix (MM)[1]	QIAcuity Probe PCR MM	4x	3
	Primer-Probe mix[2]	10x	1.2
	EcoRI mix[3]	10x	1.2
	DNA template	-	3
	RNase-free water	-	3.6
	Total		**12**

[1]All the components are mixed in a MM for the appropriate number of samples except the DNA template and dH_2O. [2]See Table 4.17. for protocol. [3]See Table 4.15. for protocol.

Table 4.17. *Reagents and volumes needed to prepare the primer-probe mix (10x) using both reference genes in wheat (Ref. gene 1 + TraesCS5A02G191700, and Ref. gene 2 + TraesCS5A02G191700). L primer = left primer. R primer = right primer.*

Reagent	Initial concentration	Volume per well (µl)
TaqMan® probe	100 µM	3.2
L primer	100 µM	6.4
R primer	100 µM	6.4
TaqMan® probe (Ref. gene*)	100 µM	3.2
L primer (Ref. gene*)	100 µM	6.4
R primer (Ref. gene*)	100 µM	6.4
RNase-free water	-	48
Total		80

* TaqMan® probe, left and right primers of reference gene 1 or 2 for two different multiplex reactions.

The Nanoplate was prepared to be run for the two multiplex reactions: one using primers and probe of Ref. gene 1 with *TraesCS5A02G191700*, and the other using Ref. gene 2 with *TraesCS5A02G191700*. Three genomic DNA samples (WEKH85A, Hobbit *sib* and CS) were used at two different concentrations (two biological replicates) for the two multiplex reactions. Concentrations used were higher than 150 ng/µl. The reason for this was to identify the optimal concentration for each DNA template. Two technical replicates per concentration were prepared, giving a total of 24 samples that filled a Nanoplate.

Then, the Nanoplate was left at room temperature for about 10-15 min for DNA digestion. The parameters used in the QIAcuity instrument for the thermal cycling are specified in Table 4.18.

Table 4.18. *ddPCR thermo-cycling parameters.*

Activity	Temperature (°C)	Cycles	Time
PCR initial heat activation	95	x1	2 min
Denaturation	95	x40	15 s
Annealing/ Extension (combined)	60		30 s

4.4. Results

4.4.1. Assessment of critical FHB resistant and susceptible RILs for DON tolerance in roots

Critical FHB type II resistant and susceptible RILs derived from the Hobbit *sib* x WEKH85A were used to test DON tolerance. Two experiments were performed at different timings. In the first experiment (Test 1), lines RIL 9A and RIL 17B were tested together with control lines RIL 97 and Hobbit *sib*. These control lines were used since the effect upon DON has been previously studied (see Chapter 3). In the second experiment (Test 2), lines RIL 10B and RIL 16A, and control lines, were tested.

Root lengths were measured every day for a total of 9 dpi, and final photos of seedling development were taken at 10 dpi, when seedlings were removed from agar tubes. Only final photos of lines tested in Test 2 are shown in Figure 4.2. (- 5A QTL lines) and Figure 4.3. (+ 5A QTL lines). Photos represent the nine seedlings (replicates) tested per line and treatment. Clear differences can be observed between control and DON (5 μM) treatments on the development of roots for all lines tested.

To identify differences in DON tolerance, control and DON treatments for each line were compared. First, the slope data (see section 4.3.1.3.) was calculated for each replicate of a line given at each day post-infection (dpi; starting at 3 dpi). This was calculated for both Test 1 and Test 2. The slope data represents the average rate of root growth change over time after the application of treatments.

For Test 1, when roots of RIL 9A (+ 5A QTL) and RIL 17B (- 5A QTL) were assessed the slope data showed that lines *(P*-value < 0.001) and treatments *(P*-value < 0.001) significantly differ while the interaction between line and treatment had no significant influence, indicating that the two factors are independent of each other (Table S18.).

For Test 2, when RIL 10B (+ 5A QTL) and RIL 16A (- 5A QTL) were tested, roots slope data showed that lines *(P*-value < 0.001 and < 0.05, respectively) and treatment *(P*-value < 0.001) significantly differ while the interaction between line and treatment had no significant influence, indicating that the two factors are independent of each other (Table S19.).

Additionally, root slope data for both Test 1 and Test 2 showed that trays *(P*-value > 0.05) did not show differences, meaning that lines and treatments were equally distributed within trays.

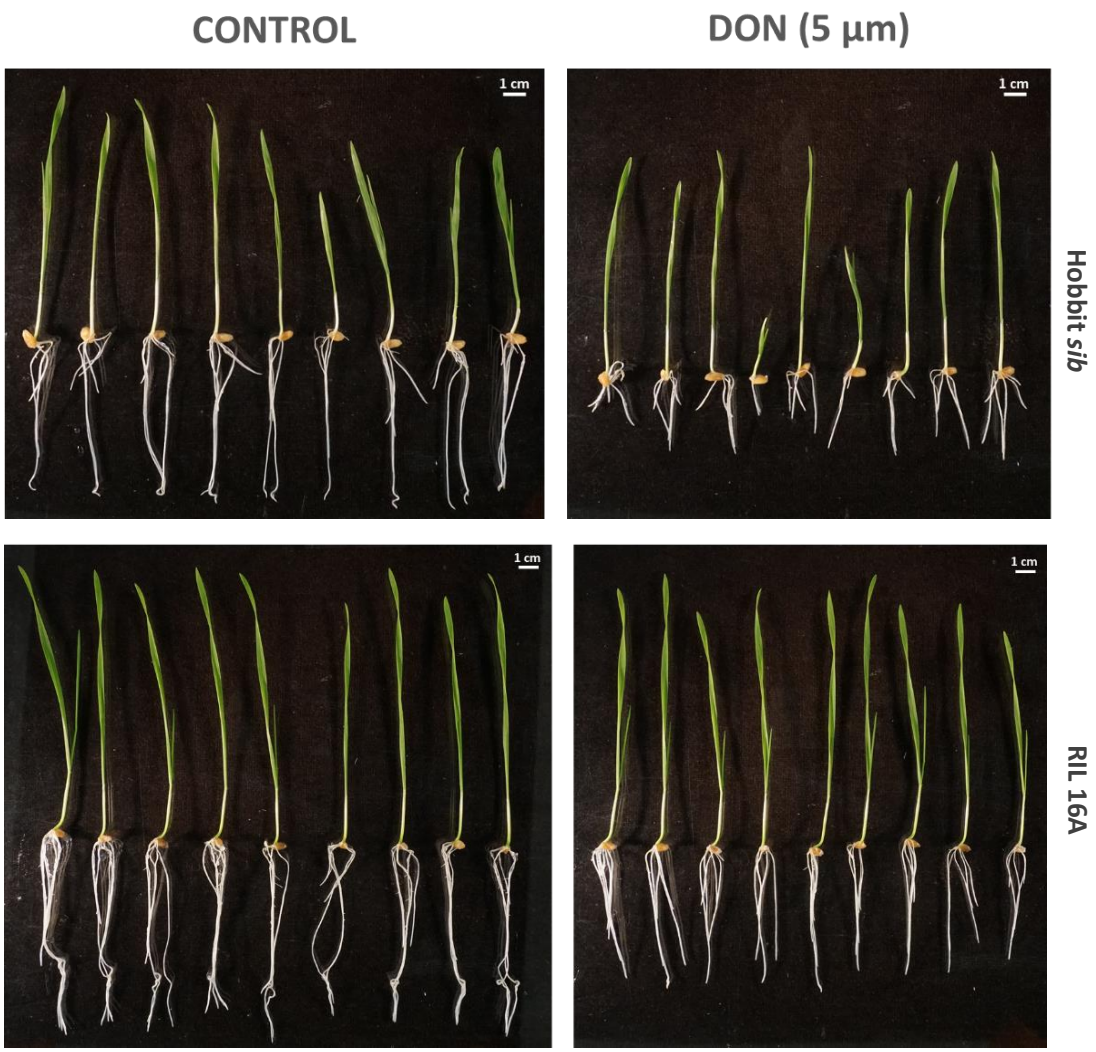

Figure 4.2. *Roots and shoots at 10 dpi of the - 5A QTL lines Hobbit sib (top) and RIL 16A (bottom) used for Test 2. Seedlings grown in agar (control) and gar + DON (5 µM).*

Table 4.19. *P-value of roots slope data of +/- 5A QTL wheat lines tested under DON (5 µM) and control treatments at different days post infection (dpi) on Test 1. Lines tested were Hobbit sib, RIL 97, RIL 9A and RIL 17B. Green = P-value < 0.001.*

	3 dpi	4 dpi	5 dpi	6 dpi	7 dpi	8 dpi	9 dpi	10 dpi
Line	<.001	<.001	<.001	<.001	<.001	<.001	<.001	<.001
Treatment	<.001	<.001	<.001	<.001	<.001	<.001	<.001	<.001
Line x Treatment	0.130	0.067	0.076	0.138	0.115	0.099	0.086	0.099
Tray	0.254	0.229	0.259	0.380	0.376	0.323	0.310	0.317

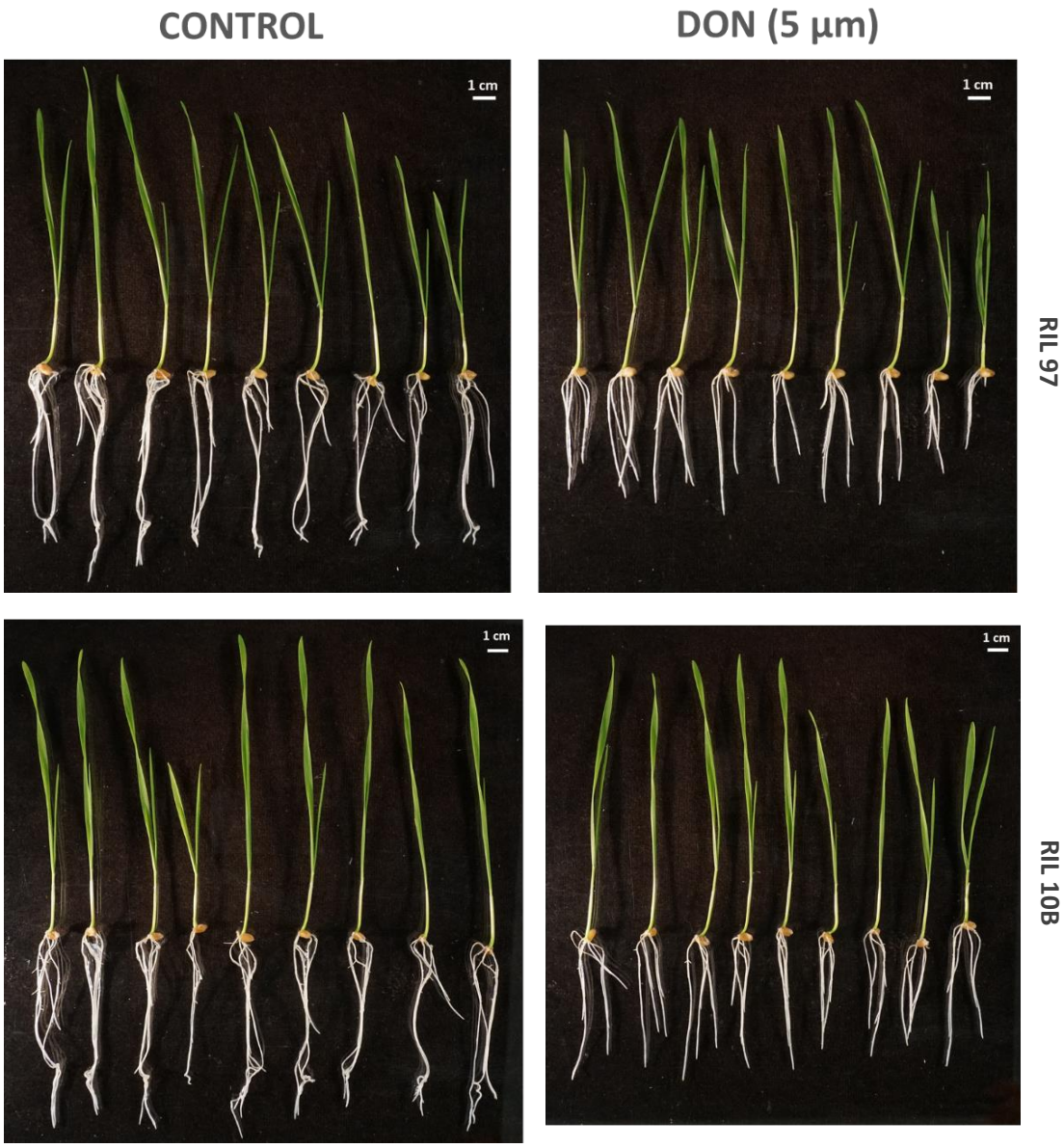

Figure 4.3. *Roots and shoots at 10 dpi of the + 5A QTL lines RIL 97 (top) and RIL 10B (bottom) used for Test 2. Seedlings grown in agar (control) and gar + DON (5 µM).*

Table 4.20. *P-value of roots slope data of +/- 5A QTL wheat lines tested under DON (5 µM) and control treatments at different days post infection (dpi) on Test 2. Lines tested were Hobbit sib, RIL 97, RIL 10B and RIL 16A. Green = P-value < 0.001.*

	3 dpi	4 dpi	5 dpi	6 dpi	7 dpi	8 dpi	9 dpi	10 dpi
Line	<.001	<.001	<.001	<.001	<.001	<.001	<.001	<.001
Treatment	<.001	<.001	<.001	<.001	<.001	<.001	<.001	<.001
Line x Treatment	0.293	0.116	0.054	0.083	0.110	0.135	0.110	0.101
Tray	0.896	0.859	0.812	0.783	0.765	0.695	0.666	0.673

The slope ratio (DON treatment/ control treatment) for each line was calculated and represented as percentage of root development. Both Test 1 and Test 2 were represented together in Figure 4.4. The ratio DON/Control shows the effect of the DON treatment compared with the control.

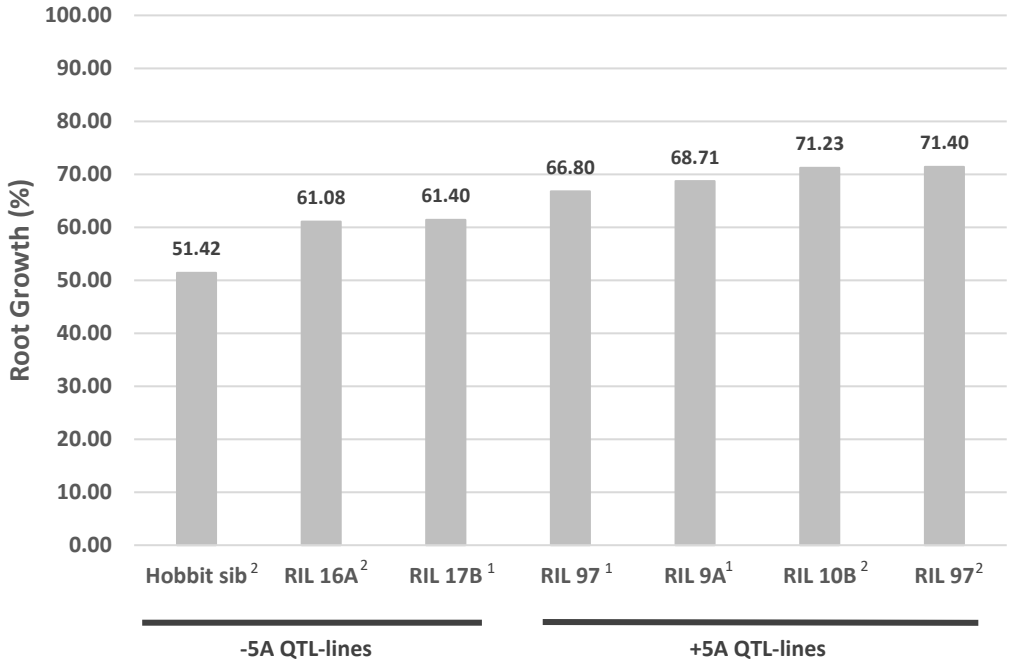

Figure 4.4. *Ratio DON/control (%) of roots at 4 dpi of +/- 5A QTL lines. [1]Lines RIL 9A, RIL 97 and RIL 17B tested in Experiment 1 (Test 1). [2]Lines RIL 10B, RIL 97, RIL 16A and Hobbit sib tested in Experiment 2 (Test 2). Predicted means were generated using an Unbalanced ANOVA. The percentage of the ratio of root length between predicted mean treated (DON) and untreated (control) was calculated for each line. Percentage values for each line are shown on the top of each bar.*

Results revealed that roots of lines containing the 6.24 Mbp-QTL associated with FHB type II resistance (RIL 97, RIL 9A and RIL 10B) were less inhibited compared with lines not containing the QTL (RIL 16A, RIL 17B and Hobbit *sib*). Data from Hobbit *sib* from Test 1 was not included due very poor seed performance leading to uneven growth. Parental lines were bulked, and new seed was harvested to be used in Test 2.

The difference in root length between RIL 97 (used in Test 2) and Hobbit *sib* at 4 dpi was 20 % (Figure 4.4.). At 5 dpi the difference is of 22 % (see Supplementary Data Table S19) and then it decreased over time. The difference of root length between RIL 97 (used in Test 2) and RIL 16A (- 5A QTL) at 4 dpi was 10 % (Figure 4.4.), and the differential also to decreased over time being around 4 % from 7 dpi. Differences between RIL 97 and RIL 10B were minimal over time (see Supplementary Data Table S19).

The level of DON tolerance of Line RIL 97 in Test 1 was not as great as in Experiment 2. The difference in root length between RIL 97 (used in Experiment 1) and RIL 17B (- 5A QTL) at 4 dpi was 5 %, and between RIL 9A (+ 5A QTL) and RIL 17B was 7 % (Figure 4.4.). These differences decreased over time (see Supplementary Data Table S18).

Lines used for both Tests 1 and 2 were screened with markers: *S4, S11, S13, S18, S20* and *S25* to confirm the presence /absence of markers to the QTL region. Genotypic data of RILs and parental line Hobbit *sib* combined with the phenotypic data obtained from the DON assay of Test 1 and 2 is represented in Table 4.21. The allele provided by the parental line Hobbit *sib* is presented as 'Hs' (red), and the one provided by parental line WEKH85A as 'WEK' (blue). Ratio DON/control (%) of roots is shown for 4 dpi.

To conclude, the lines harbouring the 'WEK' allele showed higher levels of DON resistance in roots in both experiments Tests 1 and 2 (RIL 9A with 68.71 %, RIL 10B with 71.23 %, and RIL 97 with 71.40 %) (Table 4.21.) when compared with lines harbouring the 'Hs' allele (RIL 16A with 61.08 %, RIL 17B with 61.40 %, and Hobbit *sib* with 51.42 %).

Table 4.21. *Genotypic data of RILs and parental line Hobbit sib combined with the phenotypic data obtained from the DON assay of Experiment 1 and 2 (Test 1 and 2). RILs were chosen because of the presence or absence of the 6.24 Mbp-QTL on the 5AL chromosome, between markers S11 (389.64 Mbp) and S18 (395.89 Mbp). Hs = allele provided by parental line Hobbit sib. WEK = allele provided by parental line WEKH85A. Ratio DON/control (%) of roots is represented at 4 dpi.*

	RefSeqv1.0 (Mbp)	321.89	389.64	394.75	395.89	400.79	409.32	
	Markers	**S4**	**S11**	**S13**	**S18**	**S20**	**S25**	**Ratio DON/control of roots (%)**
Experiment 1	**RIL 9A**	Hs	Hs	WEK	Hs	Hs	Hs	68.71
	RIL 97	Hs	WEK	WEK	WEK	WEK	WEK	66.80
	RIL 17B	WEK	Hs	Hs	Hs	WEK	Hs	61.40
Experiment 2	**RIL 10B**	Hs	WEK	WEK	Hs	Hs	WEK	71.23
	RIL 97	Hs	WEK	WEK	WEK	WEK	WEK	71.40
	RIL 16A	WEK	Hs	Hs	Hs	WEK	Hs	61.08
	Hobbit *sib*	Hs	Hs	Hs	Hs	Hs	Hs	51.42

4.4.2. Sequencing genes TraesCS5A02G191700 and TraesCS5A02G191800

During the RNA-Seq analysis in Chapter 3, five DEGs upon DON treatment were identified on the 5A locus in RIL 97, between 322 to 417 Mbp. Therefore, these genes are specific of the parental line providing the resistance, WEKH85A. However, only two genes, *TraesCS5A02G191700* and *TraesCS5A02G191800,* located within the 6.24 Mbp FHB QTL showed a response to DON in both lines. Furthermore, gene *TraesCS5A02G191700* was differentially expressed in response to the mycotoxin between Hobbit *sib* and RIL 97 being more highly expressed in the latter.

These two DON-candidate genes were selected for sequencing. Specific PP were manually designed to amplify the CDS and the upstream region (3000 bp) of both genes. Read files for the forward and reverse sequences were obtained of each PCR product and were aligned together with the upstream genomic sequence of 3000 bp, and the sequences of the UTR5', CDS and UTR3' of CS gene *TraesCS5A02G191700* and *TraesCS5A02G191800*, respectively.

Sequencing results in the CDS of both genes did not reveal any polymorphism with respect CS reference genome. However, polymorphisms were identified in the upstream region of both genes. The promoter of *TraesCS5A02G191700* revealed 25 SNPs between the parental lines and CS (Figure 4.5 and Table 4.22.); an insertion of 1 bp at 763 bp upstream of the transcription start site in the UTR5' of the gene; a deletion of 8 bp in both parental lines at 887 bp upstream of the transcription start site in the UTR5' of the gene; and a 3 bp-deletion in the parental line WEKH85A at 2007 bp upstream the UTR5' of the gene *TraesCS5A02G191700* (Figure 4.6 and Table 4.23.).

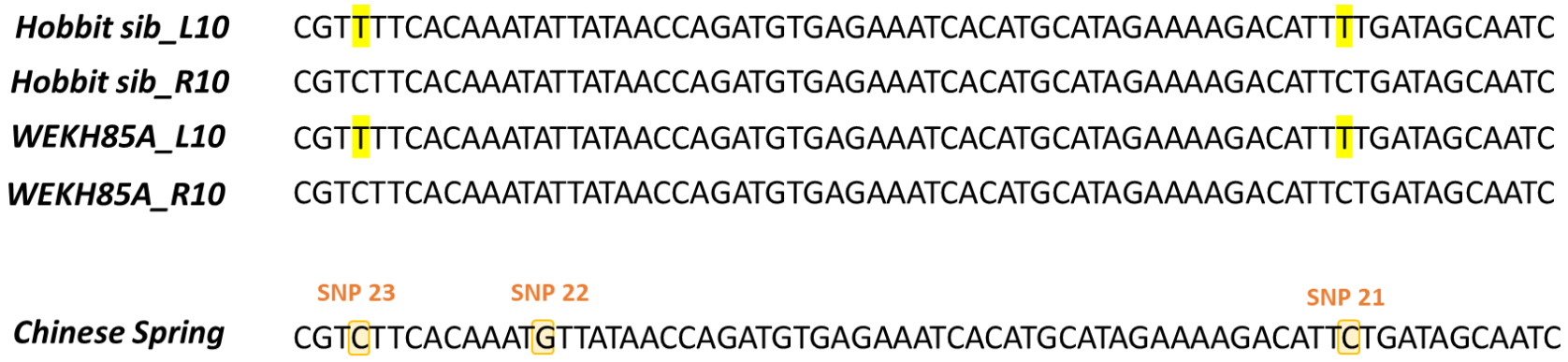

Figure 4.5. *Polymorphisms (SNPs 21-23; orange squares) identified in the promotor region of gene TraesCS5A02G191700 between parental lines Hobbit sib (Hs) and WEKH85A (WEK). This genomic region was amplified using primer pairs (PP) L10/R10. Alignment of sequenced reads from parental lines Hs and WEK against Chinese Spring reference genome was done using Geneious Prime software (version 2021.2.2).*

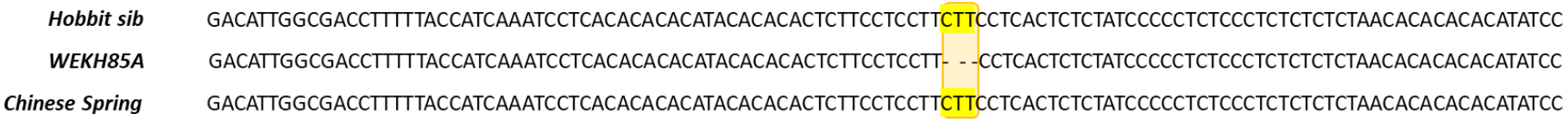

Figure 4.6. *Deletion of 3 bp identified in the promotor region of gene TraesCS5A02G191700 in parental line WEKH85A. This genomic region was amplified using primer pairs (PP) L8/R8. Alignment of sequenced reads from parental lines Hobbit sib and WEKH85A was done using Geneious Prime software (version 2021.2.2).*

From 25 SNPs identified in the promoter of *TraesCS5A02G191700* between Hs/WEK and CS, there were eight SNPs which were classified as being 'Heterozygous' (Het) (Table 4.22.). These Het SNPs were identified in the sequence from only one of the forward or reverse strands for both parental lines but not in the other direction. The allele given for each parental line and the PP used to sequence that read is specified in Table 4.22.

Table 4.22. *Polymorphisms (SNPs) identified between Chinese Spring (CS) reference genome (IWGSC RefSeq v1.0) and parental lines Hobbit sib (Hs) and WEKH85A (WEK) on the promoter region of gene TraesCS5A02G191700. The location of each SNP was calculated counting the number of base pairs (bp) upstream from the UTR5' of the gene. Several SNPs were classified as being 'Heterozygous' and next to the corresponding allele it is shown in which primer pair (right or left) was identified.*

			Alleles		
Polymorphism	**Comments**	**Location (bp)**	**CS**	**Hs**	**WEK**
SNP 1		645	C	T	T
SNP 2		647	A	G	G
SNP 3		663	A	G	G
SNP 4		714	A	G	G
SNP 5		784	A	G	G
SNP 6		789	A	G	G
SNP 7		813	G	A	A
SNP 8	Heterozygous	843	G	G (Left)/ A (Right)	G (Left)/ A (Right)
SNP 9	Heterozygous	995	C	T	C (Left)/ T (Right)
SNP 10		1018	A	G	G
SNP 11		1067	A	G	G
SNP 12		1196	A	G	G
SNP 13		1269	A	G	G
SNP 14		1293	T	C	C
SNP 15		1302	T	C	C
SNP 16		1323	T	C	C
SNP 17	Heterozygous	1329	C	C (Left)/ T (Right)	T
SNP 18		1420	G	A	A
SNP 19	Heterozygous	1618	C	T (Left)/ C (Right)	T (Left)/ C (Right)
SNP 20	Heterozygous	1625	C	T (Left)/ C (Right)	T (Left)/ C (Right)
SNP 21	Heterozygous	1678	C	T (Left)/ C (Right)	T (Left)/ C (Right)
SNP 22		1721	G	A	A
SNP 23	Heterozygous	1731	C	T (Left)/ C (Right)	T (Left)/ C (Right)
SNP 24		1899	T	C	C
SNP 25		1920	T	C	C

Table 4.23. *Deletions and insertions identified between Chinese Spring (CS) reference genome (IWGSC RefSeq v1.0) and parental lines Hobbit sib (Hs) and WEKH85A (WEK) on the promoter region of gene TraesCS5A02G191700. The location of each insertion/deletion was calculated counting the number of base pairs (bp) upstream from the UTR5' of the gene. The number of base pairs (bp) of the insertion and deletions are shown.*

			Sequence		
Deletion/Insertions	**N° of bp**	**Location (bp)**	**CS**	**Hs**	**WEK**
Insertion	1	763	-	T	T
Deletion	8	887-895	TAATGTAC	-	-
Deletion	3	2007-2010	CTT	CTT	-

Sequencing results in the promoter of *TraesCS5A02G191800* revealed 10 SNPs between the parental lines and CS (Table 4.24.). Eight SNPs were also classified as being Het, as previously described.

Table 4.24. *Polymorphisms (SNPs) identified between Chinese Spring (CS) reference genome (IWGSC RefSeq v1.0) and parental lines Hobbit sib (Hs) and WEKH85A (WEK) on the promoter region of gene TraesCS5A02G191800. The location of each SNP was calculated counting the number of base pairs (bp) upstream from the UTR5' of the gene. Several SNPs were classified as being 'Heterozygous' and next to the corresponding allele it is shown in which primer pair (right or left) was identified.*

			Allele		
Polymorphism	**Comments**	**Location (bp)**	**CS**	**Hs**	**WEK**
SNP 1	Heterozygous	62	C	T (Left)	T (Left)
SNP 2		1806	A	G	G
SNP 3	Heterozygous	2025	G	G (Left)/ A (Right)	G
SNP 4	Heterozygous	2044	G	G (Left)/ A (Right)	G
SNP 5	Heterozygous	2065	T	T	T (Left)/ G (Right)
SNP 6	Heterozygous	2141	C	T (Left)	T (Left)
SNP 7	Heterozygous	2332	C	T (Left)	T (Left)
SNP 8	Heterozygous	2336	T	T (Left)/ A (Right)	T
SNP 9	Heterozygous	2363	C	T (Left)	T (Left)
SNP 10		2917	A	T	T

In summary, the sequence of the CDS of gene *TraesCS5A02G191700* and *TraesCS5A02G191800* of both parental lines did not differ from that of the CS reference genome. However, clear differences were observed in the upstream genomic region for both genes in the parental lines Hobbit *sib* and WEKH85A with respect CS. Indeed, small but

potentially important differences were identified in the promoter region of gene *TraesCS5A02G191700* between WEKH85A and Hobbit *sib*.

4.4.3. Gene *TraesCS5A02G191700* is highly expressed in RIL 97 upon DON exposure

RNA obtained from roots of lines RIL 97 and Hobbit *sib*, exposed to DON or H_2O, were transformed into cDNA for the RT-qPCR analysis. While RIL 97 (+ 5A QTL) was a line conferring DON tolerance and harbouring the *QFhb.WEK5A* locus for FHB type II resistance, line Hobbit *sib* (- 5A QTL) was susceptible to DON and lacking the locus.

Since gene *TraesCS5A02G191700* showed several sequence differences in the promoter region between parental lines, it was checked for gene expression and further analysis. Results showed that the expression level of gene *TraesCS5A02G191700* was much higher in the line harbouring the *QFhb.WEK5A* locus (RIL 97) (log_2 FC = 8.84) than in the parental line Hobbit *sib* (log_2 FC = 1.91) when exposed to DON (Figure 4.7.). This experiment was tested twice, following the same protocol and steps, and results were confirmed.

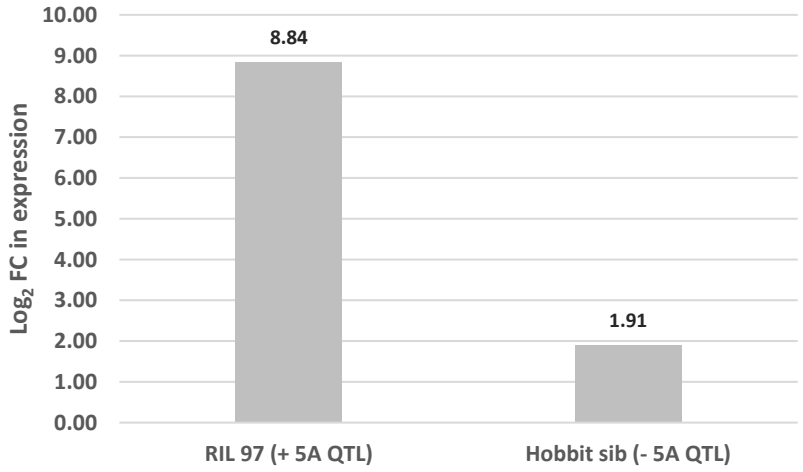

Figure 4.7. *Change in expression of gene TraesCS5A02G191700 in a line harbouring the QFhb.WEK5A locus (RIL 97) and a line lacking the QTL (Hobbit sib) when roots of those lines were exposed to DON. The expression shown is relative to that in control treated roots. The log_2 fold change (FC) in expression for both lines are shown on the top of each bar.*

Additionally, a t-Test analysis was performed to compare DON and control (H_2O) treatments for both +/- *QFhb.WEK5A*-lines, and to compare the differences between Cq values for lines upon DON and water treatments. Note that larger values indicate lower concentrations of cDNA of *TraesCS5A02G191700*. These comparations were performed for both the housekeeping gene of wheat, *hn-RNPQ,* and for the DON-candidate gene *TraesCS5A02G191700* (Table 4.25. and Table 4.26., respectively).

The housekeeping gene did not show any difference in level of expression between treatments or lines (*P*-value > 0.05), as expected (Table 4.25.). However, clear differences on the level of expression were observed for *TraesCS5A02G191700* (Table 4.26.). Differences between control and DON treatments were significant for Hobbit *sib* (*P*-value = 0.004), and highly significant for RIL 97 (*P*-value < 0.0001). Moreover, when comparing both lines upon exposure to DON, the levels of expression significantly differed (*P*-value < 0.0001) being much higher (lower Cq) for RIL97 than Hobbit *sib*.

Table 4.25. *t-Test results of the comparations of all treatments and the P-value given for each comparation when analysing the expression level of the housekeeping gene of wheat hn-RNPQ. DON and control (H_2O) treatments were used. RIL 97 was the line harbouring the QFhb.WEK5A locus, while Hobbit sib was the line lacking the QTL.*

	Hobbit *sib*		**RIL 97**		**Control**		**DON**	
	DON	**Control**	**DON**	**Control**	**Hobbit *sib***	**RIL 97**	**Hobbit *sib***	**RIL 97**
Mean	23.69	23.37	23.41	23.01	23.37	23.01	23.69	23.41
Variance	0.44	0.35	0.28	0.27	0.35	0.27	0.44	0.28
Observations	10	11	11	9	11	9	10	11
Biological reps.	4	4	4	4	4	4	4	4
Technical reps.	2 or 3	2 or 3	2 or 3	2 or 3	2 or 3	2 or 3	2 or 3	2 or 3
***P*-value**	0.2686		0.1065		0.1670		0.3197	

Table 4.26. *t-Test results of the comparations of all treatments and the P-value given for each comparation when analysing the expression level of gene TraesCS5A02G191700. DON and control (H_2O) treatments were used. RIL 97 was the line harbouring the QFhb.WEK5A locus, while Hobbit sib was the line lacking the QTL.*

	Hobbit *sib*		**RIL 97**		**Control**		**DON**	
	DON	**Control**	**DON**	**Control**	**Hobbit *sib***	**RIL 97**	**Hobbit *sib***	**RIL 97**
Mean	33.34	34.36	26.55	34.01	34.36	34.01	33.34	26.55
Variance	0.27	0.27	0.43	0.01	0.27	0.01	0.27	0.43
Observations	8	6	6	5	6	5	8	6
Biological reps.	3	2	2	2	2	2	3	2
Technical reps.	2 or 3	3	3	2 and 3	3	2 and 3	2 or 3	3
***P*-value**	0.0040		< 0.0001		0.1619		< 0.0001	

4.4.4. Is gene *TraesCS5A02G191700* duplicated in WEKH85A?

To confirm the number of copies of gene *TraesCS5A02G191700* in both parental lines when compared with CS, a ddPCR was performed. Development of the ddPCR assay was performed by me with the help and supervision of Tom Lawrenson from the transformation team (Crop Genetics, JIC). Tom was in charge of establishing the appropriate settings in the QIAcuity instrument to run the assay, and also helped me during the analysis of the data.

The gene copy number of *TraesCS5A02G191700* was calculated in relation to the number of copies of Ref. gene 1 set (equivalent to three homoeologues genes in an hexaploid genome) and in relation to the Ref. gene 2 set (single gene in an hexaploid genome (no homoeologues)). Results for the copy number of *TraesCS5A02G191700* in the three DNA samples of the CS, the FHB susceptible parental line Hobbit *sib* and the FHB resistance parental line WEKH85A were calculated and represented in Figure 4.8.

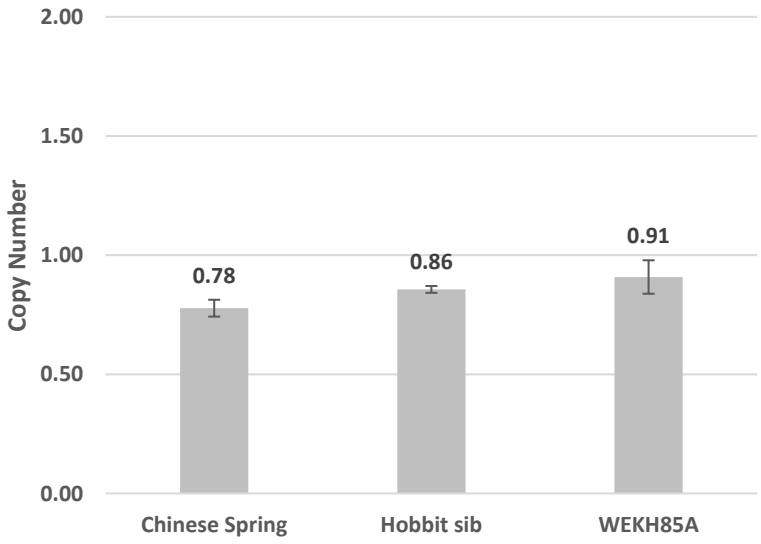

Figure 4.8. *Display of the calculated copy number of gene TraesCS5A02G191700 in the reference genome of Chinese Spring, the FHB susceptible parental line Hobbit sib and the FHB resistance parental line WEKH85A. The gene copy number of gene TraesCS5A02G191700 was calculated in relation to the number of copies of Ref. gene 1 set to three (homozygous of the three homoeologues genes in an hexaploid genome) and in relation to the Ref. gene 2 set to one (single homozygous gene in an hexaploid genome). Each bar is the average of two biological replicates and two technical replicates. Error bars are ± standard error.*

Results of the ddPCR assay did not produce an integer result as expected, but it was shown that *TraesCS5A02G191700* does not differ in copy number between parental lines Hobbit *sib* (0.86 ± 0.014) and WEKH85A (0.91 ± 0.070) when compared with CS (0.78 ± 0.035) (Figure 4.8.). Thus, these results indicate that the gene is present as a single copy in the hexaploid genome of both parental lines. Therefore, *TraesCS5A02G191700* is not duplicated in FHB resistant parental line WEKH85A.

4.5. Discussion

4.5.1. The *QFhb.WEK-5A* locus for FHB type II resistance may also provide DON tolerance

The RILs used for FHB type II resistance under polytunnel conditions during summer 2020 trial refined the *QFhb.WEK-5A* locus to an interval of 6.24 Mbp. RILs selected with the *QFhb.WEK-5A* locus were RIL 9A and RIL 10B (+ 5A QTL) and those lacking the locus were RIL 16A and RIL 17B (- 5A QTL). These selected recombinants were then tested for DON tolerance in an *in vitro* assay as previously performed in Chapter 3.

The phytotoxic effects upon DON were clearly observed in the roots of seedlings with lines harbouring the *QFhb.WEK5A* locus (RIL 9A, RIL 10B and RIL 97) showing higher levels of DON resistance in both experiments (Table 4.21. and Figure 4.4.) when compared with lines lacking the locus (RIL 16A, RIL 17B and Hobbit *sib*). Since RILs harbouring the allele provided by the *Fusarium*-resistant parental line WEKH85A (RIL 9A, RIL 10B and RIL 97) showed levels of FHB type II resistance as well as DON tolerance, it may imply that the 6.24 Mbp locus may harbour the genes associated with both traits: FHB type II resistance and DON tolerance.

As previously mentioned in Chapter 3, there were two genes (*TraesCS5A02G304000LC* and *TraesCS5A02G191800*) expressed upon DON on the 6.24 Mbp-interval and were specifically expressed in RIL 97 (+ 5A QTL). Additionally, the paralogue of

gene *TraesCS5A02G191800* is the adjacent gene *TraesCS5A02G191700*, which was also selected as a promising DON-candidate gene on the 5A locus. On the basis of these findings, I propose that the DON-candidate genes *TraesCS5A02G191700* and *TraesCS5A02G191800* identified on the *QFhb.WEK5A* locus may be associated with both traits. As I previously mentioned, resistance to DON may be underlying FHB type II resistance.

4.5.2. The gene *TraesCS5A02G191700* in WEKH85A contains a 3 bp deletion in the promoter region

To investigate whether the differences in resistance to DON/FHB were due to differences in amino acid sequence or differences in expression level of *TraesCS5A02G191700* and *TraesCS5A02G191800* between parental lines Hobbit *sib* and WEKH85A, both genes and their promotor regions were sequenced.

Sequencing data revealed that gene *TraesCS5A02G191800* and its promoter region in both parental lines Hobbit *sib* and WEKH85A did not differ from one another making it highly unlikely that the observed differences in FHB and DON tolerance were due to this gene. The same was observed for the CDS of gene *TraesCS5A02G191700*. However, a small but potentially important difference was identified in the promoter region of gene *TraesCS5A02G191700*. A 3 bp deletion (CTT) was identified in the promoter region of WEKH85A, around 2000 bp upstream of the UTR5' of the gene.

The RT-qPCR expression profile of DON-candidate gene *TraesCS5A02G191700* confirmed that it was highly expressed in RIL 97 (+ 5A QTL) upon DON exposure. Thus, gene *TraesCS5A02G191700*, located within the *QFhb.WEK5A* locus, may be regulated with or by other genes which allow the increase in its expression upon exposure to the mycotoxin. This increase in expression may be related to the differences identified in the promoter region between parental lines Hobbit *sib* and WEKH85A.

4.5.3. *TraesCS5A02G191700* may interact with two *WRKY45* transcription factors

To investigate the interaction of gene *TraesCS5A02G191700* with other genes, KnetMiner (https://knetminer.com/) was used to visualize the relationships between genes. KnetMiner is a gene discovery platform that helps to visualize links between the genetic and biological properties of complex polygenic traits.

In Figure 4.9. the interaction of the DON-candidate gene *TraesCS5A02G191700* with other genes is shown. The interaction or relationship between genes is represented with dotted lines if a gene regulates other genes; or with a line if the gene has homoeologues.

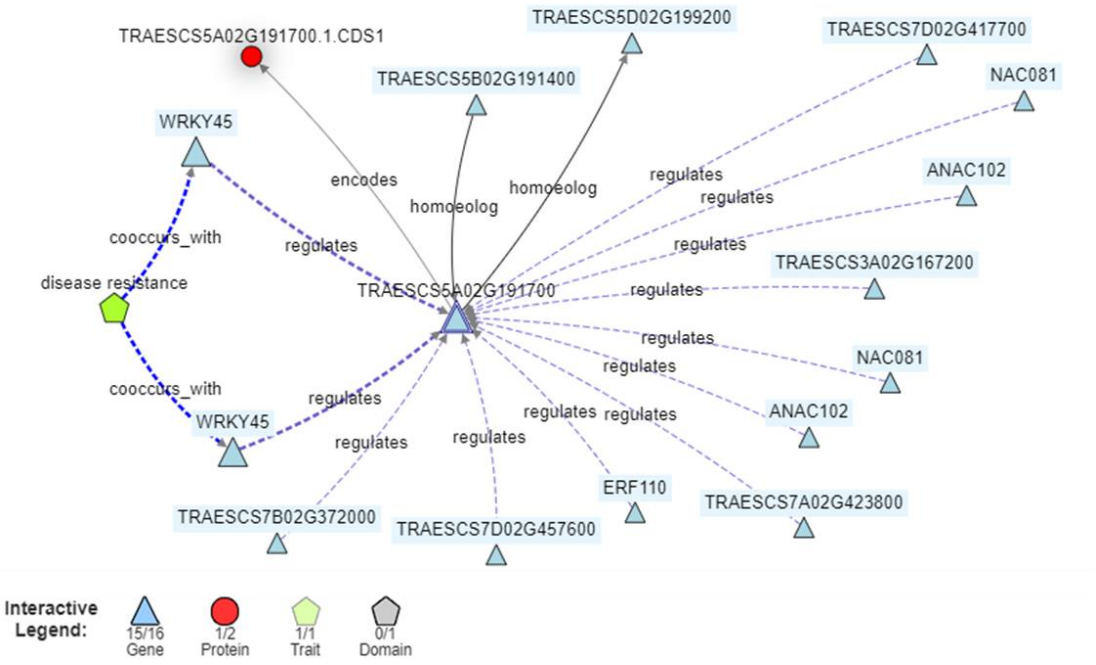

Figure 4.9. *Display of the interaction of DON-candidate gene TraesCS5A02G191700 with other genes extracted from KnetMiner (https://knetminer.com/). Legend is specified on the left: blue triangles are genes, red circles are protein, green pentagons are traits and grey pentagons are domains. The interaction or relationship between genes is represented with dotted lines if a gene regulates other genes; or with a line if the gene encodes a protein or it is an homeolog gene.*

Figure 4.9. shows that two *WRKY45* genes associated with disease resistance regulates gene *TraesCS5A02G191700*. At the same time, this gene is regulated by many other genes as is shown in Figure 4.9. (Small blue triangles). *WRKY45* genes are

TraesCS2A02G011000 and *TraesCS2B02G010500*, which are two transcription factors (TFs) located on the chromosomes 2A and 2B of bread wheat, respectively. TFs are regulatory proteins known to modulate the expression of downstream genes. They are key components of the signalling pathways and help in mitigating various developmental processes and stress responses (Ahad et al. 2021).

Additionally, the interaction of gene *TraesCS5A02G191800* with other genes is shown in Figure 4.10. The interaction or relationship between genes is represented with dotted lines if a gene regulates other genes; or with a line if the gene encodes a protein.

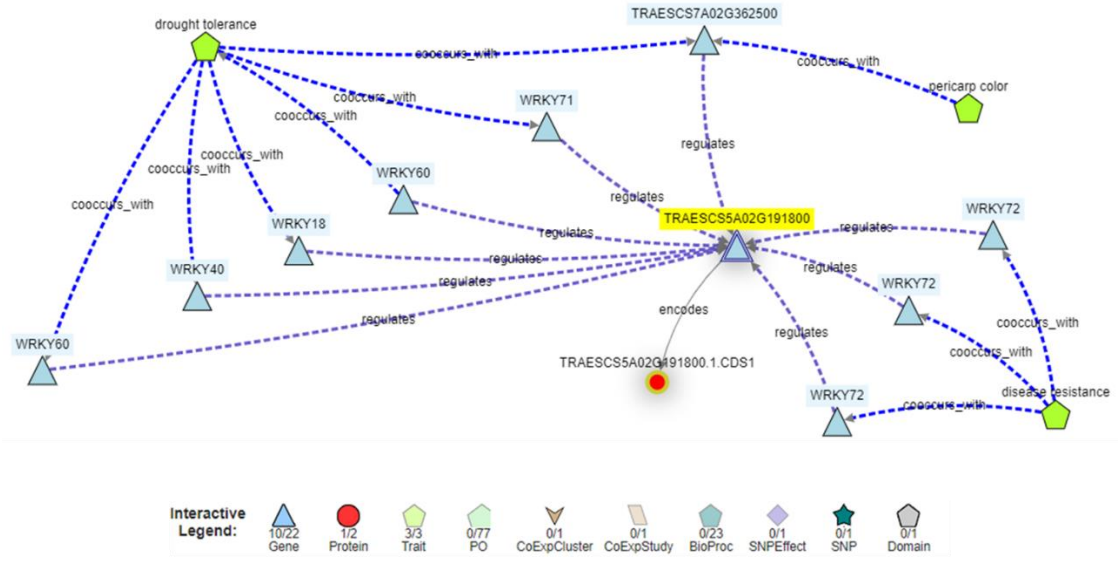

Figure 4.10. *Display of the interaction of DON-candidate gene TraesCS5A02G191800 with other genes extracted from KnetMiner (https://knetminer.com/). Legend is specified at the bottom: blue triangles are genes, red circles are protein, and green pentagons are traits. The interaction or relationship between genes is represented with dotted lines if a gene regulates other genes; or with a line if the gene encodes a protein.*

In this instance, *TraesCS5A02G191800* is related with three traits: drought tolerance, pericarp colour and disease resistance. Figure 4.10. shows that three *WRKY72* genes associated with disease resistance regulates gene *TraesCS5A02G191800.* These genes are *TraesCS3B02G130000*, *TraesCS3D02G113300* and *TraesCS7A02G096300*, which are three TFs located on the chromosomes 3B, 3D and 7A of bread wheat, respectively. Although gene

TraesCS5A02G191800 is regulated by WRKY TFs, these are different TFs from those that regulate gene *TraesCS5A02G191700.*

4.5.4. *WRKY45* transcription factor binding sites in the promoter of gene *TraesCS5A02G191700*

It is known that some TFs are involved in pathogen-induced resistance gene expression. WRKY have been characterised among the best TFs involved in pathogen defence mechanisms (Eulgem et al. 2000; Ülker and Somssich 2004). *OsWRKY45* gene was identified in rice as a positive regulator in the interaction with the blast fungus (Shimono et al. 2007). *OsWRKY45* is a component of the salicylic acid signalling pathway in rice, and its overexpression in transgenic rice enhanced the resistance to leaf blight (Shimono et al. 2007; Tao et al. 2009). The wheat ortholog of *OsWRKY45* is *TaWRKY45* and this was also demonstrated to play a role in defence against pathogen infection (Bahrini, Sugisawa, et al. 2011). In this study it was demonstrated that *TaWRKY45* was up-regulated upon infection by *F. graminearum*. Moreover, the constitutive overexpression of the *TaWRKY45* transgene conferred an enhanced resistance against the pathogen in transgenic wheat plants grown under greenhouse conditions (Bahrini, Sugisawa, et al. 2011). *TaWRKY45* is encoded by gene *TraesCS2A02G489500*, which is located at 723 Mbp in chromosome 2A of bread wheat (EMBL-EBI 2022).

To further investigate whether these *WRKY45* TFs (*TraesCS2A02G011000* and *TraesCS2B02G010500*) were predicted to bind to the promoter region of gene *TraesCS5A02G191700*, an Nsite Program analysis (Version 6.2014) from Sofberry (http://www.softberry.com/) was run to search for motifs of these TFs in the promoter of the candidate gene *TraesCS5A02G191700*. Results of the analysis revealed that the region containing the 3 bp (CTT) deletion in WEKH85A is extremely close to a region showing

similarity to a *WRKY45* transcription factor (TF) binding site, which is a CT rich region (Figure 4.11.).

Figure 4.11. *The region containing the 3 bp (CTT) deletion in the parental line WEKH85A is extremely close to a region showing similarity to a WRKY45 TFs binding sites (blue lines), which is a CT rich region in the promoter region of gene TraesCS5A02G191700. 'CTT' (red) is de deletion identified in the parental line WEKH85A.*

4.5.5. Expression of gene *TraesCS5A02G191700* may be regulated by different TFs

Additionally, a transcription factor biding site (TFBS) analysis (source from PlantPAN 2.0; http://PlantPAN2.itps.ncku.edu.tw) suggested that this CT/GA rich locus located in the promoter region of gene *TraesCS5A02G191700* may be the binding site (or the near region) of different TFs. The most relevant TFs identified are specified in Table 4.27. and visualized in Figure 4.12. Some of these TFs were two types of zinc-finger TFs, SRS and C2H2, and a DNA-binding with one finger (Dof) TF.

Table 4.27. *Main transcription factors and their binding sites on the promoter region of gene TraesCS5A02G191700 (source from PlantPAN 2.0; http://PlantPAN2.itps.ncku.edu.tw). 'CTT/GAA' (red) is de deletion identified in the parental line WEKH85A. TF = transcription factor. ID = identity.*

TF ID	TF name	Binding site (5' -> 3')
AP2	APETALA2/ERF	AGAGATAGGGGGAGAGGGAG
AP2	APETALA2/ERF	GAA**GAA**GGAGTGAGAGATAG
BBR-BPC	Barley B Recombinant/ Basic Pentacysteine	CTT**CTT**CCTCACTCTCTATCCCCCT
BBR-BPC	Barley B Recombinant/ Basic Pentacysteine	TCCTCCTT**CTT**CCTCACTCTCTATCCCCCT
C2H2	Cys 2- Hys 2	T**CTT**CCTCACTCTCT
Dof	DNA-binding with one finger	TCCTT
SRS	Shi Related Sequence	ACTCTTC

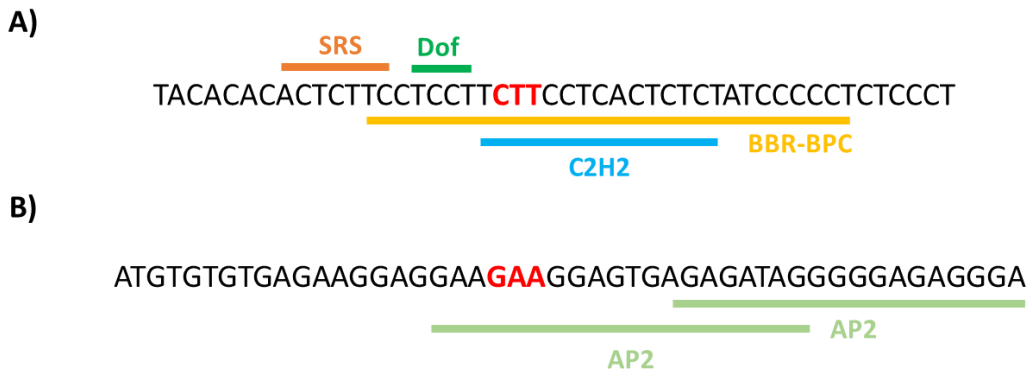

Figure 4.12. *Main transcription factors and their binding sites on the promoter region of gene TraesCS5A02G191700 in the forward strand (A; 5' -> 3') and the complementary strand (B; 5' -> 3') (source from PlantPAN 2.0; http://PlantPAN2.itps.ncku.edu.tw). 'CTT/GAA' (red) is de deletion identified in the parental line WEKH85A.*

It seems that this CT/GA rich locus may correspond to a binding region for BBR-BPC (Barley B Recombinant/ Basic Pentacysteine) family of TFs (Figure 4.12.-A). This type of type of TFs have been reported to be involved in developmental regulation in plants (Ahad et al. 2021; Theune et al. 2019). They play a role in auxin, cytokinin and ethylene signalling (Theune et al. 2019). However, these types of TFs are still poorly characterized, and no significant information is still available for *T. aestivum* (Ahad et al. 2021).

The promoter of gene *TraesCS5A02G191700* of the parental line Hobbit *sib*, which do not contain the 3 bp deletion, may allow the binding of this type of BBR-BPC TFs (wild-type version) (Figure 4.12.-A). However, when the deletion is present, as it occurs in the parental line WEKH85A, this type of TF cannot bind due to the absence of the 'CTT' region. This could suggest that this type of TF could act as a form of repressor of gene *TraesCS5A02G191700* when it binds to the wild-type version of the promoter perhaps reducing the ability of WRKY45 genes to bind and so attenuating the increase in gene expression following exposure to DON. The absence of binding of a BBR-BPC TF, due to the deletion of 3 bp, may allow greater access of the WRKY TF and lead to enhanced expression in response to DON (Figure 4.13.-A).

A) WEKH85A (FHB R parental line): Highly expression of gene *TraesCS5A02G191700*

B) Hobbit *sib* (FHB S parental line): Basal expression of gene *TraesCS5A02G191700*

Figure 4.13. *Schematic representation of the hypothetical increase in expression of gene TraesCS5A02G191700 due to the binding of the TF WRKY45 near the 'CTT' deletion in the parental line WEKH85A (A) and when binding site of the TF WRKY45 is occupied by TF BBR-BPC in the parental line Hobbit sib (B). 'CTT' (red) is de deletion identified in the parental line WEKH85A. S = susceptible. R = resistant.*

I speculate that the BBR-BPC TF binds into the CT/GA rich locus in the promoter of the wild-type version, in the susceptible line Hobbit *sib*. As the binding site for the *WRKY45* TF resides very close to this locus, this region may have been already occupied by the BBR-BPC TF preventing the *WRKY45* TF from binding to the promoter of gene *TraesCS5A02G191700.* There may be other TFs activating a basal expression of the gene, but the inability of the *WRKY45* TF to bind into the promoter may cause the reduction of the level of expression in the susceptible line Hobbit *sib* (Figure 4.13.-B).

Sequence analysis of TF binding sites also revealed an ethylene response TF (AP2) sitting directly within the BBR-BPC site but in the complementary strand (Figure 4.12.-B). The

TF associated with this target is encoded by *TraesCS2A02G417200*, which is involved with ethylene signalling. Ethylene is an endogenous plant hormone that influences many aspects of plant growth and development. This hormone induces several defence related-genes containing a cis-regulatory element known as the Ethylene-Responsive Element (ERE) (Broglie et al. 1989). Specific ERE regions contain a short motif rich in G/C nucleotides, known as the GCC-box, essential for the response to ethylene. This short motif is recognised by a family of TFs containing the ERE binding factors (ERF) domain or the APETALA2 (AP2) domain (http://www.ebi.ac.uk/interpro/entry/InterPro/IPR036955/).

Thus, an alternative hypothesis to that of the BBR-BPC TF binding site (Figure 4.13.) would involve the activation of the DON-candidate gene *TraesCS2A02G417200* by an ethylene signalling response. In this case, it would involve the binding of the AP2 TF into the CT/GA rich locus in the promoter of the wild-type version, in the susceptible line Hobbit *sib*. Therefore, the AP2 TF would be the agent preventing the WRKY45 TF from binding to the promoter of gene *TraesCS5A02G191700* and may cause the reduction of the level of expression of this gene in the susceptible line Hobbit *sib*, as similarly described in Figure 4.13.

4.5.6. Chitin and *flg22* may increase expression of DON-candidate genes *TraesCS5A02G191700* and *TraesCS5A02G191800*

Plants have evolved a multi-layered immune response in response to microbial pathogen attacks. The perception of pathogen, microbe, or damage-associated molecular patterns (PAMPs, MAMPs or DAMPs) by pattern recognition receptors (PRRs) leads to PAMPs, MAMPs or DAMPs-triggered immunity (PTI, MTI or DTI).

PTI is a complex set of physiological and molecular processes in the plant that promotes disease resistance. PTI responses include calcium ion (Ca^{2+}) influx, reactive oxygen species (ROS) burst, callose deposition and defence gene activation (Bigeard, Colcombet, and

Hirt 2015). The polysaccharide chitin is a primary component of cell walls in fungi and one of the best studied MAMPs to induce PTI against pathogen attack (Sánchez-Vallet, Mesters, and Thomma 2015). Another well-studied MAMP is the bacterial flagellar protein flagellin, which is perceived by the PRR FLAGELLIN-SENSITIVE 2 (FLS2) (Bigeard, Colcombet, and Hirt 2015). A 22-amino-acid long region of flagellin (flg22) from *Pseudomonas aeruginosa* is sufficient for the activation of the PTI via FLS2 (Gómez-Gómez and Boller 2000).

It has been shown that in *Arabidopsis thaliana*, LysM (extracellular lysin motifs)-containing receptor-like kinases are implicated in chitin signalling and resistance against fungal pathogens (Sánchez-Vallet, Mesters, and Thomma 2015; Wan et al. 2008). Chitin fragments are perceived by the LysM domain-containing OsCEBiP (chitin elicitor binding protein) and OsCERK1 (Kaku et al. 2006; Shimizu et al. 2010) in rice. Additionally, the LysM domain-containing HvCERK1 (Chitin Elicitor Receptor Kinase 1) is required for plant response to chitin in barley (Karre et al. 2017).

Moreover, it was shown that in wheat leaves, chitin and flg22 induce the expression of wheat homologues of *Arabidopsis* chitin- and flg22-responsive genes (Schoonbeek et al. 2015). It was also shown that chitin induced a ROS response in wheat rachises and rachis nodes, which are critical barriers for FHB spread in wheat, after *F. graminearum* infection (Hao, Tiley, and McCormick 2022). Hao, Tiley, and McCormick (2022) also identified that rachis nodes and wheat heads showed different defence gene expression patterns when treated with chitin. It seems that there was a tissue-specific immune responses induced by chitin, which may play a key role during FHB infection in wheat.

It was shown in Chapter 3 of the present study that both DON-candidate genes *TraesCS5A02G191700* and *TraesCS5A02G191800* are expressed upon DON and *Fusarium* infection in wheat spikes. It seems likely that both genes may function as part of a more general stress response. Both *TraesCS5A02G191700* and *TraesCS5A02G191800* genes have

been identified to be highly expressed in leaves inoculated with flg22 (log_2 FC = 5.01 and 4.45) and chitin (log_2 FC = 4.65 and 4.04) (Ramírez-González et al. 2018) (Figure 4.14.).

Figure 4.14. *Differential expression levels of genes TraesCS5A02G191700 (left column) and TraesCS5A02G191800 (right column) in leaves inoculated with water (first row), chitin (second row) and flg22 (third row), to study PAMP responses in polyploid wheat (http://www.wheat-expression.com/) (Ramírez-González et al 2018).*

Thus, these findings indicate that *TraesCS5A02G191700* and *TraesCS5A02G191800* may be involved in a more general PAMP-induced basal resistance against pathogen attack. Indeed, it was suggested that MAMPs are perceived as general danger signals and plants do not distinguish between different microbes (Zipfel et al. 2006). Therefore, PTI activation may confer cross-protection against pathogens in different kingdoms (Sarowar et al. 2019). It would also be useful to determine whether both genes are upregulated and increase resistance against other pathogens.

4.5.7. Gene *TraesCS5A02G191700* is a single copy in parental line WEKH85A

The identification of the seven and eight Het SNPs on the promoter of both *TraesCS5A02G191700* and *TraesCS5A02G191800* genes, respectively, lead to the hypothesis that these SNPs might reflect the presence of very similar duplicates of these genes. I hypothesised that *QFhb.WEK-5A* locus could have been duplicated in the FHB resistant parental line WEKH85A. An alternative possibility is that the Het SNPs arose from individual primers amplifying from the B or D homoeologues as well as the 5A homoeologous.

The ddPCR results, however, revealed that *TraesCS5A02G191700* is present as a single copy in the hexaploid genome of both parental lines. Therefore, it was not duplicated

in FHB resistant parental line WEKH85A. It is concluded that the Het SNPs arose because of amplification from either the 5B or 5D the homoeologues.

4.5.8. Higher expression of *TraesCS5A02G191700* may increase DON tolerance and FHB resistance

Under pathogen attack, some resistance genes may be overexpressed in the wheat genome, including those genes involved in hormonal stress signalling such as salicylic acid, ethylene, and methyl jasmonate (Makandar et al. 2012). The overexpression of this type of gene favours increased FHB resistance by affecting the signalling molecules and a diverse set of TFs in plants (Bahrini, Ogawa, et al. 2011). This may be the case in the present study of *TraesCS5A02G191700*, in which expression upon exposure to DON is regulated by the ability of specific TFs to bind near the CTT deletion site on the promoter region. Thus, gene *TraesCS5A02G191700* may be a potential candidate gene and its higher expression may increase DON tolerance and FHB resistance through acting within the PTI pathway.

Many different wheat genes have been identified that have been associated with DON resistance and DON production by *F. graminearum*. These genes are associated with cellular metabolism, DON detoxification by glutathione S-transferases (GSTs) or UGTs, programmed cell death, kinases, oxidoreductases, retrotransposons, transporter protein (ABC transporters), or even orphan genes such as *TaFROG* (Gunupuru, Perochon, and Doohan 2017).

Those genes which are directly involved in DON detoxification are the UGTs, which have been shown to convert DON to a less toxic compound D3G (Poppenberger et al. 2003). For instance, the barley UGT (*HvUGT13248*) showed enhanced tolerance to DON toxicity in transgenic *Arabidopsis* lines (Shin et al. 2012). When this gene was transformed into wheat, it was demonstrated that DON was rapidly and efficiently conjugated into D3G and generally

reduced the severity of FHB under field conditions (Li et al. 2015). Indeed, it was also shown that *Brachypodium distachyon* encodes two homologs of *HvUGT13248*, which also convert DON to D3G when expressed in yeast (Schweiger, Pasquet, et al. 2013). When *Brachypodium* UGT *Bradi5g03300* was overexpressed, the toxicity of DON towards root tissue decreased and the spikelet resistance to FHB disease was enhanced (Pasquet et al. 2016).

Another example of genes involved in detoxification mechanisms is *Fhb7*. This novel FHB resistance gene was identified from *Thinopyrum elongatum*. *Fhb7* encodes a GST, which confers a broad resistance to *Fusarium* species by detoxification of trichothecenes through de-epoxidation (Wang et al. 2020).

However, the mechanisms for which gene *TraesCS5A02G191700* is providing DON resistance may not be provided by any type of DON detoxification mechanism. The toxicity of the mycotoxin inside the plant cells may be reduced by other processes which are enhanced when the expression of the gene increases. This is still uncertain and therefore more studies are needed. When DON is detected in the plant cells, a cascade of TFs is activated. These TFs would regulate diverse clusters of gene signalling, from which *TraesCS5A02G191700* may be a key element in providing a general stress response, including FHB type II resistance.

4.5.9. Conclusions and future work

It appears that the *QFhb.WEK-5A* locus for FHB type II resistance of 6.24 Mbp also confers DON tolerance in the introgression line WEK8H5A. The most promising candidate gene located in the 5A locus is the DON-responsive gene *TraesCS5A02G191700.* I have shown that *gene TraesCS5A02G191700* contains a deletion of 3 bp (CTT) in the promoter region of the parental line WEKH85A.

The differences at the promoter region of gene *TraesCS5A02G191700* may permit enhanced expression of this gene upon challenge with DON in WEKH85A. Indeed, several TFs may be interacting with the promotor of gene *TraesCS5A02G191700*, and it is possible that differences in the promotor region between parental lines may be responsible for the higher expression in the introgression line WEKH85A. Differences in the promoter region of WEKH85A may be even responsible of the increase in expression of gene *TraesCS5A02G191800* when exposed to DON. Further confirmation of its expression profile is needed. In fact, additional RT-qPCR experiments are needed to show how the expression of both DON-candidate genes changes over time (time course experiment) since it seems that both genes may function as part of a more general PAMP-induced basal resistance against pathogen attack.

As a future work, the 3 bp deletion identified in the promotor of gene *TraesCS5A02G191700* could be functionally validated using CRISPR to introduce a similar disruption in the promoter of a variety containing the CTT triplet. It would also be interesting to identify breeding lines that are identical in state across the *QFhb.WEK-5A* locus and phenotype them to confirm the presence of the FHB resistance gene. In addition, *TraesCS5A02G191700* could be introduced into an FHB susceptible variety under the control of a constitutive promoter to determine the effect of overexpression of this gene on FHB resistance and DON tolerance.

Chapter 5

The QTL (*QFhb.Wuhan-2DL*) on chromosome arm 2D of Wuhan increases Fusarium Head Blight type II resistance in wheat

5.1. Abstract

Quantitative trait locus (QTL) associated with FHB have been detected on all wheat chromosomes. The 2D QTL is one of the major QTLs associated with FHB resistance and very stable across different genetic and environmental backgrounds. The 2DL QTL was identified in a population from a Wuhan-1 x Nyubai cross and confers FHB type II resistance. Several candidate genes underlying this QTL have been identified and characterized, but functional validation of those genes is still needed to confirm the findings.

A near isogenic line (NIL) population had been created using the Chinese cultivar Wuhan-1 (resistant) backcrossed with the UK elite cultivar Crusoe (susceptible). In the present study, a selection of recombinants generated using specific NILs were tested for FHB type II resistance to confirm its effectiveness under UK weather conditions. The purpose of this project was also to identify the physical location of the 2D QTL by performing a single marker analysis on those recombinant lines.

This study confirmed that the QTL was stable under UK environmental conditions and that the 2D locus, named *QFhb.Wuhan-2DL*, was located on the long arm of the 2D chromosome. *QFhb.Wuhan-2DL* was fine-mapped to a region of 55.6 Mbp, containing 575 annotated genes in the Chinese Spring reference genome. Further fine-mapping is needed.

5.2. Introduction

To understand the mechanism of resistance to FHB, numerous genetic and molecular experiments have been performed. Indeed, genomic regions associated with FHB resistance QTL have been detected on all wheat chromosomes (Buerstmayr, Ban, and Anderson 2009).

The 2DL QTL is one of the major QTL associated with FHB resistance and also one of the most stable QTL across different genetic backgrounds and various environments (Buerstmayr, Ban, and Anderson 2009). The 2DL QTL was identified in a population from a Wuhan-1 x Nyubai cross and confers rachis resistance (type II resistance) by limiting the spread of the pathogen from the initial point of infection (Somers, Fedak, and Savard 2003).

Significant efforts to identify and characterise the genes underlying the 2DL QTL using different tools have led to new insights. A gene expression profiling of NILs containing the 2DL QTL was developed and eight candidate genes were associated with FHB, with only one of these genes being localized on the 2DL chromosome (Long et al. 2015). Using the same NILs, an RNA-Seq experiment was conducted and a list of differentially expressed genes was developed, including genes with unique expression profiles associated with either the presence or the absence of the 2DL QTL (Biselli et al. 2018). Moreover, by using the same pair of NILs contrasting for the 2DL QTL, a metabolomic study performed by Kage, Yogendra, and Kushalappa (2017) led to the identification of a *WRKY70* transcription factor and three biosynthetic enzymes as possible candidate genes associated with the 2DL QTL. By using previous bioinformatic information together with additional analysis of Wuhan-1, two expressed genes (*Traes_2DL_179570792* and *UN25696*) associated with the 2DL QTL for FHB resistance were identified and mapped (Hu et al. 2019a).

The metabolomics approach of Kage et al (2017) led to the identification of a gene encoding agmatine coumaroyl transferase (*TaACT*) which was located on the 2DL QTL between the flanking markers WMC245 and GWM608. This gene seems important in

conferring type II resistance by reinforcing secondary cell walls, and indirectly, preventing further spread of the pathogen throughout the wheat rachis.

Therefore, several candidate genes on the long arm of the 2D chromosome in wheat have been identified and characterized. However, additional experiments involving functional validation will be required to confirm whether those genes are actually conferring the FHB type II resistance on the 2D chromosome or they just have a more general role in resistance. Additional experiments will also be required to confirm whether the 2DL QTL is stable in UK germplasm and in multiple environments.

5.2.1. Chapter aims

In the present study, to test if the 2DL QTL of Wuhan is useful in a UK environment, the Chinese cultivar Wuhan-1 was backcrossed with the UK elite cultivar Crusoe by Limagrain S.A. By using the derived NIL population, the objectives were:

1) Identify whether the 2DL QTL is effective in a UK background to reduce FHB type II symptoms.

2) Fine-mapping of the 2DL locus using a single marker analysis based on the physical position of single nucleotide polymorphisms (SNPs) in the Chinese Spring reference genome (IWGSC RefSeq v1.1).

5.3. Materials and Methods

5.3.1. Plant material

The cross between Wuhan-1 and Crusoe population was generated by the iCase collaborators at Limagrain S.A. The UK cultivar Crusoe was backcrossed with the resistant cultivar Wuhan-1, for which FHB type II resistance is located on the long arm of 2D chromosome (Somers, Fedak, and Savard 2003), to finally produce the BC_3F_3 generation.

Seven near-isogenic lines (NILs) were used for the 2DL QTL FHB characterisation and mapping in Summer 2019. These NILs were selected because of the different recombination events occurring across the 2D chromosome. For subsequent summer trials, only specific recombinant lines (RILs) containing the 2D locus were selected to be tested for FHB resistance.

Seed of the selected RILs were sown and transplanted into 1L-pots as previously described in Chapter 2 section 2.3.1.3. Plants were located at the John Innes Centre, Norwich (UK) and were staked and tied as appropriate.

5.3.2. Polytunnel experimental design

Plants were arranged in a polytunnel at the JIC in an Alpha Lattice design within different blocks and plots per block. Depending on the trial and number of plants selected, different numbers of blocks were used.

In Summer 2019, plants were arranged in six blocks (N1-3; S1-3) containing three plots each (P1-3) (Supplementary data Figure S3). Each plot contained one replicate of the nine lines use for the experiment. Therefore, a total of 18 replicates per line were used and were equally distributed in the poly tunnel.

In Summer 2020, a total of sixteen recombinant lines were selected and, therefore, the experimental design contained a higher number of plants. Recombinant lines were still segregating for several markers, so sister lines for each recombinant line were grouped in three groups depending on the given allele: 'A' if the allele was given by parental line Crusoe; 'B' if the allele was given by parental line Wuhan; and 'H' if the allele was still heterozygous for the marker. Five plants were selected for each group, except for 'H' group for which two plants were selected. Plants were arranged in sixteen blocks (N1-8; S1-8) containing two plots each (Supplementary data Figure S4). Randomization was generated using the Design Computing Gendex DOE Toolkit 8.0. (Module IBD, http://designcomputing.net/).

In Summer 2021, two smaller sets of recombinant lines were selected so two trials (Test 1 and Test 2) were performed. Both trials were arranged in a randomised incomplete block design. For the first trial (Test 1), a total of 68 plants were selected and arranged in three blocks. The second trial (Test 2) containing a total of 44 lines was arranged in two blocks. Each block also contained Crusoe-like and Wuhan-like parental lines. For these trials, each RIL was treated as a single plant.

5.3.3. Evaluation of type II FHB resistance

Selected RILs, Crusoe-like and Wuhan-like were evaluated for FHB type II resistance by using the point-inoculation method as previously specified in Chapter 2 section 2.3.2.1.

FHB disease symptoms were scored after different days post-infection (dpi), as previously specified in Chapter 2 section 2.3.2.2. Scoring of symptoms was done depending on the flowering time for each set of plants, and data was analysed together as 'Score 1', 'Score 2', and so on. Data for Summer 2019 was collected at 9-10 dpi (Score 1), at 13-14 dpi (Score 2), at 17-18 dpi (Score 3), at 20-21 dpi (Score 4) and at 25 dpi (Score 5); for Summer 2020 scoring was carried out at 14 dpi (Score 1), at 16 dpi (Score 2), at 18-19 dpi (Score 3), at 20-21 dpi (Score 4) and at 22-23 dpi (Score 5); for the first trial (Test 1) in Summer 2021

scoring was carried out at 12-13 dpi (Score 1), at 14-15 dpi (Score 2), at 16-18 dpi (Score 3), at 19-20 dpi (Score 4), at 21-22 dpi (Score 5) and at 23-25 dpi (Score 6); and for the second trial (Test 2) in Summer 2021 scoring was carried out at 15 dpi (Score 1), at 18 dpi (Score 2), at 20-21 dpi (Score 3), at 22-23 dpi (Score 4), at 25 dpi (Score 5) and at 27-28 dpi (Score 6).

FHB disease symptoms were recorded by counting the number of infected or bleached spikelets below and above the point of infection (PI), respectively. Complete bleached spikes above the PI were given a '10' score, the approximate number of total spikelets above the PI. Resistant spikes showed a reduced spread of FHB infection and un-inoculated spikelets remained green. Spikes in Figure 5.1.A-C were inoculated with *F. culmorum* and disease spread was observed, since there was bleaching: A) one and a half-infected spikelets above the PI (1.5 score) and one and a half below the PI (1.5 score); B) one and a half-infected spikelets above the PI (1.5 score) and four and a half below the PI (4.5 score); C) complete bleached spike above the PI (10 score) and five and a half below the PI (5.5 score).

Figure 5.1. *Scoring FHB disease symptoms in wheat spikes. FHB symptoms were recorded by counting the number of infected or bleached spikelets above and under the PI in the middle of the spike (red arrow): A) one and a half-infected spikelets above the PI (1.5 score) and one and a half below the PI (1.5 score); B) one and a half-infected spikelets above the PI (1.5 score) and four and a half below the PI (4.5 score); C) complete bleached spike above the PI (10 score) and five and a half below the PI (5.5 score).*

5.3.4. Genotyping

5.3.4.1. Leaf sampling and DNA extraction

Leaf sampling and DNA extraction was performed as previously specified in Chapter 2 section 2.3.3.1.

5.3.4.2. Developing and using KASP markers

Several markers were developed by me as previously specified in Chapter 2 section 2.3.3.2. The main source which I used to identify SNPs was the Cereals DB web site (www.cerealsdb.uk.net). Most SNPs were, however, identified by the iCase collaborators who also developed KASP markers to screen the Wuhan x Crusoe population. The source they used was an in-house SNP array and Exome capture data (Limagrain S.A., personal

communication). Sequence information of KASP markers used to genotype the 2D QTL population over the trials is found in Table 5.1.

5.3.5. Statistical analysis

Disease data was analysed using a linear mixed model (LMM) in the statistical software R 3.5.3 (https://cran.r-project.org/bin/windows/base/). Genstat software (v18.1) was also used to confirm results (https://www.vsni.co.uk/software/genstat/). The LMM analysis was used to assess the variation attributable to block (random), line (random), inoculation date (fixed) and marker (fixed). The analysis was performed for each individual marker located on the 2D chromosome. Visual analysis of residues was undertaken for all analyses to assess normality of data. All data was log10 transformed to achieve normality of residuals and to ensure residuals were independent of fitted values. Predicted mean and standard error values were calculated for those lines included in the analysis.

Table 5.1. *KASP markers used for the genotyping of the 2D chromosome. Associated RefSeqv1.1 gene models (where available) and physical position on RefSeqv1.0 assembly are shown. Fam, Vic and common primers (seq from 5' to 3') are shown for each KASP. Source of markers used for the analysis is described.*

Marker	SNP position (RefSeqv1.0)	Reference allele	Alternative allele	Associated gene (RefSeqv1.1)	Fam (seq 5' to 3')	Vic (seq 5' to 3')	Common (seq 5' to 3')	Source
S1	380.082.519	C	G/T	*intergenic*	-	-	-	18K SNP array
S2	411.408.120	C	A/G	*intergenic*	-	-	-	18K SNP array
BA00144665	446.047.025	C	T	*TraesCS2D02G347900*	CGGTGCTTGAGTTGGCGT	CGGTGCTTGAGTTGGCGC	CTGGCCACGTTGATCGCC	CerealsDB
S3	447.551.300	G	C	*intergenic*	-	-	-	18K SNP array
S4	459.848.229	C	T	*intergenic*	-	-	-	Exome capture
S5	473.437.125	C	T	*TraesCS2D02G369200*	-	-	-	Exome capture
S6	476.350.706	A	C	*TraesCS2D02G372300*	-	-	-	Exome capture
S7	488.871.873	G	A	*intergenic*	-	-	-	Exome capture
S8	490.119.157	A	G	*intergenic*	-	-	-	Exome capture
S9	497.905.031	A	G	*TraesCS2D02G390100*	-	-	-	18K SNP array
S10	507.260.371	T	C	*TraesCS2D02G396200*	-	-	-	Exome capture
S11	518.184.736	A	G	*TraesCS2D02G403400*	-	-	-	Exome capture
S12	520.584.574	T	C	*intergenic*	-	-	-	Exome capture
S13	520.645.535	G	A	*TraesCS2D02G405600*	-	-	-	Exome capture
S14	522.525.653	G	A	*TraesCS2D02G406900*	-	-	-	Exome capture
S15	527.646.686	A	G	*TraesCS2D02G413100*	-	-	-	Exome capture
S16	531.236.257	C	T	*TraesCS2D02G416800*	-	-	-	Exome capture
S17	531.677.862	G	T	*TraesCS2D02G417300*	-	-	-	Exome capture
S18	531.895.955	T	G	*intergenic*	-	-	-	Exome capture
S19	562.855.808	T	A/G	*intergenic*	-	-	-	18K SNP array
S20	563.660.447	C	A/G	*intergenic*	-	-	-	18K SNP array
BA00862086	583,231,124	C	T	*TraesCS2D02G480700*	GCAAGGTGCATACAAGTTCAC	GCAAGGTGCATACAAGTTCAT	AGCTAGTGAAAGTGAACTTCTATGA	CerealsDB
S21	601.204.785	C	T	*TraesCS2D02G507600*	-	-	-	18K SNP array
S22	619.412.506	C	G	*TraesCS2D02G537900*	-	-	-	18K SNP array
S23	630.765.860	G	C/T	*intergenic*	-	-	-	18K SNP array

5.4. Results

5.4.1. Characterisation of the 2D QTL under polytunnel conditions

FHB disease trials to assess type II resistance were performed over three Summers (2019-2021) under polytunnel conditions at the JIC (Norwich, UK). FHB type II disease symptoms were scored when symptoms (bleaching) were observed/spread within wheat spikes as in Figure 5.1.A-C. Scoring of symptoms above and below the PI of wheat spikes was done every 2-4 days post-infection (dpi).

The genomic information was obtained by screening each line with polymorphic markers identified between the parental lines. This allows the determination of which parental allele is present in each line for each marker within the 2D locus. Most of the SNPs identified in the long arm of the 2D chromosome were identified by the iCase collaborator who used them to develop KASP markers. Different numbers of markers were used for each year's analysis depending on the availability and discovery of new SNPs along the 2D interval (Table 5.1.). To begin with, two markers from Cereals BD could be used to screen the population, followed by markers developed by the iCase collaborators using an in-house SNP array and the Exome capture data (Limagrain S.A., personal communication).

A LMM analysis was then performed for each individual marker located on the 2DL chromosome using the phenotypic data obtained from above and below the point of infection in each summer season and the genotypic data of the parental-like lines and RILs.

5.4.1.1. Summer 2019

Graphical genotype of parental-like lines and NILs used in Summer 2019 is provided in Figure 5.2. The physical position of the KASP markers used on the 2D chromosome are based on the Chinese Spring RefSeq 1.0 assembly. Line names are specified on each raw and

markers used are specified on each column. Yellow is the allele provided by Wuhan and blue the one by Crusoe.

Figure 5.3. represents the distribution of disease spread above the PI changes for these lines over time using phenotypic data collected at 9-10 dpi (Score 1), at 13-14 dpi (Score 2), at 17-18 dpi (Score 3), at 20-21 dpi (Score 4) and at 25 dpi (Score 5). As expected, Crusoe-like parental line was more susceptible than parent Wuhan-like when observing disease spread above and below the PI. The resistance of Wuhan-like to FHB disease spread above the PI was maintained over time (Figure 5.2.).

Phenotypic data in 2019 showed different levels of FHB disease spread depending on the line. Lines showing a high level of FHB resistance over time were NILs Rec 3, Rec 6 and Rec 7. In contrast, Rec 1, Rec 2, Rec 4, and Rec 5 were very susceptible (Figure 5.2. and Figure 5.3.).

(a)

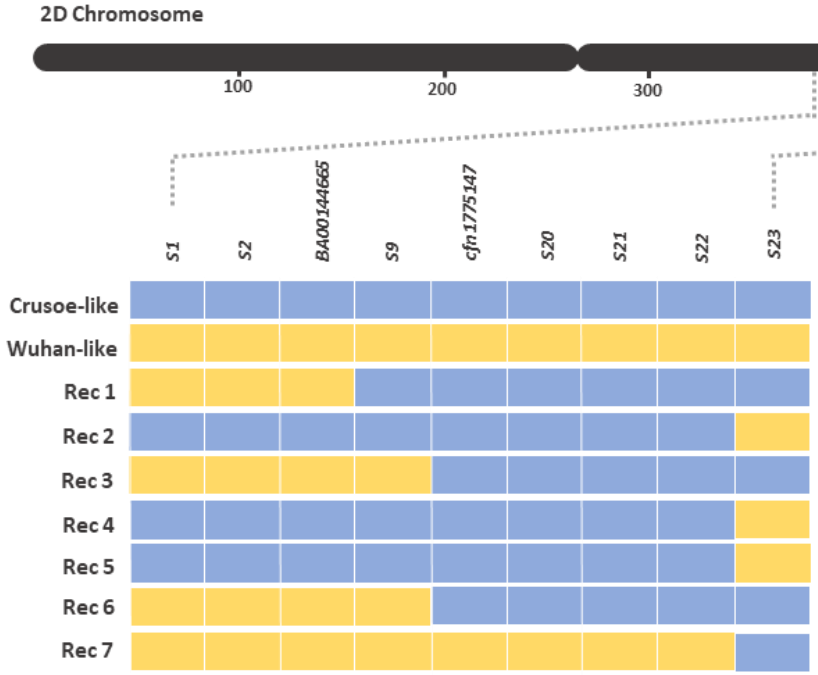

(b)

Total number of FHB infected-spikelets

Score 1	Score 2	Score 3	Score 4	Score 5
1.07	4.29	6.51	9.60	12.61
0.44	0.81	1.47	2.60	4.94
1.78	6.45	10.23	12.19	15.08
1.43	4.29	6.59	8.93	11.72
0.70	2.40	3.90	5.57	8.05
1.50	4.44	8.54	11.40	13.27
1.05	3.88	5.99	8.14	10.41
0.65	1.47	2.22	3.44	6.01
0.58	1.11	2.05	3.09	5.85

Figure 5.2. *a) Graphical genotype of near isogenic lines, Crusoe-like and Wuhan-like parental lines used on Summer. Line names are specified on each raw and markers used are specified on each column. Yellow is the allele provided by Wuhan and blue the one by Crusoe. b) Total number of FHB infected-spikelets (scoring data above and below the point of infection) obtained for each line at different scoring dates: Score 1 (9-10 dpi), Score 2 (13-14 dpi), Score 3 (17-18 dpi), Score 4 (20-21 dpi) and Score 5 (25 dpi).*

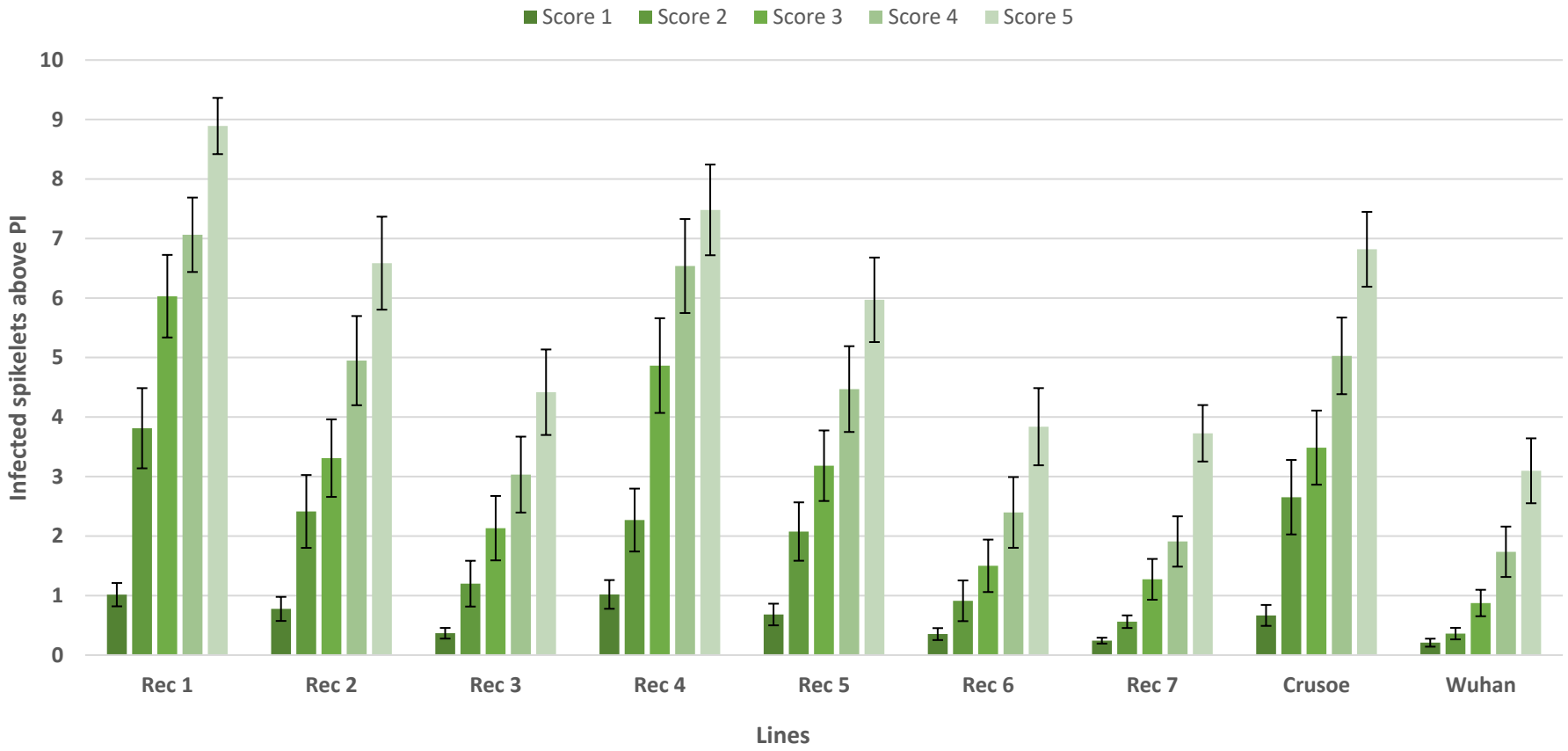

Figure 5.3. *FHB disease above the PI or number of bleached spikelets above the PI of NILs and parental-like lines (Crusoe and Wuhan) tested for type II on Summer 2019. Scoring symptoms were collected at 9-10 dpi (Score 1), at 13-14 dpi (Score 2), at 17-18 dpi (Score 3), at 20-21 dpi (Score 4) and at 25 dpi (Score 5). Predicted means were generated using a LMM analysis. Error bars are ± standard error.*

P-value data obtained from the LMM analysis performed for each individual marker located on the 2D chromosome is shown in Table 5.2. and Table 5.3., for scoring data above and below the PI, respectively. Source of markers used for the analysis are described. Associated RefSeqv1.1 gene models (where available) and physical position on RefSeqv1.0 assembly are shown.

LMM analysis of Summer 2019 data revealed that one marker was very closely associated with FHB type II resistance (*P-value* = 0.003) at 17-18 dpi on the long arm of chromosome 2D. This marker is *S9* (source: 18K SNP array) located at 497.90 Mbp (Table 5.2.). The association with the resistance increased over time (*P-value* = 0.001) at 20-21 and 25 dpi when using scoring data above the PI. The same marker was also associated with the disease when using the scoring data below the PI, being strongest (*P-value* < 0.001) at 17-18, 20-21 and 25 dpi, and thus confirming the genomic region of the 2DL QTL (Table 5.3.).

Other markers were associated with FHB type II resistance when using scoring data above the PI at 13-14 dpi and at 20-21 dpi, but to a less extent (*P-value* < 0.05). These markers were *S20*, *BA00862086*, *S21* and *S22* located at 563.66, 583.23, 601.20 and 619.41 Mbp, respectively (Table 5.2.). The same markers were also associated with the disease when using the scoring data below the PI (*P-value* < 0.05) at 17-18, 20-21 and 25 dpi. There was also an association at 20-21 dpi (*P-value* < 0.05) for markers *S1*, *S2* and *BA00144665* located at 380.08, 411.40, 446.04 Mbp, respectively (Table 5.3.).

Table 5.2. *P-value data obtained from a LMM analysis performed for each individual marker located on the 2D chromosome. Source of markers used for the analysis is described. Associated RefSeqv1.1 gene models (where available) and physical position on RefSeqv1.0 assembly are shown. Symptoms above the point of infection were assessed in five sets at different dpi: at 9-10 dpi (Score 1), at 13-14 dpi (Score 2), at 17-18 dpi (Score 3), at 20-21 dpi (Score 4) and at 25 dpi (Score 5) in Summer 2019. Data was transformed using a log10 transformation. P-value data of markers associated with FHB Type II resistance are highlighted in light green (P < 0.05) and markers strongly associated with the resistance in dark green (P < 0.01).*

Source	18K SNP array	18K SNP array	Cereals DB	18K SNP array	18K SNP array	Cereals DB	18K SNP array	18K SNP array	18K SNP array
RefSeqv1.1 Gene model	*intergenic*	*intergenic*	*TraesCS2D02G347900*	*TraesCS2D02G390100*	*intergenic*	*TraesCS2D02G480700*	*TraesCS2D02G507600*	*TraesCS2D02G537900*	*intergenic*
RefSeqv1.0 (bp)	380,082,519	411,408,120	446,047,025	497,905,031	563,660,447	583,231,124	601,204,785	619,412,506	630,765,860
Marker	***S1***	***S2***	***BA00144665***	***S9***	***S20***	***BA00862086***	***S21***	***S22***	***S23***
Score 1	0.136	0.136	0.136	0.002	0.062	0.062	0.062	0.062	0.645
Score 2	0.169	0.169	0.169	0.001	0.038	0.038	0.038	0.038	0.930
Score 3	0.205	0.205	0.205	0.003	0.053	0.053	0.053	0.053	0.880
Score 4	0.119	0.119	0.119	0.001	0.046	0.046	0.046	0.046	0.775
Score 5	0.135	0.135	0.135	0.001	0.079	0.079	0.079	0.079	0.939

Table 5.3. *P-value data obtained from a LMM analysis performed for each individual marker located on the 2D chromosome. Source of markers used for the analysis is described. Associated RefSeqv1.1 gene models (where available) and physical position on RefSeqv1.0 assembly are shown. Symptoms below the point of infection were assessed in five sets at different dpi: at 9-10 dpi (Score 1), at 13-14 dpi (Score 2), at 17-18 dpi (Score 3), at 20-21 dpi (Score 4) and at 25 dpi (Score 5) in Summer 2019. Data was transformed using a log10 transformation. P-value data of markers associated with FHB Type II resistance are highlighted in light green (P < 0.05) and markers strongly associated with the resistance in dark green (P < 0.01).*

Source	18K SNP array	18K SNP array	Cereals DB	18K SNP array	18K SNP array	Cereals DB	18K SNP array	18K SNP array	18K SNP array
RefSeqv1.1 Gene model	*intergenic*	*intergenic*	*TraesCS2D02G347900*	*TraesCS2D02G390100*	*intergenic*	*TraesCS2D02G480700*	*TraesCS2D02G507600*	*TraesCS2D02G537900*	*intergenic*
RefSeqv1.0 (bp)	380,082,519	411,408,120	446,047,025	497,905,031	563,660,447	583,231,124	601,204,785	619,412,506	630,765,860
Marker	***S1***	***S2***	***BA00144665***	***S9***	***S20***	***BA00862086***	***S21***	***S22***	***S23***
Score 1	0.723	0.723	0.723	0.098	0.497	0.497	0.497	0.497	0.918
Score 2	0.093	0.093	0.093	< 0.001	0.592	0.592	0.592	0.592	0.658
Score 3	0.069	0.069	0.069	< 0.001	0.048	0.048	0.048	0.048	0.706
Score 4	0.048	0.048	0.048	< 0.001	0.468	0.468	0.468	0.468	0.765
Score 5	0.526	0.526	0.526	< 0.001	0.038	0.038	0.038	0.038	0.836

The phenotypic data is related to the alleles provided by parental lines (Crusoe or Wuhan) in each recombinant at each marker position, while the genomic data reveals the location of the QTL in these lines. Once the single marker analysis is performed, any marker associated with the resistance (provided by Wuhan allele) can be identified.

The genomic region on the 2DL locus most associated with FHB resistance in Summer 2019 was of 117.62 Mbp, between markers *BA00144665* (at 446.04 Mbp) and *S20* (at 563.66 Mbp). Recombinant lines tested in Summer 2019 contained the resistant allele (Wuhan) on that genomic region on the 2DL were Rec 3, Rec 6, and Rec 7. The other recombinants (Rec 1, Rec 2, Rec 4, and Rec 5) were like Crusoe (Figure 5.2.). Lines showing the greatest resistance were, indeed, Rec 3, Rec 6, and Rec 7 (the total number of infected spikelets were 3.90, 2.22 and 2.05, respectively) at 17-18 dpi (Figure 5.2.). In contrast, Rec 1, Rec 2, Rec 4, and Rec 5 (the total number of infected spikelets were 10.23, 6.59, 8.54, 5.99, respectively) showed higher levels of susceptibility at 17-18 dpi (Figure 5.2.).

Heterozygous lines across the 2D chromosome were selected from previous provided NILs. These heterozygous lines were bulked to identify new recombinant lines containing the 2DL locus. A total of sixteen heterozygous lines were selected to obtain different recombination points on the 2DL. These lines were genotyped and divided in different groups for FHB type II disease assessment in the 2020 summer trial to confirm the mapping of the QTL interval. Some of these lines were sister lines, like for example Rec 1_A, Rec 1_B and Rec 1_H, which were obtained from Rec 1 (Table 5.4.).

Table 5.4. *Graphical genotype of parental-like lines (Crusoe and Wuhan) and RILs selected to be tested for FHB type II resistance in Summer 2020. Source of markers is described. Associated RefSeqv1.1 gene models (where available) and physical position on RefSeqv1.0 assembly are shown. 'Cru' is the allele provided by parental line Crusoe; 'Wu' is the allele provided by parental line Wuhan; 'Het' is the heterozygous allele.*

Source	18K SNP array	18K SNP array	18K SNP array	18K SNP array	18K SNP array	18K SNP array	18K SNP array
RefSeqv1.1 Gene model	*intergenic*	*intergenic*	*TraesCS2D02G390100*	*intergenic*	*TraesCS2D02G507600*	*TraesCS2D02G537900*	*intergenic*
RefSeqv1.0 (bp)	380,082,519	411,408,120	497,905,031	563,660,447	601,204,785	619,412,506	630,765,860
Marker	***S1***	***S2***	***S9***	***S20***	***S21***	***S22***	***S23***
Rec 1	Het	Het	Cru	Cru	Cru	Cru	Cru
Rec 2	Cru	Cru	Het	Het	Het	Het	Het
Rec 3	Het	Het	Het	Cru	Cru	Het	Het
Rec 4	Het	Het	Het	Cru	Cru	Cru	Cru
Rec 5	Het	Het	Wu	Wu	Wu	Wu	Wu
Rec 6	Het	Het	Wu	Het	Het	Het	Het
Rec 7	Het	Het	Wu	Wu	Wu	Het	Het
Rec 8	Wu	Wu	Het	Het	Het	Het	Wu
Rec 9	Wu	Wu	Wu	Het	Cru	Cru	Cru
Rec 10	Wu	Wu	Het	Het	Het	Het	Het
Rec 11	Cru	Cru	Cru	Het	Het	Het	Wu
Rec 12	Cru	Cru	Cru	Het	Het	Het	Het
Rec 13	Het	Het	Wu	Wu	Wu	Wu	Het
Rec 14	Het	Het	-	Cru	Cru	Cru	Cru
Rec 15	Cru	Cru	-	Het	Het	Het	Wu
Rec 16	Cru	Cru	-	Het	Het	Het	Cru
Crusoe-like	Wu	Wu	Wu	Wu	Wu	Wu	Wu
Wuhan-like	Cru	Cru	Cru	Cru	Cru	Cru	Cru

5.4.1.2. Summer 2020

For this trial, a larger set of RILs (Rec 1-16) were selected to fine-map the 2DL QTL. These lines were bulked and sister lines with different recombination events across the 2D chromosome were selected and distributed into different groups ('A', 'B', and 'H') as previously commented. Crusoe-like and Wuhan-like lines were also tested. Graphical genotype of parental-like lines and RILs used in Summer 2020 is provided in Figure 5.4.

The distribution of disease spread above the PI changed for these lines over time. Figure 5.5. represents only the phenotypic data of RILs and parental-like lines collected at 16 dpi (Score 2) and at 20-21 dpi (Score 4). As it can be observed, the S.E. for each RIL is higher than previously seen because sister lines were group and analysed together.

As expected, the 'Crusoe-like' line was more susceptible than 'Wuhan-like' line when observing disease spread above the PI. The resistance of lines with Wuhan-like alleles to FHB disease spread above the PI was maintained over time (Figure 5.4.).

In general, disease severity of Summer 2020 was not as high as for Summer 2019 trial. It can be observed in Figure 5.5. that most of the RILs remained quite resistant with less than five infected-spikelets above the PI at 20-21 dpi (Score 4). However, there were different levels of FHB disease spread depending on the line. Recombinant lines showing a higher level of FHB resistance than the 'Wuhan-like' line were Rec 13_H, Rec 15_H, Rec 16_B, Rec 13_A, Rec 2_B, Rec 7_H, Rec 7_B, Rec 15_B, Rec 14_H and Rec 4_B. In contrast, lines more susceptible than the 'Crusoe-like' line were Rec 10_A, Rec 3_H, Rec 4_H, Rec 3_A, Rec 11_H, Rec 4_A, Rec 1_H, Rec 5_H, Rec 3_B, Rec 11_B, Rec 1_A, Rec 8_H, Rec 11_A, Rec 1_B and Rec 8_A (Figure 5.5.).

(a)

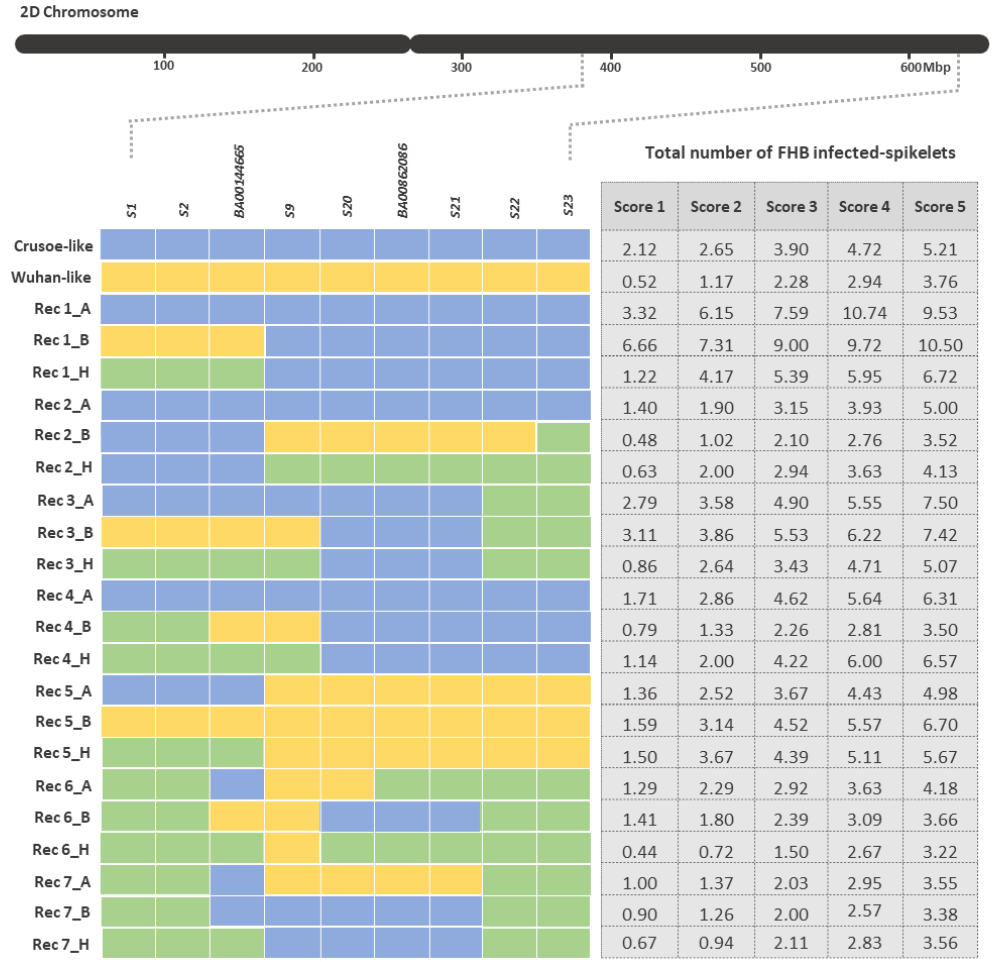

(b)

Total number of FHB infected-spikelets

Score 1	Score 2	Score 3	Score 4	Score 5
2.12	2.65	3.90	4.72	5.21
0.52	1.17	2.28	2.94	3.76
3.32	6.15	7.59	10.74	9.53
6.66	7.31	9.00	9.72	10.50
1.22	4.17	5.39	5.95	6.72
1.40	1.90	3.15	3.93	5.00
0.48	1.02	2.10	2.76	3.52
0.63	2.00	2.94	3.63	4.13
2.79	3.58	4.90	5.55	7.50
3.11	3.86	5.53	6.22	7.42
0.86	2.64	3.43	4.71	5.07
1.71	2.86	4.62	5.64	6.31
0.79	1.33	2.26	2.81	3.50
1.14	2.00	4.22	6.00	6.57
1.36	2.52	3.67	4.43	4.98
1.59	3.14	4.52	5.57	6.70
1.50	3.67	4.39	5.11	5.67
1.29	2.29	2.92	3.63	4.18
1.41	1.80	2.39	3.09	3.66
0.44	0.72	1.50	2.67	3.22
1.00	1.37	2.03	2.95	3.55
0.90	1.26	2.00	2.57	3.38
0.67	0.94	2.11	2.83	3.56

Figure 5.4. *a) Graphical genotype of parental-like lines (Crusoe and Wuhan) and RILs used in Summer 2020. Line names are specified on each raw and markers used are specified on each column. Yellow is the allele provided by Wuhan and blue the one by Crusoe. Green is the heterozygous allele. b) Total number of FHB infected-spikelets (scoring data above and below the point of infection) obtained for each line at different scoring dates: Score 1 (14 dpi), Score 2 (16 dpi), Score 3 (18-19 dpi), Score 4 (20-21 dpi) and Score 5 (22-23 dpi).*

(a)

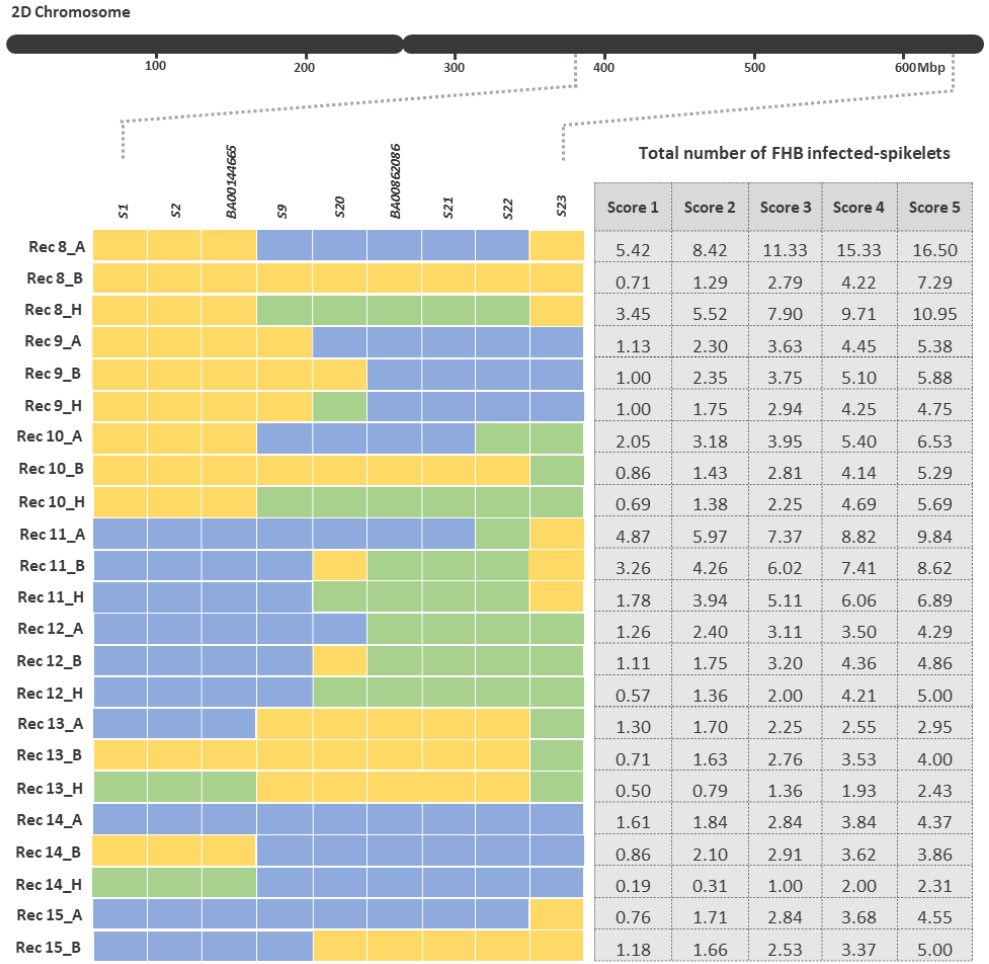

(b)

Total number of FHB infected-spikelets

	Score 1	Score 2	Score 3	Score 4	Score 5
Rec 8_A	5.42	8.42	11.33	15.33	16.50
Rec 8_B	0.71	1.29	2.79	4.22	7.29
Rec 8_H	3.45	5.52	7.90	9.71	10.95
Rec 9_A	1.13	2.30	3.63	4.45	5.38
Rec 9_B	1.00	2.35	3.75	5.10	5.88
Rec 9_H	1.00	1.75	2.94	4.25	4.75
Rec 10_A	2.05	3.18	3.95	5.40	6.53
Rec 10_B	0.86	1.43	2.81	4.14	5.29
Rec 10_H	0.69	1.38	2.25	4.69	5.69
Rec 11_A	4.87	5.97	7.37	8.82	9.84
Rec 11_B	3.26	4.26	6.02	7.41	8.62
Rec 11_H	1.78	3.94	5.11	6.06	6.89
Rec 12_A	1.26	2.40	3.11	3.50	4.29
Rec 12_B	1.11	1.75	3.20	4.36	4.86
Rec 12_H	0.57	1.36	2.00	4.21	5.00
Rec 13_A	1.30	1.70	2.25	2.55	2.95
Rec 13_B	0.71	1.63	2.76	3.53	4.00
Rec 13_H	0.50	0.79	1.36	1.93	2.43
Rec 14_A	1.61	1.84	2.84	3.84	4.37
Rec 14_B	0.86	2.10	2.91	3.62	3.86
Rec 14_H	0.19	0.31	1.00	2.00	2.31
Rec 15_A	0.76	1.71	2.84	3.68	4.55
Rec 15_B	1.18	1.66	2.53	3.37	5.00

Figure 5.4. Continued. *a) Graphical genotype of parental-like lines (Crusoe and Wuhan) and RILs used in Summer 2020. Line names are specified on each raw and markers used are specified on each column. Yellow is the allele provided by Wuhan and blue the one by Crusoe. Green is the heterozygous allele. b) Total number of FHB infected-spikelets (scoring data above and below the point of infection) obtained for each line at different scoring dates: Score 1 (14 dpi), Score 2 (16 dpi), Score 3 (18-19 dpi), Score 4 (20-21 dpi) and Score 5 (22-23 dpi).*

(a)

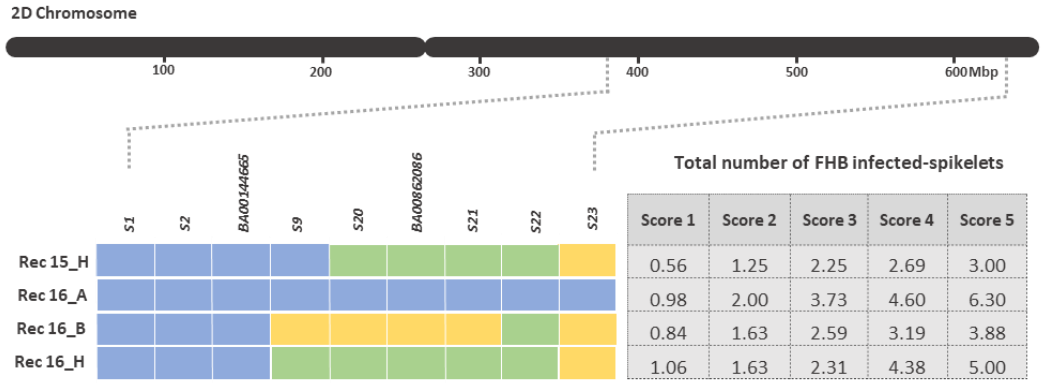

(b)

Total number of FHB infected-spikelets

	Score 1	Score 2	Score 3	Score 4	Score 5
Rec 15_H	0.56	1.25	2.25	2.69	3.00
Rec 16_A	0.98	2.00	3.73	4.60	6.30
Rec 16_B	0.84	1.63	2.59	3.19	3.88
Rec 16_H	1.06	1.63	2.31	4.38	5.00

Figure 5.4. Continued. *a) Graphical genotype of parental-like lines (Crusoe and Wuhan) and RILs used in Summer 2020. Line names are specified on each raw and markers used are specified on each column. Yellow is the allele provided by Wuhan and blue the one by Crusoe. Green is the heterozygous allele. b) Total number of FHB infected-spikelets (scoring data above and below the point of infection) obtained for each line at different scoring dates: Score 1 (14 dpi), Score 2 (16 dpi), Score 3 (18-19 dpi), Score 4 (20-21 dpi) and Score 5 (22-23 dpi).*

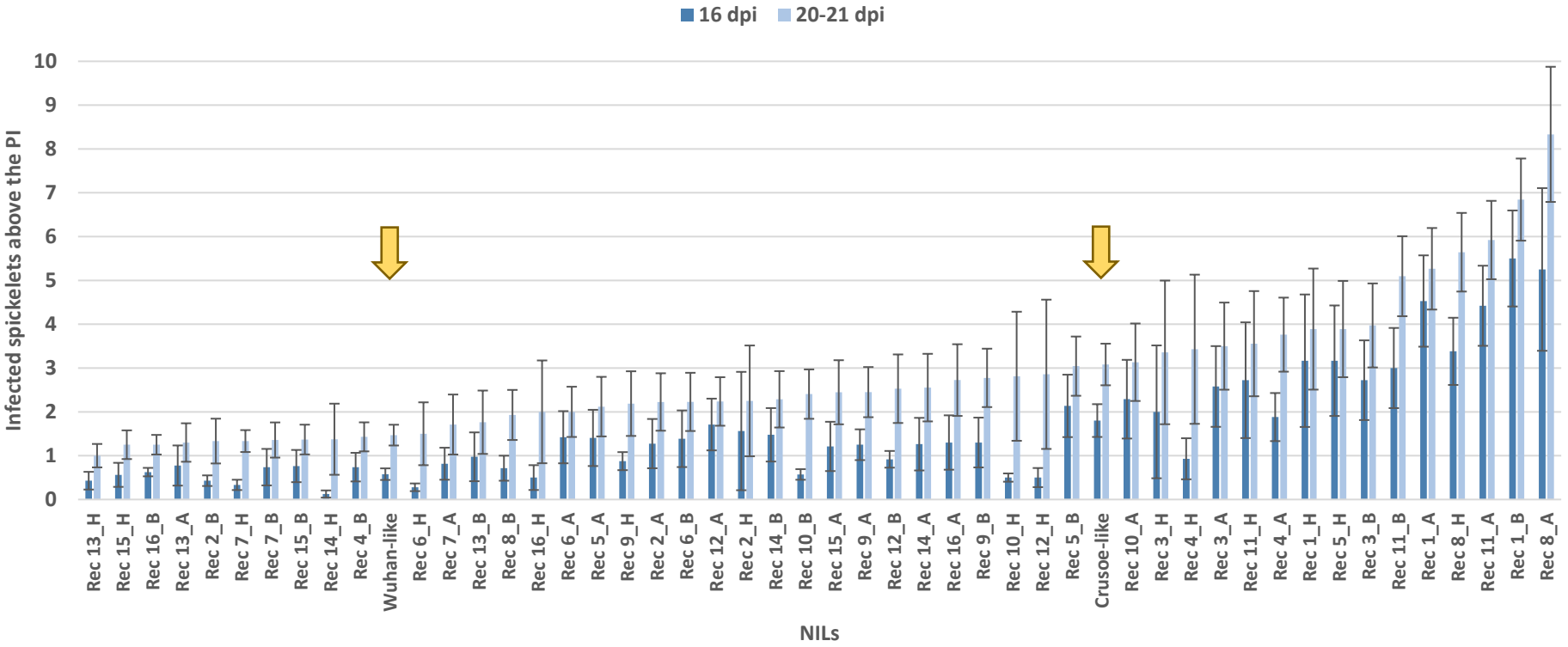

***Figure 5.5**. FHB disease above the PI or number of bleached spikelets above the PI of RILs and parental-like lines (Crusoe and Wuhan; yellow arrows) tested for Type II on Summer 2020. Scoring symptoms represented at 16 dpi (Score 2) and at 20-21 dpi (Score 4). Predicted means were generated using a LMM analysis. Error bars are ± standard error.*

LMM analysis of Summer 2020 data revealed that one marker was strongly associated with FHB type II resistance (*P-value* < 0.001) at 20-21 dpi on the long arm of chromosome 2D. This marker is *S9* (source: 18K SNP array) located at 497.90 Mbp (Table 5.5.). There was a stronger association with the resistance over time (*P-value* < 0.001) at 22-23 dpi when using scoring data above the PI. Analysis also shown that markers *S20, BA00862086*, *S21* and *S22* were also associated with the resistance (*P-value* < 0.05). Additionally, marker *S9* was also associated with the disease when using the scoring data below the PI (*P-value* = 0.018) at 20-21 dpi, and thus confirming the genomic region of the 2DL. Marker S23 at 630.76 Mbp was also associated with FHB type II resistance (*P-value* < 0.05) (Table 5.6.), although this marker was not statistically significant when using the scoring data above the PI (*P-value* > 0.05) (Table 5.5.).

The genomic region on the 2DL locus most associated with FHB resistance in Summer 2020 was still of 117.62 Mbp, between markers *BA00144665* (at 446.04 Mbp) and *S20* (at 563.66 Mbp). Recombinant lines tested in Summer 2020 containing the resistant allele 'Wu' in that genomic region on the 2DL were Rec 2_B, Rec 5_A-H, Rec 6_A, Rec 7_A-H, Rec 8_B, Rec 9_B, Rec 10_B, Rec 13_A-H and Rec 16_B. There were several recombinant lines from 497 to 563 Mbp for which the breaking point of Crusoe-Wuhan allele was still unknown due to lack of polymorphic markers on that genomic region. These lines were Rec 3_B, Rec 4_B, Rec 6_B, Rec 9_A, Rec 11_B, Rec 12_B and Rec 15_B. Moreover, there were still lines segregating within that region at one or both markers. These lines were Rec 2_H, Rec 3_H, Rec 4_H, Rec 6_H, Rec 8_H, Rec 9_H, Rec 10_H, Rec 11_H, Rec 12_H, Rec 15_H and Rec 16_H (Figure 5.4.).

Recombinant lines showing the greatest resistance at 20-21 dpi were Rec 13_H, Rec 13_A, Rec 7_B, Rec 6_H, Rec 15_H, Rec 2_B, Rec 4_B and Rec 7_H (the total number of infected spikelets ranging from 1.93 to 2.83). Line Rec 14_H showed higher levels of FHB type

II resistance but contains ‘Crusoe’ allele for the markers flanking the 2DL locus. In contrast, Rec 10_A, Rec 3_A, Rec 4_A, Rec 1_H, Rec 4_H, Rec 11_H, Rec 3_B, Rec 11_B, Rec 11_A, Rec 8_H, Rec 1_B, Rec 1_A and Rec 8_A (the total number of infected spikelets ranging from 5.4 to 15.33) showed higher levels of susceptibility at 20-21 dpi. Nevertheless, the exception was Rec 5_B, Rec 5_H and Rec 9_B which showed higher levels of FHB type II susceptibility but appears to contain ‘Wuhan’ alleles for the markers flanking the 2DL locus (Figure 5.4. and Figure 5.5.).

To conclude, summer 2020 trial helped to confirm the QTL location on the long arm of the 2D chromosome of wheat. However, several inconsistences between genotypic and phenotypic results were observed as mentioned above. For instance, Rec 5_A, Rec 5_B and Rec 5_H were all susceptible despite having the ‘Wuhan’ allele throughout the interval, and Rec 2_A was resistant despite having the ‘Crusoe’ allele throughout the interval. These anomalies prevent unequivocal assignment of the QTL interval.

Seed obtained from Summer 2020 trial was not harvested so could not be used for subsequent trials. That is why, to obtain more recombinant lines on the 2DL locus, seed selected to be used for Summer 2021 trial was bulked again to identify new breaking points on the 2DL locus. Heterozygous RILs selected were Rec 4, Rec 6, Rec 9, Rec 11, and Rec 12 (Table 5.7.). This material was then used to work on the fine-mapping of the 2DL QTL.

Table 5.5. *P-value data obtained from a LMM analysis performed for each individual marker located on the 2D chromosome. Source of markers used for the analysis is described. Associated RefSeqv1.1 gene models (where available) and physical position on RefSeqv1.0 assembly are shown. Symptoms above the point of infection were assessed in five sets at different dpi: at 14 dpi (Score 1), at 16 dpi (Score 2), at 18-19 dpi (Score 3), at 20-21 dpi (Score 4) and at 22-23 dpi (Score 5) in Summer 2020. Data was transformed using a log10 transformation. P-value data of markers associated with FHB Type II resistance are highlighted in light green (P < 0.05) and markers strongly associated with the resistance in dark green (P < 0.01).*

Source	18K SNP array	18K SNP array	Cereals DB	18K SNP array	18K SNP array	Cereals DB	18K SNP array	18K SNP array	18K SNP array
RefSeqv1.1 Gene model	*intergenic*	*intergenic*	*TraesCS2D02G347900*	*TraesCS2D02G390100*	*intergenic*	*TraesCS2D02G480700*	*TraesCS2D02G507600*	*TraesCS2D02G537900*	*intergenic*
RefSeqv1.0 (bp)	380,082,519	411,408,120	446,047,025	497,905,031	563,660,447	583,231,124	601,204,785	619,412,506	630,765,860
Marker	***S1***	***S2***	***BA00144665***	***S9***	***S20***	***BA00862086***	***S21***	***S22***	***S23***
Score 1	0.643	0.643	0.487	<0.001	0.028	0.032	0.032	0.052	0.084
Score 2	0.644	0.644	0.689	<0.001	0.002	0.002	0.002	0.011	0.069
Score 3	0.901	0.901	0.823	<0.001	0.004	0.003	0.003	0.009	0.141
Score 4	0.970	0.970	0.881	<0.001	0.003	0.002	0.002	0.014	0.147
Score 5	0.816	0.816	0.732	<0.001	0.004	0.005	0.005	0.013	0.493

Table 5.6. *P-value data obtained from a LMM analysis performed for each individual marker located on the 2D chromosome. Source of markers used for the analysis is described. Associated RefSeqv1.1 gene models (where available) and physical position on RefSeqv1.0 assembly are shown. Symptoms below the point of infection were assessed in five sets at different dpi: at 14 dpi (Score 1), at 16 dpi (Score 2), at 18-19 dpi (Score 3), at 20-21 dpi (Score 4) and at 22-23 dpi (Score 5) in Summer 2020. Data was transformed using a log10 transformation. P-value data of markers associated with FHB Type II resistance are highlighted in light green (P < 0.05) and markers strongly associated with the resistance in dark green (P < 0.01).*

Source	18K SNP array	18K SNP array	Cereals DB	18K SNP array	18K SNP array	Cereals DB	18K SNP array	18K SNP array	18K SNP array
RefSeqv1.1 Gene model	*intergenic*	*intergenic*	*TraesCS2D02G347900*	*TraesCS2D02G390100*	*intergenic*	*TraesCS2D02G480700*	*TraesCS2D02G507600*	*TraesCS2D02G537900*	*intergenic*
RefSeqv1.0 (bp)	380,082,519	411,408,120	446,047,025	497,905,031	563,660,447	583,231,124	601,204,785	619,412,506	630,765,860
Marker	***S1***	***S2***	***BA00144665***	***S9***	***S20***	***BA00862086***	***S21***	***S22***	***S23***
Score 1	0.304	0.304	0.529	0.007	0.471	0.521	0.521	0.117	0.001
Score 2	0.171	0.171	0.385	0.028	0.372	0.379	0.379	0.302	0.000
Score 3	0.338	0.338	0.661	0.037	0.357	0.303	0.303	0.246	0.005
Score 4	0.150	0.150	0.490	0.018	0.318	0.312	0.312	0.236	0.024
Score 5	0.252	0.252	0.516	0.015	0.412	0.446	0.446	0.207	0.032

Table 5.7. *Graphical genotype of parental-like lines (Crusoe and Wuhan) and RILs selected to be tested for FHB type II resistance in Summer 2021. Source of markers is described. Associated RefSeqv1.1 gene models (where available) and physical position on RefSeqv1.0 assembly are shown. 'Cru' is the allele provided by parental line Crusoe; 'Wu' is the allele provided by parental line Wuhan; 'Het' is the heterozygous allele.*

Source	18K SNP array	18K SNP array	18K SNP array	18K SNP array	18K SNP array	18K SNP array	18K SNP array
RefSeqv1.1 Gene model	*intergenic*	*intergenic*	*TraesCS2D02G390100*	*intergenic*	*TraesCS2D02G507600*	*TraesCS2D02G537900*	*intergenic*
RefSeqv1.0 (bp)	380,082,519	411,408,120	497,905,031	563,660,447	601,204,785	619,412,506	630,765,860
Marker	***S1***	***S2***	***S9***	***S20***	***S21***	***S22***	***S23***
Rec 4	Het	Het	Het	Cru	Cru	Cru	Cru
Rec 6	Het	Het	Wu	Het	Het	Het	Het
Rec 9	Wu	Wu	Wu	Het	Cru	Cru	Cru
Rec 11	Cru	Cru	Cru	Het	Het	Het	Wu
Rec 12	Cru	Cru	Cru	Het	Het	Het	Het
Crusoe-like	Wu	Wu	Wu	Wu	Wu	Wu	Wu
Wuhan-like	Cru	Cru	Cru	Cru	Cru	Cru	Cru

5.4.1.3. Summer 2021

For summer 2021 trial, two sets of recombinant plants were screened with new markers developed by the iCase collaborators and were arranged as first trial (Test 1) and second trial (Test 2). The first trial (Test 1) contained recombinants Rec 4, Rec 6, Rec 9, Rec 11 and Rec 12, while in the second trial (Test 2) only Rec 4 and Rec 12 were tested. Crusoe-like and Wuhan-like lines were also tested in both experiments. Graphical genotype of parental-like lines and RILs used in Summer 2021 is provided Figure 5.6., for Test 1, and in Figure 5.7., for test 2.

The distribution of disease spread above the PI changed for these recombinants over time. Figure 5.8. and Figure 5.9. represent the phenotypic data of RILs and parental-like lines collected at 14-15 dpi (Score 2) and at 19-20 dpi (Score 4) for Test 1; and Figure 5.10. and Figure 5.11. at 18 dpi (Score 2) and at 22-23 dpi (Score 4) for Test 2.

In both trials, the 'Crusoe-like' line was more susceptible than the 'Wuhan-like' line when observing disease spread above the PI (Figure 5.8. and Figure 5.10.) and below the PI (Figure 5.9. and Figure 5.11.). The resistance of Wuhan-like line to FHB disease spread above the PI was maintained over time for both trials (see Figure 5.6. for Test 1; and Figure 5.7. for Test 2). At 19-20 dpi in Test 1, Wuhan-like line had a total of 5.92 infected spikelets, and at 18 dpi in Test 2, this line had 1.67 infected spikelets. In the case of Crusoe-like line, at 19-20 dpi in Test 1 it had a total of 9.32 infected spikelets, and at 18 dpi in Test 2, this line had 7.14 infected spikelets. Although not shown, the S.E. for each RIL is higher than previously seen because only one plant per recombinant line was tested and analysed. However, higher number of spikes were infected per plant to reduce the variation as much as possible.

It seems that disease severity of Summer 2021 was higher in Test 1 than in Test 2 as it can be observed in the parental-like lines at 25 dpi. During Test 1, Crusoe-like had a total of 12.05 infected spikelets, and Wuhan-like 9.40 infected spikelets, while during Test 2

Crusoe-like had 10.69 infected spikelets and Wuhan-like had 2.42 infected spikelets (see Figure 5.6. for Test 1; and Figure 5.7. for Test 2).

It can be observed in Figure 5.8. that 22 of the RILs remained quite resistant with less than three and a half infected-spikelets above the PI at 19-20 dpi (Score 4) during Test 1. Some recombinant lines showing a higher level of FHB resistance than the Wuhan-like line were Rec 12_01, Rec 9_07, Rec 6_04, Rec 12_07, Rec 9_10, Rec 9_05 and Rec 4_08. In contrast, lines more susceptible than the Crusoe-like line at 19-20 dpi (Score 4) during Test 1 were Rec 4_10, Rec 4_01, Rec 11_02, Rec 6_01, Rec 11_06, Rec 12_23, Rec 12_16, Rec 9_17, Rec 11_11, Rec 11_23, Rec 11_25, Rec 4_18, Rec 9_12, Rec 11_10, Rec 11_05, Rec 11_20, Rec 4_15 and Rec 11_07.

When observing data of infected spikelets below the PI (Figure 5.9.) there were 12 lines (Rec 9_07, Rec 9_08, Rec 12_07, Rec 4_19, Rec 12_01, Rec 4_08, Rec 6_04, Rec 9_10, Rec 9_15, Rec 9_05, Rec 9_18 and Rec 4_21) showing higher levels of FHB resistance with less than two infected-spikelets. When comparing data of infected spikelets above and under the PI (Figure 5.8. and Figure 5.9.), the most resistant lines to FHB type II resistance in Test 1 were Rec 12_01, Rec 9_07, Rec 6_04, Rec 12_07, Rec 9_10, Rec 9_05 and Rec 4_08.

Additionally, during Test 2 seven of the RILs remained quite resistant with less than one infected-spikelet above the PI at 22-23 dpi (Score 4). These recombinant lines were Rec 4_018, Rec 4_027, Rec 12_039, Rec 12_258, Rec 12_059, Rec 12_029 and Rec 4_022. Lines more susceptible than the Crusoe-like line at 22-23 dpi (Score 4) during Test 2 were Rec 12_179, Rec 12_004, Rec 12_118, Rec 12_099 and Rec 12_003 (Figure 5.10.).

When observing data of infected spikelets below the PI (Figure 5.11.) there were 9 lines (Rec 12_039, Rec 4_018, Rec 12_101, Rec 12_029, Rec 12_251, Rec 12_059, Rec 4_026, Rec 12_050 and Rec 12_256) showing higher levels of FHB resistance than Wuhan-like line. When comparing data of infected spikelets above and under the PI (Figure 5.10. and Figure

5.11.), the most resistant lines to FHB type II resistance in Test 2 were Rec 4_018, Rec 12_039, Rec 12_059 and Rec 12_029 (Figure 5.11.).

However, as I will describe later in the results after the LMM analysis, data of Summer 2021 also affected the ability to reduce the QTL interval since inconsistences between genotype and phenotype were also observed. Some plants with 'Wuhan' alleles across the interval appeared to be susceptible, and plants with 'Crusoe' alleles appeared to be resistant.

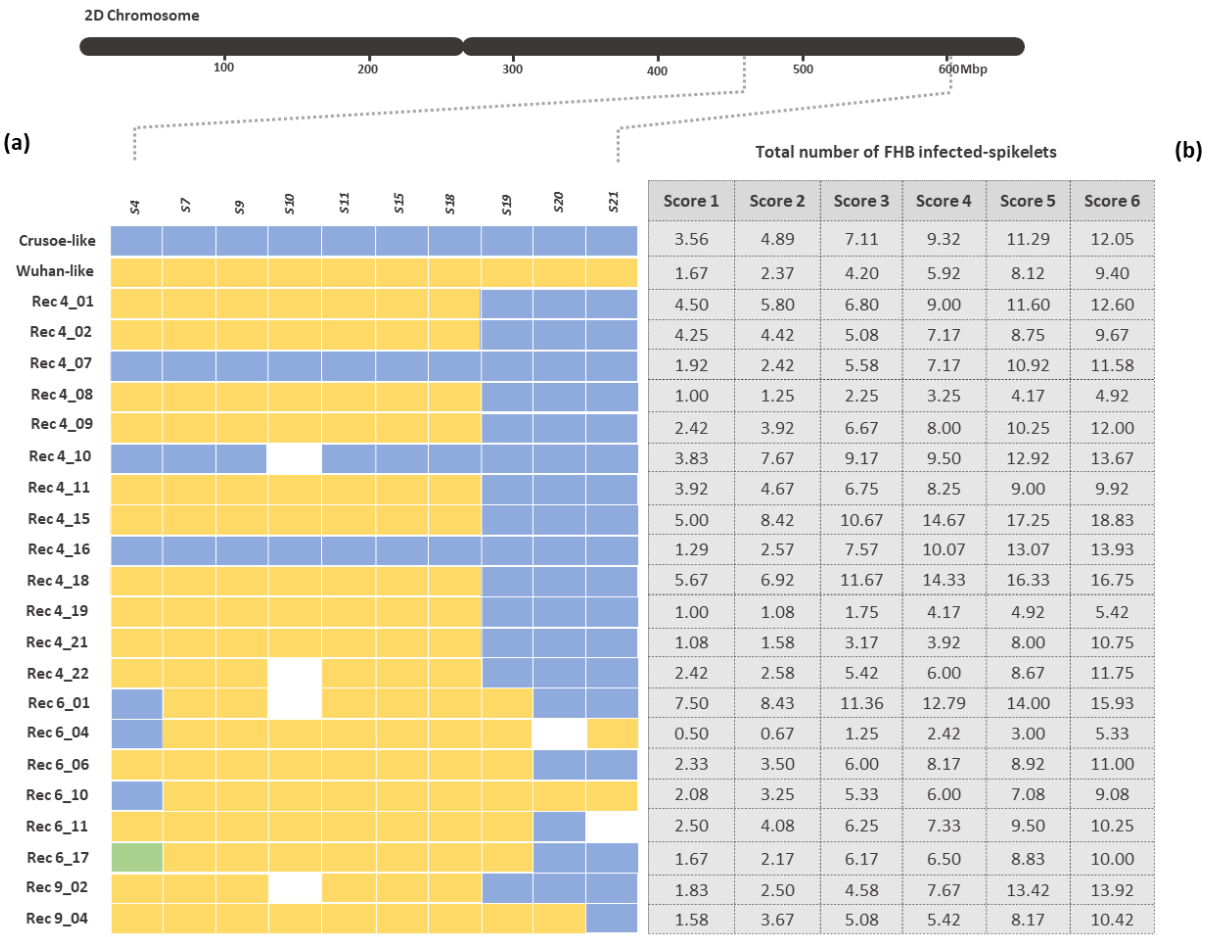

(b) Total number of FHB infected-spikelets

	Score 1	Score 2	Score 3	Score 4	Score 5	Score 6
Crusoe-like	3.56	4.89	7.11	9.32	11.29	12.05
Wuhan-like	1.67	2.37	4.20	5.92	8.12	9.40
Rec 4_01	4.50	5.80	6.80	9.00	11.60	12.60
Rec 4_02	4.25	4.42	5.08	7.17	8.75	9.67
Rec 4_07	1.92	2.42	5.58	7.17	10.92	11.58
Rec 4_08	1.00	1.25	2.25	3.25	4.17	4.92
Rec 4_09	2.42	3.92	6.67	8.00	10.25	12.00
Rec 4_10	3.83	7.67	9.17	9.50	12.92	13.67
Rec 4_11	3.92	4.67	6.75	8.25	9.00	9.92
Rec 4_15	5.00	8.42	10.67	14.67	17.25	18.83
Rec 4_16	1.29	2.57	7.57	10.07	13.07	13.93
Rec 4_18	5.67	6.92	11.67	14.33	16.33	16.75
Rec 4_19	1.00	1.08	1.75	4.17	4.92	5.42
Rec 4_21	1.08	1.58	3.17	3.92	8.00	10.75
Rec 4_22	2.42	2.58	5.42	6.00	8.67	11.75
Rec 6_01	7.50	8.43	11.36	12.79	14.00	15.93
Rec 6_04	0.50	0.67	1.25	2.42	3.00	5.33
Rec 6_06	2.33	3.50	6.00	8.17	8.92	11.00
Rec 6_10	2.08	3.25	5.33	6.00	7.08	9.08
Rec 6_11	2.50	4.08	6.25	7.33	9.50	10.25
Rec 6_17	1.67	2.17	6.17	6.50	8.83	10.00
Rec 9_02	1.83	2.50	4.58	7.67	13.42	13.92
Rec 9_04	1.58	3.67	5.08	5.42	8.17	10.42

Figure 5.6. *a) Graphical genotype of parental-like lines (Crusoe and Wuhan) and RILs used for the first trial (Test 1) in Summer 2021. Line names are specified on each raw and markers used are specified on each column. Yellow is the allele provided by Wuhan and blue the one by Crusoe. Green is the heterozygous allele. White is missing value. b) Total number of FHB infected-spikelets (scoring data above and below the point of infection) obtained for each line at different scoring dates: Score 1 (12-13 dpi), Score 2 (14-15 dpi), Score 3 (16-18 dpi), Score 4 (19-20 dpi), Score 5 (21-22 dpi) and Score 6 (23-25 dpi).*

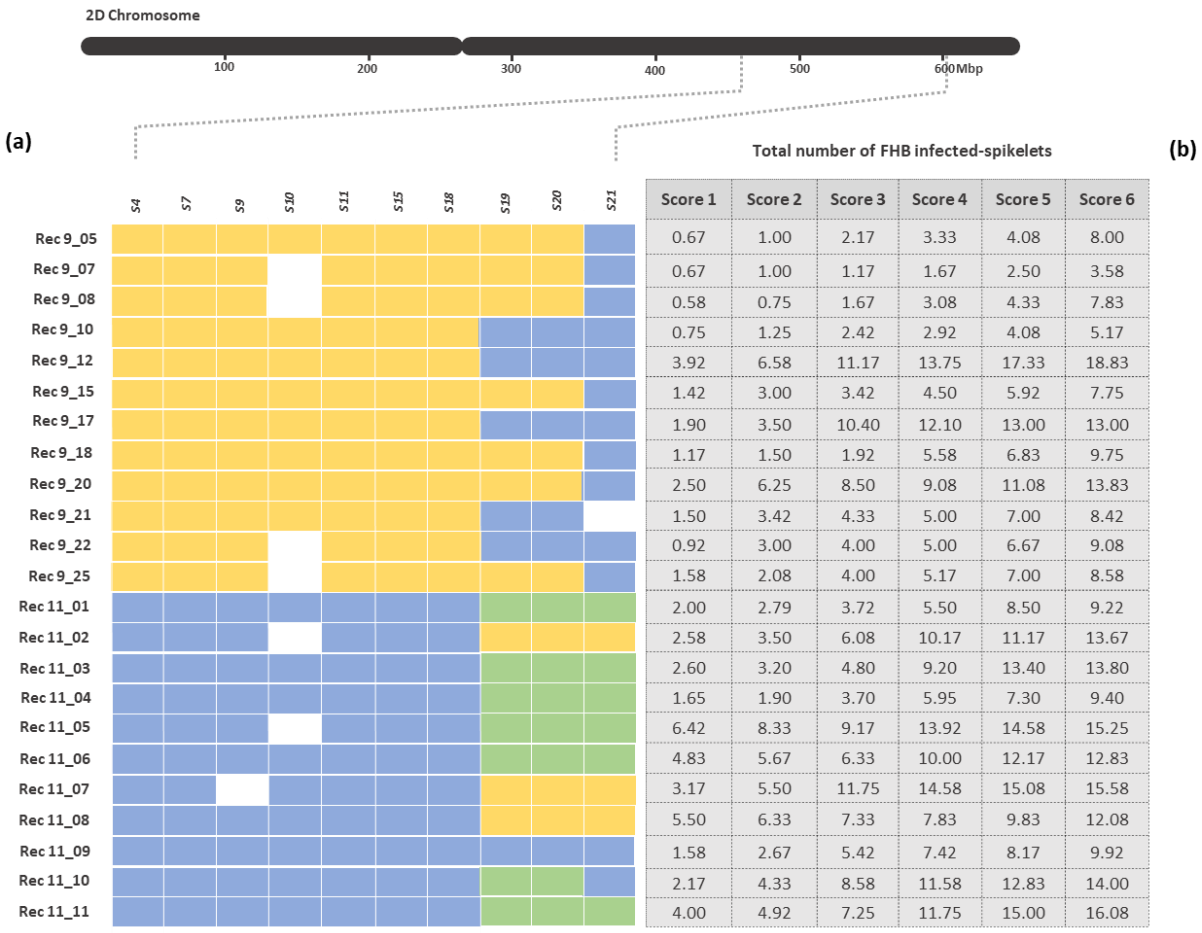

(b) Total number of FHB infected-spikelets

	Score 1	Score 2	Score 3	Score 4	Score 5	Score 6
Rec 9_05	0.67	1.00	2.17	3.33	4.08	8.00
Rec 9_07	0.67	1.00	1.17	1.67	2.50	3.58
Rec 9_08	0.58	0.75	1.67	3.08	4.33	7.83
Rec 9_10	0.75	1.25	2.42	2.92	4.08	5.17
Rec 9_12	3.92	6.58	11.17	13.75	17.33	18.83
Rec 9_15	1.42	3.00	3.42	4.50	5.92	7.75
Rec 9_17	1.90	3.50	10.40	12.10	13.00	13.00
Rec 9_18	1.17	1.50	1.92	5.58	6.83	9.75
Rec 9_20	2.50	6.25	8.50	9.08	11.08	13.83
Rec 9_21	1.50	3.42	4.33	5.00	7.00	8.42
Rec 9_22	0.92	3.00	4.00	5.00	6.67	9.08
Rec 9_25	1.58	2.08	4.00	5.17	7.00	8.58
Rec 11_01	2.00	2.79	3.72	5.50	8.50	9.22
Rec 11_02	2.58	3.50	6.08	10.17	11.17	13.67
Rec 11_03	2.60	3.20	4.80	9.20	13.40	13.80
Rec 11_04	1.65	1.90	3.70	5.95	7.30	9.40
Rec 11_05	6.42	8.33	9.17	13.92	14.58	15.25
Rec 11_06	4.83	5.67	6.33	10.00	12.17	12.83
Rec 11_07	3.17	5.50	11.75	14.58	15.08	15.58
Rec 11_08	5.50	6.33	7.33	7.83	9.83	12.08
Rec 11_09	1.58	2.67	5.42	7.42	8.17	9.92
Rec 11_10	2.17	4.33	8.58	11.58	12.83	14.00
Rec 11_11	4.00	4.92	7.25	11.75	15.00	16.08

Figure 5.6. Continued. *a) Graphical genotype of parental-like lines (Crusoe and Wuhan) and RILs used for the first trial (Test 1) in Summer 2021. Line names are specified on each raw and markers used are specified on each column. Yellow is the allele provided by Wuhan and blue the one by Crusoe. Green is the heterozygous allele. White is missing value. b) Total number of FHB infected-spikelets (scoring data above and below the point of infection) obtained for each line at different scoring dates: Score 1 (12-13 dpi), Score 2 (14-15 dpi), Score 3 (16-18 dpi), Score 4 (19-20 dpi), Score 5 (21-22 dpi) and Score 6 (23-25 dpi).*

Score 1	Score 2	Score 3	Score 4	Score 5	Score 6
2.25	2.83	3.25	6.92	7.83	8.67
1.67	2.67	6.42	7.25	9.83	10.92
2.50	4.58	8.33	8.67	9.25	10.08
1.83	2.75	6.42	6.92	9.08	9.42
3.08	4.75	7.75	8.17	11.00	14.00
3.83	4.50	8.33	9.42	11.25	11.58
3.58	4.25	6.17	8.67	10.67	10.92
5.08	6.50	9.92	12.67	12.92	13.75
1.83	4.58	6.42	7.42	9.42	11.17
4.83	5.92	7.58	9.58	12.25	12.50
2.58	3.92	8.58	11.50	13.67	14.00
3.83	4.92	5.17	6.58	8.92	10.17
2.25	3.92	8.67	10.92	13.33	14.00
0.83	0.83	1.17	2.17	3.17	3.67
2.17	2.67	3.58	5.75	9.17	15.08
0.25	0.67	1.42	2.00	2.33	2.58
2.00	4.25	4.25	6.08	7.83	11.42
6.67	8.75	9.75	12.17	13.92	16.00
1.40	1.80	3.10	4.80	8.30	9.50
4.25	5.00	6.58	8.58	12.00	14.33
1.00	1.83	4.00	4.50	6.33	6.67
3.83	6.08	8.08	10.42	11.17	12.75

Figure 5.6. Continued. *a) Graphical genotype of parental-like lines (Crusoe and Wuhan) and RILs used for the first trial (Test 1) in Summer 2021. Line names are specified on each raw and markers used are specified on each column. Yellow is the allele provided by Wuhan and blue the one by Crusoe. Green is the heterozygous allele. White is missing value. b) Total number of FHB infected-spikelets (scoring data above and below the point of infection) obtained for each line at different scoring dates: Score 1 (12-13 dpi), Score 2 (14-15 dpi), Score 3 (16-18 dpi), Score 4 (19-20 dpi), Score 5 (21-22 dpi) and Score 6 (23-25 dpi).*

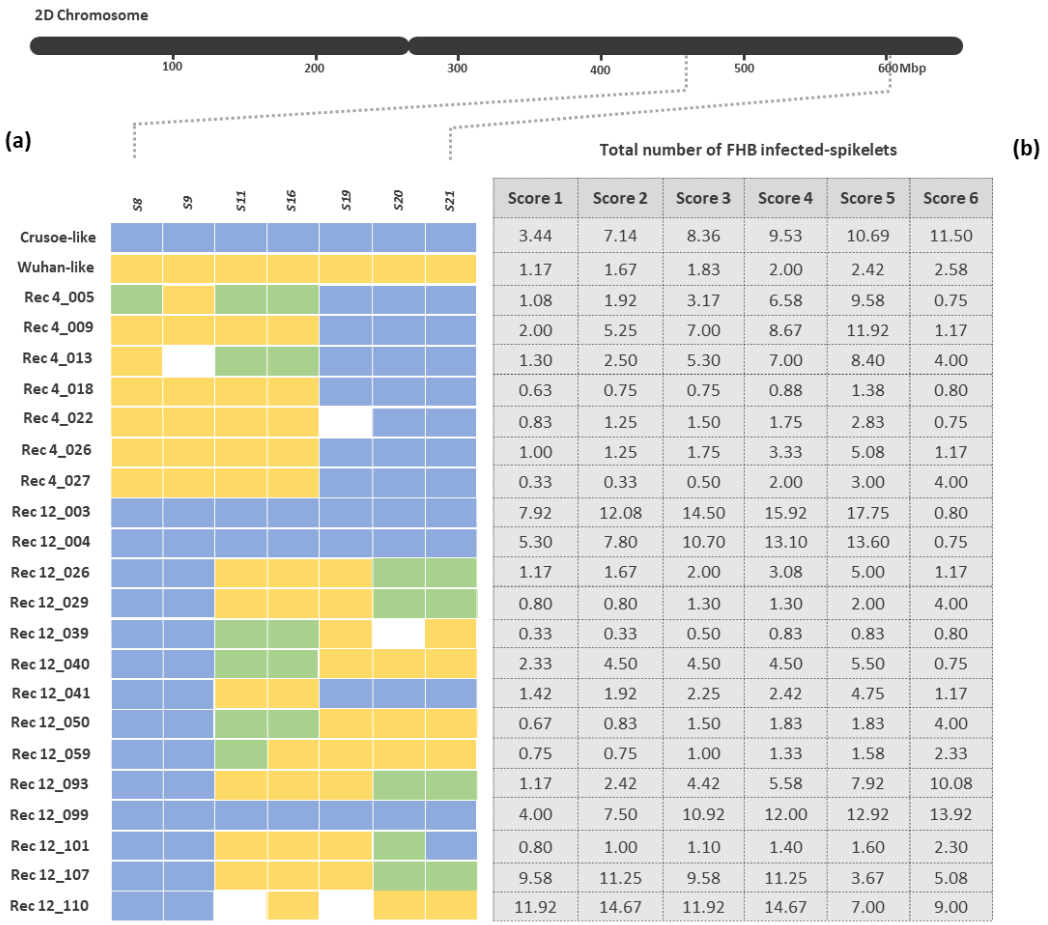

	Score 1	Score 2	Score 3	Score 4	Score 5	Score 6
Crusoe-like	3.44	7.14	8.36	9.53	10.69	11.50
Wuhan-like	1.17	1.67	1.83	2.00	2.42	2.58
Rec 4_005	1.08	1.92	3.17	6.58	9.58	0.75
Rec 4_009	2.00	5.25	7.00	8.67	11.92	1.17
Rec 4_013	1.30	2.50	5.30	7.00	8.40	4.00
Rec 4_018	0.63	0.75	0.75	0.88	1.38	0.80
Rec 4_022	0.83	1.25	1.50	1.75	2.83	0.75
Rec 4_026	1.00	1.25	1.75	3.33	5.08	1.17
Rec 4_027	0.33	0.33	0.50	2.00	3.00	4.00
Rec 12_003	7.92	12.08	14.50	15.92	17.75	0.80
Rec 12_004	5.30	7.80	10.70	13.10	13.60	0.75
Rec 12_026	1.17	1.67	2.00	3.08	5.00	1.17
Rec 12_029	0.80	0.80	1.30	1.30	2.00	4.00
Rec 12_039	0.33	0.33	0.50	0.83	0.83	0.80
Rec 12_040	2.33	4.50	4.50	4.50	5.50	0.75
Rec 12_041	1.42	1.92	2.25	2.42	4.75	1.17
Rec 12_050	0.67	0.83	1.50	1.83	1.83	4.00
Rec 12_059	0.75	0.75	1.00	1.33	1.58	2.33
Rec 12_093	1.17	2.42	4.42	5.58	7.92	10.08
Rec 12_099	4.00	7.50	10.92	12.00	12.92	13.92
Rec 12_101	0.80	1.00	1.10	1.40	1.60	2.30
Rec 12_107	9.58	11.25	9.58	11.25	3.67	5.08
Rec 12_110	11.92	14.67	11.92	14.67	7.00	9.00

Figure 5.7. *a) Graphical genotype of parental-like lines (Crusoe and Wuhan) and RILs used for the first trial (Test 2) in Summer 2021. Line names are specified on each raw and markers used are specified on each column. Yellow is the allele provided by Wuhan and blue the one by Crusoe. Green is the heterozygous allele. White is missing value. b) Total number of FHB infected-spikelets (scoring data above and below the point of infection) obtained for each line at different scoring dates: Score 1 (15 dpi), Score 2 (18 dpi), Score 3 (20-21 dpi), Score 4 (22-23 dpi), Score 5 (25 dpi) and Score 6 (27-28 dpi).*

(b) Total number of FHB infected-spikelets

Score 1	Score 2	Score 3	Score 4	Score 5	Score 6
8.40	9.40	8.40	9.40	13.58	14.00
1.38	3.88	1.38	3.88	5.33	6.25
2.83	4.08	2.83	4.08	5.00	5.80
5.08	7.92	5.08	7.92	6.50	9.33
3.00	4.00	3.00	4.00	4.80	6.50
17.75	18.58	17.75	18.58	10.00	10.00
13.60	14.50	13.60	14.50	10.92	13.58
5.00	6.08	5.00	6.08	7.30	9.00
2.00	5.40	2.00	5.40	5.63	7.88
0.83	1.00	0.83	1.00	3.75	5.25
5.50	5.83	5.50	5.83	6.30	6.70
4.75	6.33	4.75	6.33	3.10	5.90
1.83	2.17	1.83	2.17	5.67	7.92
1.58	2.33	1.58	2.33	2.20	2.30
7.92	10.08	7.92	10.08	2.17	2.92
12.92	13.92	12.92	13.92	2.20	2.80

Figure 5.7. Continued. *a) Graphical genotype of parental-like lines (Crusoe and Wuhan) and RILs used for the first trial (Test 2) in Summer 2021. Line names are specified on each raw and markers used are specified on each column. Yellow is the allele provided by Wuhan and blue the one by Crusoe. Green is the heterozygous allele. White is missing value. b) Total number of FHB infected-spikelets (scoring data above and below the point of infection) obtained for each line at different scoring dates: Score 1 (15 dpi), Score 2 (18 dpi), Score 3 (20-21 dpi), Score 4 (22-23 dpi), Score 5 (25 dpi) and Score 6 (27-28 dpi).*

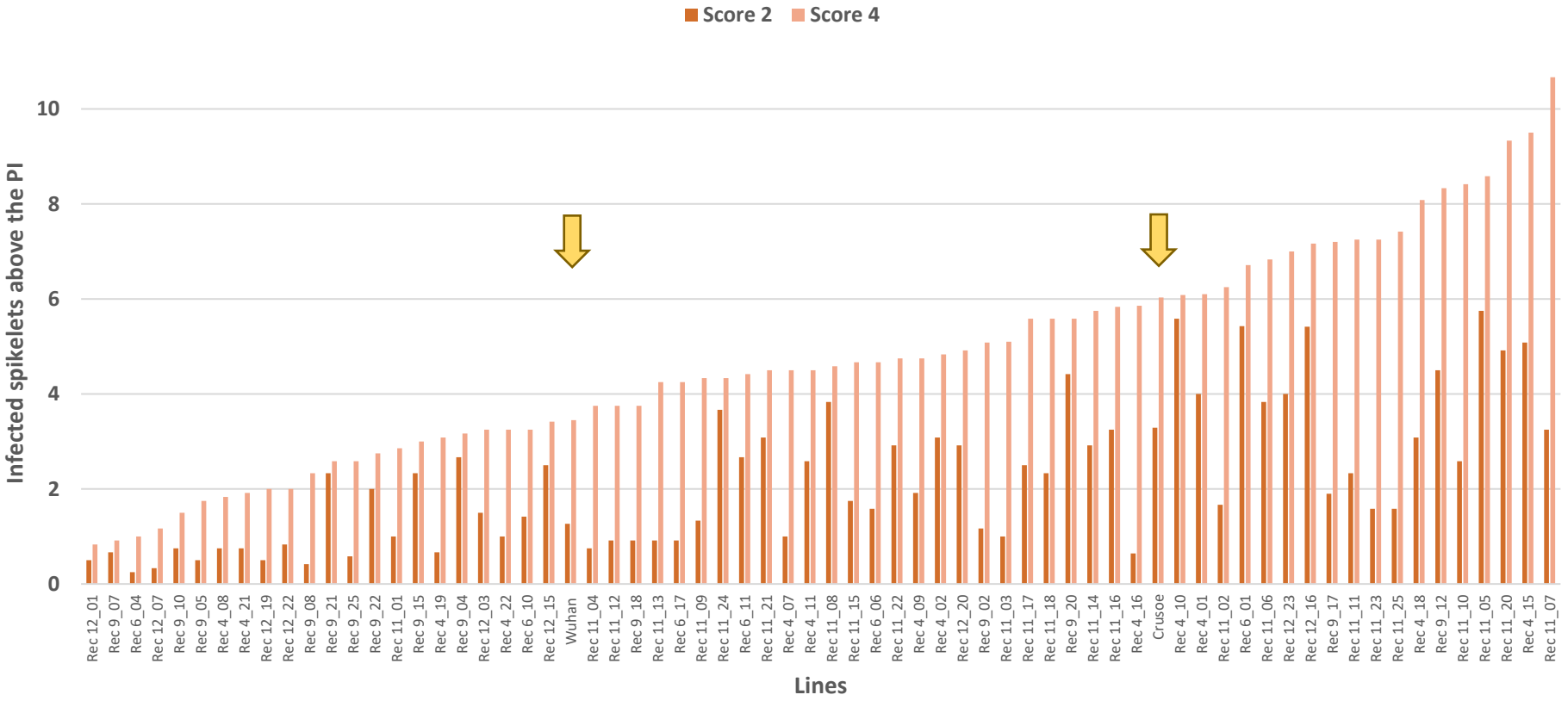

Figure 5.8. *FHB disease above the PI or number of bleached spikelets above the PI of RILs and parental-like lines (Crusoe and Wuhan; yellow arrows) tested for Type II on Summer 2021 (Test 1). Scoring symptoms represented at 14-15 dpi (Score 2) and at 19-20 dpi (Score 4). Predicted means were generated using a LMM analysis. Standard errors of the mean were not shown due to the high error.*

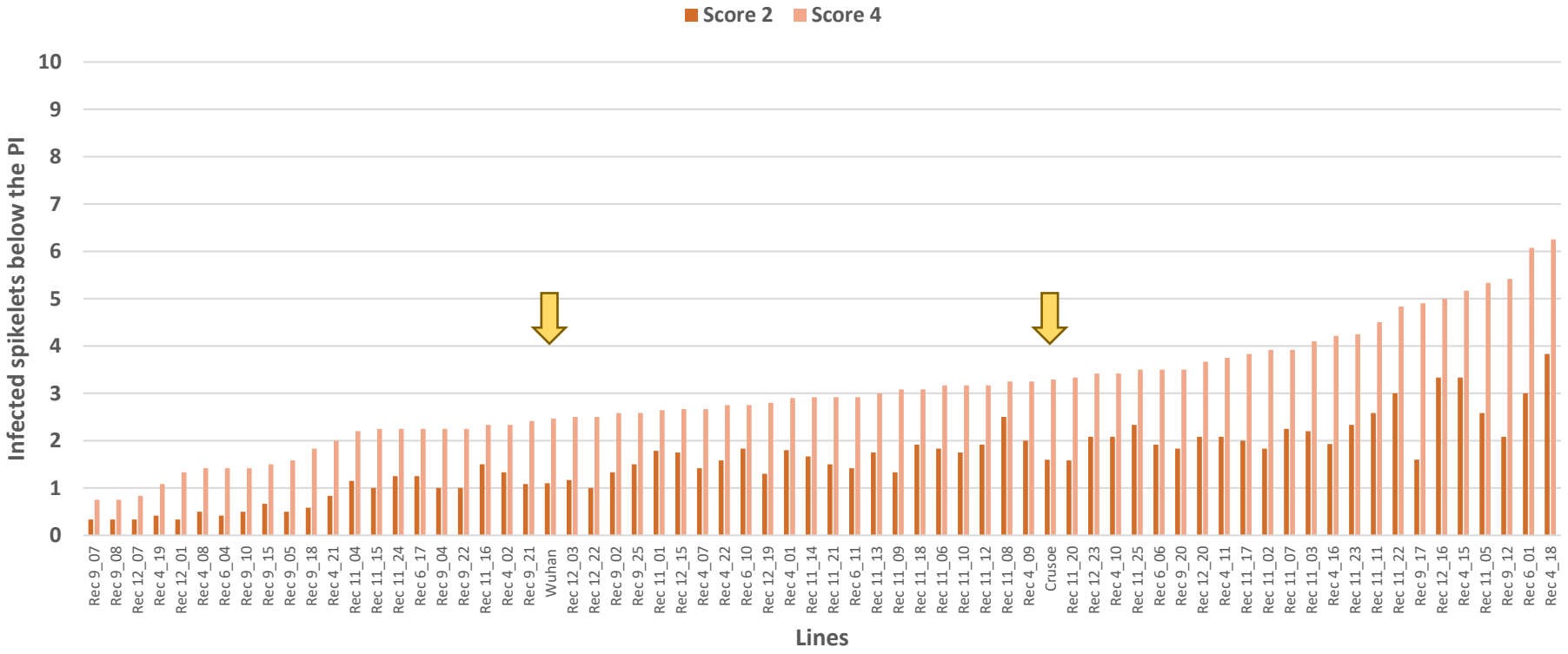

Figure 5.9. *FHB disease* below *the PI or number of bleached spikelets* below *the PI of RILs and parental-like lines (Crusoe and Wuhan; yellow arrows) tested for Type II on Summer 2021 (Test 1). Scoring symptoms represented at 14-15 dpi (Score 2) and at 19-20 dpi (Score 4). Predicted means were generated using a LMM analysis. Standard errors of the mean were not shown due to the high error.*

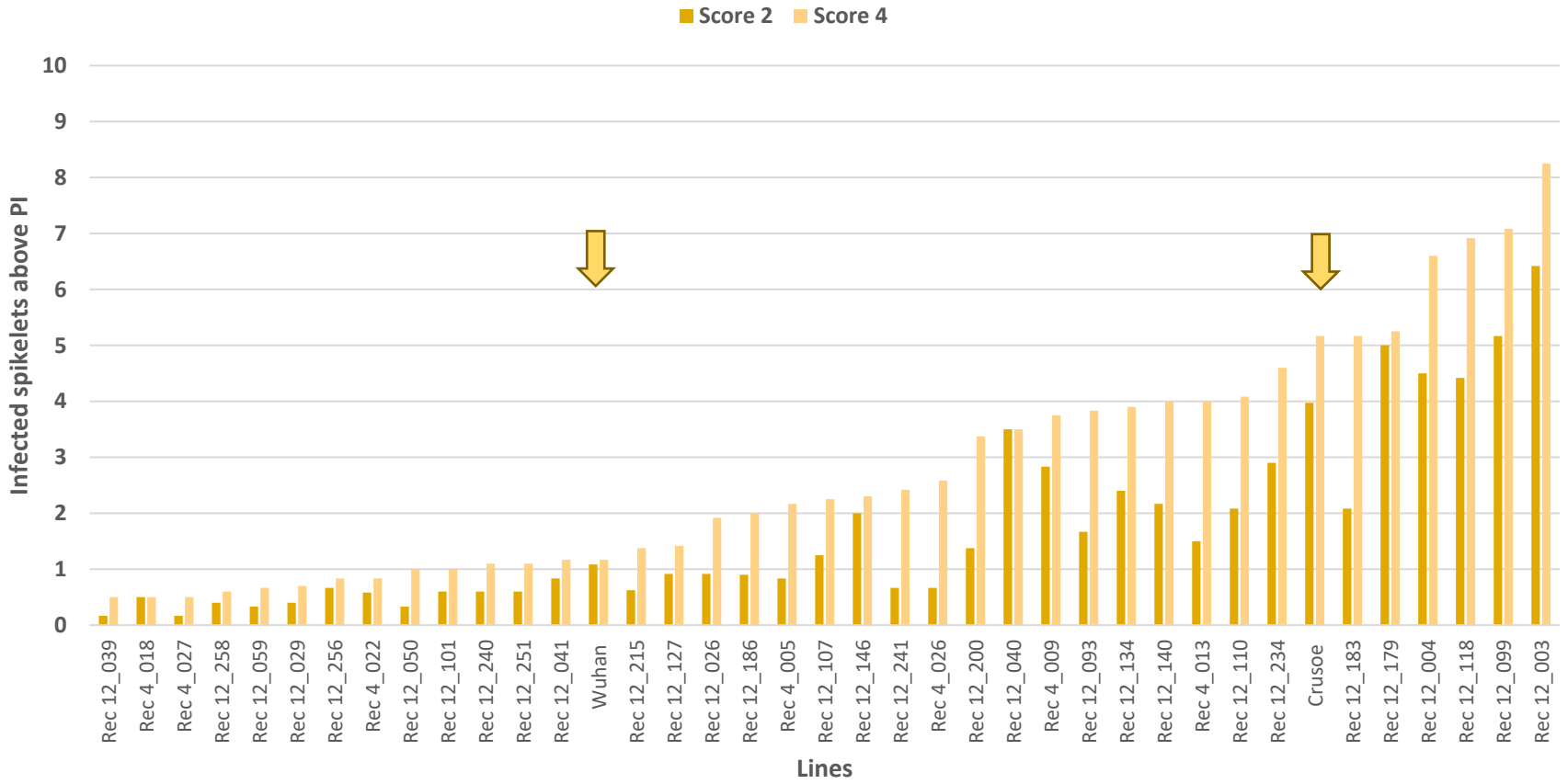

Figure 5.10. *FHB disease above the PI or number of bleached spikelets above the PI of RILs and parental-like lines (Crusoe and Wuhan; yellow arrows) tested for Type II on Summer 2021 (Test 2). Scoring symptoms represented at 18 dpi (Score 2) and at 22-23 dpi (Score 4). Predicted means were generated using a LMM analysis. Standard errors of the mean were not shown due to the high error.*

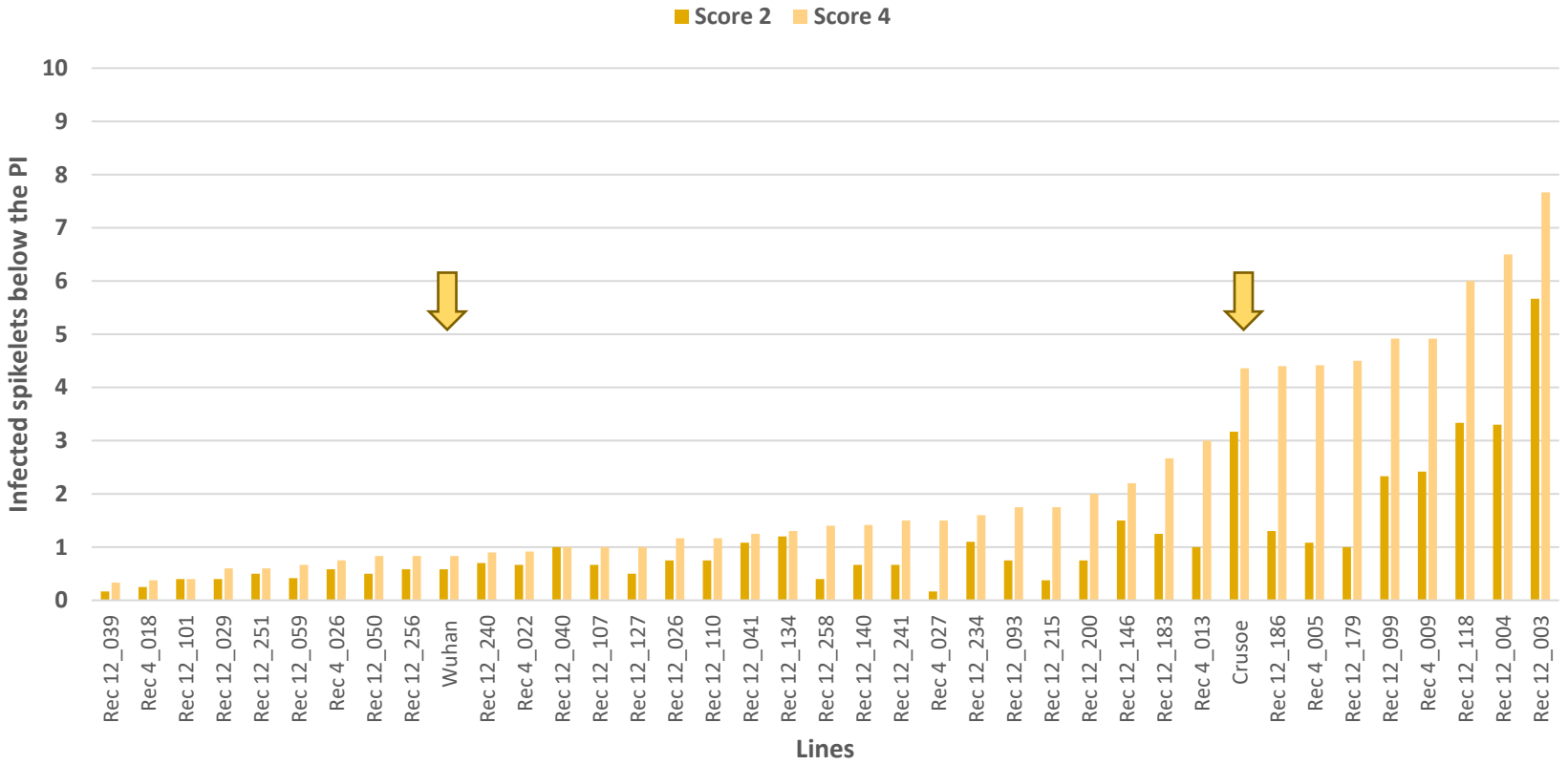

Figure 5.11. *FHB disease* below *the PI or number of bleached spikelets* below *the PI of RILs and parental-like lines (Crusoe and Wuhan; yellow arrows) tested for Type II on Summer 2021 (Test 2). Scoring symptoms represented at 18 dpi (Score 2) and at 22-23 dpi (Score 4). Predicted means were generated using a LMM analysis. Standard errors of the mean were not shown due to the high error.*

LMM analysis of Summer 2021 using the data of Test 1 revealed that eight markers were associated (*P-value* < 0.05) with FHB type II resistance over time, and they were very strongly associated with resistance above the PI (*P-value* < 0.001) at 21-22 dpi. These markers were S11, S12, S13, S14, S15, S16, S17 and S18 (source: Exome capture) located at 518.18, 520.58, 520.64, 522.52, 527.64, 531.23, 531.67 and 531.89 Mbp, respectively (Table 5.8.). This block of markers was also associated with the disease when using the scoring data below the PI (P-value < 0.01), and thus highlighting the genomic region most strongly associated with the FHB resistance conferred by the 2DL locus (Table 5.9.).

LMM analysis of Test 2 revealed that four markers were strongly associated (P-value < 0.001) with FHB type II resistance above the PI from Score 1 (at 5 dpi) to Score 4 (at 22-23 dpi). These markers were S11, S16, S17 and S18 (source: Exome capture) located at 518.18, 531.23, 531.67 and 531.89 Mbp, respectively (Table 5.10.). This block of markers was also strongly associated with the disease when using the scoring data below the PI (P-value < 0.001), and thus confirming the genomic region of the 2DL (Table 5.11.).

The genomic region on the 2DL locus most associated with FHB resistance in Summer 2021 Test 1 was of 55.6 Mbp, between markers *S10* (at 507.26 Mbp) and *S19* (at 562.86 Mbp), while in Test 2 was of 64.95 Mbp, between markers *S9* (at 497.91 Mbp) and *S19* (at 562.86 Mbp). This slight increase in the QTL interval identified in Test 2 was due to the number of markers used for the screening of the recombinant lines used for this test, since not all the markers were included by the iCase collaborators.

Recombinant lines tested in the Test 1 in Summer 2021 that contained the resistant allele 'Wu' in the 2DL locus were Rec 4 (except Rec 4_07, Rec 4_10 and Rec 4_16), Rec 6, Rec 9, Rec 12_01, Rec 12_03, Rec 12_07 and Rec 12_22 (Figure 5.6). However, some contradictory data was identified since Rec 4_11, Rec 4_15 and Rec 4_18 had the 'Wuhan'

allele but were very susceptible to FHB with 8.25, 14.67 and 14.13 infected spikelets, respectively at 19-20 dpi (Figure 5.6).

Recombinant line showing the greatest effect on resistance in Test 1 at 21-22 dpi were Rec 9_07, Rec 12_07, Rec 12_01, Rec 6_04, Rec 9_10, Rec 9_08, Rec 4_08, Rec 9_05 and Rec 4_21 (the total number of infected spikelets ranging from 1.67 to 3.92), all of them containing the 'Wu' allele across the region. In contrast, Rec 11_17, Rec 4_10, Rec 11_22, Rec 11_06, Rec 4_16, Rec 11_02, Rec 12_23, Rec 11_25, Rec 11_23, Rec 11_10, Rec 11_11, Rec 9_17, Rec 12_16, Rec 11_20, Rec 6_01, Rec 9_12, Rec 11_05, Rec 4_18, Rec 11_07 and Rec 4_15 (the total number of infected spikelets ranging from 9.42 to 14.67) showed higher levels of susceptibility at 21-22 dpi (Figure 5.6., Figure 5.8. and Figure 5.9.). These lines contained the susceptible allele 'Cru' except lines Rec 9_17, Rec 6_01, Rec 9_12, Rec 4_18 and Rec 4_15 (Figure 5.6.).

Recombinant lines tested in the Test 2 in Summer 2021 were still segregating at different markers across the 2DL QTL from 497.91 to 562.86 Mbp. Some lines contained the resistant allele 'Wu' through the entire 2DL QTL interval and these lines were Rec 4_009, Rec 4_018, Rec 4_026, Rec 4_027, Rec 12_026, Rec 12_029, Rec 12_041, Rec 12_093, Rec 12_101, Rec 12_127, Rec 12_183, Rec 12_200, Rec 12_256 and Rec 12_258 (Figure 5.7.). However, several contradictions between genotype and resistance were observed in some of those lines. For instance, Rec 4_009 contained the 'Wuhan' allele but was susceptible to FHB with 8.67 infected spikelets at 22-23 dpi; Rec 12-183 contained the 'Wu' allele and had 7.83 infected spikelets at 22-23 dpi; and even lines Rec 12_093 and Rec 12_200 with 5.58 and 5.38 infected spikelets, respectively, at 22-23 dpi (Figure 5.7.).

Recombinant lines showing the most resistant effect at 22-23 dpi were Rec 12_039, Rec 4_018, Rec 12_029, Rec 12_059, Rec 12_101, Rec 12_256, Rec 12_251, Rec 4_022, Rec 12_050, Rec 4_027, Rec 12_240 and Rec 12_258 (the total number of infected spikelets

ranging from 0.83 to 2.00) (Figure 5.7., Figure 5.10. and Figure 5.11.). These lines had the 'Wu' allele although some of these lines (Rec 12_039, Rec 12_050, Rec 12_059 and Rec 12_240) were still segregating on the 2DL locus, while other lines (Rec 4_022 and Rec 12_251) had missing alleles since genotyping at specific markers failed.

In contrast, lines containing the 'Crusoe' allele across the long arm of the 2D chromosome were Rec 12_003, Rec 12_004 and Rec 12_099 (Figure 5.7.). These lines were very susceptible at 22-23 dpi with 15.92, 13.10 and 12.00 infected spikelets, respectively. Additionally, lines Rec 12_179 and Rec 12_118 (the total number of infected spikelets ranging from 9.75 to 15.92) also exhibited higher levels of susceptibility at 22-23 dpi (Figure 5.7., Figure 5.10. and Figure 5.11.). These lines contained the susceptible allele 'Cru' except lines Rec 12_118, which was still segregating at the locus, and Rec 12_179, which had some missing data on the locus (Figure 5.7.).

To conclude, data from summer 2021 trials is not conclusive in helping to fine-map the 2DL QTL. Both trials in Summer 2021 (Test 1 and Test 2) revealed inconsistencies between genotype and phenotype for several recombinant lines. Nevertheless, this data confirmed the position of the QTL on the long arm of the 2D chromosome, although more work is needed to refine its location.

Table 5.8. *P-value data obtained from a LMM analysis of Test 1 (first trial in Summer 2021) performed for each individual marker located on the 2D chromosome. Source of markers used for the analysis is described. Associated RefSeqv1.1 gene models (where available) and physical position on RefSeqv1.0 assembly are shown. Symptoms above the point of infection were assessed in five sets at different dpi: at 12-13 dpi (Score 1), at 14-15 dpi (Score 2), at 16-18 dpi (Score 3), at 19-20 dpi (Score 4), at 21-22 dpi (Score 5) and at 23-25 dpi (Score 6). Data was transformed using a log10 transformation. P-value data of markers associated with FHB Type II resistance are highlighted in light green (P < 0.05) and markers strongly associated with the resistance in dark green (P < 0.01).*

Source	Exome capture	Exome capture	Exome capture	18K SNP array	Exome capture	Exome capture	Exome capture
RefSeqv1.1 Gene model	*intergenic*	*TraesCS2D02G369200*	*intergenic*	*TraesCS2D02G390100*	*TraesCS2D02G396200*	*TraesCS2D02G403400*	*intergenic*
RefSeqv1.0 (bp)	459,848,229	473,437,125	490,119,157	497,905,031	507,260,371	518,184,736	520.584.574
Marker	***S4***	***S5***	***S8***	***S9***	***S10***	***S11***	***S12***
Score 1	0.092	0.058	0.058	0.058	0.058	0.008	0.008
Score 2	0.293	0.130	0.130	0.130	0.130	0.013	0.013
Score 3	0.590	0.204	0.204	0.204	0.204	0.010	0.010
Score 4	0.286	0.059	0.059	0.059	0.059	0.002	0.002
Score 5	0.137	0.013	0.013	0.013	0.013	<0.001	<0.001
Score 6	0.223	0.039	0.039	0.039	0.039	0.001	0.001

Source	Exome capture	Exome capture	Exome capture	18K SNP array	18K SNP array
RefSeqv1.1 Gene model	*TraesCS2D02G406900*	*TraesCS2D02G413100*	*TraesCS2D02G416800*	*intergenic*	*TraesCS2D02G507600*
RefSeqv1.0 (bp)	522,525,653	527,646,686	531,236,257	562,855,808	601,204,785
Marker	***S14***	***S15***	***S16***	***S19***	***S21***
Score 1	0.008	0.008	0.008	0.132	0.289
Score 2	0.013	0.013	0.013	0.072	0.199
Score 3	0.010	0.010	0.010	0.035	0.121
Score 4	0.002	0.002	0.002	0.010	0.262
Score 5	<0.001	<0.001	<0.001	0.003	0.166
Score 6	0.001	0.001	0.001	0.018	0.262

Table 5.9. *P-value data obtained from a LMM analysis of Test 1 (first trial in Summer 2021) performed for each individual marker located on the 2D chromosome. Source of markers used for the analysis is described. Associated RefSeqv1.1 gene models (where available) and physical position on RefSeqv1.0 assembly are shown. Symptoms below the point of infection were assessed in five sets at different dpi: at 12-13 dpi (Score 1), at 14-15 dpi (Score 2), at 16-18 dpi (Score 3), at 19-20 dpi (Score 4), at 21-22 dpi (Score 5) and at 23-25 dpi (Score 6). Data was transformed using a log10 transformation. P-value data of markers associated with FHB Type II resistance are highlighted in light green (P < 0.05) and markers strongly associated with the resistance in dark green (P < 0.01).*

Source	Exome capture	Exome capture	Exome capture	18K SNP array	Exome capture	Exome capture	Exome capture
RefSeqv1.1 Gene model	*intergenic*	*TraesCS2D02G369200*	*intergenic*	*TraesCS2D02G390100*	*TraesCS2D02G396200*	*TraesCS2D02G403400*	*intergenic*
RefSeqv1.0 (bp)	459,848,229	473,437,125	490,119,157	497,905,031	507,260,371	518,184,736	520.584.574
Marker	***S4***	***S5***	***S8***	***S9***	***S10***	***S11***	***S12***
Score 1	0.055	0.027	0.027	0.027	0.027	0.001	0.001
Score 2	0.078	0.029	0.029	0.029	0.029	0.001	0.001
Score 3	0.176	0.074	0.074	0.074	0.074	0.004	0.004
Score 4	0.065	0.027	0.027	0.027	0.027	0.001	0.001
Score 5	0.380	0.144	0.144	0.144	0.144	0.007	0.007
Score 6	0.548	0.339	0.339	0.339	0.339	0.046	0.046

Source	Exome capture	Exome capture	Exome capture	18K SNP array	18K SNP array
RefSeqv1.1 Gene model	*TraesCS2D02G406900*	*TraesCS2D02G413100*	*TraesCS2D02G416800*	*intergenic*	*TraesCS2D02G507600*
RefSeqv1.0 (bp)	522,525,653	527,646,686	531,236,257	562,855,808	601,204,785
Marker	***S14***	***S15***	***S16***	***S19***	***S21***
Score 1	0.001	0.001	0.001	0.011	0.227
Score 2	0.001	0.001	0.001	0.012	0.236
Score 3	0.004	0.004	0.004	0.036	0.524
Score 4	0.001	0.001	0.001	0.014	0.349
Score 5	0.007	0.007	0.007	0.015	0.241
Score 6	0.046	0.046	0.046	0.136	0.320

Table 5.10. *P-value data obtained from a LMM analysis of Test 2 (second trial in Summer 2021) performed for each individual marker located on the 2D chromosome. Source of markers used for the analysis is described. Associated RefSeqv1.1 gene models (where available) and physical position on RefSeqv1.0 assembly are shown. Symptoms above the point of infection were assessed in five sets at different dpi: at 15 dpi (Score 1), at 18 dpi (Score 2), at 20-21 dpi (Score 3), at 22-23 dpi (Score 4), at 25 dpi (Score 5) and at 27-28 dpi (Score 6). Data was transformed using a log10 transformation. P-value data of markers associated with FHB Type II resistance are highlighted in light green (P < 0.05) and markers strongly associated with the resistance in dark green (P < 0.01).*

Source	Exome capture	Exome capture	18K SNP array	Exome capture	Exome capture	18K SNP array	18K SNP array
RefSeqv1.1 Gene model	*intergenic*	*intergenic*	*TraesCS2D02G390100*	*TraesCS2D02G403400*	*TraesCS2D02G416800*	*intergenic*	*intergenic*
RefSeqv1.0 (bp)	488,871,873	490,119,157	497,905,031	518,184,736	531,236,257	562,855,808	563,660,447
Marker	***S7***	***S8***	***S9***	***S11***	***S16***	***S19***	***S20***
Score 1	0.397	0.397	0.192	<0.001	<0.001	0.059	0.262
Score 2	0.494	0.494	0.289	<0.001	<0.001	0.072	0.275
Score 3	0.534	0.534	0.395	<0.001	<0.001	0.093	0.252
Score 4	0.500	0.500	0.446	<0.001	<0.001	0.114	0.264
Score 5	0.521	0.521	0.702	0.004	0.009	0.096	0.211
Score 6	0.606	0.606	0.744	0.024	0.039	0.104	0.171

Table 5.11. *P-value data obtained from a LMM analysis of Test 2 (second trial in Summer 2021) performed for each individual marker located on the 2D chromosome. Source of markers used for the analysis is described. Associated RefSeqv1.1 gene models (where available) and physical position on RefSeqv1.0 assembly are shown. Symptoms below the point of infection were assessed in five sets at different dpi: at 15 dpi (Score 1), at 18 dpi (Score 2), at 20-21 dpi (Score 3), at 22-23 dpi (Score 4), at 25 dpi (Score 5) and at 27-28 dpi (Score 6). Data was transformed using a log10 transformation. P-value data of markers associated with FHB Type II resistance are highlighted in light green (P < 0.05) and markers strongly associated with the resistance in dark green (P < 0.01).*

Source	Exome capture	Exome capture	18K SNP array	Exome capture	Exome capture	18K SNP array	18K SNP array
RefSeqv1.1 Gene model	*intergenic*	*intergenic*	*TraesCS2D02G390100*	*TraesCS2D02G403400*	*TraesCS2D02G416800*	*intergenic*	*intergenic*
RefSeqv1.0 (bp)	488,871,873	490,119,157	497,905,031	518,184,736	531,236,257	562,855,808	563,660,447
Marker	***S7***	***S8***	***S9***	***S11***	***S16***	***S19***	***S20***
Score 1	0.384	0.384	0.338	<0.001	<0.001	0.079	0.214
Score 2	0.597	0.597	0.505	<0.001	<0.001	0.035	0.108
Score 3	0.573	0.573	0.581	<0.001	<0.001	0.017	0.040
Score 4	0.524	0.524	0.898	<0.001	<0.001	0.008	0.016
Score 5	0.419	0.419	0.951	0.002	<0.001	0.002	0.002
Score 6	0.245	0.245	0.780	0.012	0.001	0.001	0.001

5.4.2. Location of the 2DL locus over Summers 2019-2021

The fine-mapping of the 2DL locus over the period of three Summers (2019-2021) on the long arm of the 2DL chromosome is graphically represented in Figure 5.12. Graphical genotypes of the 2DL QTL location for each of the three summer trials are represented in light yellow bars.

The genomic region on the 2DL locus most associated with FHB type II resistance in Summer 2019 was of 117.62 Mbp, between markers *BA00144665* (at 446.04 Mbp) and *S20* (at 563.66 Mbp); in Summer 2020 the size of the region was still of 117.62 Mbp, between markers *BA00144665* (at 446.04 Mbp) and *S20* (at 563.66 Mbp); in Summer 2021 the interval defined in Test 1 was 55.6 Mbp, between markers *S10* (at 507.26 Mbp) and *S19* (at 562.86 Mbp), while in Test 2 the interval was 64.95 Mbp, between markers *S9* (at 497.91 Mbp) and *S19* (at 562.86 Mbp).

The 2DL locus was stable over a period of three years under UK poly tunnel environmental conditions. The genomic region on the 2DL consistently associated with FHB type II resistance was located between markers *S10* (at 507.26 Mbp) and *S19* (at 562.86 Mbp). To conclude, this genomic region of 55.6 Mbp confers a robust and stable increase in FHB type II resistance over three summer trials. However, further fine mapping is still needed to reduce the interval further before identifying a list of potential candidate genes.

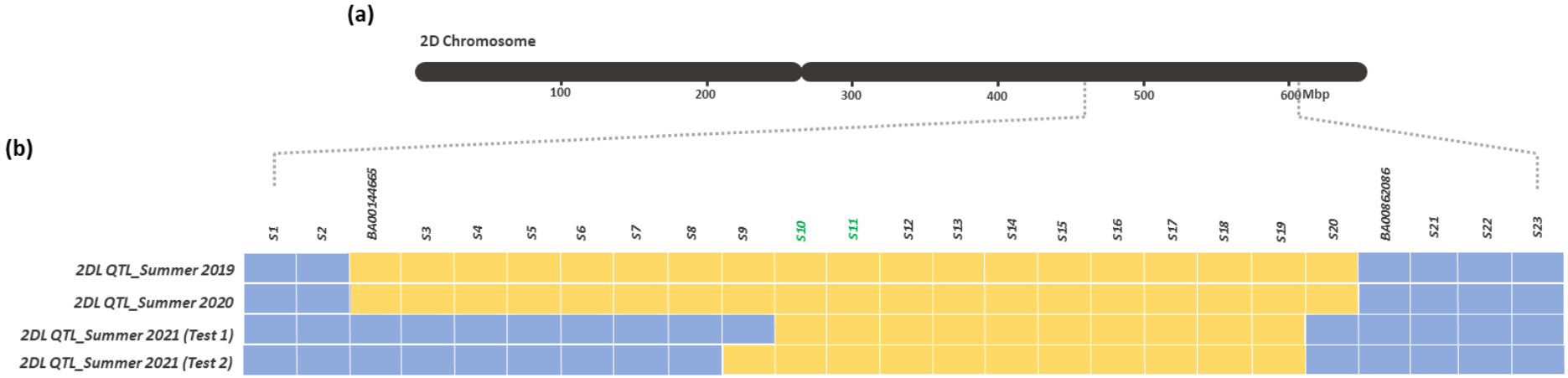

Figure 5.12. *a) Physical map of the wheat chromosome 2DL of 652 Mbp. (b) Graphical genotypes of the 2DL QTL over three summer trials (2019-2021). Light yellow bars represent the size and location of the QTL for that specific year. KASP markers (S1-S23) location is represented. The genomic region on the 2DL consistently associated with FHB type II resistance is located between markers S10 (at 507.26 Mbp) and S19 (at 562.86 Mbp), a genomic region of 55.6 Mbp. The hypothesised fine-mapping of the 2DL QTL is shown in green between markers S10 and S11.*

5.4.3. Refining the 2DL locus

A selection of recombinants (Rec 12) tested in Summer 2021 were screened by the iCase collaborators using the new KASPs and will be used for a Summer 2022 trial. These lines contained the same block of 'Crusoe' and 'Wuhan' alleles but appeared to differ in their FHB type II resistance or susceptibility (see Figure 5.13.). The break point between 'Crusoe' (blue) and 'Wuhan' (yellow) in those lines is located between markers S10 (at 507.26 Mbp) and S11 (at 518.18 Mbp). Figure 5.13. also represents that 'Wuhan-like' line was showing FHB resistance at 20-21 dpi with a total of 1.83 infected spikelets, while 'Crusoe-like' was very susceptible with 8.36 infected spikelets.

On the basis of this preliminary evidence, I might expect that, genes responsible for FHB resistance in the 2DL QTL (*QFhb.Wuhan-2DL*) may be located in the 10.92 Mbp genomic region between markers S10 and S11 (Figure 5.12.; markers and location highlighted in green). This evidence is not conclusive since during summer 2021 trial, single plants were tested for the analysis and inconsistences between genotype and phenotype were identified. Therefore, I still do not have strong evidence to support the refined QTL interval between these S10 and S11 markers. To accomplish it, more markers need to be developed on the interval and more recombinants need to be re-tested for FHB resistance with appropriate replication.

Additionally, the fine-mapping of the locus has not been properly done since the availability of recombinant lines did not allow it. However, those specific recombinants stated above (Figure 5.13.) will be re-tested for FHB type II resistance in Summer 2022 to compile better conclusions.

To conclude, the identification of additional SNPs within this genomic region is of critical importance for efforts to reduce the interval and identify break points in the

recombinant lines selected for the FHB trial in Summer 2022. Further fine-mapping of the *QFhb.Wuhan-2DL* locus needs to be done.

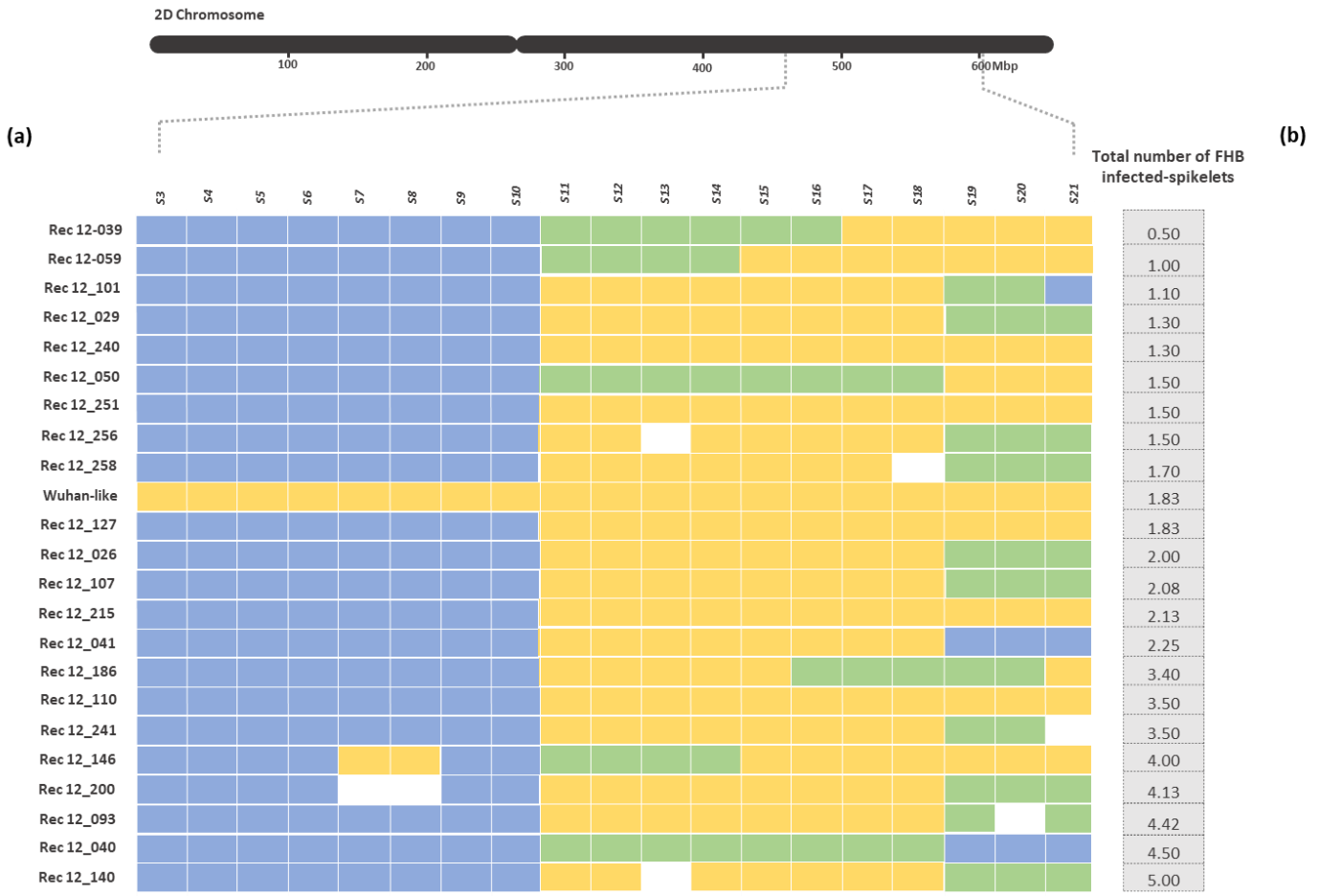

Figure 5.13. *a) Graphical genotype of RILs selected to be tested for FHB type II resistance in Summer 2022. b) Total number of infected spikelets at 20-21 dpi (above + below) for each RIL. Scoring data from Summer 2021 poly tunnel trial.*

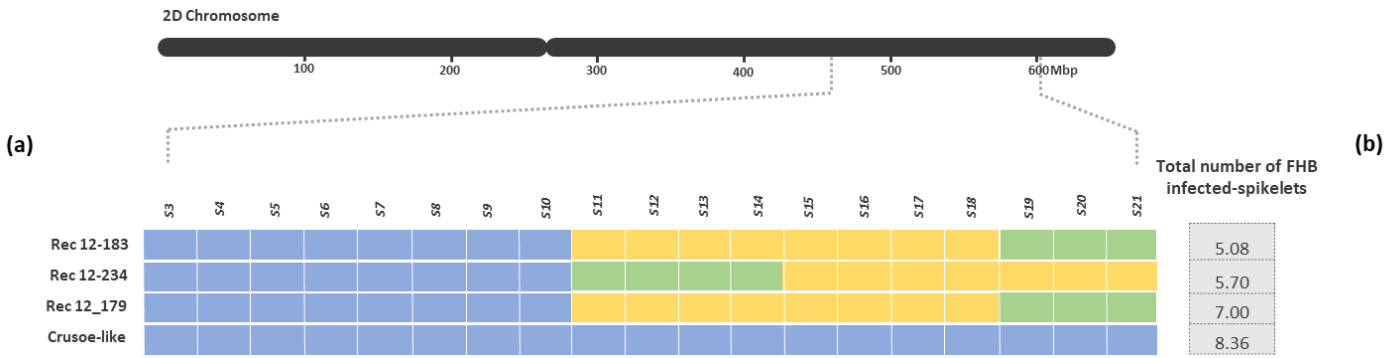

Figure 5.13. Continued. *a) Graphical genotype of RILs selected to be tested for FHB type II resistance in Summer 2022. b) Total number of infected spikelets at 20-21 dpi (above + below) for each RIL. Scoring data from Summer 2021 poly tunnel trial.*

5.5. Discussion

5.5.1. *QFhb.Wuhan-2DL* is located on the long arm of the 2D chromosome

In this study, a set of NILs derived from the cross between the resistant line Wuhan and the susceptible line Crusoe were provided by the iCase collaborators, Limagrain S.A. Since the source of FHB type II resistance provided by Wuhan is known to be located on the long arm of the 2D chromosome, this population was genotyped using a diverse set of KASP markers developed on that genomic region. Most of the screening was performed by the collaborators, but I could identify two SNPs between parental lines for which I developed KASPs to screen the population.

Different selections of recombinant lines were phenotyped for FHB type II resistance over three summer trials (2019-2021). A single marker analysis for each KASP along the 2DL chromosome was performed to map the resistance. Indeed, based on the Chinese Spring reference genome (IWGSC RefSeq v1.0) a physical map of the wheat 2D chromosome was developed using KASP markers (Figure 5.12.) to visualize the fine mapping of the 2DL QTL over time.

This study confirms that the source of resistance provided by Wuhan is type II. Data collected from three summer poly tunnel trials in Norwich (UK) confirmed the location of the 2D locus, named *QFhb.Wuhan-2DL*, on the long arm of the 2D chromosome between markers *S10* (at 507.26 Mbp) and *S19* (at 562.86 Mbp). Thus, the genomic region stable for the three summer trials was of 55.6 Mbp and contains 575 annotated genes, which were extracted from Ensembl Plants (EMBL-EBI 2022).

5.5.2. FHB QTLs on the 2D chromosome

Somers, Fedak, and Savard (2003) identified a moderately potent resistance QTL for FHB Type II resistance that was mapped on the long arm of chromosome 2D. These findings were also confirmed by Long et al. (2015), who showed that the presence of the 2DL QTL reduced the spread of infection, the amount of fungal biomass and DON accumulation both in greenhouse and field conditions.

A group of genes including *TaWRKY70* (*TraesCS2D02G489700*), *TaACT* (*TraesCS2D02G490400*), *TaDGK* (*TraesCS2D02G534600*) and *TaGLI1* (*TraesCS2D02G517200*), have recently been proposed as candidate genes for the 2DL QTL (Kage et al. 2017; Kage, Yogendra, and Kushalappa 2017). Kage, Yogendra, and Kushalappa (2017) identified and characterized *TaWRKY70* transcription factor (TF) from bread wheat to be located within the 2DL region. *TaWRKY70* allows FHB resistance by accumulation of phosphatidic acids (PAs) and hydroxycinnamic acid amides (HCAAs) through regulation of downstream biosynthetic resistance genes *TaACT*, *TaDGK* and *TaGLI1*.

Allelic variation in a *NPR1*-like gene (*TraesCS2D02G572000*), which is also located on the long arm of chromosome 2D, has been shown to be also associated with FHB resistance in European wheat (Diethelm et al. 2014). *NPR1* (non-expresser of pathogenesis related protein 1) is one of the key regulators of different hormone-dependent pathways. The activation of *NPR1* promotes salicylic acid (SA)-mediated signal transduction and influences jasmonate (JA) biosynthesis and signal transduction, leading to a systemic acquired resistance (Beckers and Spoel 2006).

Although those five genes - *TaWRKY70* (*TraesCS2D02G489700*), *TaACT* (*TraesCS2D02G490400*), *TaGLI1* (*TraesCS2D02G517200*), *TaDGK* (*TraesCS2D02G534600*), and NPR1-like gene (*TraesCS2D02G572000*) - are located on the long arm of the 2D chromosome, their physical locations in IWGSC RefSeq v1.0 (588.67, 589.28, 608.19, 618.14

and 638.14 Mbp, respectively) were outside of the genetic interval for the *QFhb.Wuhan-2DL* of the present study (Figure 5.14.), which is located between 507.26 to 562.86 Mbp.

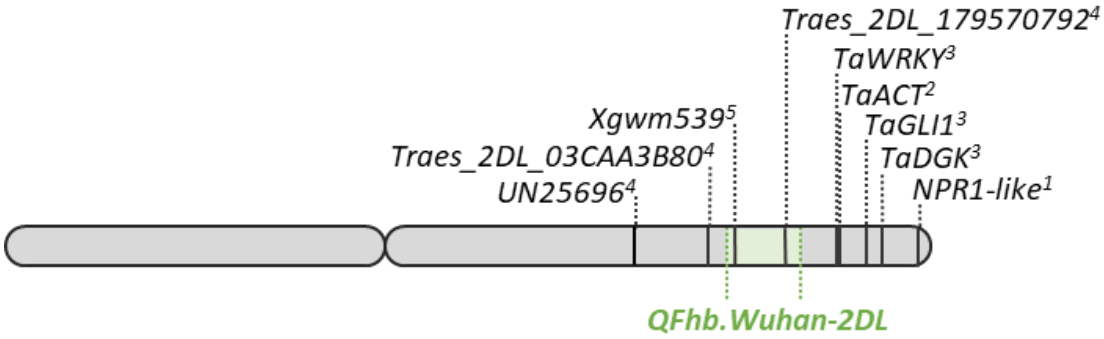

Figure 5.14. *Putative physical distribution of the genes or markers associated with Fusarium head blight resistance on chromosome 2D of wheat (Triticum aestivum): [1]Diethelm et al. (2014), [2]Kage et al. (2017), [3]Kage, Yogendra, and Kushalappa (2017), [4]Hu et al. (2019), [5]Zhu et al. (2020). The QFhb.Wuhan-2DL of the present study is located between 507.26 and 562.86 Mbp (green area).*

An RNA-Seq study than by Biselli et al. (2018) between a pair of NILs with or without the resistant allele for the 2DL QTL identified more than 1400 DEGs located on the 2DL chromosome arm. The list of DEGs was then reduced by Hu et al (2019), and selected genes were further characterized to identify candidate genes on the 2DL. *Traes_2DL_03CAA3B80*, *Traes_2DL_179570792* and *UN25696* showed a consistent difference in expression between two genotypes carrying the resistant allele for the FHB-resistance QTL on 2DL (Wuhan 1 and HC374) and two genotypes carrying the susceptible allele (Nyubai and Shaw); in three pairs of NILs; and in a DH population. The expression QTL (eQTL) for *Traes_2DL_179570792* (*TraesCS2D02G440500*) and *UN25696* were mapped in the vicinity of the 2DL QTL for FHB, but the location of *Traes_2DL_179570792* was within the boundaries of the QTL. This led to Hu et al (2019) to conclude that *Traes_2DL_179570792* was the first expression marker associated with the 2DL QTL for FHB resistance, contributing directly to its activity. *Traes_2DL_03CAA3B80* (*TraesCS2D02G495500LC)* has been annotated as a copper-transporting ATPase PPA2 located in the chloroplast and it showed a significant increase in

expression, both in rachis and spikelets, in NILs carrying the 2DL QTL after *Fusarium* infection (Hu et al. 2019a).

Two of those genes previously mentioned, *UN25696* at 446.26 Mbp and *Traes_2DL_03CAA3B80* at 493.19 Mbp, are located outside of the genomic interval of the *QFhb.Wuhan-2DL* locus defined in the present study. Nevertheless, gene *Traes_2DL_179570792* at 550.63 Mbp is residing on the interval supported in the present study (Figure 5.14.).

In a recent study, a panel of Chinese wheat cultivars and elite breeding lines including more than 50 widely grown cultivars were analysed to study the FHB response and to determine the genetic architecture of the resistance (Zhu et al. 2020). In this study several loci for FHB resistance were identified with the 2DL QTL provided by Wuhan 1 detected using marker *Xgwm539* at 513.1 Mbp on the long arm of chromosome 2D of wheat. Interestingly, this means that this QTL is located within the *QFhb.Wuhan-2DL* locus (Figure 5.14.). The original QTL identified on 2DL in Wuhan also centred about marker *Xgwm539* reinforcing the view that the QTL defined in the present work is the same as that in the first report (Somers, Fedak, and Savard 2003).

5.5.3. Conclusions and future work

In summary, data from the present study has confirmed that the *QFhb.Wuhan-2DL* for FHB type II resistance is effective under a poly tunnel environment in the UK. It was confirmed by my iCase partners that the 2DL locus from Wuhan 1 is also providing FHB type II resistance in different locations in France (data not shown), and it was maintained over subsequent summer trials on a genomic region of 55.6 Mbp. The *QFhb.Wuhan-2DL* identified from the cross Wuhan x Crusoe may be a potential source of FHB resistance but it still contains 575 annotated candidate genes.

Nevertheless, the locus needs to be further fine mapped to select potential candidate genes associated with the resistance. This will be performed in Summer 2022 with specific FHB resistant and susceptible RILs selected from Summer 2021 poly tunnel trial. Additional SNPs within the 2DL locus will need to be identify using different sources in order to reduce the QTL interval on the selected RILs.

Furthermore, an RNA-Seq analysis using selected resistant and susceptible RILs identified over summer trials in the present study could be performed to identify genes differentially expressed in response to FHB over a period of time (time course experiment). This experiment in combination with the fine-mapping of the 2DL locus will provide a better understanding of the candidate genes involved in the *Fusarium* resistance provided by the Chinese cultivar Wuhan.

Chapter 6

General Discussion

Fusarium head blight (FHB) is an economically important cereal disease worldwide caused by *Fusarium* spp. FHB is among the most extensively studied fungal diseases of wheat and other small grain cereals due to its impact on yield and grain quality, but more importantly due to its potential to produce mycotoxins, which are harmful to humans and animals (Buerstmayr, Steiner, and Buerstmayr 2020). Trichothecene mycotoxins such as deoxynivalenol (DON), act as virulence factors and enable the pathogen to spread within wheat heads.

Chemical and agricultural methods aimed to reduce the impact of FHB are only moderately effective at limiting crop losses. The most sustainable method to reduce the impact of FHB in commercial wheat cultivars is to improve genetic resistance (Marburger et al. 2015). Introducing FHB resistance is a major challenge since it is a quantitative trait influenced by many genes dispersed through the genome. Moreover, FHB resistance QTLs are often environmentally sensitive and, therefore, they may only be effective under certain climatic conditions.

The aim of this PhD research project was to refine the physical location of two FHB QTLs for type II resistance (resistance to pathogen spread from the infected to the non-infected spikelets) located on chromosomes 5A and 2D in bread wheat (*Triticum aestivum*). The ultimate aim was to identify the underlying gene, or genes, associated with the FHB type II resistance.

6.1. The 5A and the 2D QTLs of bread wheat

A very extensively used method for discovering QTLs associated with FHB resistance traits and to quantify their effects has been the use of mapping populations. This involves generating and analysing segregating mapping populations, derived from crosses of genotypes with contrasting resistances. For this type of QTL studies, the primary type of populations used are recombinant inbred lines (RILs), backcross-derived RILs (near isogenic lines or NILs), and double haploids (DH) (Buerstmayr, Steiner, and Buerstmayr 2020).

A detailed compilation of FHB resistance QTL information was performed by Buerstmayr et al (2009) and was updated later by Buerstmayr et al (2020). Around 500 QTL studies have been reported since the first FHB resistance QTL identified in wheat at the end of the 20th century (Waldron et al. 1999). Nevertheless, only around 104 (20%) were described as major QTL by the authors. Buerstmayr et al (2020) suggested that these numbers may be an overestimation of the reality, since it is not known how many of these QTL are identical referring to the same genes and how many of the minor QTL are statistical artefacts.

For the present PhD project, my focus has been the 5A and the 2D QTLs in bread wheat. Both loci have been very extensively and well-studied in hexaploid wheat as was described in Chapters 2 and 5, respectively. In both instances, the respective populations were developed and seed was available at the start of the project.

The 5A QTL was previously identified during work done in the Nicholson group and reported by Gosman et al (2001). The 5A QTL for FHB resistance was mapped by using a DH population from the cross WEK0609 x Hobbit *sib* (resistant and susceptible lines, respectively). A single chromosome substitution line, WEKH85A, was created by the introgression of the 5A chromosome from the resistant cultivar WEK0609 in a susceptible Hobbit *sib* background. To fine map the QTL region during this project, a population was then

created by using the susceptible parental line Hobbit *sib* and the resistant parental line WEKH85A.

Additionally, the 2D QTL has been studied repeatedly in the past decade since it provides a potent source of FHB type II resistance. This QTL was identified in a population from a Wuhan-1 x Nyubai (resistant and susceptible lines, respectively) cross by Somers, Fedak, and Savard (2003). To fine map the QTL region for the present study, the iCase collaborators in Limagrain S.A., generated a population from the Chinese cultivar Wuhan-1, which was backcrossed with the UK elite cultivar Crusoe.

6.2. Fine-mapping the 5A (*QFhb.WEK-5A*) and the 2D (*QFhb.Wuhan-2DL*) QTLs in bread wheat

Most of the studies related with FHB resistant QTLs only provide an estimation of the QTL position on the chromosome by using genetic maps, with QTL intervals encompassing up to 20 cM or more. By using this methodology, identified linked markers may not be close enough to the gene of interest for use in marker assisted selection (MAS) breeding. Recombination events between QTL effect and marker may compromise efficient marker-assisted breeding. Thus, tightly linked, or diagnostic markers are preferred in breeding, and dense marker saturation is required for map-based gene cloning (Buerstmayr, Steiner, and Buerstmayr 2020).

Fine-mapping and cloning of QTLs in wheat has been highly improved due to the development of genotyping technology, which deliver data for thousands of markers. Single marker polymorphism (SNP) detection technologies represent a significant advance to evaluate thousands of loci simultaneously. For instance, the Axiom® wheat HD Genotyping Array, also known as Axiom® 820K SNP array, is a high-density array containing 819,571

exome-captured SNP sequences derived from hexaploid wheat, diploid and tetraploid progenitors and wheat relatives (Winfield et al. 2016). Additionally, the Breeders' 35K Axiom® array contains 35,143 SNPs and has been used to screen a large global collection of elite and landrace varieties including hexaploid and tetraploid accessions of wheat. The SNP information in bread wheat (*T. aestivum*) and its relatives can be found in CerealsDB (https://www.cerealsdb.uk.net/).

Other technologies to identify SNPs are the use of RNA sequencing (RNA-Seq) (Ramirez-Gonzalez et al. 2015) and Exome capture (Krasileva et al. 2017). Exome capture technologies aim to cover most of the coding regions. Indeed, the iCase collaborators used this technology to detect variants in the populations used for the present project and developed KASP markers for these.

Moreover, another step-change in wheat research has been the completion and annotation of the wheat genome (IWGSC 2018), and the large amount of transcriptomic data, including the one related to FHB response, available in the user-friendly platform expVIP (Borrill, Ramirez-Gonzalez, and Uauy 2016; Ramírez-González et al. 2018). These recent advances in wheat research have facilitated the finding of SNPs and developing of polymorphic markers and has made a huge impact in the development and achievements of this PhD project. Indeed, fine-mapping of both 5A and 2D loci was carried out by using a single marker analysis based on the physical position of SNPs in the Chinese Spring reference genome (IWGSC RefSeq v1.1).

On the one hand, in Chapter 2, I demonstrated that the 5A QTL (*QFhb.WEK-5A*) was stable across three summer trials (2018-2020) in the UK and that *QFhb.WEK-5A* locus was refined to 6.24 Mbp on the long arm of chromosome 5A. When comparing with literature related with FHB resistance on the 5A, my findings suggested that the *QFhb.WEK-5A* locus of WEK0609 is not on the same chromosome arm as those reported for Sumai 3 or Fundulea

F201R. As the origin of the source of type II resistance provided by cv. WEK0609 is still not clear, it is possible that *QFhb.WEK-5A* may be a novel source of FHB resistance on chromosome 5A.

Moreover, I showed in Chapters 3 and 4 that not only does the *QFhb.WEK-5A* locus of 6.24 Mbp confer FHB type II resistance but it confers DON tolerance. Therefore, I also demonstrated that the *QFhb.WEK-5A* locus may be associated with two traits: DON tolerance and FHB resistance.

In addition, In Chapter 5, I demonstrated that the 2D (*QFhb.Wuhan-2DL*) was stable in a UK environment across three summer trials (2019-2021) in a genomic region of 55.6 Mbp on the long arm of the 2D chromosome. Although further fine-mapping is still in process.

6.3. Using *QFhb.WEK-5A and QFhb.Wuhan-2DL* loci for FHB improvement

From all identified QTL for FHB resistance in the literature, only a few have been fine-mapped so far: *Fhb1* (Cuthbert, Somers, Thomas, Cloutier, and Brule-Babel 2006; Jia et al. 2018; Li, Zhou, et al. 2019; Liu et al. 2006; Rawat et al. 2016; Schweiger et al. 2016; Su et al. 2019), *Fhb2* (Cuthbert, Somers, and Brule-Babel 2007; Jia et al. 2018), *Fhb4*, *Fhb5* (Jia et al. 2018), *Qfhs.ifa-5A* (Steiner et al. 2019), *Qfhs.ndsu-3AS* (Zhu et al. 2016), *Qfhb.nau-2B* (Li, Jia, et al. 2019) and *Qfhb.mgb-2A* (Gadaleta et al. 2019). *Fhb1* has been the most frequently studied resistance QTL and evaluated either individually or in combination with other QTLs (*Fhb5*/*Qfhs.ifa-5A*, *Fhb2* and *QFhs.nau-2DL*) (Buerstmayr, Steiner, and Buerstmayr 2020).

Many resistance sources have been identified but relatively few have been deployed in breeding programmes for the development of improved cultivars, with high levels of resistance to FHB (Buerstmayr, Steiner, and Buerstmayr 2020; Steiner et al. 2017; Zhu et al.

2019). The major QTLs for FHB resistance are *Fhb1* and *Qfhs.ifa-5A* provided by the Chinese spring wheat cultivar Sumai 3 and these have been used worldwide. These loci have been verified in different genetic backgrounds and environments and have shown to be suitable for application in breeding programmes (Buerstmayr, Steiner, and Buerstmayr 2020).

The combination of *Fhb1* and *Fhb5/Qfhs.ifa-5A* is effective in diverse genetic backgrounds (Salameh et al. 2011; Suzuki, Sato, and Takeuchi 2012; von der Ohe et al. 2010). In most cases, the presence of a single QTL significantly improved FHB resistance but the presence of both *Fhb1* and *Fhb5* loci was more efficient and stable in increasing resistance compared to the presence of one locus. The integration of major resistance genes, such as *Fhb1* and *Fhb2*, from Asian spring wheat germplasm in adopted European winter wheat breeding material was shown to increase FHB resistance (Häberle et al. 2009). Additionally, the effective and additive effect of *Fhb1 i*n combination with *QFhs.nau-2DL* has also been reported (Agostinelli et al. 2012; Clark et al. 2016).

By using markers closely linked to both *QFhb.WEK-5A* and *QFhb.Wuhan-2DL* loci identified in the present study (although further fine-mapping of the *QFhb.Wuhan-2DL* loci is needed), breeders could incorporate them, together with other resistances, into UK breeding programmes to achieve more effective FHB resistance. These resistances would need to be validated under other climate conditions to prove their efficacy, and in different genetic backgrounds. In fact, the *QFhb.Wuhan-2DL* loci has been already tested by the iCase collaborators in France and introduced into the Limagrain breeding programme for validation.

6.4. Sequencing of target genomic regions of selected loci

Advances in genomics and the generation of genome assemblies have been more challenging in wheat (*Triticum* spp.) due to its large (16 Gbp), hexaploid, and complex genome that contains more than 85% of repetitive DNA (IWGSC 2018).

The first steps into sequencing the hexaploid wheat genome began in 2005, with the creation of the International Wheat Genome Consortium (IWGSC) (Guan et al. 2020). The draft of the wheat bread genome revealed the evolutionary dynamics of the genome through gene loss, gain, and duplication (IWGSC 2014). Later studies produced whole-genome assemblies of bread wheat genome but lacked full annotation and did not present the genome in the correct physical order (Chapman et al. 2015; Clavijo et al. 2017; Zimin et al. 2017). An ordered and annotated assembly (IWGSC RefSeq v1.0) of the 21 chromosomes of the hexaploid wheat cultivar Chinese Spring (CS) (IWGSC 2018) was later achieved and provided a huge insight into the global wheat genome composition. The new annotation has really helped and advanced the genetic dissection of quantitative traits and the implementation of modern breeding strategies for future wheat improvement.

The CS genome assembly was the first step towards understanding the diversity available. However, reference-quality genome assemblies have been also produced for other wheat cultivars. The most contiguous and complete chromosome-scale assembly of bread wheat genome to date has been recently released in the French cultivar Renan. Its genome has been assembled by using an optimized procedure based on long-reads produced on the Oxford Nanopore Technology (ONT) PromethION device (Aury et al. 2022).

The genetic variation within wheat species is referred to as the wheat 'pan genome', which is being characterized by the 10+ Wheat Genomes Project (http://www.10wheatgenomes.com/). Information about the genomes of other wheat cultivars advances the identification of quantitative traits in the germplasm.

For this present PhD research, none of the cultivars used have been sequenced. Although improvements have been made in wheat research in the recent years, sequencing costs are still high, and bioinformatic knowledge is essential for the success of generating a high-quality genome assembly, as previously described. Nevertheless, the methodology I have used through the project has helped to localize and fine-map both *QFhb.WEK-5A* and *QFhb.Wuhan-2DL* loci in their respective chromosomes. This methodology is mainly based in the identification of SNPs (obtained from different sources such as Cereals DB web site, an RNA-Seq data set, an in-house 18K SNP array and exome capture data) which provide information of the parental allele at that specific location in the chromosome. The analysis that followed, allowed the identification of SNPs (markers) associated with the allele of the resistant cultivar (WEKH85A or Wuhan parental lines) with FHB type II resistance.

As both loci have been greatly reduced in size and research is still ongoing to further fine-map the *QFhb.Wuhan-2DL* locus, an alternative option to whole-genome sequencing could be to sequence only a genomic region of interest, maybe where several genes of interest are colocalised. This could be performed using an ONT with target enrichment, since by dedicating more sequencing time to regions of interest, their depth and coverage could be greatly increased. This type of precise sequencing may help to identify those differences in the selected region of the locus with respect to the CS reference genome. However, this type of technology may still be challenging in wheat, since the sequencing of a small genomic region of < 60 Kbp from the whole genome of 16 Gbp would provide a very poor coverage.

Another alternative for fine-mapping a locus and not sequencing the entire genome may be the combination of CRISPR-Cas9 targeted cleavage of a region of interest, followed by enrichment and long-read sequencing using the ONT. This method was recently used to sequence a locus spanning 8 Kbp in the apple (*Malus* x *domestica*) genome (López-Girona et al. 2020). As for this PhD project a great advance was made in the identification of a candidate

gene for DON tolerance and FHB resistance on the *QFhb.WEK-5A* locus, this type of sequencing technologies may be of interest for the *QFhb.Wuhan-2DL* locus.

The *QFhb.Wuhan-2DL* locus was of 55.6 Mbp and contains 575 annotated genes (EMBL-EBI 2022). This genomic interval is the same as that in the first report of the 2DL QTL (Somers, Fedak, and Savard 2003). However, most of the published 2DL QTL candidate genes reside outside this locus interval, as discussed in Chapter 5. Preliminary evidence from selected RILs (to be re-tested in Summer 2022) suggest that the resistance may be located in a 10.92 Mbp genomic region, containing 73 annotated genes (EMBL-EBI 2022). Nevertheless, the *QFhb.Wuhan-2DL* locus needs further fine-mapping to reduce further the number of candidate genes and enable production of a physical map of the interval.

6.5. Identifying the underlying genes of the *QFhb.WEK-5A* locus

Only two FHB QTLs have been claimed to be cloned so far: *Fhb1* (*Qfhs.ndsu-3BS*) (Li, Zhou, et al. 2019; Rawat et al. 2016; Su et al. 2019) and *Qfhb.mgb-2A* (Gadaleta et al. 2019).

Genes associated with either *Fusarium* or DON resistance have been identified from numerous studies on *Fhb1*. These identified genes are involved in numerous defence responses in plants, including pathogenesis related proteins, the synthesis of antimicrobial compounds, antioxidative stress responses, DON detoxification, cell morphogenesis and cell wall fortification (Foroud et al. 2012; Schweiger et al. 2016; Walter and Doohan 2011).

Fhb1 gene has been the focus of many recent studies trying to elucidate the mechanisms of its resistance. Indeed, a number of studies have reported the cloning of this locus, although they came to contradictory results regarding the causative gene as previously mentioned. Three different contradictory papers were compared by Lagudah and Krattinger (2019) who suggested that both the Pore-forming toxin-like gene (Rawat et al. 2016) and

histidine-rich calcium-binding-protein gene (Li, Zhou, et al. 2019; Su et al. 2019) could possibly be contributing independently towards FHB resistance. In this last instance, both independent research teams disagree in the mode of action of HRC1 in *Fhb1*. While Su et al (2019) reported that the wild type allele caused susceptibility and the resistance allele in Sumai 3 results from a deletion embracing the start codon in the histidine-rich calcium-binding-protein gene (loss-of-function mutation), Li, Zhou, et al. (2019) stated that the resistant Wangshuibai allele confers resistance in an active manner (gain-of-function mutation). However, further efforts are needed to clarify *Fhb1* gene isolation (Lagudah and Krattinger 2019).

Interestingly, *Fhb1* locus has not been found in tetraploid wheat species including durum wheat. However, orthologues genes of *Fhb1* have been identified in wild emmer wheat (*T. turgidum* ssp. *dicoccoides*, AABB) and durum wheat (Haile et al. 2019; Li, Zhou, et al. 2019; Ruan et al. 2020; Su et al. 2019).

The cloning of the *Qfhb.mgb-2A* locus has been reported on the 2A chromosome of durum wheat, introgressed from a resistant line derived from Sumai 3. The underlying gene identified was a wall-associated receptor-like kinase (WAK2) (Gadaleta et al. 2019).

In the present study, I have reported that DON-responsive candidate genes *TraesCS5A02G191700* and *TraesCS5A02G191800* identified on the FHB *QFhb.WEK-5A* locus may be promising candidate genes for FHB resistance by increasing their level of expression upon DON exposure. Significantly, *TraesCS5A02G191700* was the only gene differentially expressed in the +/- 5A QTL lines in response to DON. Both genes, particularly *TraesCS5A02G191700*, were also highly responsive to challenge by *Fusarium* species according to expression levels in expVIP (Borrill, Ramirez-Gonzalez, and Uauy 2016; Ramírez-González et al. 2018). Differences in the promoter region of gene *TraesCS5A02G191700* were identified in Chapter 4. Indeed, the 3 bp (CTT) deletion in the promoter region of gene

TraesCS5A02G191700 may be responsible for the enhanced expression of this gene upon challenge with DON or *F. graminearum* in the introgression line WEKH85A.

To conclude, in the present PhD project I have identified a highly plausible candidate for the third FHB resistance gene (*TraesCS5A02G191700*), one that may have a wider role in response to stress.

6.6. Functionally validation of gene *TraesCS5A02G191700*

Efficient wheat transformation via an in-planta *Agrobacterium*-mediated inoculation method has been very challenging. Generating stable transgenic lines in wheat most commonly involves transforming immature wheat embryos followed by callus regeneration (Harwood 2011). Recently, a high-throughput, highly efficient and repeatable transformation system for wheat was developed and optimised using *Agrobacterium*-mediated transformation system (Hayta et al. 2019). In this study, transformation efficiencies of up to 25 % were reported in the spring wheat *T. aestivum* cv. Fielder. Indeed, this system was successfully used to introduce genes of interest in cv. Fielder as well as for CRISPR/Cas9 based genome editing (Rey et al. 2018).

Gene expression can be also altered in a variety of ways such as, for example, overexpressing the gene of interest using either a constitutive, tissue-specific, or inducible promoters (Hensel et al. 2011). Additionally, genome editing (GE) technologies have recently provided new opportunities to manipulate genes in wheat. For instance, TALEN and CRISPR/Cas9-mediated GE have been successfully used in transient expression in wheat (Shan et al. 2014) and stable transformation of plants (Luo et al. 2019; Wang et al. 2014).

In the present PhD project, a 3 bp (CTT) deletion was identified in the promotor of gene *TraesCS5A02G191700* in the resistant introgression line WEK8H5A. To functionally

validate gene TraesCS*5A02G191700*, two different approaches are being used. Limagrain S.A. are using CRISPR/Cas9-mediated GE technology to disrupt the 3 bp region upstream of the coding sequence in order to validate this target as being responsible for the increase in DON tolerance and FHB resistance associated with the 5A QTL. Additionally, gene synthesis and overexpression using the rice actin promoter (OsAct) has been applied into cv. Fielder (susceptible to FHB). This procedure has recently been performed by the Transformation team at the JIC using the GRF-GIF fusion technology (Debernardi et al. 2020).

Wheat plants of the F_1 generation have been produced and are being bulked to obtained seed. Plants of the F_2 generation will be screen on the *QFhb.WEK-5A* locus to confirm segregation and those homozygous lines will be then selected to be further characterised for FHB type II resistance.

6.7. Concluding remarks

In the present PhD project, two *QFhb.WEK-5A* and *QFhb.Wuhan-2DL* loci have been fine mapped on the long arm of the 5A and 2D chromosomes of bread wheat, respectively. The main objectives of the project have been achieved since both loci have been delimited with specific markers to be used into breeding programmes.

A promising candidate gene *TraesCS5A02G191700* for DON tolerance and FHB resistance on the *QFhb.WEK-5A* locus was identified. In addition, differences in the promoter region of gene *TraesCS5A02G191700* have been identified that may account for the enhanced expression of this gene upon challenge with DON in the FHB resistant line WEKH85A. Nevertheless, further research is needed to functionally validate the candidate gene on the *QFhb.WEK-5A* locus and the fine-mapping of the *QFhb.Wuhan-2DL* locus.

It would be important to implement the discovery of new sources of resistances, even with small effects, into breeding programmes together with well-known and studied sources of resistance such as *Fhb1*. Although there is not a complete source of FHB resistance, the combination of different sources and the contribution of its underlying gene or genes enhance FHB resistance. Pyramiding different sources of FHB resistance into breeding programmes would need to be achieved as new loci are identified. It would be also important to identify whether the introgression of specific loci, or the combination of different loci, affects the nutritional values, such as protein content, of a specific cultivar. Thus, the trade-offs of stacking several FHB QTLs would also need to be further examined.

Additionally, the identification and the functional validation of genes underlying FHB QTLs may revolutionize breeding for FHB resistance. For example, *TraesCS5A02G191700* is part of a network of interacting genes with a potential role in stress response. The other genes involved in this network also provide additional potential targets for improving FHB resistance.

References

Agostinelli, Andres M., Anthony J. Clark, Gina Brown-Guedira, and David A. Van Sanford. 2012. 'Optimizing phenotypic and genotypic selection for Fusarium head blight resistance in wheat', *Euphytica*, 186: 115-26.

Ahad, Arzoo, Roohi Aslam, Alvina Gul, Rabia Amir, Faiza Munir, Tuba Sharf Batool, Mahnoor Ilyas, Muhammad Sarwar, Muhammad Azhar Nadeem, Faheem Shehzad Baloch, Sajid Fiaz, and Muhammad Abu Bakar Zia. 2021. 'Genome-wide analysis of bZIP, BBR, and BZR transcription factors in Triticum aestivum', *Plos One*, 16: e0259404.

Anderson, J.A., R.W. Stack, S. Liu, B.L. Waldron, A.D. Fjeld, C. Coyne, B. Moreno-Sevilla, J.M. Fetch, Q.J. Song, P.B. Cregan, and R.C. Frohberg. 2001. 'DNA markers for Fusarium head blight resistance QTLs in two wheat populations', *Theoretical and Applied Genetics*, 102: 1164-68.

Aury, Jean-Marc, Stefan Engelen, Benjamin Istace, Cécile Monat, Pauline Lasserre-Zuber, Caroline Belser, Corinne Cruaud, Hélène Rimbert, Philippe Leroy, Sandrine Arribat, Isabelle Dufau, Arnaud Bellec, David Grimbichler, Nathan Papon, Etienne Paux, Marion Ranoux, Adriana Alberti, Patrick Wincker, and Frédéric Choulet. 2022. 'Long-read and chromosome-scale assembly of the hexaploid wheat genome achieves high resolution for research and breeding', *bioRxiv*: 2021.08.24.457458.

Bagga, Paramjits S. 2012. 'Efficacy of triazole and strobilurin fungicides for controlling Fusarium Head Blight (Scab) and Brown rust of wheat in Punjab', *Indian Phytopathology*.

Bahrini, Insaf, Taiichi Ogawa, Fuminori Kobayashi, Hiroyuki Kawahigashi, and Hirokazu Handa. 2011. 'Overexpression of the pathogen-inducible wheat TaWRKY45 gene confers disease resistance to multiple fungi in transgenic wheat plants', *Breeding Science*, 61: 319-26.

Bahrini, Insaf, Motoki Sugisawa, Rie Kikuchi, Taiichi Ogawa, Hiroyuki Kawahigashi, Tomohiro Ban, and Hirokazu Handa. 2011. 'Characterization of a wheat transcription factor, TaWRKY45, and its effect on Fusarium head blight resistance in transgenic wheat plants', *Breeding Science*, 61: 121-29.

Bai, G.-H., R. Plattner, A. Desjardins, F. Kolb, and R. A. McIntosh. 2008. 'Resistance to Fusarium head blight and deoxynivalenol accumulation in wheat', *Plant Breeding*, 120: 1-6.

Bai, G.-H., G. Shaner, and H. Ohm. 2000. 'Inheritance of resistance to *Fusarium graminearum* in wheat', *Theoretical and Applied Genetics*, 100: 1-8.

Bai, G. and G. Shaner. 2004. 'Management and resistance in wheat and barley to Fusarium head blight', *Annu Rev Phytopathol*, 42: 135-61.

Bai, G. H., A. E. Desjardins, and R. D. Plattner. 2002. 'Deoxynivalenol-nonproducing Fusarium graminearum Causes Initial Infection, but does not Cause Disease Spread in Wheat Spikes', *Mycopathologia*, 153: 91-98.

Bai, G., F. L. Kolb, G. Shaner, and L. L. Domier. 1999. 'Amplified fragment length polymorphism markers linked to a major quantitative trait locus controlling scab resistance in wheat', *Phytopathology*, 89: 343-8.

Bai, G., and G. Shaner. 1994. 'Scab of wheat: prospects for control', *Plant Disease*, 78: 760-66.

Bai, Guihua, Zhenqi Su, and Jin Cai. 2018. 'Wheat resistance to Fusarium head blight', *Canadian Journal of Plant Pathology*, 40: 336-46.

Bankes-Jones, Elizabeth Anna. 2021. 'Identifying genes underlying Fusarium and mycotoxin susceptibility in Brachypodium distachyon', University of East Anglia.

Beckers, G. J. M., and S. H. Spoel. 2006. 'Fine-Tuning Plant Defence Signalling: Salicylate versus Jasmonate', *Plant Biology*, 8: 1-10.

Berthiller, F., M. Lemmens, U. Werner, R. Krska, M. T. Hauser, G. Adam, and R. Schuhmacher. 2007. 'Short review: Metabolism of theFusarium mycotoxins deoxynivalenol and zearalenone in plants', *Mycotoxin Research*, 23: 68-72.

Bigeard, J., J. Colcombet, and H. Hirt. 2015. 'Signaling mechanisms in pattern-triggered immunity (PTI)', *Mol Plant*, 8: 521-39.

Biselli, Chiara, Paolo Bagnaresi, Primetta Faccioli, Xinkun Hu, Margaret Balcerzak, Maria G. Mattera, Zehong Yan, Therese Ouellet, Luigi Cattivelli, and Giampiero Valè. 2018. 'Comparative Transcriptome Profiles of Near-Isogenic Hexaploid Wheat Lines Differing for Effective Alleles at the 2DL FHB Resistance QTL', *Frontiers in Plant Science*, 9.

Boddu, J., S. Cho, and G. J. Muehlbauer. 2007. 'Transcriptome analysis of trichothecene-induced gene expression in barley', *Mol Plant Microbe Interact*, 20: 1364-75.

Boedi, S., H. Berger, C. Sieber, M. Munsterkotter, I. Maloku, B. Warth, M. Sulyok, M. Lemmens, R. Schuhmacher, U. Guldener, and J. Strauss. 2016. 'Comparison of *Fusarium graminearum* Transcriptomes on Living or Dead Wheat Differentiates Substrate-Responsive and Defense-Responsive Genes', *Front Microbiol*, 7: 1113.

Boenisch, M.J., and W. Schaefer. 2011. '*Fusarium graminearum* forms mycotoxin producing infection structures on wheat', *BMC Plant Biol*, 11: 1471-2229.

Borrill, Philippa, Ricardo Ramirez-Gonzalez, and Cristobal Uauy. 2016. 'expVIP: a Customizable RNA-seq Data Analysis and Visualization Platform ', *Plant Physiology*, 170: 2172-86.

Bottalico, A., and G. Perrone. 2002. 'Toxigenic *Fusarium* species and mycotoxins associated with head blight in small-grain cereals in Europe', *Eur J Plant Pathol*, 108: 611-24.

Boycheva, Svetlana, Laurent Daviet, Jean-Luc Wolfender, and Teresa B. Fitzpatrick. 2014. 'The rise of operon-like gene clusters in plants', *Trends in Plant Science*, 19: 447-59.

Brennan, J.M., B. Fagan, A. van Maanen, B.M. Cooke, and F.M. Doohan. 2003. 'Studies on *in vitro* Growth and Pathogenicity of European *Fusarium* Fungi', *Eur J Plant Pathol*, 109: 577-87.

Broglie, K. E., P. Biddle, R. Cressman, and R. Broglie. 1989. 'Functional analysis of DNA sequences responsible for ethylene regulation of a bean chitinase gene in transgenic tobacco', *The Plant Cell*, 1: 599-607.

Buerstmayr, H. , T. Ban, and J.A. Anderson. 2009. 'QTL mapping and marker-assisted selection for *Fusarium* head blight resistance in wheat: a review', *Plant Breeding*, 128: 1-26.

Buerstmayr, H., M. Lemmens, G. Fedak, P. Ruckenbauer, and Communicated B. S. Gill. 1999. 'Back-cross reciprocal monosomic analysis of *Fusarium* head blight resistance in wheat (*Triticum aestivum* L.)', *Theor Appl Genet*, 98: 76-85.

Buerstmayr, H., M. Lemmens, L. Hartl, L. Doldi, B. Steiner, M. Stierschneider, and P. Ruckenbauer. 2002. 'Molecular mapping of QTLs for Fusarium head blight resistance in spring wheat. I. Resistance to fungal spread (Type II resistance)', *Theoretical and Applied Genetics*, 104: 84-91.

Buerstmayr, H., B. Steiner, L. Hartl, M. Griesser, N. Angerer, D. Lengauer, T. Miedaner, B. Schneider, and M. Lemmens. 2003. 'Molecular mapping of QTLs for Fusarium head blight resistance in spring wheat. II. Resistance to fungal penetration and spread', *Theor Appl Genet*, 107: 503-8.

Buerstmayr, M., M. Lemmens, B. Steiner, and H. Buerstmayr. 2011. 'Advanced backcross QTL mapping of resistance to Fusarium head blight and plant morphological traits in a Triticum macha × T. aestivum population', *Theor Appl Genet*, 123: 293-306.

Buerstmayr, Maria, Barbara Steiner, and Hermann Buerstmayr. 2020. 'Breeding for Fusarium head blight resistance in wheat—Progress and challenges', *Plant Breeding*, 139: 429-54.

Buerstmayr, Maria, Barbara Steiner, Christian Wagner, Petra Schwarz, Klaus Brugger, Delfina Barabaschi, Andrea Volante, Giampiero Valè, Luigi Cattivelli, and Hermann Buerstmayr. 2018. 'High-resolution mapping of the pericentromeric region on wheat chromosome arm 5AS harbouring the Fusarium head blight resistance QTL Qfhs.ifa-5A', *Plant Biotechnol J*, 16: 1046-56.

Bushnell, W.R., B.E. Hazen, and C. Pritsch. 2003. *Histology and physiology of Fusarium head blight* (APS Press, St. Paul, MN).

Cainong, Joey C., William W. Bockus, Yigao Feng, Peidu Chen, Lili Qi, Sunish K. Sehgal, Tatiana V. Danilova, Dal-Hoe Koo, Bernd Friebe, and Bikram S. Gill. 2015. 'Chromosome engineering, mapping, and transferring of resistance to Fusarium head blight disease from Elymus tsukushiensis into wheat', *Theoretical and Applied Genetics*, 128: 1019-27.

Chapman, Jarrod A., Martin Mascher, Aydın Buluç, Kerrie Barry, Evangelos Georganas, Adam Session, Veronika Strnadova, Jerry Jenkins, Sunish Sehgal, Leonid Oliker, Jeremy Schmutz, Katherine A. Yelick, Uwe Scholz, Robbie Waugh, Jesse A. Poland, Gary J.

Muehlbauer, Nils Stein, and Daniel S. Rokhsar. 2015. 'A whole-genome shotgun approach for assembling and anchoring the hexaploid bread wheat genome', *Genome Biology*, 16: 26.

Chen, J., C. A. Griffey, M. A. Saghai Maroof, E. L. Stromberg, R. M. Biyashev, W. Zhao, M. R. Chappell, T. H. Pridgen, Y. Dong, and Z. Zeng. 2006. 'Validation of two major quantitative trait loci for fusarium head blight resistance in Chinese wheat line W14', *Plant Breeding*, 125: 99-101.

Chen, Xunfen, Justin D. Faris, Jinguo Hu, Robert W. Stack, Tika Adhikari, Elias M. Elias, Shahryar F. Kianian, and Xiwen Cai. 2007. 'Saturation and comparative mapping of a major Fusarium head blight resistance QTL in tetraploid wheat', *Molecular Breeding*, 19: 113-24.

Chu, Chenggen, Zhixia Niu, Shaobin Zhong, Shiaoman Chao, Timothy L. Friesen, Scott Halley, Elias M. Elias, Yanhong Dong, Justin D. Faris, and Steven S. Xu. 2011. 'Identification and molecular mapping of two QTLs with major effects for resistance to Fusarium head blight in wheat', *Theoretical and Applied Genetics*, 123: 1107.

Clark, Anthony J., Daniela Sarti-Dvorjak, Gina Brown-Guedira, Yanhong Dong, Byung-Kee Baik, and David A. Van Sanford. 2016. 'Identifying Rare FHB-Resistant Segregants in Intransigent Backcross and F2 Winter Wheat Populations', *Frontiers in Microbiology*, 7.

Clavijo, B. J., L. Venturini, C. Schudoma, G. G. Accinelli, G. Kaithakottil, J. Wright, P. Borrill, G. Kettleborough, D. Heavens, H. Chapman, J. Lipscombe, T. Barker, F. H. Lu, N. McKenzie, D. Raats, R. H. Ramirez-Gonzalez, A. Coince, N. Peel, L. Percival-Alwyn, O. Duncan, J. Trösch, G. Yu, D. M. Bolser, G. Namaati, A. Kerhornou, M. Spannagl, H. Gundlach, G. Haberer, R. P. Davey, C. Fosker, F. D. Palma, A. L. Phillips, A. H. Millar, P. J. Kersey, C. Uauy, K. V. Krasileva, D. Swarbreck, M. W. Bevan, and M. D. Clark. 2017. 'An improved assembly and annotation of the allohexaploid wheat genome identifies complete families of agronomic genes and provides genomic evidence for chromosomal translocations', *Genome Res*, 27: 885-96.

Collard, B.C.Y., M.Z.Z. Jahufer, J.B. Brouwer, and E.C.K. Pang. 2005. 'An introduction to markers, quantitative trait loci (QTL) mapping and marker-assisted selection for crop improvement: The basic concepts', *Euphytica*, 142: 169-96.

Collier, R., K. Dasgupta, Y. P. Xing, B. T. Hernandez, M. Shao, D. Rohozinski, E. Kovak, J. Lin, M. L. P. de Oliveira, E. Stover, K. F. McCue, F. G. Harmon, A. Blechl, J. G. Thomson, and R. Thilmony. 2017. 'Accurate measurement of transgene copy number in crop plants using droplet digital PCR', *Plant J*, 90: 1014-25.

Cuomo, C. A., U. Guldener, J. R. Xu, F. Trail, B. G. Turgeon, A. Di Pietro, J. D. Walton, L. J. Ma, S. E. Baker, M. Rep, G. Adam, J. Antoniw, T. Baldwin, S. Calvo, Y. L. Chang, D. Decaprio, L. R. Gale, S. Gnerre, R. S. Goswami, K. Hammond-Kosack, L. J. Harris, K. Hilburn, J. C. Kennell, S. Kroken, J. K. Magnuson, G. Mannhaupt, E. Mauceli, H. W. Mewes, R. Mitterbauer, G. Muehlbauer, M. Munsterkotter, D. Nelson, K. O'Donnell, T. Ouellet, W. Qi, H. Quesneville, M. I. Roncero, K. Y. Seong, I. V. Tetko, M. Urban, C. Waalwijk, T. J. Ward, J. Yao, B. W. Birren, and H. C. Kistler. 2007. 'The Fusarium graminearum genome reveals a link between localized polymorphism and pathogen specialization', *Science*, 317: 1400-2.

Cuthbert, P. A., D. J. Somers, J. Thomas, S. Cloutier, and A. Brulé-Babel. 2006. 'Fine mapping Fhb1, a major gene controlling fusarium head blight resistance in bread wheat (Triticum aestivum L.)', *Theor Appl Genet*, 112: 1465-72.

Cuthbert, P.A., D.J. Somers, and A. Brule-Babel. 2007. 'Mapping of *Fhb2* on chromosome 6BS: a gene controlling Fusarium head blight field resistance in bread wheat (*Triticum aestivum* L.)', *Theor Appl Genet*, 114: 429-37.

Cuthbert, P.A., D.J. Somers, J. Thomas, S. Cloutier, and A. Brule-Babel. 2006. 'Fine mapping *Fhb1*, a major gene controlling fusarium head blight resistance in bread wheat (*Triticum aestivum* L.)', *Theor Appl Genet*, 112: 1465-72.

Dean, R., J.A. Van Kan, Z.A. Pretorius, K.E. Hammond-Kosack, A. Di Pietro, P.D. Spanu, J.J. Rudd, M. Dickman, R. Kahmann, J. Ellis, and G.D. Foster. 2012. 'The Top 10 fungal pathogens in molecular plant pathology', *Mol Plant Pathol*, 13: 414-30.

Debernardi, Juan M., David M. Tricoli, Maria F. Ercoli, Sadiye Hayta, Pamela Ronald, Javier F. Palatnik, and Jorge Dubcovsky. 2020. 'A GRF–GIF chimeric protein improves the regeneration efficiency of transgenic plants', *Nature Biotechnology*, 38: 1274-79.

Desjardins, A.E., and R.H. Proctor. 2007. 'Molecular biology of *Fusarium* mycotoxins', *Int J Food Microbiol*, 119: 47-50.

Dhaliwal, A.S., D Mares, J., and D Marshall, R. 1987. 'Effect of 1B/1R chromosome-translocation on milling and quality of bread wheats', *Cereal Chem*, 64: 72-76.

Dhokane, D., S. Karre, A.C. Kushalappa, and C. McCartney. 2016. 'Integrated Metabolo-Transcriptomics Reveals Fusarium Head Blight Candidate Resistance Genes in Wheat QTL-*Fhb2*', *Plos One*, 11: e0155851.

Diethelm, Manuela, Michael Schmolke, Jennifer Groth, Wolfgang Friedt, Günther Schweizer, and Lorenz Hartl. 2014. 'Association of allelic variation in two NPR1-like genes with Fusarium head blight resistance in wheat', *Molecular Breeding*, 34: 31-43.

Dill-Macky, R., and R.K. Jones. 2000. 'The Effect of Previous Crop Residues and Tillage on Fusarium Head Blight of Wheat', *Plant Disease*, 84: 71-76.

Ding, Lina, Haibin Xu, Hongying Yi, Liming Yang, Zhongxin Kong, Lixia Zhang, Shulin Xue, Haiyan Jia, and Zhengqiang Ma. 2011. 'Resistance to hemi-biotrophic F. graminearum infection is associated with coordinated and ordered expression of diverse defense signaling pathways', *Plos One*, 6: e19008-e08.

Doohan, F.M., J. Brennan, and B.M. Cooke. 2003. 'Influence of Climatic Factors on *Fusarium* Species Pathogenic to Cereals', *Eur J Plant Pathol*, 109: 755-68.

Dweba, C. C., S. Figlan, H. A. Shimelis, T. E. Motaung, S. Sydenham, L. Mwadzingeni, and T. J. Tsilo. 2017. 'Fusarium head blight of wheat: Pathogenesis and control strategies', *Crop Protection*, 91: 114-22.

Ederli, Luisa, Giovanni Beccari, Francesco Tini, Irene Bergamini, Ilaria Bellezza, Roberto Romani, and Lorenzo Covarelli. 2021. 'Enniatin B and Deoxynivalenol Activity on Bread Wheat and on Fusarium Species Development', *Toxins*, 13: 728.

Edwards, S. . 2011. 'Zearalenone risk in European wheat', *World Mycotoxin Journal*, 4: 433-38.

EMBL-EBI. 2022. "Ensembl Plants release 43." In http://plants.ensembl.org/.

Eulgem, T., P. J. Rushton, S. Robatzek, and I. E. Somssich. 2000. 'The WRKY superfamily of plant transcription factors', *Trends Plant Sci*, 5: 199-206.

FAOSTAT. 2021. " Food and Agriculture Organization of the United Nations Database." In, http://www.fao.org/faostat/ (March, 2021).

Foresight. 2011. "*The Future of Food and Farming, Final Project Report.*" In. London: The Government Office for Science.

Foroud, N. A., T. Ouellet, A. Laroche, B. Oosterveen, M. C. Jordan, B. E. Ellis, and F. Eudes. 2012. 'Differential transcriptome analyses of three wheat genotypes reveal different host response pathways associated with Fusarium head blight and trichothecene resistance', *Plant Pathology*, 61: 296-314.

Gadaleta, Agata, Pasqualina Colasuonno, Stefania Lucia Giove, Antonio Blanco, and Angelica Giancaspro. 2019. 'Map-based cloning of QFhb.mgb-2A identifies a WAK2 gene responsible for Fusarium Head Blight resistance in wheat', *Sci Rep*, 9: 6929.

Gardiner, D.M., K. Kazan, and J.M. Manners. 2009. 'Novel genes of *Fusarium graminearum* that negatively regulate deoxynivalenol production and virulence', *Mol Plant Microbe Interact*, 22: 1588-600.

Gardiner, S.A., J. Boddu, F. Berthiller, C. Hametner, R.M. Stupar, G. Adam, and G.J. Muehlbauer. 2010. 'Transcriptome Analysis of the Barley-Deoxynivalenol Interaction: Evidence for a Role of Glutathione in Deoxynivalenol Detoxification', *Molecular Plant-Microbe Interactions*, 23: 962-76.

Gatti, M., F. Cambon, C. Tassy, C. Macadre, F. Guerard, T. Langin, and M. Dufresne. 2019. 'The Brachypodium distachyon UGT Bradi5gUGT03300 confers type II fusarium head blight resistance in wheat', *Plant Pathology*, 68: 334-43.

Gervais, L., F. Dedryver, J. Y. Morlais, V. Bodusseau, S. Negre, M. Bilous, C. Groos, and M. Trottet. 2003. 'Mapping of quantitative trait loci for field resistance to Fusarium head blight in an European winter wheat', *Theor Appl Genet*, 106: 961-70.

Gilsinger, J., L. Kong, X. Shen, and H. Ohm. 2005. 'DNA markers associated with low Fusarium head blight incidence and narrow flower opening in wheat', *Theor Appl Genet*, 110: 1218-25.

Goddard, R.J. 2015. 'Avoiding trade-off when enhancing Fusarium head blight resistance of barley', University of East Anglia.

Golkari, S., J. Gilbert, S. Prashar, and J. D. Procunier. 2007. 'Microarray analysis of *Fusarium graminearum*-induced wheat genes: identification of organ-specific and differentially expressed genes', *Plant Biotechnol J*, 5: 38-49.

Gómez-Gómez, L., and T. Boller. 2000. 'FLS2: an LRR receptor-like kinase involved in the perception of the bacterial elicitor flagellin in Arabidopsis', *Mol Cell*, 5: 1003-11.

Gosman, N., R. Bayles, P. Jennings, J. Kirby, and P. Nicholson. 2007. 'Evaluation and characterization of resistance to fusarium head blight caused by *Fusarium culmorum* in UK winter wheat cultivars', *Plant Pathol*, 56: 264-76.

Gosman, N., E. Chandler, M. Thomsett, R. Draeger, and P. Nicholson. 2005. 'Analysis of the relationship between parameters of resistance to Fusarium head blight and in vitro tolerance to deoxynivalenol of the winter wheat cultivar WEK0609 ®', *European Journal of Plant Pathology*, 111: 57-66.

Gosman, N.E. 2001. 'Analysis of the genetic basis of resistance to *Fusarium culmorum* in wheat', University of East Anglia.

Goswami, R. S., and H. C. Kistler. 2005. 'Pathogenicity and In Planta Mycotoxin Accumulation Among Members of the Fusarium graminearum Species Complex on Wheat and Rice', *Phytopathology*, 95: 1397-404.

Goswami, R.S., and H.C. Kistler. 2004. 'Heading for disaster: *Fusarium graminearum* on cereal crops', *Mol Plant Pathol*, 5: 515-25.

Gou, Lulu, Jiro Hattori, George Fedak, Margaret Balcerzak, Andrew Sharpe, Paul Visendi, David Edwards, Nicholas Tinker, Yu-Ming Wei, Guo-Yue Chen, and Thérèse Ouellet. 2016. 'Development and Validation of Thinopyrum elongatum–Expressed Molecular Markers Specific for the Long Arm of Chromosome 7E', *Crop Science*, 56: 354-64.

Gratz, Silvia W., Gary Duncan, and Anthony J. Richardson. 2013. 'The Human Fecal Microbiota Metabolizes Deoxynivalenol and Deoxynivalenol-3-Glucoside and May Be Responsible for Urinary Deepoxy-Deoxynivalenol', *Applied and Environmental Microbiology*, 79: 1821.

Guan, Jiantao, Diego F. Garcia, Yun Zhou, Rudi Appels, Aili Li, and Long Mao. 2020. 'The Battle to Sequence the Bread Wheat Genome: A Tale of the Three Kingdoms', *Genomics, Proteomics & Bioinformatics*, 18: 221-29.

Guan, Shu, Jianwei He, J. Christopher Young, Honghui Zhu, Xiu-Zhen Li, Cheng Ji, and Ting Zhou. 2009. 'Transformation of trichothecene mycotoxins by microorganisms from fish digesta', *Aquaculture*, 290: 290-95.

Guenther, J.C., and F. Trail. 2005. 'The development and differentiation of *Gibberella zeae* (anamorph : *Fusarium graminearum*) during colonization of wheat', *Mycologia*, 97: 229-37.

Gunupuru, L. R., A. Perochon, and F. M. Doohan. 2017. 'Deoxynivalenol resistance as a component of FHB resistance', *Tropical Plant Pathology*, 42: 175-83.

Häberle, J., G. Schweizer, J. Schondelmaier, G. Zimmermann, and L. Hartl. 2009. 'Mapping of QTL for resistance against Fusarium head blight in the winter wheat population Pelikan//Bussard/Ning8026', *Plant Breeding*, 128: 27-35.

Haidoulis, John Francis. 2021. 'Investigating the role of phytohormones in Fusarium head blight and Fusarium root rot of Brachypodium distachyon', University of East Anglia.

Hao, G., H. Tiley, and S. McCormick. 2022. 'Chitin Triggers Tissue-Specific Immunity in Wheat Associated With Fusarium Head Blight', *Front Plant Sci*, 13: 832502.

Harwood, Wendy A. 2011. 'Advances and remaining challenges in the transformation of barley and wheat', *Journal of Experimental Botany*, 63: 1791-98.

Hayta, Sadiye, Mark A. Smedley, Selcen U. Demir, Robert Blundell, Alison Hinchliffe, Nicola Atkinson, and Wendy A. Harwood. 2019. 'An efficient and reproducible Agrobacterium-mediated transformation method for hexaploid wheat (Triticum aestivum L.)', *Plant Methods*, 15: 121.

He, J. W., G. S. Bondy, T. Zhou, D. Caldwell, G. J. Boland, and P. M. Scott. 2015. 'Toxicology of 3-epi-deoxynivalenol, a deoxynivalenol-transformation product by Devosia mutans 17-2-E-8', *Food and Chemical Toxicology*, 84: 250-9.

He, Xinyao, Morten Lillemo, Jianrong Shi, Jirong Wu, Åsmund Bjørnstad, Tatiana Belova, Susanne Dreisigacker, Etienne Duveiller, and Pawan Singh. 2016. 'QTL Characterization of Fusarium Head Blight Resistance in CIMMYT Bread Wheat Line Soru#1', *Plos One*, 11: e0158052-e52.

He, Yi, Lei Wu, Xiang Liu, Peng Jiang, Lixuan Yu, Jianbo Qiu, Gang Wang, Xu Zhang, and Hongxiang Ma. 2020. 'TaUGT6, a Novel UDP-Glycosyltransferase Gene Enhances the Resistance to FHB and DON Accumulation in Wheat', *Frontiers in Plant Science*, 11.

Hensel, Götz, Axel Himmelbach, Wanxin Chen, Dimitar K. Douchkov, and Jochen Kumlehn. 2011. 'Transgene expression systems in the Triticeae cereals', *Journal of Plant Physiology*, 168: 30-44.

Hu, Xinkun, Hélène Rocheleau, Curt McCartney, Chiara Biselli, Paolo Bagnaresi, Margaret Balcerzak, George Fedak, Zehong Yan, Giampiero Valè, Shahrokh Khanizadeh, and Thérèse Ouellet. 2019a. 'Identification and mapping of expressed genes associated with the 2DL QTL for fusarium head blight resistance in the wheat line Wuhan 1', *BMC genetics*, 20: 47-47.

IDRC. 2010. 'Facts and Figures on Food and Biodiversity'. https://www.idrc.ca/en/research-in-action/facts-figures-food-and-biodiversity.

Ikunaga, Yoko, Ikuo Sato, Stephanie Grond, Nobutaka Numaziri, Shigenobu Yoshida, Hiroko Yamaya, Syuntaro Hiradate, Morifumi Hasegawa, Hiroaki Toshima, Motoo Koitabashi, Michihiro Ito, Petr Karlovsky, and Seiya Tsushima. 2011. 'Nocardioides sp. strain WSN05-2, isolated from a wheat field, degrades deoxynivalenol, producing the novel intermediate 3-epi-deoxynivalenol', *Applied Microbiology and Biotechnology*, 89: 419-27.

International Wheat Genome Sequencing Consortium. 2014. 'A chromosome-based draft sequence of the hexaploid bread wheat (Triticum aestivum) genome', *Science*, 345: 1251788.

Islam, R., T. Zhou, J. C. Young, P. H. Goodwin, and K. P. Pauls. 2012. 'Aerobic and anaerobic de-epoxydation of mycotoxin deoxynivalenol by bacteria originating from agricultural soil', *World J Microbiol Biotechnol*, 28: 7-13.

Ittu, M., N.N. Saulescu, M. Ciuca, and G. Ittu. 2006. 'Effect of single QTLs for wheat FHB resistance from Sumai 3 and F 201R on phenotypic resistance traits and DON content', *Rom Agric Res*, 23: 13-20.

Ittu, M., N.N. Sãulescu, I. Hagima, G. Ittu, and P. Mustãtea. 2000. 'Association of Fusarium head blight resistance with gliadin loci in a winter wheat cross', *Crop Sci*, 40: 62-67.

Ittu, M., N.N. Săulescu, and G. Ittu. 2001. "Progress in breeding for scab resistance in Romania on wheat. ." In *National Fusarium Head Blight Forum Proceedings*. Cincinnati. 10-12 Dec. 2000.

IWGSC. 2014. 'A chromosome-based draft sequence of the hexaploid bread wheat (Triticum aestivum) genome', *Science*, 345: 1251788.

IWGSC. 2018. 'Shifting the limits in wheat research and breeding using a fully annotated reference genome', *Science*, 361.

Jansen, C., D. von Wettstein, W. Schafer, K.H. Kogel, A. Felk, and F.J. Maier. 2005. 'Infection patterns in barley and wheat spikes inoculated with wild-type and trichodiene synthase gene disrupted *Fusarium graminearum*', *Proc Natl Acad Sci U S A*, 102: 16892-97.

Jayatilake, D. V., G. H. Bai, and Y. H. Dong. 2011. 'A novel quantitative trait locus for Fusarium head blight resistance in chromosome 7A of wheat', *Theoretical and Applied Genetics*, 122: 1189-98.

Jia, Gaofeng, Peidu Chen, Genji Qin, Guihua Bai, Xiue Wang, Suling Wang, Bo Zhou, Shouzhong Zhang, and Dajun Liu. 2005. 'QTLs for Fusarium head blight response in a wheat DH population of Wangshuibai/Alondra's'', *Euphytica*, 146: 183-91.

Jia, H.Y., J. Zhou, S.L. Xue, G. Li, H. Yan, C. Ran, Y. Zhang, J. Shi, L. Jia, X. Wang, J. Luo, and Z.Q. Ma. 2018. 'A journey to understand wheat Fusarium head blight resistance in the Chinese wheat landrace Wangshuibai', *Crop J*, 6: 48-59.

Jiang, Guo-Liang, Yanhong Dong, JianRong Shi, and Richard W. Ward. 2007. 'QTL analysis of resistance to Fusarium head blight in the novel wheat germplasm CJ 9306. II. Resistance to deoxynivalenol accumulation and grain yield loss', *Theoretical and Applied Genetics*, 115: 1043-52.

Jiang, P., X. Zhang, L. Wu, Y. He, W. Zhuang, X. Cheng, W. Ge, H. Ma, and L. Kong. 2020. 'A novel QTL on chromosome 5AL of Yangmai 158 increases resistance to Fusarium head blight in wheat', *Plant Pathology*, 69: 249-58.

Joffe, A.Z. 1978. '*Fusarium poae* and *F. sporotrichoides* as principal causal agents of alimentary toxic aleukia.' in T.D. Wyllie, Morehouse, L.G., Eds. (ed.), *Mycotoxic Fungi, Mycotoxins, Mycotoxicoses: An Encyclopedic Handbook* (Deker: New York, USA).

Kage, U., K. N. Yogendra, and A. C. Kushalappa. 2017. 'TaWRKY70 transcription factor in wheat QTL-2DL regulates downstream metabolite biosynthetic genes to resist Fusarium graminearum infection spread within spike', *Sci Rep*, 7: 42596.

Kage, Udaykumar, Shailesh Karre, Ajjamada C. Kushalappa, and Curt McCartney. 2017. 'Identification and characterization of a fusarium head blight resistance gene TaACT in wheat QTL-2DL', *Plant Biotechnol J*, 15: 447-57.

Kaku, H., Y. Nishizawa, N. Ishii-Minami, C. Akimoto-Tomiyama, N. Dohmae, K. Takio, E. Minami, and N. Shibuya. 2006. 'Plant cells recognize chitin fragments for defense signaling through a plasma membrane receptor', *Proc Natl Acad Sci U S A*, 103: 11086-91.

Kang, Zhensheng, and Heinrich Buchenauer. 1999. 'Immunocytochemical localization of fusarium toxins in infected wheat spikes by Fusarium culmorum', *Physiological and Molecular Plant Pathology*, 55: 275-88.

Karre, S., A. Kumar, D. Dhokane, and A. C. Kushalappa. 2017. 'Metabolo-transcriptome profiling of barley reveals induction of chitin elicitor receptor kinase gene (HvCERK1) conferring resistance against Fusarium graminearum', *Plant Mol Biol*, 93: 247-67.

Kazan, K., and D.M. Gardiner. 2018. 'Transcriptomics of cereal–*Fusarium graminearum* interactions: what we have learned so far', *Mol Plant Pathol*, 19: 764-78.

Khalturin, K., G. Hemmrich, S. Fraune, R. Augustin, and T. C. Bosch. 2009. 'More than just orphans: are taxonomically-restricted genes important in evolution?', *Trends Genet*, 25: 404-13.

Khan, Mohd Kamran, Anamika Pandey, Tabinda Athar, Saumya Choudhary, Ravi Deval, Sait Gezgin, Mehmet Hamurcu, Ali Topal, Emel Atmaca, Pamela Aracena Santos, Makbule Rumeysa Omay, Hatice Suslu, Kamer Gulcan, Merve Inanc, Mahinur S. Akkaya, Abdullah Kahraman, and George Thomas. 2020. 'Fusarium head blight in wheat: contemporary status and molecular approaches', *3 Biotech*, 10: 172.

Kim, D., B. Langmead, and S. L. Salzberg. 2015. 'HISAT: a fast spliced aligner with low memory requirements', *Nat Methods*, 12: 357-60.

Krasileva, Ksenia V., Hans A. Vasquez-Gross, Tyson Howell, Paul Bailey, Francine Paraiso, Leah Clissold, James Simmonds, Ricardo H. Ramirez-Gonzalez, Xiaodong Wang, Philippa Borrill, Christine Fosker, Sarah Ayling, Andrew L. Phillips, Cristobal Uauy, and Jorge Dubcovsky. 2017. 'Uncovering hidden variation in polyploid wheat', *Proceedings of the National Academy of Sciences*, 114: E913-E21.

Kugler, Karl G., Gerald Siegwart, Thomas Nussbaumer, Christian Ametz, Manuel Spannagl, Barbara Steiner, Marc Lemmens, Klaus F. X. Mayer, Hermann Buerstmayr, and Wolfgang Schweiger. 2013. 'Quantitative trait loci-dependent analysis of a gene co-expression network associated with Fusarium head blight resistance in bread wheat (Triticum aestivumL.)', *BMC Genomics*, 14: 728.

Lagudah, Evans S., and Simon G. Krattinger. 2019. 'A new player contributing to durable Fusarium resistance', *Nature Genetics*, 51: 1070-71.

Landjeva, S., V. Korzun, and A. Börner. 2007. 'Molecular markers: Actual and potential contributions to wheat genome characterization and breeding', *Euphytica*, 156: 271-96.

Langevin, François, François Eudes, and André Comeau. 2004. 'Effect of Trichothecenes Produced by Fusarium graminearum during Fusarium Head Blight Development in Six Cereal Species', *European Journal of Plant Pathology*, 110: 735-46.

Lemmens, M., U. Scholz, F. Berthiller, C. Dall'Asta, A. Koutnik, R. Schuhmacher, G. Adam, H. Buerstmayr, A. Mesterhazy, R. Krska, and P. Ruckenbauer. 2005. 'The ability to detoxify the mycotoxin deoxynivalenol colocalizes with a major quantitative trait locus for Fusarium head blight resistance in wheat', *Mol Plant Microbe Interact*, 18: 1318-24.

Li, Guoqiang, Li Jia, Jiyang Zhou, Jicai Fan, Haisheng Yan, Jinxing Shi, Xin Wang, Min Fan, Shulin Xue, Shouyang Cao, Shunshun Tian, Haiyan Jia, and Zhengqiang Ma. 2019. 'Evaluation and precise mapping of QFhb.nau-2B conferring resistance against Fusarium infection and spread within spikes in wheat (Triticum aestivum L.)', *Molecular Breeding*, 39: 62.

Li, Guoqiang, Jiyang Zhou, Haiyan Jia, Zhongxia Gao, Min Fan, Yanjun Luo, Panting Zhao, Shulin Xue, Na Li, Yang Yuan, Shengwei Ma, Zhongxin Kong, Li Jia, Xia An, Ge Jiang, Wenxing Liu, Wenjin Cao, Rongrong Zhang, Jicai Fan, Xiaowu Xu, Yanfang Liu, Qianqian Kong, Shouhang Zheng, Yao Wang, Bin Qin, Shouyang Cao, Yunxiao Ding, Jinxing Shi, Haisheng Yan, Xin Wang, Congfu Ran, and Zhengqiang Ma. 2019. 'Mutation of a histidine-rich calcium-binding-protein gene in wheat confers resistance to Fusarium head blight', *Nature Genetics*, 51: 1106-12.

Li, Tao, Guihua Bai, Shuangye Wu, and Shiliang Gu. 2011. 'Quantitative trait loci for resistance to fusarium head blight in a Chinese wheat landrace Haiyanzhong', *Theoretical and Applied Genetics*, 122: 1497-502.

Li, Tao, Guihua Bai, Shuangye Wu, and Shiliang Gu. 2012. 'Quantitative trait loci for resistance to Fusarium head blight in the Chinese wheat landrace Huangfangzhu', *Euphytica*, 185: 93-102.

Li, X., H. Michlmayr, W. Schweiger, A. Malachova, S. Shin, Y. Huang, Y. Dong, G. Wiesenberger, S. McCormick, M. Lemmens, P. Fruhmann, C. Hametner, F. Berthiller, G. Adam, and G.J. Muehlbauer. 2017. 'A barley UDP-glucosyltransferase inactivates nivalenol and provides Fusarium Head Blight resistance in transgenic wheat', *J Exp Bot*, 68: 2187-97.

Li, X., S. Shin, S.J. Heinen, R. Dill-Macky, F. Berthiller, N. Nersesian, T. Clemente, S. McCormick, and G.J. Muehlbauer. 2015. 'Transgenic Wheat Expressing a Barley UDP-Glucosyltransferase Detoxifies Deoxynivalenol and Provides High Levels of Resistance to *Fusarium graminearum*', *Mol Plant Microbe Interact*, 28: 1237-46.

Li, X. Z., C. Zhu, C. F. M. de Lange, T. Zhou, J. He, H. Yu, J. Gong, and J. C. Young. 2011. 'Efficacy of detoxification of deoxynivalenol-contaminated corn by Bacillus sp. LS100 in reducing the adverse effects of the mycotoxin on swine growth performance', *Food Additives & Contaminants: Part A*, 28: 894-901.

Lin, F., S. L. Xue, Z. Z. Zhang, C. Q. Zhang, Z. X. Kong, G. Q. Yao, D. G. Tian, H. L. Zhu, C. J. Li, Y. Cao, J. B. Wei, Q. Y. Luo, and Z. Q. Ma. 2006. 'Mapping QTL associated with resistance to Fusarium head blight in the Nanda2419 x Wangshuibai population. II: Type I resistance', *Theoretical and Applied Genetics*, 112: 528-35.

Lin, F. Y., Q. X. Lu, J. H. Xu, and J. R. Shi. 2008. '[Cloning and expression analysis of two salt and Fusarium graminearum stress associated UDP-glucosyltransferases genes in wheat]', *Yi Chuan*, 30: 1608-14.

Liu, S., Z. A. Abate, H. Lu, T. Musket, G. L. Davis, and A. L. McKendry. 2007. 'QTL associated with Fusarium head blight resistance in the soft red winter wheat Ernie', *Theoretical and Applied Genetics*, 115: 417-27.

Liu, S. Y., M. D. Hall, C. A. Griffey, and A. L. McKendry. 2009. 'Meta-analysis of QTL associated with Fusarium head blight resistance in wheat', *Crop Science*, 49: 1955-68.

Liu, S., X. Zhang, M.O. Pumphrey, R.W. Stack, B.S. Gill, and J.A. Anderson. 2006. 'Complex microcolinearity among wheat, rice, and barley revealed by fine mapping of the genomic region harboring a major QTL for resistance to Fusarium head blight in wheat', *Funct Integr Genomics*, 6: 83-9.

Liu, Sixin, Michael O. Pumphrey, Bikram S. Gill, Harold N. Trick, Julia X. Zhang, Jaroslav Dolezel, Boulos Chalhoub, and James A. Anderson. 2008. 'Toward positional cloning of Fhb1, a major QTL for Fusarium head blight resistance in wheat', *Cereal Research Communications*, 36: 195-201.

Löffler, Martin, Chris-Carolin Schön, and Thomas Miedaner. 2009. 'Revealing the genetic architecture of FHB resistance in hexaploid wheat (Triticum aestivum L.) by QTL meta-analysis', *Molecular Breeding*, 23: 473-88.

Long, XiangYu, Margaret Balcerzak, Sigrun Gulden, Wenguang Cao, George Fedak, Yu-Ming Wei, You-Liang Zheng, Daryl Somers, and Thérèse Ouellet. 2015. 'Expression profiling identifies differentially expressed genes associated with the fusarium head blight resistance QTL 2DL from the wheat variety Wuhan-1', *Physiological and Molecular Plant Pathology*, 90: 1-11.

López-Girona, Elena, Marcus W. Davy, Nick W. Albert, Elena Hilario, Maia E. M. Smart, Chris Kirk, Susan J. Thomson, and David Chagné. 2020. 'CRISPR-Cas9 enrichment and long read sequencing for fine mapping in plants', *Plant Methods*, 16: 121.

Lulin, Ma, Yi Shang, AiZhong Cao, ZengJun Qi, LiPing Xing, PeiDu Chen, DaJun Liu, and E. Wang Xiu. 2010. 'Molecular cloning and characterization of an up-regulated UDP-glucosyltransferase gene induced by DON from Triticum aestivum L. cv. Wangshuibai', *Molecular Biology Reports*, 37: 785-95.

Luo, Ming, Hongyu Li, Soma Chakraborty, Robert Morbitzer, Amy Rinaldo, Narayana Upadhyaya, Dhara Bhatt, Smitha Louis, Terese Richardson, Thomas Lahaye, and Michael Ayliffe. 2019. 'Efficient TALEN-mediated gene editing in wheat', *Plant Biotechnol J*, 17: 2026-28.

Ma, H. X., K. M. Zhang, L. Gao, G. H. Bai, H. G. Chen, Z. X. Cai, and W. Z. Lu. 2006. 'Quantitative trait loci for resistance to fusarium head blight and deoxynivalenol accumulation in Wangshuibai wheat under field conditions', *Plant Pathology*, 55: 739-45.

Ma, Li-Jun, David M. Geiser, Robert H. Proctor, Alejandro P. Rooney, Kerry O'Donnell, Frances Trail, Donald M. Gardiner, John M. Manners, and Kemal Kazan. 2013. 'Fusarium Pathogenomics', *Annual Review of Microbiology*, 67: 399-416.

Ma, Xin, Xu-ye Du, Guo-juan Liu, Zai-dong Yang, Wen-qian Hou, Hong-wei Wang, De-shun Feng, An-fei Li, and Ling-rang Kong. 2015. 'Cloning and characterization of a novel UDP-glycosyltransferase gene induced by DON from wheat', *Journal of Integrative Agriculture*, 14: 830-38.

Maier, Frank J., Thomas Miedaner, Birgit Hadeler, Angelika Felk, Siegfried Salomon, Marc Lemmens, Helmut Kassner, and Wilhelm Schäfer. 2006. 'Involvement of trichothecenes in fusarioses of wheat, barley and maize evaluated by gene disruption of the trichodiene synthase (Tri5) gene in three field isolates of different chemotype and virulence', *Mol Plant Pathol*, 7: 449-61.

Makandar, R., V. J. Nalam, H. Lee, H. N. Trick, Y. Dong, and J. Shah. 2012. 'Salicylic acid regulates basal resistance to Fusarium head blight in wheat', *Mol Plant Microbe Interact*, 25: 431-9.

Maldonado-Ramirez, S.L., D.G. Schmale, E.J. Shields, and G.C. Bergstrom. 2005. 'The relative abundance of viable spores of *Gibberella zeae* in the planetary boundary layer suggests the role of long-distance transport in regional epidemics of Fusarium head blight', *Agricultural and Forest Meteorology*, 132: 20-27.

Mao, Shuang-Lin, Yu-Ming Wei, Wenguang Cao, Xiu-Jin Lan, Ma Yu, Zheng-Mao Chen, Guo-Yue Chen, and You-Liang Zheng. 2010. 'Confirmation of the relationship between plant height and Fusarium head blight resistance in wheat (Triticum aestivum L.) by QTL meta-analysis', *Euphytica*, 174: 343-56.

Marburger, David A., Shawn P. Conley, Paul D. Esker, Joseph G. Lauer, and Jean-Michel Ané. 2015. 'Yield Response to Crop/Genotype Rotations and Fungicide Use to Manage Fusarium-related Diseases', *Crop Science*, 55: 889-98.

Masuda, Daisuke, Mamoru Ishida, Kazuo Yamaguchi, Isamu Yamaguchi, Makoto Kimura, and Takumi Nishiuchi. 2007. 'Phytotoxic effects of trichothecenes on the growth and morphology of Arabidopsis thaliana', *Journal of Experimental Botany*, 58: 1617-26.

McCartney, C. A., D. J. Somers, G. Fedak, and W. Cao. 2004. 'Haplotype diversity at fusarium head blight resistance QTLs in wheat', *Theoretical and Applied Genetics*, 109: 261-71.

McCartney, C. A., D. J. Somers, G. Fedak, R. M. DePauw, J. Thomas, S. L. Fox, D. G. Humphreys, O. Lukow, M. E. Savard, B. D. McCallum, J. Gilbert, and W. Cao. 2007. 'The evaluation of FHB resistance QTLs introgressed into elite Canadian spring wheat germplasm', *Molecular Breeding*, 20: 209-21.

McCormick, S.P., A.M. Stanley, N.A. Stover, and N.J. Alexander. 2011. 'Trichothecenes: From Simple to Complex Mycotoxins', *Toxins*, 3: 802-14.

McCormick, Susan P. 2013. 'Microbial Detoxification of Mycotoxins', *Journal of Chemical Ecology*, 39: 907-18.

McLean, Michelle. 1995. 'The phytotoxicity of selected mycotoxins on mature, germinatingZea mays embryos', *Mycopathologia*, 132: 173-83.

McMullen, M., R. Jones, and D. Gallenberg. 1997. 'Scab of Wheat and Barley: A Re-emerging Disease of Devastating Impact', *Plant Dis*, 81: 1340-48.

Mesterházy, A. 1995. 'Types and components of resistance to Fusarium head blight of wheat', *Plant Breeding*, 114: 377-86.

Mesterházy, Á., T. Bartók, C. G. Mirocha, and R. Komoróczy. 1999. 'Nature of wheat resistance to Fusarium head blight and the role of deoxynivalenol for breeding', *Plant Breeding*, 118: 97-110.

Miedaner, T., F. Wilde, V. Korzun, E. Ebmeyer, M. Schmolke, L. Hartl, and C.C. Schön. 2009. 'Marker selection for Fusarium head blight resistance based on quantitative trait loci (QTL) from two European sources compared to phenotypic selection in winter wheat', *Euphytica*, 166: 219-27.

Miedaner, T., F. Wilde, B. Steiner, H. Buerstmayr, V. Korzun, and E. Ebmeyer. 2006. 'Stacking quantitative trait loci (QTL) for Fusarium head blight resistance from non-adapted sources in an European elite spring wheat background and assessing their effects on deoxynivalenol (DON) content and disease severity', *Theor Appl Genet*, 112: 562-9.

Miller, J.D. , J.C. Young, and D.R. Sampson. 1985. 'Deoxynivalenol and Fusarium Head Blight Resistance in Spring Cereals', *J Phytopath*, 113: 359-67.

Nicholson, P. 2009. *Fusarium and Fusarium-cereal interactions. John Wiley & Sons, Ltd.*

Niwa, S., K. Kubo, J. Lewis, R. Kikuchi, M. Alagu, and T. Ban. 2014. 'Variations for Fusarium head blight resistance associated with genomic diversity in different sources of the resistant wheat cultivar 'Sumai 3'', *Breeding Science*, 64: 90-96.

O'Donnell, Kerry, Todd J. Ward, David M. Geiser, H. Corby Kistler, and Takayuki Aoki. 2004. 'Genealogical concordance between the mating type locus and seven other nuclear genes supports formal recognition of nine phylogenetically distinct species within the Fusarium graminearum clade', *Fungal Genetics and Biology*, 41: 600-23.

OECD/FAO. 2019. "OECD-FAO Agricultural Outlook." In. Paris: OECD Agriculture Statistics.

Oliveros, J. C. . 2007-2015. "Venny. An interactive tool for comparing lists with Venn's diagrams. ." In.

Osborne, L.E., and J.M. Stein. 2007. 'Epidemiology of Fusarium head blight on small-grain cereals', *Int J Food Microbiol*, 119: 103-8.

Paillard, S., T. Schnurbusch, R. Tiwari, M. Messmer, M. Winzeler, B. Keller, and G. Schachermayr. 2004. 'QTL analysis of resistance to Fusarium head blight in Swiss winter wheat (Triticum aestivum L.)', *Theoretical and Applied Genetics*, 109: 323-32.

Pallotta, M , P Warner, RL Fox, H Kuchel, SJ Jefferies, and P Langridge. 2003. *Marker assisted wheat breeding in the southern region of Australia* (Istituto Sperimentale per per la Cerealicoltura: Paestum, Italy).

Parry, D.W., P. Jenkinson, and L. McLeod. 1995. 'Fusarium ear blight (scab) in small grain cereals - a review', *Plant Pathol*, 44: 207-38.

Pasquet, Jean-Claude, Valentin Changenet, Catherine Macadré, Edouard Boex-Fontvieille, Camille Soulhat, Oumaya Bouchabké-Coussa, Marion Dalmais, Vessela Atanasova-Pénichon, Abdelhafid Bendahmane, Patrick Saindrenan, and Marie Dufresne. 2016. 'A Brachypodium UDP-Glycosyltransferase Confers Root Tolerance to Deoxynivalenol and Resistance to Fusarium Infection', *Plant Physiology*, 172: 559-74.

Pasquet, Jean-Claude, Séjir Chaouch, Catherine Macadré, Sandrine Balzergue, Stéphanie Huguet, Marie-Laure Martin-Magniette, Floriant Bellvert, Xavier Deguercy, Vincent Thareau, Dimitri Heintz, Patrick Saindrenan, and Marie Dufresne. 2014. 'Differential gene expression and metabolomic analyses of Brachypodium distachyon infected by deoxynivalenol producing and non-producing strains of Fusarium graminearum', *BMC Genomics*, 15: 629-29.

Pereyra, S.A., R. Dill-Macky, and A.L. Sims. 2004. 'Survival and Inoculum Production of *Gibberella zeae* in Wheat Residue', *Plant Disease*, 88: 724-30.

Perochon, A., J. Jianguang, A. Kahla, C. Arunachalam, S. R. Scofield, S. Bowden, E. Wallington, and F. M. Doohan. 2015. 'TaFROG Encodes a Pooideae Orphan Protein That Interacts with SnRK1 and Enhances Resistance to the Mycotoxigenic Fungus Fusarium graminearum', *Plant Physiol*, 169: 2895-906.

Perochon, Alexandre, Amal Kahla, Monika Vranić, Jianguang Jia, Keshav B. Malla, Melanie Craze, Emma Wallington, and Fiona M. Doohan. 2019. 'A wheat NAC interacts with an orphan protein and enhances resistance to Fusarium head blight disease', *Plant Biotechnol J*, 17: 1892-904.

Pestka, J.J. 2010a. 'Deoxynivalenol-Induced Proinflammatory Gene Expression: Mechanisms and Pathological Sequelae', *Toxins*, 2: 1300.

Pestka, James J., Hui-Ren Zhou, Y. Moon, and Y. J. Chung. 2004. 'Cellular and molecular mechanisms for immune modulation by deoxynivalenol and other trichothecenes: unraveling a paradox', *Toxicology Letters*, 153: 61-73.

Pestka, JJ. 2010b. 'Deoxynivalenol: mechanisms of action, human exposure, and toxicological relevance', *Arch Toxicol*, 84: 663-79.

Petersen, G., O. Seberg, M. Yde, and K. Berthelsen. 2006. 'Phylogenetic relationships of Triticum and Aegilops and evidence for the origin of the A, B, and D genomes of common wheat (Triticum aestivum)', *Mol Phylogenet Evol*, 39: 70-82.

Poppenberger, B., F. Berthiller, D. Lucyshyn, T. Sieberer, R. Schuhmacher, R. Krska, K. Kuchler, J. Glossl, C. Luschnig, and G. Adam. 2003. 'Detoxification of the Fusarium mycotoxin deoxynivalenol by a UDP-glucosyltransferase from *Arabidopsis thaliana*', *J Biol Chem*, 278: 47905-14.

Puri, K.D., and S. Zhong. 2010. 'The 3ADON Population of *Fusarium graminearum* Found in North Dakota Is More Aggressive and Produces a Higher Level of DON than the Prevalent 15ADON Population in Spring Wheat', *Phytopathol*, 100: 1007-14.

Qi, L. L., M. O. Pumphrey, Bernd Friebe, P. D. Chen, and B. S. Gill. 2008. 'Molecular cytogenetic characterization of alien introgressions with gene Fhb3 for resistance to Fusarium head blight disease of wheat', *Theoretical and Applied Genetics*, 117: 1155-66.

Rahman, Shanjida, Shahidul Islam, Zitong Yu, Maoyun She, Eviatar Nevo, and Wujun Ma. 2020. 'Current Progress in Understanding and Recovering the Wheat Genes Lost in Evolution and Domestication', *International journal of molecular sciences*, 21: 5836.

Ramírez-González, R. H., P. Borrill, D. Lang, S. A. Harrington, J. Brinton, L. Venturini, M. Davey, J. Jacobs, F. van Ex, A. Pasha, Y. Khedikar, S. J. Robinson, A. T. Cory, T. Florio, L. Concia, C. Juery, H. Schoonbeek, B. Steuernagel, D. Xiang, C. J. Ridout, B. Chalhoub, K. F. X. Mayer, M. Benhamed, D. Latrasse, A. Bendahmane, B. B. H. Wulff, R. Appels, V. Tiwari, R. Datla, F. Choulet, C. J. Pozniak, N. J. Provart, A. G. Sharpe, E. Paux, M. Spannagl, A. Bräutigam, C. Uauy, Abraham Korol, Andrew G. Sharpe, Angéla Juhász, Antje Rohde, Arnaud Bellec, Assaf Distelfeld, Bala Ani Akpinar, Beat Keller, Benoit Darrier, Bikram Gill, Boulos Chalhoub, Burkhard Steuernagel, Catherine Feuillet, Chanderkant Chaudhary, Cristobal Uauy, Curtis Pozniak, Danara Ormanbekova, Daoquan Xiang, David Latrasse, David Swarbreck, Delfina Barabaschi, Dina Raats, Ekaterina Sergeeva, Elena Salina, Etienne Paux, Federica Cattonaro, Frédéric Choulet, Fuminori Kobayashi, Gabriel Keeble-Gagnere, Gaganpreet Kaur, Gary Muehlbauer, George Kettleborough, Guotai Yu, Hana Šimková, Heidrun Gundlach, Hélène Berges, Hélène Rimbert, Hikmet Budak, Hirokazu Handa, Ian Small, Jan Bartoš, Jane Rogers, Jaroslav Doležel, Jens Keilwagen, Jesse Poland, Joanna Melonek, John Jacobs, Jon Wright, Jonathan D. G. Jones, Juan Gutierrez-Gonzalez, Kellye Eversole, Kirby Nilsen, Klaus F.X. Mayer, Kostya Kanyuka, Kuldeep Singh, Liangliang Gao, Lorenzo Concia, Luca Venturini, Luigi Cattivelli, Manuel Spannagl, Martin Mascher, Matthew Hayden, Michael Abrouk, Michael Alaux, Mingcheng Luo, Miroslav Valárik, Moussa Benhamed, Nagendra K. Singh, Naveen Sharma, Nicolas Guilhot, Nikolai Ravin, Nils Stein, Odd-Arne Olsen, Om Prakash Gupta, Paramjit Khurana, Parveen Chhuneja, Philipp E. Bayer, Philippa Borrill, Philippe Leroy, Philippe Rigault, Pierre Sourdille, Pilar Hernandez, Raphael Flores, Ricardo H. Ramirez-Gonzalez, Robert King, Ron Knox, Rudi Appels, Ruonan Zhou, Sean Walkowiak, Sergio Galvez, Sezgi Biyiklioglu, Shuhei Nasuda, Simen Sandve, Smahane Chalabi, Song Weining, Sunish Sehgal, Suruchi Jindal, Tatiana Belova, Thomas Letellier, Thomas Wicker, Tsuyoshi Tanaka, Tzion Fahima, Valérie Barbe, Vijay Tiwari, Vinod Kumar, and Yifang Tan. 2018. 'The transcriptional landscape of polyploid wheat', *Science*, 361: eaar6089.

Ramirez-Gonzalez, Ricardo H., Vanesa Segovia, Nicholas Bird, Paul Fenwick, Sarah Holdgate, Simon Berry, Peter Jack, Mario Caccamo, and Cristobal Uauy. 2015. 'RNA-Seq bulked segregant analysis enables the identification of high-resolution genetic markers for breeding in hexaploid wheat', *Plant Biotechnol J*, 13: 613-24.

Ramirez-Gonzalez, Ricardo H., Cristobal Uauy, and Mario Caccamo. 2015. 'PolyMarker: A fast polyploid primer design pipeline', *Bioinformatics*, 31: 2038-39.

Rawat, N., M.O. Pumphrey, S. Liu, X. Zhang, V.K. Tiwari, K. Ando, H.N. Trick, W.W. Bockus, E. Akhunov, J.A. Anderson, and B.S. Gill. 2016. 'Wheat *Fhb1* encodes a chimeric lectin

with agglutinin domains and a pore-forming toxin-like domain conferring resistance to Fusarium head blight', *Nature Genet*, 48: 1576.

Rey, María-Dolores, Azahara C. Martín, Mark Smedley, Sadiye Hayta, Wendy Harwood, Peter Shaw, and Graham Moore. 2018. 'Magnesium Increases Homoeologous Crossover Frequency During Meiosis in ZIP4 (Ph1 Gene) Mutant Wheat-Wild Relative Hybrids', *Frontiers in Plant Science*, 9.

Ribichich, K.F., S.E. Lopez, and A.C. Vegetti. 2000. 'Histopathological spikelet changes produced by *Fusarium graminearum* in susceptible and resistant wheat cultivars', *Plant Disease*, 84: 794-802.

Rocha, O., K. Ansari, and F. M. Doohan. 2005. 'Effects of trichothecene mycotoxins on eukaryotic cells: A review', *Food Additives & Contaminants*, 22: 369-78.

Rudd, J., R. Horsley, A. McKendry, and E. Elias. 2001. 'Host plant resistance genes for fusarium head blight: Sources, mechanisms, and utility in conventional breeding systems', *Crop Sci*, 41: 620-27.

Rynkiewicz, Michael J., David E. Cane, and David W. Christianson. 2001. 'Structure of trichodiene synthase from Fusarium sporotrichioides provides mechanistic inferences on the terpene cyclization cascade', *Proceedings of the National Academy of Sciences*, 98: 13543-48.

Saharan, M. S. 2020. 'Current status of resistant source to Fusarium head blight disease of wheat: a review', *Indian Phytopathology*, 73: 3-9.

Salameh, A., M. Buerstmayr, B. Steiner, A. Neumayer, M. Lemmens, and H. Buerstmayr. 2011. 'Effects of introgression of two QTL for fusarium head blight resistance from Asian spring wheat by marker-assisted backcrossing into European winter wheat on fusarium head blight resistance, yield and quality traits', *Molecular Breeding*, 28: 485-94.

Sánchez-Vallet, A., J. R. Mesters, and B. P. Thomma. 2015. 'The battle for chitin recognition in plant-microbe interactions', *FEMS Microbiol Rev*, 39: 171-83.

Santos, M. A. Costa e Silva dos. 2021. 'Brachypodium distachyon as a model to understand resistance to wheat root diseases', University of East Anglia.

Sarowar, S., S. T. Alam, R. Makandar, H. Lee, H. N. Trick, Y. Dong, and J. Shah. 2019. 'Targeting the pattern-triggered immunity pathway to enhance resistance to Fusarium graminearum', *Mol Plant Pathol*, 20: 626-40.

Sato, Ikuo, Michihiro Ito, Masumi Ishizaka, Yoko Ikunaga, Yukari Sato, Shigenobu Yoshida, Motoo Koitabashi, and Seiya Tsushima. 2012. 'Thirteen novel deoxynivalenol-degrading bacteria are classified within two genera with distinct degradation mechanisms', *FEMS Microbiology Letters*, 327: 110-17.

Schenk, P.M., K. Kazan, I. Wilson, J.P. Anderson, T. Richmond, S.C. Somerville, and J.M. Manners. 2000. 'Coordinated plant defense responses in *Arabidopsis* revealed by microarray analysis', *Proc Natl Acad Sci U S A*, 97: 11655-60.

Schoonbeek, H. J., H. H. Wang, F. L. Stefanato, M. Craze, S. Bowden, E. Wallington, C. Zipfel, and C. J. Ridout. 2015. 'Arabidopsis EF-Tu receptor enhances bacterial disease resistance in transgenic wheat', *New Phytol*, 206: 606-13.

Schroeder, H.W., and J.J. Christensen. 1963. 'Factors affecting resistance of Wheat to scab caused by *Gibberella zeae*', *Phytopathol*, 53: 831-38.

Schweiger, W., J. Boddu, S. Shin, B. Poppenberger, F. Berthiller, M. Lemmens, G.J. Muehlbauer, and G. Adam. 2010. 'Validation of a Candidate Deoxynivalenol-Inactivating UDP-Glucosyltransferase from Barley by Heterologous Expression in Yeast', *Mol Plant Microbe Interact*, 23: 977-86.

Schweiger, W., B. Steiner, C. Ametz, G. Siegwart, G. Wiesenberger, F. Berthiller, M. Lemmens, H. Y. Jia, G. Adam, G.J. Muehlbauer, D.P. Kreil, and H. Buerstmayr. 2013. 'Transcriptomic characterization of two major Fusarium resistance quantitative trait loci (QTLs), Fhb1 and Qfhs.ifa-5A, identifies novel candidate genes', *Mol Plant Pathol*, 14: 772-85.

Schweiger, W., B. Steiner, S. Vautrin, T. Nussbaumer, G. Siegwart, M. Zamini, F. Jungreithmeier, V. Gratl, M. Lemmens, K. F. X. Mayer, H. Bérgès, G. Adam, and H. Buerstmayr. 2016. 'Suppressed recombination and unique candidate genes in the divergent haplotype encoding Fhb1, a major Fusarium head blight resistance locus in wheat', *Theor Appl Genet*, 129: 1607-23.

Schweiger, Wolfgang, Jean-Claude Pasquet, Thomas Nussbaumer, Maria Paula Kovalsky Paris, Gerlinde Wiesenberger, Catherine Macadré, Christian Ametz, Franz Berthiller, Marc Lemmens, Patrick Saindrenan, Hans-Werner Mewes, Klaus F. X. Mayer, Marie Dufresne, and Gerhard Adam. 2013. 'Functional Characterization of Two Clusters of Brachypodium distachyon UDP-Glycosyltransferases Encoding Putative Deoxynivalenol Detoxification Genes', *Molecular Plant-Microbe Interactions®*, 26: 781-92.

Seong, K.Y., M. Pasquali, X. Zhou, J. Song, K. Hilburn, S. McCormick, Y. Dong, J.R. Xu, and H.C. Kistler. 2009. 'Global gene regulation by *Fusarium* transcription factors *Tri6* and *Tri10* reveals adaptations for toxin biosynthesis', *Mol Microbiol*, 72: 354-67.

Shah, D. A., E. D. De Wolf, P. A. Paul, and L. V. Madden. 2014. 'Predicting Fusarium head blight epidemics with boosted regression trees', *Phytopathology*, 104: 702-14.

Shah, L., A. Ali, Y.L. Zhu, S.X. Wang, H.Q. Si, and C.X. Ma. 2017. 'Wheat Resistance to Fusarium Head Blight and Possibilities of its Improvement using Molecular Marker-Assisted Selection', *Czech J Genet Plant* 53: 47-54.

Shan, Qiwei, Yanpeng Wang, Jun Li, and Caixia Gao. 2014. 'Genome editing in rice and wheat using the CRISPR/Cas system', *Nature Protocols*, 9: 2395-410.

Shaner, G. 2002. "Resistance in hexaploid wheat to Fusarium head blight." In *In: Proceedings of National Fusarium Head Blight Forum*, pp 208-11. Erlanger, KY: Michigan State Univ., East Lansing.

Shen, X.R., M. Ittu, and H.W. Ohm. 2003. 'Quantitative Trait Loci Conditioning Resistance to Fusarium Head Blight in Wheat Line F201R ', *Crop Sci*, 43: 850-57.

Shewry, P.R. 2009. 'Wheat', *J Exp Bot*, 60: 1537-53.

Shi, J. R., D. H. Xu, H. Y. Yang, Q. X. Lu, and T. Ban. 2008. 'DNA marker analysis for pyramided of Fusarium head blight (FHB) resistance QTLs from different germplasm', *Genetica*, 133: 77-84.

Shimada, T., and M. Otani. 1990. 'EFFECTS OF FUSARIUM MYCOTOXINS ON THE GROWTH OF SHOOTS AND ROOTS AT GERMINATION IN SOME JAPANESE WHEAT CULTIVARS', *Cereal Research Communications*, 18: 229-32.

Shimizu, T., T. Nakano, D. Takamizawa, Y. Desaki, N. Ishii-Minami, Y. Nishizawa, E. Minami, K. Okada, H. Yamane, H. Kaku, and N. Shibuya. 2010. 'Two LysM receptor molecules, CEBiP and OsCERK1, cooperatively regulate chitin elicitor signaling in rice', *Plant J*, 64: 204-14.

Shimono, Masaki, Shoji Sugano, Akira Nakayama, Chang-Jie Jiang, Kazuko Ono, Seiichi Toki, and Hiroshi Takatsuji. 2007. 'Rice WRKY45 Plays a Crucial Role in Benzothiadiazole-Inducible Blast Resistance', *The Plant Cell*, 19: 2064-76.

Shin, S., J.A. Torres-Acosta, S.J. Heinen, S. McCormick, M. Lemmens, M.P.K. Paris, F. Berthiller, G. Adam, and G.J. Muehlbauer. 2012. 'Transgenic *Arabidopsis thaliana* expressing a barley UDP-glucosyltransferase exhibit resistance to the mycotoxin deoxynivalenol', *J Exp Bot*, 63: 4731-40.

Simpson, D.R., G.E. Weston, J.A. Turner, P. Jennings, and P. Nicholson. 2001. 'Differential Control of Head Blight Pathogens of Wheat by Fungicides and Consequences for Mycotoxin Contamination of Grain', *Eur J Plant Pathol*, 107: 421-31.

Skinnes, H., K. Semagn, Y. Tarkegne, A. G. Maroy, and A. Bjornstad. 2010. 'The inheritance of anther extrusion in hexaploid wheat and its relationship to Fusarium head blight resistance and deoxynivalenol content', *Plant Breeding*, 129: 149-55.

Smith, W.G. 1884. *Diseases of Field and Garden Crops* (MacMillan and Co: London).

Snijders, C. H. 2004. 'Resistance in wheat to Fusarium infection and trichothecene formation', *Toxicol Lett*, 153: 37-46.

Somers, D.J., G. Fedak, and M. Savard. 2003. 'Molecular mapping of novel genes controlling Fusarium head blight resistance and deoxynivalenol accumulation in spring wheat', *Genome*, 46: 555-64.

Srinivasachary, N. Gosman, A. Steed, T.W. Hollins, R. Bayles, P. Jennings, and P. Nicholson. 2009. 'Semi-dwarfing *Rht-B1* and *Rht-D1* loci of wheat differ significantly in their influence on resistance to Fusarium head blight', *Theor Appl Genet*, 118: 695-702.

Steiner, B., M. Lemmens, M. Griesser, U. Scholz, J. Schondelmaier, and H. Buerstmayr. 2004. 'Molecular mapping of resistance to Fusarium head blight in the spring wheat cultivar Frontana', *Theor Appl Genet*, 109: 215-24.

Steiner, Barbara, Maria Buerstmayr, Sebastian Michel, Wolfgang Schweiger, Marc Lemmens, and Hermann Buerstmayr. 2017. 'Breeding strategies and advances in line selection for Fusarium head blight resistance in wheat', *Tropical Plant Pathology*, 42: 165-74.

Steiner, Barbara, Maria Buerstmayr, Christian Wagner, Andrea Danler, Babur Eshonkulov, Magdalena Ehn, and Hermann Buerstmayr. 2019. 'Fine-mapping of the Fusarium head blight resistance QTL Qfhs.ifa-5A identifies two resistance QTL associated with anther extrusion', *Theor Appl Genet*, 132: 2039-53.

Su, Zhenqi, Amy Bernardo, Bin Tian, Hui Chen, Shan Wang, Hongxiang Ma, Shibin Cai, Dongtao Liu, Dadong Zhang, Tao Li, Harold Trick, Paul St. Amand, Jianming Yu, Zengyan Zhang, and Guihua Bai. 2019. 'A deletion mutation in TaHRC confers Fhb1 resistance to Fusarium head blight in wheat', *Nature Genetics*, 51: 1099-105.

Sun, Jin-Yue, Denis Gaudet, Zhen-Xiang Lu, Michele Frick, Byron Puchalski, and André Laroche. 2008. 'Characterization and Antifungal Properties of Wheat Nonspecific Lipid Transfer Proteins', *Mol Plant Microbe Interact*, 21: 346-60.

Suzuki, T., M. Sato, and T. Takeuchi. 2012. 'Evaluation of the effects of five QTL regions on Fusarium head blight resistance and agronomic traits in spring wheat (Triticum aestivum L.)', *Breed Sci*, 62: 11-7.

Tao, Zeng, Hongbo Liu, Deyun Qiu, Yan Zhou, Xianghua Li, Caiguo Xu, and Shiping Wang. 2009. 'A Pair of Allelic WRKY Genes Play Opposite Roles in Rice-Bacteria Interactions ', *Plant Physiology*, 151: 936-48.

Theune, Marius L., Ulrich Bloss, Luise H. Brand, Friederike Ladwig, and Dierk Wanke. 2019. 'Phylogenetic Analyses and GAGA-Motif Binding Studies of BBR/BPC Proteins Lend to Clues in GAGA-Motif Recognition and a Regulatory Role in Brassinosteroid Signaling', *Frontiers in Plant Science*, 10.

Thompson, C.J. . 2010. 'Evaluation of an inoculation method and quantitative trait loci for Fusarium Head Blight resistance in wheat', University of Illinois at Urbana-Champaign.

Tian, Ye, Yanglan Tan, Na Liu, Yucai Liao, Changpo Sun, Shuangxia Wang, and Aibo Wu. 2016. 'Functional Agents to Biologically Control Deoxynivalenol Contamination in Cereal Grains', *Frontiers in Microbiology*, 7.

Trail, F. 2009. 'For Blighted Waves of Grain: *Fusarium graminearum* in the Postgenomics Era', *Plant Physiol*, 149: 103-10.

Trapp, S. C., T. M. Hohn, S. McCormick, and B. B. Jarvis. 1998. 'Characterization of the gene cluster for biosynthesis of macrocyclic trichothecenes in Myrothecium roridum', *Molecular and General Genetics MGG*, 257: 421-32.

Truman, William, Mark H. Bennett, Ines Kubigsteltig, Colin Turnbull, and Murray Grant. 2007. 'Arabidopsis systemic immunity uses conserved defense signaling pathways and is mediated by jasmonates', *Proceedings of the National Academy of Sciences*, 104: 1075-80.

Ülker, Bekir, and Imre E. Somssich. 2004. 'WRKY transcription factors: from DNA binding towards biological function', *Current Opinion in Plant Biology*, 7: 491-98.

Union, The European. 2006. "Commission Regulation (EC) No 1881/2006 setting maximum levels of certain contaminants in foodsstuffs." In *Official Journal of the European Union*, 5-24.

Untergasser, Andreas, Harm Nijveen, Xiangyu Rao, Ton Bisseling, René Geurts, and Jack A. M. Leunissen. 2007. 'Primer3Plus, an enhanced web interface to Primer3', *Nucleic acids research*, 35: W71-W74.

van der Lee, Theo, Hao Zhang, Anne van Diepeningen, and Cees Waalwijk. 2015. 'Biogeography of Fusarium graminearum species complex and chemotypes: a review', *Food additives & contaminants. Part A, Chemistry, analysis, control, exposure & risk assessment*, 32: 453-60.

Venske, Eduardo, Railson Schreinert Dos Santos, Daniel da Rosa Farias, Vianei Rother, Luciano Carlos da Maia, Camila Pegoraro, and Antonio Costa de Oliveira. 2019. 'Meta-Analysis of the QTLome of Fusarium Head Blight Resistance in Bread Wheat: Refining the Current Puzzle', *Frontiers in Plant Science*, 10: 727-27.

von der Ohe, C., E. Ebmeyer, V. Korzun, and T. Miedaner. 2010. 'Agronomic and Quality Performance of Winter Wheat Backcross Populations Carrying Non-Adapted Fusarium Head Blight Resistance QTL', *Crop Science*, 50: 2283-90.

Waldron, B. L., B. Moreno-Sevilla, J. A. Anderson, R. W. Stack, and R. C. Frohberg. 1999. 'RFLP Mapping of QTL for Fusarium Head Blight Resistance in Wheat', *Crop Science*, 39: cropsci1999.0011183X003900030032x.

Walter, S., and F.M. Doohan. 2011. 'Transcript profiling of the phytotoxic response of wheat to the *Fusarium* mycotoxin deoxynivalenol', *Mycotoxin Res*, 27: 221-30.

Walter, S., A. Kahla, C. Arunachalam, A. Perochon, M. R. Khan, S. R. Scofield, and F. M. Doohan. 2015. 'A wheat ABC transporter contributes to both grain formation and mycotoxin tolerance', *J Exp Bot*, 66: 2583-93.

Walter, Stephanie, Paul Nicholson, and Fiona M. Doohan. 2010. 'Action and reaction of host and pathogen during Fusarium head blight disease', *New Phytologist*, 185: 54-66.

Wan, Jinrong, Xue-Cheng Zhang, David Neece, Katrina M. Ramonell, Steve Clough, Sung-Yong Kim, Minviluz G. Stacey, and Gary Stacey. 2008. 'A LysM receptor-like kinase plays a critical role in chitin signaling and fungal resistance in Arabidopsis', *The Plant Cell*, 20: 471-81.

Wang, Hongwei, Silong Sun, Wenyang Ge, Lanfei Zhao, Bingqian Hou, Kai Wang, Zhongfan Lyu, Liyang Chen, Shoushen Xu, Jun Guo, Min Li, Peisen Su, Xuefeng Li, Guiping Wang, Cunyao Bo, Xiaojian Fang, Wenwen Zhuang, Xinxin Cheng, Jianwen Wu, Luhao Dong, Wuying Chen, Wen Li, Guilian Xiao, Jinxiao Zhao, Yongchao Hao, Ying Xu, Yu Gao, Wenjing Liu, Yanhe Liu, Huayan Yin, Jiazhu Li, Xiang Li, Yan Zhao, Xiaoqian Wang, Fei Ni, Xin Ma, Anfei Li, Steven S. Xu, Guihua Bai, Eviatar Nevo, Caixia Gao, Herbert Ohm, and Lingrang Kong. 2020. 'Horizontal gene transfer of Fhb7 from fungus underlies Fusarium head blight resistance in wheat', *Science*: eaba5435.

Wang, Y. Z., and J. D. Miller. 1988. 'Effects of Fusarium graminearum Metabolites on Wheat Tissue in Relation to Fusarium Head Blight Resistance', *Journal of Phytopathology*, 122: 118-25.

Wang, Yanpeng, Xi Cheng, Qiwei Shan, Yi Zhang, Jinxing Liu, Caixia Gao, and Jin-Long Qiu. 2014. 'Simultaneous editing of three homoeoalleles in hexaploid bread wheat confers heritable resistance to powdery mildew', *Nature Biotechnology*, 32: 947-51.

Wegulo, S.N. 2012. 'Factors influencing deoxynivalenol accumulation in small grain cereals', *Toxins* 4: 1157-80.

Wegulo, Stephen N., and Floyd E. Dowell. 2008. 'Near-infrared versus visual sorting of Fusarium-damaged kernels in winter wheat', *Canadian Journal of Plant Science*, 88: 1087-89.

Wilde, F., V. Korzun, E. Ebmeyer, H. H. Geiger, and T. Miedaner. 2007. 'Comparison of phenotypic and marker-based selection for Fusarium head blight resistance and DON content in spring wheat', *Molecular Breeding*, 19: 357-70.

Winfield, Mark O., Alexandra M. Allen, Amanda J. Burridge, Gary L. A. Barker, Harriet R. Benbow, Paul A. Wilkinson, Jane Coghill, Christy Waterfall, Alessandro Davassi, Geoff Scopes, Ali Pirani, Teresa Webster, Fiona Brew, Claire Bloor, Julie King, Claire West, Simon Griffiths, Ian King, Alison R. Bentley, and Keith J. Edwards. 2016. 'High-density SNP genotyping array for hexaploid wheat and its secondary and tertiary gene pool', *Plant Biotechnol J*, 14: 1195-206.

Xiao, J., X. Jin, X. Jia, H. Wang, A. Cao, W. Zhao, H. Pei, Z. Xue, L. He, Q. Chen, and X. Wang. 2013. 'Transcriptome-based discovery of pathways and genes related to resistance against Fusarium head blight in wheat landrace Wangshuibai', *BMC Genomics*, 14: 197.

Xing, L.-P., L.-Q. He, J. Xiao, Q.-G. Chen, M.-H. Li, Y. Shang, Y.-F. Zhu, P.-D. Chen, A.-Z. Cao, and X.-E. Wang. 2017. 'An UDP-Glucosyltransferase Gene from Barley Confers Disease Resistance to Fusarium Head Blight', *Plant Mol Biol Report*, 35: 224-36.

Xu, DH, HF Juan, M Nohda, and T Ban. 2001. "QTLs mapping of type I and type II resistance to FHB in wheat." In *National Fusarium heading blight. Forum Proceedings, Erlanger, KY. Michigan State University, East Lansing. pp*, 40-42.

Xu, X., and P. Nicholson. 2009. 'Community Ecology of Fungal Pathogens Causing Wheat Head Blight', *Annu Rev Phytopathol*, 47: 83-103.

Xu, Xiangming, P. Nicholson, and A. Ritieni. 2007. 'Effects of fungal interactions among Fusarium head blight pathogens on disease development and mycotoxin accumulation', *International Journal of Food Microbiology*, 119: 67-71.

Xue, S.L., G. Li, H. Jia, F. Xu, F. Lin, M. Tang, Y. Wang, X. An, H. Xu, L. Zhang, Z.X. Kong, and Z.Q. Ma. 2010. 'Fine mapping *Fhb4*, a major QTL conditioning resistance to *Fusarium* infection in bread wheat *(Triticum aestivum* L.)', *Theor Appl Genet*, 121: 147-56.

Xue, Shulin, Feng Xu, Mingzhi Tang, Yan Zhou, Guoqiang Li, Xia An, Feng Lin, Haibin Xu, Haiyan Jia, Lixia Zhang, Zhongxin Kong, and Zhengqiang Ma. 2011. 'Precise mapping Fhb5, a

major QTL conditioning resistance to Fusarium infection in bread wheat (Triticum aestivum L.)', *Theoretical and Applied Genetics*, 123: 1055-63.

Yang, Z., J. Gilbert, G. Fedak, and D. J. Somers. 2005. 'Genetic characterization of QTL associated with resistance to Fusarium head blight in a doubled-haploid spring wheat population', *Genome*, 48: 187-96.

Yang, Z. P., J. Gilbert, D. J. Somers, G. Fedak, J. D. Procunier, and I. H. McKenzie. 2003. 'Marker Assisted Selection of Fusarium Head Blight Resistance Genes in Two Doubled-Haploid Populations of Wheat', *Molecular Breeding*, 12: 309-17.

Yi, Xin, Jingye Cheng, Zhengning Jiang, Wenjing Hu, Tongde Bie, Derong Gao, Dongsheng Li, Ronglin Wu, Yuling Li, Shulin Chen, Xiaoming Cheng, Jian Liu, Yong Zhang, and Shunhe Cheng. 2018. 'Genetic Analysis of Fusarium Head Blight Resistance in CIMMYT Bread Wheat Line C615 Using Traditional and Conditional QTL Mapping', *Frontiers in Plant Science*, 9.

Young, J. Christopher, Ting Zhou, Hai Yu, Honghui Zhu, and Jianhua Gong. 2007. 'Degradation of trichothecene mycotoxins by chicken intestinal microbes', *Food and Chemical Toxicology*, 45: 136-43.

Zain, M. E., A. H. Bahkali, and Mounerah R. Al-Othman. 2012. 'Effect of chemical compounds on amino acid content of some Fusarium species and its significance to fungal chemotaxonomy', *Journal of Saudi Chemical Society*, 16: 183-92.

Zhang, Li. 2011. 'Controlling fusarium head blight of wheat (triticum aestivum L.) with genetics', *Advances in Bioscience and Biotechnology*, 02: 263-70.

Zhang, Qijun, Jason E. Axtman, Justin D. Faris, Shiaoman Chao, Zengcui Zhang, Timothy L. Friesen, Shaobin Zhong, Xiwen Cai, Elias M. Elias, and Steven S. Xu. 2014. 'Identification and molecular mapping of quantitative trait loci for Fusarium head blight resistance in emmer and durum wheat using a single nucleotide polymorphism-based linkage map', *Molecular Breeding*, 34: 1677-87.

Zhang, Wentao, Tammy Francis, Peng Gao, Kerry Boyle, Fengying Jiang, François Eudes, Richard Cuthbert, Andrew Sharpe, and Pierre R. Fobert. 2018. 'Genetic characterization of type II Fusarium head blight resistance derived from transgressive segregation in a cross between Eastern and Western Canadian spring wheat', *Molecular Breeding*, 38: 13.

Zhang, Yuwen, Ziwen Li, Biao Ma, Quancan Hou, and Xiangyuan Wan. 2020. 'Phylogeny and Functions of LOB Domain Proteins in Plants', *International journal of molecular sciences*, 21: 2278.

Zhao, C., F. Cui, X. Wang, S. Shan, X. Li, Y. Bao, and H. Wang. 2012. 'Effects of 1BL/1RS translocation in wheat on agronomic performance and quality characteristics', *Field Crops Res*, 127: 79-84.

Zhao, L., X. Ma, P. Su, W. Ge, H. Wu, X. Guo, A. Li, H. Wang, and L. Kong. 2018. 'Cloning and characterization of a specific UDP-glycosyltransferase gene induced by DON and Fusarium graminearum', *Plant Cell Rep*, 37: 641-52.

Zhao, M., Y. Leng, S. Chao, S. S. Xu, and S. Zhong. 2018. 'Molecular mapping of QTL for Fusarium head blight resistance introgressed into durum wheat', *Theor Appl Genet*, 131: 1939-51.

Zhou, W. C., F. L. Kolb, G. H. Bai, L. L. Domier, and J. B. Yao. 2002. 'Effect of individual Sumai 3 chromosomes on resistance to scab spread within spikes and deoxynivalenol accumulation within kernels in wheat', *Hereditas*, 137: 81-9.

Zhou, Xiaohong, Ke Wang, Lipu Du, Yongwei Liu, Zhishan Lin, and Xingguo Ye. 2016. 'Effects of the wheat UDP-glucosyltransferase gene TaUGT-B2 on Agrobacterium-mediated plant transformation', *Acta Physiologiae Plantarum*, 39: 15.

Zhu, Xianwen, Shaobin Zhong, Shiaoman Chao, Yong Qiang Gu, Shahryar F. Kianian, Elias Elias, and Xiwen Cai. 2016. 'Toward a better understanding of the genomic region harboring Fusarium head blight resistance QTL Qfhs.ndsu-3AS in durum wheat', *Theoretical and Applied Genetics*, 129: 31-43.

Zhu, Zhanwang, Ling Chen, Wei Zhang, Lijun Yang, Weiwei Zhu, Junhui Li, Yike Liu, Hanwen Tong, Luping Fu, Jindong Liu, Awais Rasheed, Xianchun Xia, Zhonghu He, Yuanfeng Hao, and Chunbao Gao. 2020. 'Genome-Wide Association Analysis of Fusarium Head Blight Resistance in Chinese Elite Wheat Lines', *Frontiers in Plant Science*, 11.

Zhu, Zhanwang, Yuanfeng Hao, Mohamed Mergoum, Guihua Bai, Gavin Humphreys, Sylvie Cloutier, Xianchun Xia, and Zhonghu He. 2019. 'Breeding wheat for resistance to Fusarium head blight in the Global North: China, USA, and Canada', *The Crop Journal*, 7: 730-38.

Zimin, Aleksey V, Daniela Puiu, Richard Hall, Sarah Kingan, Bernardo J Clavijo, and Steven L Salzberg. 2017. 'The first near-complete assembly of the hexaploid bread wheat genome, Triticum aestivum', *GigaScience*, 6.

Zipfel, Cyril, Gernot Kunze, Delphine Chinchilla, Anne Caniard, Jonathan D. G. Jones, Thomas Boller, and Georg Felix. 2006. 'Perception of the Bacterial PAMP EF-Tu by the Receptor EFR Restricts Agrobacterium-Mediated Transformation', *Cell*, 125: 749-60.

Supplementary data

***Table S1**. Standard compost mixes used by Horticultural Services at the John Innes Centre.*

John Innes Cereals mix	John Innes F2 Starter
65 % Peat	100 % Peat
25 % Loam	4 kg/m³ Dolomitic Limestone
10 % Grit	1.2 kg/m³ Osmocote start
3 kg/m³ Dolomitic Limestone	
1.3 kg/m³ PG mix	
3 kg/m³ Osmocote exact	

Table S2. *Table of predicted means for the alleles given at markers BA00061052, BA00919063 and BA00710203 located on the 5A chromosome. Source of markers used for the analysis is described. Associated RefSeqv1.1 gene models (where available) and physical position on RefSeqv1.0 assembly are shown. Symptoms above the point of infection were assessed at 10 dpi, 14 dpi and 18 dpi in Summer 2018. Allelic results for each marker are given as 'Hs', if the allele is provided by Hobbit sib (the susceptible parent), as 'WEK', if the allele is provided by WEKH85A (the resistant parent), and as 'Hs/WEK' if it is heterozygous for the allele.*

Source	CerealsDB			CerealsDB			CerealsDB		
RefSeqv1.1 Gene model	TraesCS5A02G202200			*intergenic*			*TraesCS5A02G207400*		
RefSeqv1.0 (bp)	408,930,186			412,226,288			419,363,482		
Marker	***BA00061052***			***BA00919063***			***BA00710203***		
Alleles	**Hs**	**WEK**	**Hs/WEK**	**Hs**	**WEK**	**Hs/WEK**	**Hs**	**WEK**	**Hs/WEK**
10 dpi	2.82	2.65	2.59	2.82	2.63	2.86	2.82	2.64	2.96
14 dpi	6.87	6.20	6.80	6.87	6.18	7.34	6.86	6.20	7.12
18 dpi	7.98	7.49	7.76	7.98	7.47	8.14	7.98	7.48	8.09

Table S3. *Table of predicted means for the alleles given at markers BA00061052, BA00919063 and BA00710203 located on the 5A chromosome. Source of markers used for the analysis is described. Associated RefSeqv1.1 gene models (where available) and physical position on RefSeqv1.0 assembly are shown. Symptoms below the point of infection were assessed at 10 dpi, 14 dpi and 18 dpi in Summer 2018. Allelic results for each marker are given as 'Hs', if the allele is provided by Hobbit sib (the susceptible parent), as 'WEK', if the allele is provided by WEKH85A (the resistant parent), and as 'Hs/WEK' if it is heterozygous for the allele.*

Source	CerealsDB			CerealsDB			CerealsDB		
RefSeqv1.1 Gene model	TraesCS5A02G202200			*intergenic*			*TraesCS5A02G207400*		
RefSeqv1.0 (bp)	408,930,186			412,226,288			419,363,482		
Marker	***BA00061052***			***BA00919063***			***BA00710203***		
Alleles	**Hs**	**WEK**	**Hs/WEK**	**Hs**	**WEK**	**Hs/WEK**	**Hs**	**WEK**	**Hs/WEK**
10 dpi	1.88	1.74	1.78	1.88	1.73	1.92	1.88	1.74	1.83
14 dpi	3.69	3.43	3.38	3.69	3.42	3.54	3.71	3.43	3.42
18 dpi	6.01	5.72	5.36	6.01	5.71	5.61	6.02	5.72	5.40

Table S4. *Table of predicted means for the alleles given at markers S22, S23, S24, BA00061052, S25, S26, S27, BA00919063 and S28 located on the 5A chromosome. Source of markers used for the analysis is described. Associated RefSeqv1.1 gene models (where available) and physical position on RefSeqv1.0 assembly are shown. Symptoms above the point of infection were assessed in five sets at different dpi: at 11-12 dpi (Score 1), at 14-15 dpi (Score 2), at 17-18 dpi (Score 3), at 21 dpi (Score 4) and at 23-24 dpi (Score 5), in Summer 2019. Allelic results for each marker are given as 'Hs', if the allele is provided by Hobbit sib (the susceptible parent), as 'WEK', if the allele is provided by WEKH85A (the resistant parent), and as 'Hs/WEK' if it is heterozygous for the allele.*

Source	18K SNP array			18K SNP array			18K SNP array			CerealsDB			RNA-Seq			RNA-Seq			18K SNP array		
RefSeqv1.1 Gene model	intergenic			intergenic			intergenic			*TraesCS5A02G202200*			*TraesCS5A02G202300*			*TraesCS5A02G202700*			*TraesCS5A02G203000*		
RefSeqv1.0 (bp)	404,438,674			405,034,925			407,955,815			408,930,186			409,319,878			410,499,218			410,803,424		
Marker	***S22***			***S23***			***S24***			***BA00061052***			***S25***			***S26***			***S27***		
Alleles	**Hs**	**WEK**	**Hs/WEK**	**Hs**	**WEK**	**Hs/WEK**	**Hs**	**WEK**	**Hs/WEK**	**Hs**	**WEK**	**Hs/WEK**	**Hs**	**WEK**	**Hs/WEK**	**Hs**	**WEK**	**Hs/WEK**	**Hs**	**WEK**	**Hs/WEK**
Score 1	2.06	1.12	-	2.06	1.12	-	2.06	1.12	-	2.06	1.12	-	2.06	1.12	-	2.06	1.12	-	2.06	1.12	-
Score 2	4.25	2.59	-	4.25	2.59	-	4.25	2.59	-	4.25	2.59	-	4.25	2.59	-	4.25	2.59	-	4.25	2.59	-
Score 3	5.58	3.49	-	5.58	3.49	-	5.58	3.49	-	5.58	3.49	-	5.58	3.49	-	5.58	3.49	-	5.58	3.49	-
Score 4	6.81	4.74	-	6.81	4.74	-	6.81	4.74	-	6.81	4.74	-	6.81	4.74	-	6.81	4.74	-	6.81	4.74	-
Score 5	7.86	5.97	-	7.86	5.97	-	7.86	5.97	-	7.86	5.97	-	7.86	5.97	-	7.86	5.97	-	7.86	5.97	-

Source	CerealsDB			RNA-Seq		
RefSeqv1.1 Gene model	intergenic			*TraesCS5A02G203500*		
RefSeqv1.0 (bp)	412,226,288			413,043,503		
Marker	***BA00919063***			***S28***		
Alleles	**Hs**	**WEK**	**Hs/WEK**	**Hs**	**WEK**	**Hs/WEK**
Score 1	2.06	1.12	-	2.06	1.12	-
Score 2	4.25	2.59	-	4.25	2.59	-
Score 3	5.58	3.49	-	5.58	3.49	-
Score 4	6.81	4.74	-	6.81	4.74	-
Score 5	7.86	5.97	-	7.86	5.97	-

Table S5. *Table of predicted means for the alleles given at markers S22, S23, S24, BA00061052, S25, S26, S27, BA00919063 and S28 located on the 5A chromosome. Source of markers used for the analysis is described. Associated RefSeqv1.1 gene models (where available) and physical position on RefSeqv1.0 assembly are shown. Symptoms below the point of infection were assessed in five sets at different dpi: at 11-12 dpi (Score 1), at 14-15 dpi (Score 2), at 17-18 dpi (Score 3), at 21 dpi (Score 4) and at 23-24 dpi (Score 5), in Summer 2019. Allelic results for each marker are given as 'Hs', if the allele is provided by Hobbit sib (the susceptible parent), as 'WEK', if the allele is provided by WEKH85A (the resistant parent), and as 'Hs/WEK' if it is heterozygous for the allele.*

Source	18K SNP array			18K SNP array			18K SNP array			CerealsDB			RNA-Seq			RNA-Seq			18K SNP array		
RefSeqv1.1 Gene model	intergenic			intergenic			intergenic			*TraesCS5A02G202200*			*TraesCS5A02G202300*			*TraesCS5A02G202700*			*TraesCS5A02G203000*		
RefSeqv1.0 (bp)	404,438,674			405,034,925			407,955,815			408,930,186			409,319,878			410,499,218			410,803,424		
Marker	***S22***			***S23***			***S24***			***BA00061052***			***S25***			***S26***			***S27***		
Alleles	**Hs**	**WEK**	**Hs/WEK**	**Hs**	**WEK**	**Hs/WEK**	**Hs**	**WEK**	**Hs/WEK**	**Hs**	**WEK**	**Hs/WEK**	**Hs**	**WEK**	**Hs/WEK**	**Hs**	**WEK**	**Hs/WEK**	**Hs**	**WEK**	**Hs/WEK**
Score 1	1.48	0.95	-	1.48	0.95	-	1.48	0.95	-	1.48	0.95	-	1.48	0.95	-	1.48	0.95	-	1.48	0.95	-
Score 2	2.99	2.13	-	2.99	2.13	-	2.99	2.13	-	2.99	2.13	-	2.99	2.13	-	2.99	2.13	-	2.99	2.13	-
Score 3	4.24	3.11	-	4.24	3.11	-	4.24	3.11	-	4.24	3.11	-	4.24	3.11	-	4.24	3.11	-	4.24	3.11	-
Score 4	6.09	4.44	-	6.09	4.44	-	6.09	4.44	-	6.09	4.44	-	6.09	4.44	-	6.09	4.44	-	6.09	4.44	-
Score 5	7.29	5.60	-	7.29	5.60	-	7.29	5.60	-	7.29	5.60	-	7.29	5.60	-	7.29	5.60	-	7.29	5.60	-

Source	CerealsDB			RNA-Seq		
RefSeqv1.1 Gene model	intergenic			*TraesCS5A02G203500*		
RefSeqv1.0 (bp)	412,226,288			413,043,503		
Marker	***BA00919063***			***S28***		
Alleles	**Hs**	**WEK**	**Hs/WEK**	**Hs**	**WEK**	**Hs/WEK**
Score 1	1.48	0.95	-	1.48	0.95	-
Score 2	2.99	2.13	-	2.99	2.13	-
Score 3	4.24	3.11	-	4.24	3.11	-
Score 4	6.09	4.44	-	6.09	4.44	-
Score 5	7.29	5.60	-	7.29	5.60	-

Table S6. *Table of predicted means for the alleles given at markers BA00228977 and S15 located on the 5A chromosome. Source of markers used for the analysis is described. Associated RefSeqv1.1 gene models (where available) and physical position on RefSeqv1.0 assembly are shown. Symptoms above the point of infection were assessed in five sets at different dpi: at 12-13 dpi (Score 1), at 14-15 dpi (Score 2), at 16-17 dpi (Score 3), at 18-19 dpi (Score 4) and at 21-22 dpi (Score 5) in Summer 2020. Allelic results for each marker are given as 'Hs', if the allele is provided by Hobbit sib (the susceptible parent), as 'WEK', if the allele is provided by WEKH85A (the resistant parent), and as 'Hs/WEK' if it is heterozygous for the allele.*

Source	CerealsDB			RNA-Seq		
RefSeqv1.1 Gene model	*TraesCS5A02G190600*			*TraesCS5A02G191500*		
RefSeqv1.0 (bp)	395,057,684			395,833,610		
Marker	***BA00228977***			***S15***		
Alleles	**Hs**	**WEK**	**Hs/WEK**	**Hs**	**WEK**	**Hs/WEK**
Score 1	1.78	0.79	-	1.78	0.79	-
Score 2	2.82	1.17	-	2.82	1.17	-
Score 3	3.82	1.60	-	3.82	1.6	-
Score 4	4.89	2.44	-	4.89	2.44	-
Score 5	5.97	3.57	-	5.97	3.57	-

Table S7. *Table of predicted means for the alleles given at markers BA00228977 and S15 located on the 5A chromosome. Source of markers used for the analysis is described. Associated RefSeqv1.1 gene models (where available) and physical position on RefSeqv1.0 assembly are shown. Symptoms below the point of infection were assessed in five sets at different dpi: at 12-13 dpi (Score 1), at 14-15 dpi (Score 2), at 16-17 dpi (Score 3), at 18-19 dpi (Score 4) and at 21-22 dpi (Score 5) in Summer 2020. Allelic results for each marker are given as 'Hs', if the allele is provided by Hobbit sib (the susceptible parent), as 'WEK', if the allele is provided by WEKH85A (the resistant parent), and as 'Hs/WEK' if it is heterozygous for the allele.*

Source	CerealsDB			RNA-Seq		
RefSeqv1.1 Gene model	*TraesCS5A02G190600*			*TraesCS5A02G191500*		
RefSeqv1.0 (bp)	395,057,684			395,833,610		
Marker	***BA00228977***			***S15***		
Alleles	**Hs**	**WEK**	**Hs/WEK**	**Hs**	**WEK**	**Hs/WEK**
Score 1	1.10	0.77	-	1.10	0.77	-
Score 2	1.83	1.35	-	1.83	1.35	-
Score 3	2.60	2.06	-	2.60	2.06	-
Score 4	3.73	2.97	-	3.73	2.97	-
Score 5	5.29	4.10	-	5.29	4.10	-

Table S8. *Percentage of the root ratio between predicted means treated (DON) and untreated (control) for each +/- 5A QTL lines at different days post infection (dpi).*

		3 dpi	4 dpi	5 dpi	6 dpi	7 dpi	8 dpi	9 dpi
+ 5A QTL line	**RIL 97**	76.96	70.91	66.88	66.09	64.88	64.19	62.95
- 5A QTL lines	**RIL 103**	54.95	58.96	56.96	56.21	55.72	55.25	54.32
	RIL 107	58.37	56.80	54.72	53.23	50.93	50.81	50.77
	Hobbit *sib*	51.08	49.70	48.06	47.16	48.25	48.90	49.40
RIL 97 vs. Hobbit *sib*		25.87	21.21	18.82	18.93	16.63	15.29	13.55

Table S9. *Percentage of the shoot ratio between predicted means treated (DON) and untreated (control) for each +/- 5A QTL lines at different days post infection (dpi).*

		3 dpi	4 dpi	5 dpi	6 dpi	7 dpi	8 dpi	9 dpi
+ 5A QTL line	**RIL 97**	92.18	94.38	93.60	94.89	95.01	96.41	95.83
- 5A QTL lines	**RIL 103**	98.31	97.62	96.87	96.81	96.79	96.55	96.73
	RIL 107	83.45	85.24	87.30	88.74	89.80	90.21	91.24
	Hobbit sib	77.14	77.56	79.12	81.33	82.72	82.57	84.18
RIL 97 vs. Hobbit *sib*		15.03	16.82	14.48	13.57	12.29	13.84	11.65

Table S10. *Up-regulated genes (P-value ≤ 0.01; log2 FC ≥ 2.0) in RIL 97 (+ 5A QTL) extracted from the 5A chromosome of wheat. Genes ordered from higher to lower expressed.*

Gene ID	Annotation	Gene start (bp)	Gene end (bp)	log_2 (FC)	*P*-value
TraesCS5A02G545100LC	N/A	N/A	N/A	7.02	6.00E-66
TraesCS5A02G065500	-	71397158	71398871	5.24	4.56E-103
TraesCS5A02G182500	-	382291561	382292892	4.57	1.90E-20
TraesCS5A02G368900	-	569283133	569285041	4.45	2.21E-19
TraesCS5A02G196400	-	400410933	400413943	4.44	3.43E-21
TraesCS5A02G368800	Protein DETOXIFICATION [Source:UniProtKB/TrEMBL;Acc:A0A341UZ89]	569221139	569225973	4.36	2.03E-91
TraesCS5A02G298500LC	N/A	N/A	N/A	4.25	1.79E-17
TraesCS5A02G270000	-	480503178	480504041	4.09	1.14E-40
TraesCS5A02G368600	Protein DETOXIFICATION [Source:UniProtKB/TrEMBL;Acc:A0A341VF21]	569181349	569184876	4.00	1.74E-39
TraesCS5A02G024900LC	N/A	N/A	N/A	3.92	2.00E-15
TraesCS5A02G149600	Glycosyltransferase [Source:UniProtKB/TrEMBL;Acc:A0A1D5YPX1]	327573796	327581013	3.86	1.76E-37
TraesCS5A02G397900	-	592122205	592125380	3.53	2.91E-40
TraesCS5A02G368700	Protein DETOXIFICATION [Source:UniProtKB/TrEMBL;Acc:A0A341V5V1]	569217168	569219804	3.40	4.19E-81
TraesCS5A02G131300	-	295726499	295732900	3.25	5.16E-68
TraesCS5A02G233100	-	448539712	448541474	3.16	1.01E-77
TraesCS5A02G180800	-	379353913	379354845	3.11	1.51E-15
TraesCS5A02G137400	-	309311254	309313048	3.05	6.27E-51
TraesCS5A02G270100	-	480507905	480508712	2.89	4.97E-09
TraesCS5A02G449400	-	631503086	631505615	2.88	9.47E-34
TraesCS5A02G427400	Alpha/beta hydrolase fold-3 domain containing protein [Source: Projected from Oryza sativa (Os03g0790500)]	612158055	612159662	2.84	4.55E-16
TraesCS5A02G321000	-	534011669	534014153	2.75	4.07E-08
TraesCS5A02G339200	-	546684326	546687119	2.70	3.31E-27
TraesCS5A02G069000	-	77365858	77367087	2.70	5.27E-31
TraesCS5A02G236700	-	452122768	452125017	2.67	2.26E-23
TraesCS5A02G195300LC	N/A	N/A	N/A	2.61	4.46E-07
TraesCS5A02G528000	-	688292625	688295351	2.61	4.52E-07
TraesCS5A02G729810LC	N/A	N/A	N/A	2.56	6.94E-15
TraesCS5A02G304000LC	N/A	N/A	N/A	2.52	1.10E-06
TraesCS5A02G325100	-	535786872	535787957	2.51	1.20E-06
TraesCS5A02G343000	-	548219178	548221179	2.45	1.60E-14
TraesCS5A02G416900	-	605232016	605233025	2.45	4.14E-28
TraesCS5A02G369700LC	N/A	N/A	N/A	2.43	5.82E-18
TraesCS5A02G183500	-	383191065	383192590	2.37	4.62E-06
TraesCS5A02G099000	-	141031388	141032548	2.33	6.60E-06
TraesCS5A02G149700	-	327575915	327577750	2.30	8.26E-06
TraesCS5A02G191800	-	395847109	395848224	2.29	3.68E-06
TraesCS5A02G180900	-	379355434	379356264	2.24	1.19E-05
TraesCS5A02G397800	-	592034007	592036417	2.13	9.54E-76
TraesCS5A02G513000	-	676949097	676951841	2.09	2.05E-17

Table S11. *Down-regulated genes (P-value ≤ 0.01; log2 FC ≥ -2.0) in RIL 97 (+ 5A QTL) extracted from the 5A chromosome of wheat.*

Gene ID	Annotation	Gene start (bp)	Gene end (bp)	log_2 (FC)	*P*-value
TraesCS5A02G535900	-	692371595	692373001	-2.02	7.61E-07
TraesCS5A02G023700	-	18812811	18817203	-2.36	4.90E-06

Table S12. *Up-regulated genes (P-value ≤ 0.01; log2 FC ≥ 2.0) in Hobbit sib (- 5A QTL) extracted from the 5A chromosome of wheat. Genes ordered from higher to lower expressed.*

Gene ID	Annotation	Gene start (bp)	Gene end (bp)	log_2 (FC)	*P*-value
TraesCS5A02G325100	-	535786872	535787957	4.22	2.04E-36
TraesCS5A02G182500	-	382291561	382292892	3.60	8.37E-30
TraesCS5A02G545000LC	N/A	N/A	N/A	3.44	2.54E-23
TraesCS5A02G065500	-	71397158	71398871	3.26	4.43E-33
TraesCS5A02G368800	Protein DETOXIFICATION [Source:UniProtKB/TrEMBL;Acc:A0A341UZ89]	569221139	569225973	3.05	1.96E-41
TraesCS5A02G196400	-	400410933	400413943	2.99	1.07E-19
TraesCS5A02G368600	Protein DETOXIFICATION [Source:UniProtKB/TrEMBL;Acc:A0A341VF21]	569181349	569184876	2.71	5.85E-24
TraesCS5A02G368700	Protein DETOXIFICATION [Source:UniProtKB/TrEMBL;Acc:A0A341V5V1]	569217168	569219804	2.65	3.00E-40
TraesCS5A02G183500	-	383191065	383192590	2.57	1.89E-14
TraesCS5A02G300000LC	N/A	N/A	N/A	2.55	2.36E-13
TraesCS5A02G180800	-	379353913	379354845	2.47	2.11E-18
TraesCS5A02G149600	Glycosyltransferase [Source:UniProtKB/TrEMBL;Acc:A0A1D5YPX1]	327573796	327581013	2.35	4.90E-33
TraesCS5A02G099000	-	141031388	141032548	2.28	5.89E-11
TraesCS5A02G233100	-	448539712	448541474	2.20	1.51E-17
TraesCS5A02G131300	-	295726499	295732900	2.19	3.32E-42
TraesCS5A02G137400	-	309311254	309313048	2.01	6.24E-14

Table S13. *Common up-regulated genes (P-value ≤ 0.01; log2 FC ≥ 2.0) for both RIL 97 (+ 5A QTL) and Hobbit sib (- 5A QTL) extracted from the 5A chromosome of wheat. Genes ordered from higher to lower expressed in RIL 97.*

Gene ID	Annotation	Gene start (bp)	Gene end (bp)	RIL 97 (+ 5A QTL)		Hobbit *sib* (- 5A QTL)	
				log_2 (FC)	*P*-value	log_2 (FC)	*P*-value
TraesCS5A02G065500	-	71397158	71398871	5.24	4.56E-103	3.26	4.43E-33
TraesCS5A02G182500	-	382291561	382292892	4.57	1.90E-20	3.60	8.37E-30
TraesCS5A02G196400	-	400410933	400413943	4.44	3.43E-21	2.99	1.07E-19
TraesCS5A02G368800	Protein DETOXIFICATION [Source:UniProtKB/TrEMBL;Acc:A0A341UZ89]	569221139	569225973	4.36	2.03E-91	3.05	1.96E-41
TraesCS5A02G368600	Protein DETOXIFICATION [Source:UniProtKB/TrEMBL;Acc:A0A341VF21]	569181349	569184876	4.00	1.74E-39	2.71	5.85E-24
TraesCS5A02G149600	Glycosyltransferase [Source:UniProtKB/TrEMBL;Acc:A0A1D5YPX1]	327573796	327581013	3.86	1.76E-37	2.35	4.90E-33
TraesCS5A02G368700	Protein DETOXIFICATION [Source:UniProtKB/TrEMBL;Acc:A0A341V5V1]	569217168	569219804	3.40	4.19E-81	2.65	3.00E-40
TraesCS5A02G131300	-	295726499	295732900	3.25	5.16E-68	2.19	3.32E-42
TraesCS5A02G233100	-	448539712	448541474	3.16	1.01E-77	2.20	1.51E-17
TraesCS5A02G180800	-	379353913	379354845	3.11	1.51E-15	2.47	2.11E-18
TraesCS5A02G137400	-	309311254	309313048	3.05	6.27E-51	2.01	6.24E-14
TraesCS5A02G325100	-	535786872	535787957	2.51	1.20E-06	4.22	2.04E-36
TraesCS5A02G183500	-	383191065	383192590	2.37	4.62E-06	2.57	1.89E-14
TraesCS5A02G099000	-	141031388	141032548	2.33	6.60E-06	2.28	5.89E-11

Table S14. *Gene counts obtained from the RNA-Seq analysis of genes identified on the 5A QTL on RIL 97, located from 322 Mbp to 417 Mbp.*

	RIL 97								**Hobbit *sib***							
	DON				**Control**				**DON**				**Control**			
Gene ID	**Sample 1**	**Sample 2**	**Sample 3**	**Sample 4**	**Sample 1**	**Sample 2**	**Sample 3**	**Sample 4**	**Sample 1**	**Sample 2**	**Sample 3**	**Sample 4**	**Sample 1**	**Sample 2**	**Sample 3**	**Sample 4**
TraesCS5A02G149600	4190	4065	3663	5833	353	83	228	265	972	1322	1239	2449	311	555	428	167
TraesCS5A02G149700	108	154	153	120	9	4	11	0	26	50	30	83	4	36	12	26
TraesCS5A02G180900	269	370	431	602	36	11	23	10	72	106	125	250	39	46	37	22
TraesCS5A02G183500	1711	1419	1594	2694	16	0	25	18	224	585	459	896	40	114	13	14
TraesCS5A02G191700	188	209	90	223	33	38	29	54	17	72	65	61	35	16	50	8
TraesCS5A02G191800	39	51	33	56	8	2	6	0	4	28	13	0	8	6	14	1
TraesCS5A02G196400	1955	1332	1350	2528	29	3	13	23	486	331	407	429	14	57	10	17
TraesCS5A02G298500LC	19	7	45	51	0	0	0	0	3	0	9	27	0	0	0	0
TraesCS5A02G304000LC	6	11	25	16	0	0	0	0	3	4	0	5	1	0	4	0

Table S15. *Transcripts per million (TPM) obtained from the RNA-Seq analysis of genes identified on the 5A QTL on RIL 97, located from 322 Mbp to 417 Mbp.*

	RIL 97								Hobbit *sib*							
	DON				Control				DON				Control			
Gene ID	**Sample 1**	**Sample 2**	**Sample 3**	**Sample 4**	**Sample 1**	**Sample 2**	**Sample 3**	**Sample 4**	**Sample 1**	**Sample 2**	**Sample 3**	**Sample 4**	**Sample 1**	**Sample 2**	**Sample 3**	**Sample 4**
TraesCS5A02G149600	7	137	129	158	8	3	7	10	69	66	82	91	9	17	13	12
TraesCS5A02G149700	26	48	48	29	2	1	3	0	17	23	19	27	1	10	3	17
TraesCS5A02G180900	466	790	948	997	55	23	47	24	310	336	509	577	77	90	72	96
TraesCS5A02G183500	73	76	90	116	1	0	1	1	25	47	49	53	2	5	1	2
TraesCS5A02G191700	11	16	7	13	2	3	2	5	3	8	10	5	2	1	3	1
TraesCS5A02G191800	2	4	3	3	0	0	0	0	1	3	2	0	1	0	1	0
TraesCS5A02G196400	203	175	183	262	3	0	2	3	136	64	107	61	2	7	1	5
TraesCS5A02G298500LC	2	1	5	4	0	0	0	0	1	0	2	3	0	0	0	0
TraesCS5A02G304000LC	0	1	2	1	0	0	0	0	0	0	0	0	0	0	0	0

Table S16. *Log_2 FC and P-value data extracted from the RNA-Seq analysis performed in roots upon DON and control treatments for lines RIL 97 (+ 5A QTL) and Hobbit sib (- 5A QTL) for homoeologues of gene TraesCS5A02G191700.*

		Gene ID	log_2 (FC)	*P*-value
DON vs. control	**RIL 97**	***TraesCS5A02G191700***	1.84	0.0000001
		TraesCS5B02G191400	1.59	0.0000004
		TraesCS5D02G199200	0.89	0.0563773
	Hobbit *sib*	***TraesCS5A02G191700***	1.06	0.0013911
		TraesCS5B02G191400	0.69	0.0404076
		TraesCS5D02G199200	0.62	0.0610897
RIL 97 vs. Hobbit *sib*	**DON**	***TraesCS5A02G191700***	0.71	0.0195055
		TraesCS5B02G191400	0.52	0.0741996
		TraesCS5D02G199200	0.62	0.0723209
	control	***TraesCS5A02G191700***	0.30	0.3319103
		TraesCS5B02G191400	0.02	0.9459936
		TraesCS5D02G199200	0.47	0.1034124

Table S17. *Log2 FC and P-value data extracted from the RNA-Seq analysis performed in roots upon DON and control treatments for lines RIL 97 (+ 5A QTL) and Hobbit sib (- 5A QTL) for homoeologues of gene TraesCS5A02G191800.*

		Gene ID	log_2 (FC)	*P*-value
DON vs. control	**RIL 97**	***TraesCS5A02G191800***	2.29	0.00000368
		TraesCS5B02G191300	1.84	0.00001012
		TraesCS5D02G199100	2.43	0.00000001
	Hobbit *sib*	***TraesCS5A02G191800***	0.40	0.19716399
		TraesCS5B02G191300	0.96	0.00472586
		TraesCS5D02G199100	0.26	0.34437197
RIL 97 vs. Hobbit *sib*	**DON**	***TraesCS5A02G191800***	0.40	0.23365539
		TraesCS5B02G191300	1.00	0.00059382
		TraesCS5D02G199100	0.56	0.09533612
	control	***TraesCS5A02G191800***	-0.24	0.38896058
		TraesCS5B02G191300	0.28	0.38449692
		TraesCS5D02G199100	0.00	0.98710043

Table S18. *Percentage of the root ratio between predicted means treated (DON) and untreated (control) for each +/- 5A QTL lines at different days post infection (dpi) on Test 1. Lines tested were Hobbit sib, RIL 97, RIL 9A and RIL 17B.*

		3 dpi	4 dpi	5 dpi	6 dpi	7 dpi	8 dpi	9 dpi	10 dpi
+ 5A QTL line	**RIL 97**	72.96	66.80	63.01	60.04	58.83	58.38	58.03	57.50
	RIL 9A	73.89	68.71	63.07	59.78	60.05	59.37	59.11	58.68
- 5A QTL lines	**RIL 17B**	64.92	61.40	59.31	59.03	58.53	57.79	57.09	56.95
RIL 9A vs. RIL 17B		8.97	7.30	3.77	0.76	1.52	1.58	2.02	1.73

Table S19. *Percentage of the root ratio between predicted means treated (DON) and untreated (control) for each +/- 5A QTL lines at different days post infection (dpi) on Test 2. Lines tested were Hobbit sib, RIL 97, RIL 9A and RIL 17B.*

		3 dpi	4 dpi	5 dpi	6 dpi	7 dpi	8 dpi	9 dpi	10 dpi
+ 5A QTL line	**RIL 97**	76.91	71.40	66.30	62.99	61.63	61.06	60.42	59.67
	RIL 10B	78.19	71.23	66.56	64.05	61.94	59.72	57.91	56.63
- 5A QTL lines	**RIL 16A**	66.50	61.08	58.32	58.07	57.64	56.80	56.02	55.45
	Hobbit *sib*	55.71	51.42	44.76	43.96	44.10	-	-	-
RIL 97 vs. Hobbit *sib*		21.20	19.98	21.53	19.02	17.54			

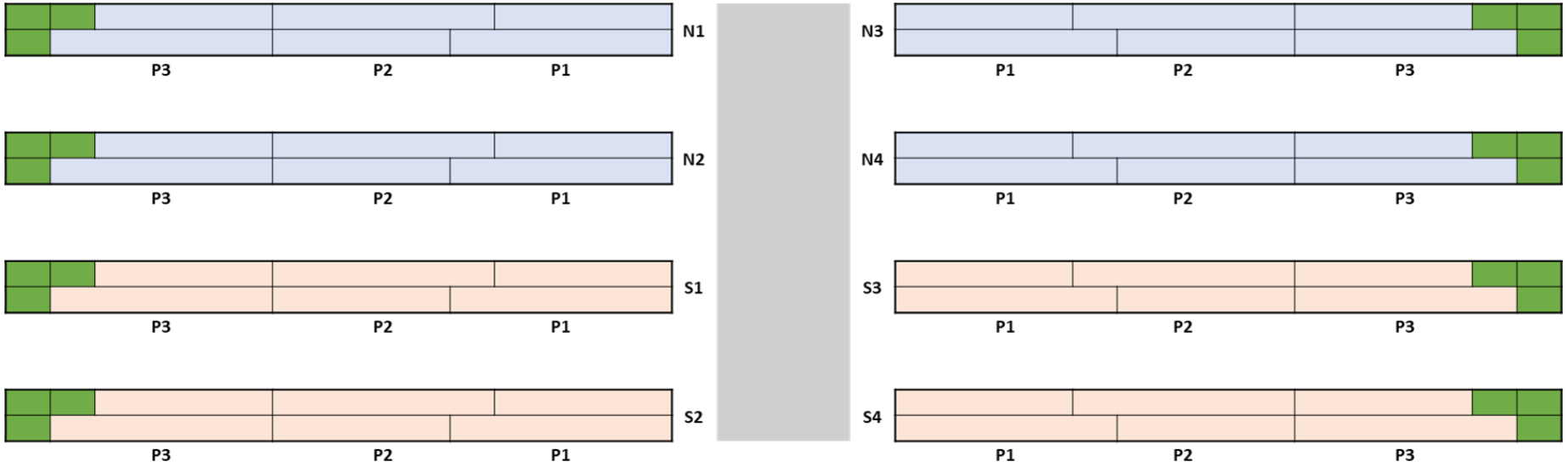

Figure S1. *Experimental design of the polytunnel 2019 trial at the JIC. Plants were arranged in eight blocks (N1-4, light blue; S1-4, light pink) containing three plots each (P1-3). Wheat lines for seed multiplication were placed on the outer edges of each block (green rectangles). There was a total of 30 plants per block. Grey vertical rectangle represents the path in the middle of the polytunnel.*

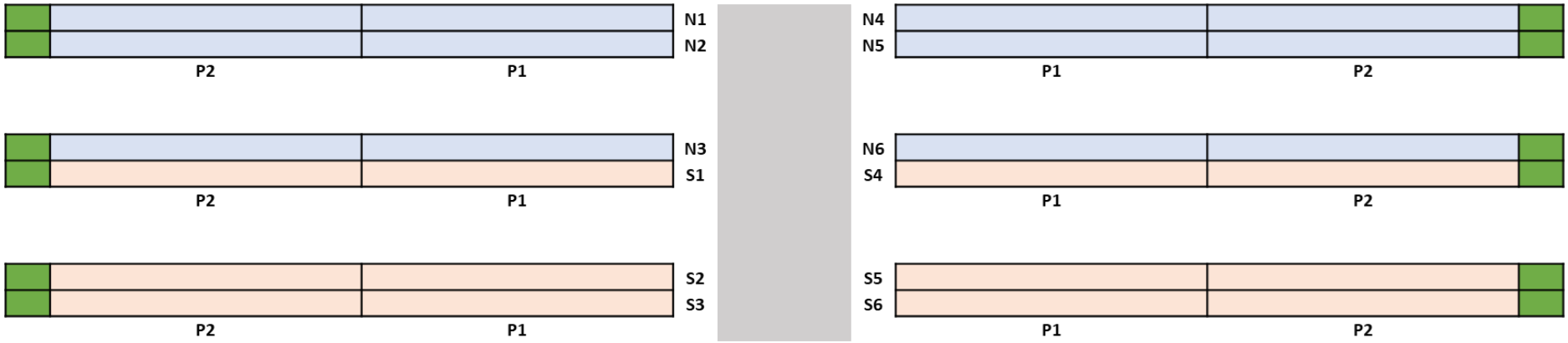

Figure S2. *Experimental design of the polytunnel 2020 trial at the JIC. Plants were arranged in twelve blocks (N1-6, light blue; S1-6, light pink) containing two plots each (P1-2). Wheat lines for seed multiplication were placed on the outer edges of each block (green rectangles). There was a total of 30 plants per two blocks. Grey vertical rectangle represents the path in the middle of the polytunnel.*

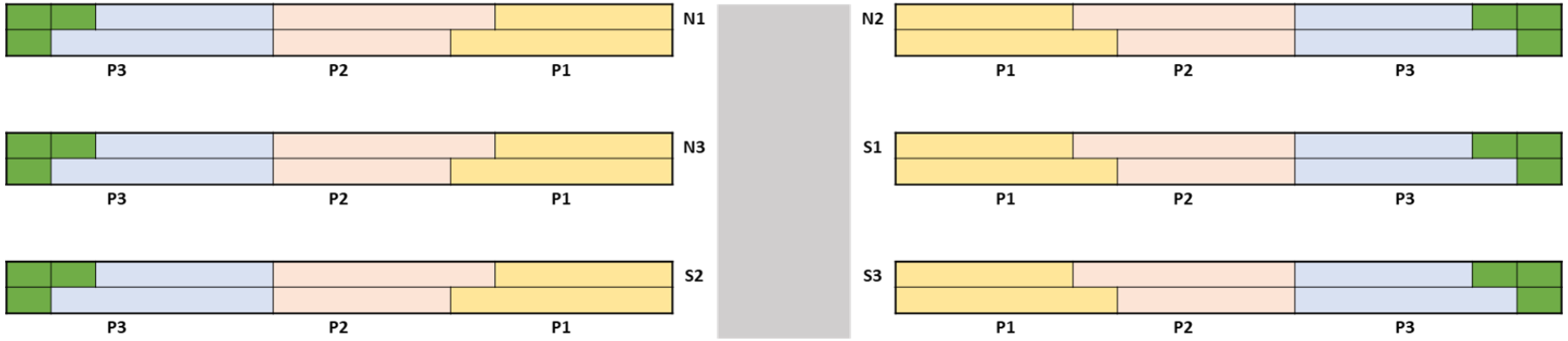

Figure S3. *Experimental design of the polytunnel 2019 trial at the JIC. Plants were arranged in six blocks (N1-3; S1-3) containing three plots each (P1-3). Wheat lines for seed multiplication were placed on the outer edges of each block (green rectangles). There was a total of 30 plants per block. Grey vertical rectangle represents the path in the middle of the polytunnel.*

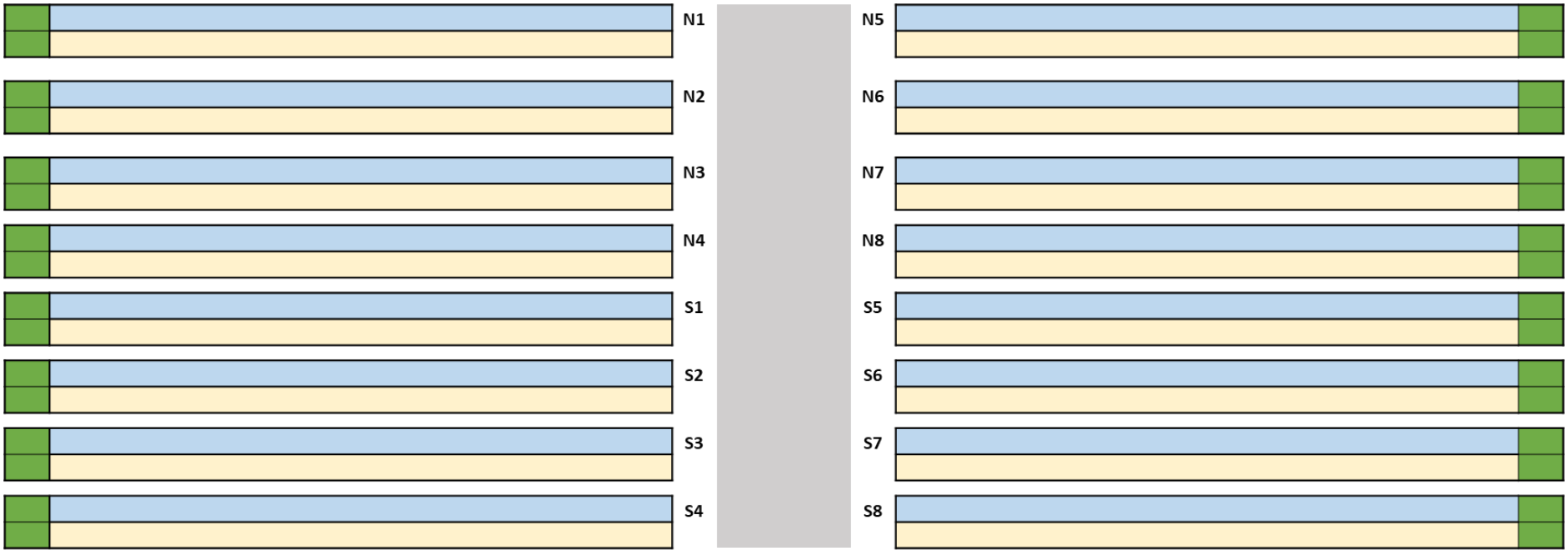

Figure S4. *Experimental design of the polytunnel 2020 trial at the JIC. Plants were arranged in sixteen blocks (N1-8; S1-8). Wheat lines for seed multiplication were placed on the outer edges of each block (green rectangles). There was a total of 30 plants per block. Grey vertical rectangle represents the path in the middle of the polytunnel.*

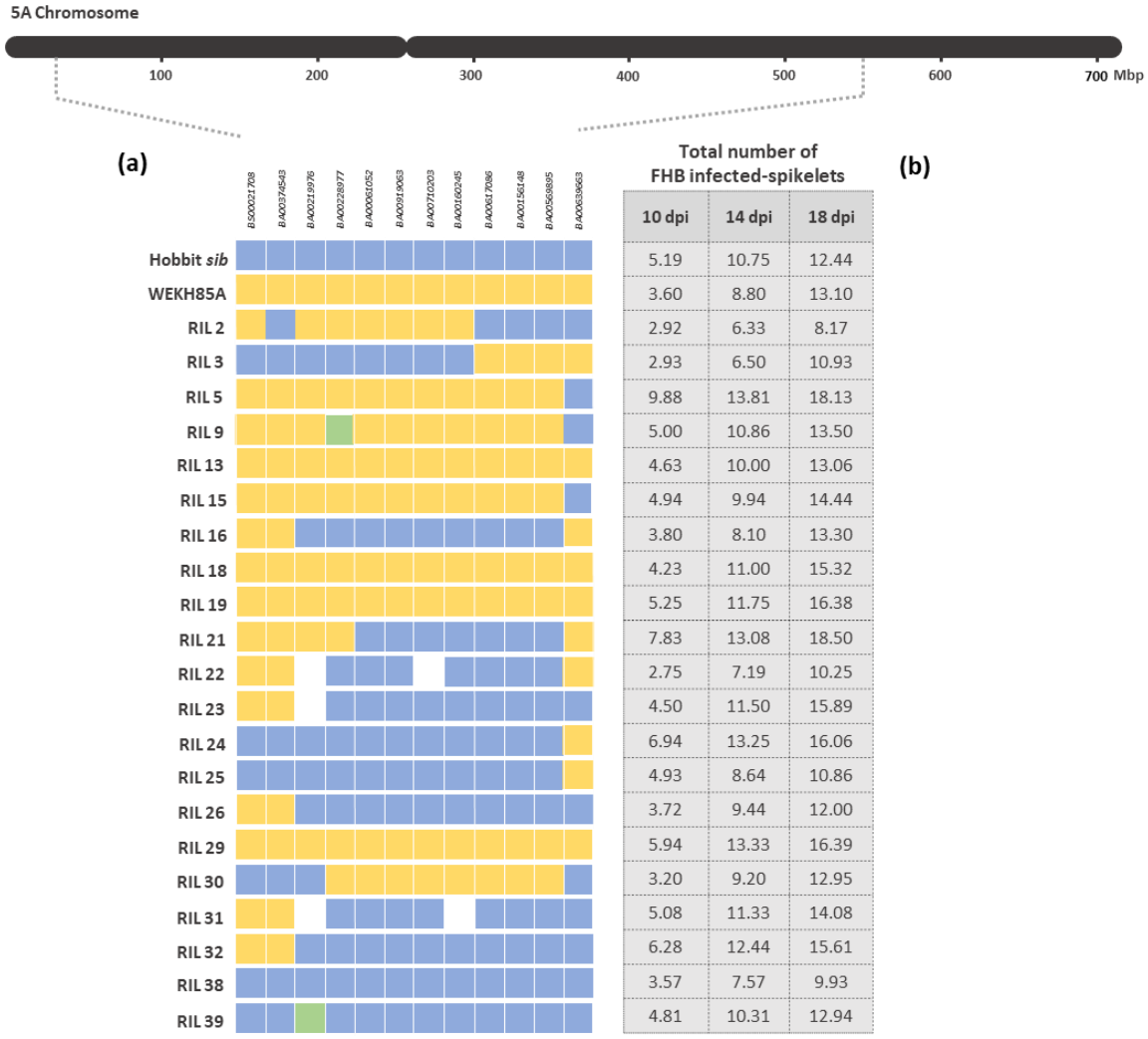

	Total number of FHB infected-spikelets		
	10 dpi	14 dpi	18 dpi
Hobbit *sib*	5.19	10.75	12.44
WEKH85A	3.60	8.80	13.10
RIL 2	2.92	6.33	8.17
RIL 3	2.93	6.50	10.93
RIL 5	9.88	13.81	18.13
RIL 9	5.00	10.86	13.50
RIL 13	4.63	10.00	13.06
RIL 15	4.94	9.94	14.44
RIL 16	3.80	8.10	13.30
RIL 18	4.23	11.00	15.32
RIL 19	5.25	11.75	16.38
RIL 21	7.83	13.08	18.50
RIL 22	2.75	7.19	10.25
RIL 23	4.50	11.50	15.89
RIL 24	6.94	13.25	16.06
RIL 25	4.93	8.64	10.86
RIL 26	3.72	9.44	12.00
RIL 29	5.94	13.33	16.39
RIL 30	3.20	9.20	12.95
RIL 31	5.08	11.33	14.08
RIL 32	6.28	12.44	15.61
RIL 38	3.57	7.57	9.93
RIL 39	4.81	10.31	12.94

Figure S5. *a) Graphical genotype of parental lines (Hobbit sib and WEKH85A) and recombinant inbred lines used on Summer 2018. Line names are specified on each raw and markers used are specified on each column. Yellow is the allele provided by WEKH85A and blue the one by Hobbit sib. Green is the heterozygous allele. White is missing value. b) Total number of FHB infected-spikelets (scoring data above and below the point of infection) obtained for each line at different scoring dates: 10 dpi, 14 dpi and 18 dpi.*

(a)

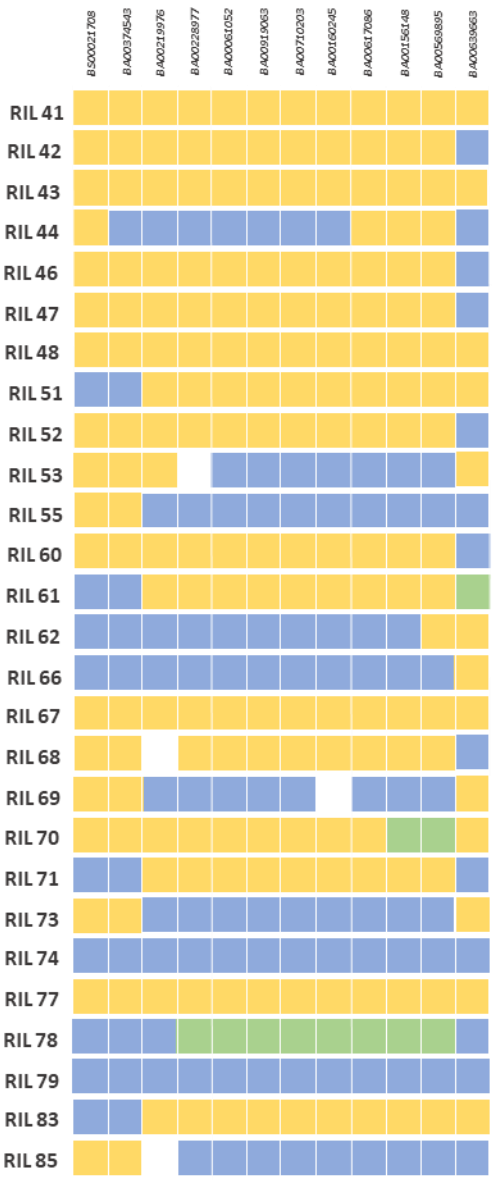

(b)

Total number of FHB infected-spikelets		
10 dpi	14 dpi	18 dpi
2.15	6.65	10.65
3.50	7.19	11.62
5.11	10.50	13.50
5.50	12.36	17.21
2.29	5.57	9.86
3.83	7.58	10.67
5.93	12.14	16.21
2.25	4.25	5.75
3.70	11.60	14.10
5.00	12.64	14.93
4.22	9.56	14.17
3.08	8.58	12.58
3.57	8.93	11.14
3.19	8.44	11.19
4.50	10.45	14.15
4.88	10.75	15.25
2.28	4.67	7.22
4.43	10.36	13.57
4.10	9.95	14.80
4.14	10.07	12.64
3.89	10.11	13.28
6.50	12.56	15.06
5.00	11.60	14.00
3.69	7.63	10.25
4.89	11.67	15.56
4.83	9.95	12.44
4.19	9.75	12.13

Figure S5. Continued. *a) Graphical genotype of parental lines (Hobbit sib and WEKH85A) and recombinant inbred lines used on Summer 2018. Line names are specified on each raw and markers used are specified on each column. Yellow is the allele provided by WEKH85A and blue the one by Hobbit sib. Green is the heterozygous allele. White is missing value. b) Total number of FHB infected-spikelets (scoring data above and below the point of infection) obtained for each line at different scoring dates: 10 dpi, 14 dpi and 18 dpi.*

(a)

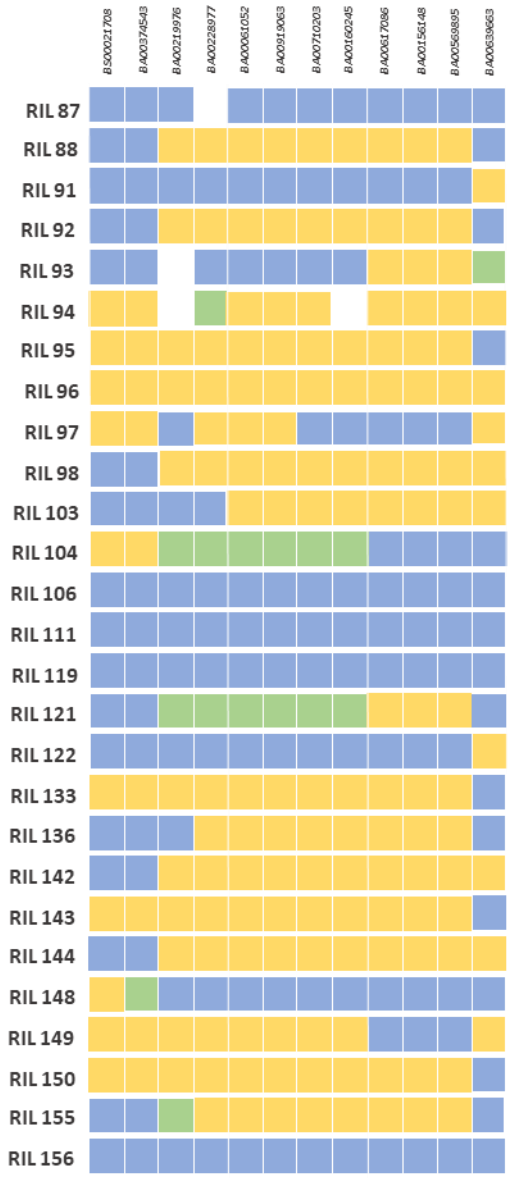

(b)

	Total number of FHB infected-spikelets		
	10 dpi	14 dpi	18 dpi
RIL 87	5.33	11.78	14.61
RIL 88	2.00	6.75	8.50
RIL 91	3.06	8.13	11.19
RIL 92	4.38	9.31	12.75
RIL 93	6.00	13.06	16.31
RIL 94	2.72	6.07	10.29
RIL 95	6.50	12.75	15.31
RIL 96	3.56	10.56	14.12
RIL 97	2.13	5.63	10.00
RIL 98	3.07	6.72	11.43
RIL 103	2.92	6.33	8.08
RIL 104	4.14	10.50	14.21
RIL 106	4.44	11.06	14.44
RIL 111	4.64	9.86	14.64
RIL 119	3.50	8.33	11.50
RIL 121	4.44	10.89	13.28
RIL 122	3.78	9.95	13.56
RIL 133	5.13	9.69	13.00
RIL 136	1.95	6.22	8.78
RIL 142	3.85	11.60	15.95
RIL 143	2.95	8.55	11.35
RIL 144	4.46	10.14	14.91
RIL 148	5.56	11.87	14.69
RIL 149	3.95	8.50	11.30
RIL 150	3.79	9.71	14.29
RIL 155	4.39	8.44	12.28
RIL 156	2.93	7.14	10.79

Figure S5. Continued. *a) Graphical genotype of parental lines (Hobbit sib and WEKH85A) and recombinant inbred lines used on Summer 2018. Line names are specified on each raw and markers used are specified on each column. Yellow is the allele provided by WEKH85A and blue the one by Hobbit sib. Green is the heterozygous allele. White is missing value. b) Total number of FHB infected-spikelets (scoring data above and below the point of infection) obtained for each line at different scoring dates: 10 dpi, 14 dpi and 18 dpi.*

(a)

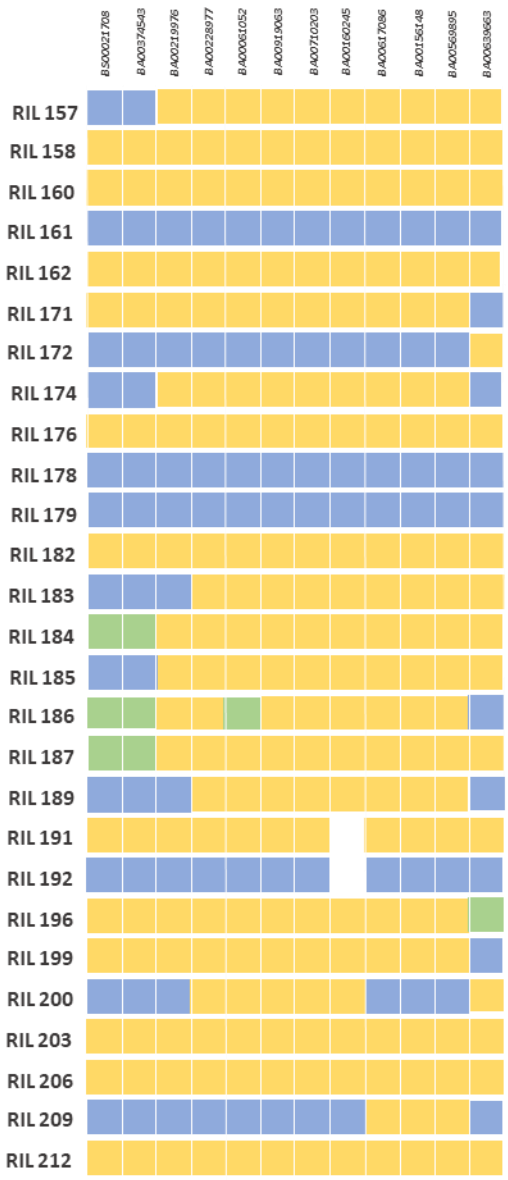

(b)

Total number of FHB infected-spikelets		
10 dpi	14 dpi	18 dpi
2.57	7.14	10.50
3.86	11.57	13.86
2.25	4.31	9.37
3.33	9.72	14.28
1.62	4.00	6.06
3.81	8.38	14.00
2.79	6.36	10.14
2.83	6.00	10.56
2.33	7.22	10.44
2.50	7.00	11.57
1.29	4.86	7.71
3.81	9.75	14.81
5.06	9.69	12.75
2.50	6.00	11.75
4.00	11.10	12.95
2.44	6.75	10.06
7.39	10.67	17.00
5.07	10.07	11.93
2.07	6.00	9.57
5.72	13.78	18.06
4.70	11.75	15.55
3.19	10.00	14.56
5.00	11.39	14.67
7.20	13.40	17.40
4.61	9.28	12.33
4.75	11.81	15.13
6.06	12.75	15.00

Figure S5. Continued. *a) Graphical genotype of parental lines (Hobbit sib and WEKH85A) and recombinant inbred lines used on Summer 2018. Line names are specified on each raw and markers used are specified on each column. Yellow is the allele provided by WEKH85A and blue the one by Hobbit sib. Green is the heterozygous allele. White is missing value. b) Total number of FHB infected-spikelets (scoring data above and below the point of infection) obtained for each line at different scoring dates: 10 dpi, 14 dpi and 18 dpi.*

(a)

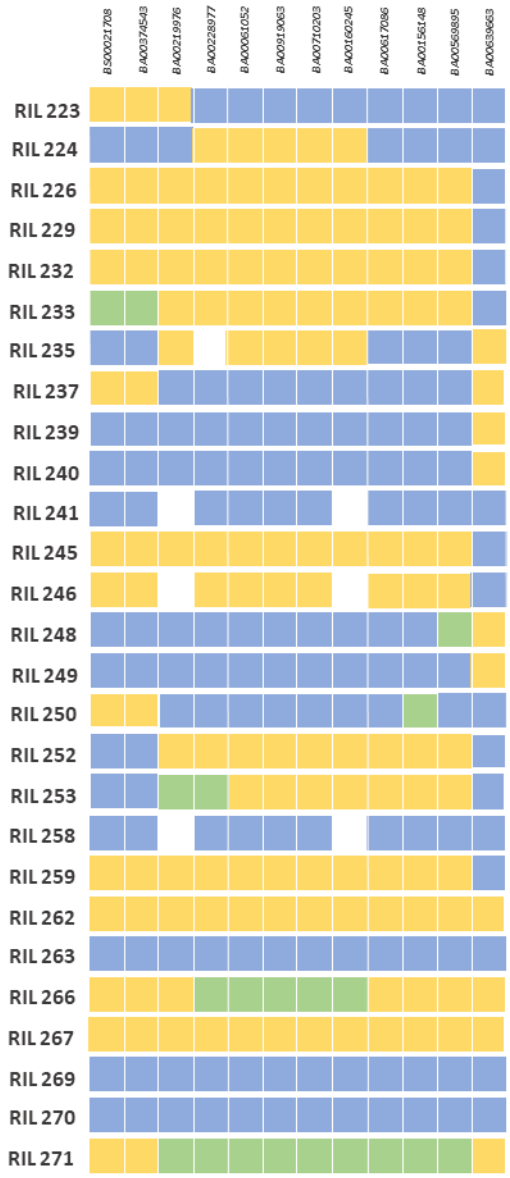

(b)

Total number of FHB infected-spikelets		
10 dpi	14 dpi	18 dpi
4.78	10.33	13.50
5.19	10.19	12.44
3.75	9.75	15.50
4.87	11.75	15.56
7.30	12.90	14.70
5.44	11.44	14.25
5.13	10.06	13.00
5.31	13.38	16.38
5.08	13.33	17.33
6.83	12.56	16.83
3.71	8.64	11.07
4.38	11.25	17.44
5.36	10.79	14.14
3.67	11.22	13.56
5.36	10.21	14.00
3.60	10.05	12.80
3.29	6.50	8.64
4.56	9.11	14.11
4.81	11.75	14.19
4.43	13.22	16.00
6.00	12.36	16.22
3.75	11.08	17.08
6.31	13.50	17.06
7.69	12.88	15.13
3.60	10.05	12.15
4.89	9.33	12.00
5.19	11.75	13.88

Figure S5. Continued. *a) Graphical genotype of parental lines (Hobbit sib and WEKH85A) and recombinant inbred lines used on Summer 2018. Line names are specified on each raw and markers used are specified on each column. Yellow is the allele provided by WEKH85A and blue the one by Hobbit sib. Green is the heterozygous allele. White is missing value. b) Total number of FHB infected-spikelets (scoring data above and below the point of infection) obtained for each line at different scoring dates: 10 dpi, 14 dpi and 18 dpi.*

(a)

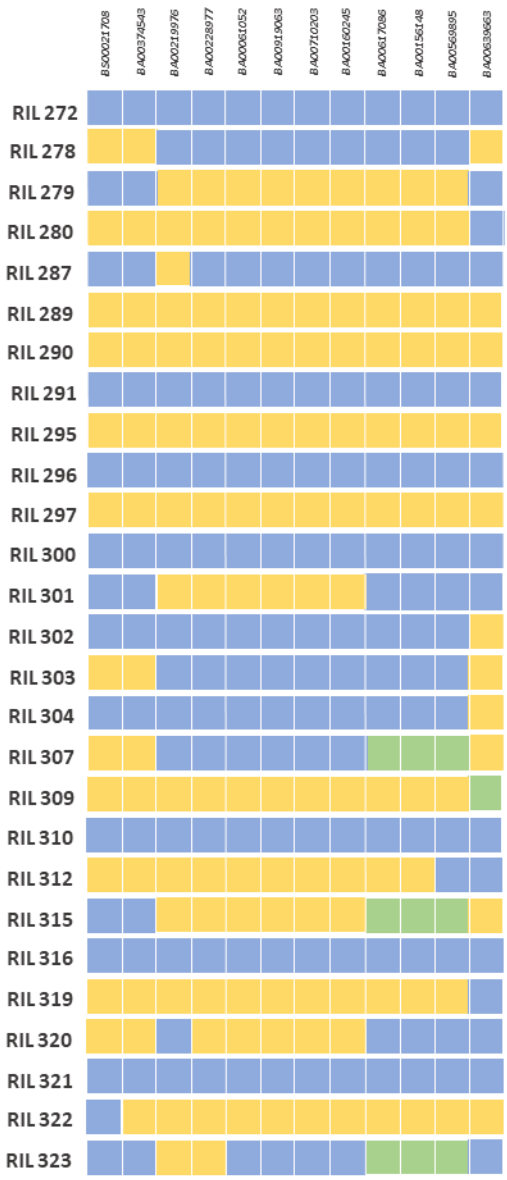

(b)

Total number of FHB infected-spikelets		
10 dpi	14 dpi	18 dpi
5.17	9.00	12.08
4.56	10.44	13.11
6.83	13.50	16.83
6.17	10.72	13.94
4.64	12.14	14.71
5.31	9.50	13.25
5.43	10.22	13.64
4.17	7.58	11.00
5.50	11.38	14.00
3.42	10.17	14.50
5.06	12.33	16.67
8.25	13.00	18.17
5.67	13.25	16.67
3.86	11.64	13.36
3.00	8.07	11.57
3.94	9.13	13.13
3.00	9.69	13.44
2.67	5.00	7.50
7.50	12.14	15.71
3.63	6.63	10.69
2.72	5.67	11.11
5.40	14.30	19.10
8.33	13.17	18.00
2.75	5.88	10.75
4.20	9.40	15.40
4.19	10.81	14.06
6.22	12.56	15.33

Figure S5. Continued. *a) Graphical genotype of parental lines (Hobbit sib and WEKH85A) and recombinant inbred lines used on Summer 2018. Line names are specified on each raw and markers used are specified on each column. Yellow is the allele provided by WEKH85A and blue the one by Hobbit sib. Green is the heterozygous allele. White is missing value. b) Total number of FHB infected-spikelets (scoring data above and below the point of infection) obtained for each line at different scoring dates: 10 dpi, 14 dpi and 18 dpi.*

(a)

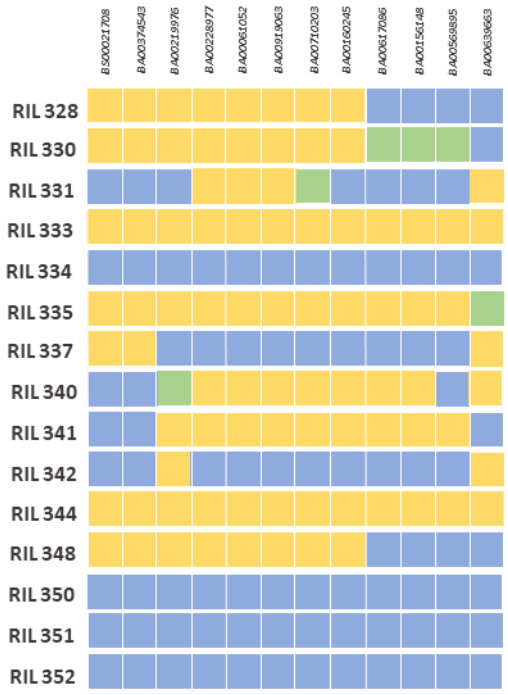

(b)

Total number of FHB infected-spikelets		
10 dpi	14 dpi	18 dpi
1.80	5.30	10.40
3.33	8.92	12.83
5.00	9.25	12.60
5.22	8.93	12.29
6.83	12.75	13.58
7.79	13.43	18.14
6.33	13.22	16.83
3.25	11.63	13.44
6.83	13.39	16.72
6.06	12.69	15.75
4.00	9.44	14.00
4.83	12.08	16.08
7.19	12.50	17.13
5.00	9.33	14.17
5.75	13.06	17.00

Figure S5. Continued. *a) Graphical genotype of parental lines (Hobbit sib and WEKH85A) and recombinant inbred lines used on Summer 2018. Line names are specified on each raw and markers used are specified on each column. Yellow is the allele provided by WEKH85A and blue the one by Hobbit sib. Green is the heterozygous allele. White is missing value. b) Total number of FHB infected-spikelets (scoring data above and below the point of infection) obtained for each line at different scoring dates: 10 dpi, 14 dpi and 18 dpi.*